PROCEEDINGS OF THE WORKSHOP ON VISUOMOTOR COORDINATION IN FROG AND TOAD: MODELS AND EXPERIMENTS[1]

organized by

Michael A. Arbib

COINS Technical Report 82-16

"Theories pass. The Frog remains."

- Jean Rostand: Notebooks of a Biologist

Computer and Information Science Department
Center for Systems Neuroscience
University of Massachusetts
Amherst, Massachusetts 01003

[1] The Workshop, held at the University of Massachusetts at Amherst on November 16-18, 1981, was supported in part by NIH under a BSRG grant to the University of Massachusetts and grant RO1 NS14971-03, and by the Sloan Foundation grant for "A Training Program in Cognitive Science".

Authors and their Addresses

Michael Arbib	Center for Systems Neuroscience, University of Massachusetts, Amherst, MA 01003
Andrew Barto	Center for Systems Neuroscience, University of Massachusetts, Amherst, MA 01003
Hans-Wilhelm Borchers	Neuro-ethology & Biocybernetic Laboratories, University of Kassel, Pf. 101380, 3500 Kassel, WEST GERMANY
C. Curtis Boylls	Rehabilitative Engineering Research & Development Ctr. (153), V.A. Medical Center, 3801 Miranda Ave., Palo Alto, CA 94304
T.S. Cartwright	Biological Sciences Dept., University of Sussex, Brighton BN1 6QG, ENGLAND
Francisco Cervantes-Perez	Computer & Information Science Dept., University of Massachusetts, Amherst, MA 01003
Thomas Collett	Biological Sciences Dept., University of Sussex, Brighton BN1 6QG, ENGLAND
Andrew Cromarty	Computer & Information Science Dept., University of Massachusetts, Amherst, MA 01003
Steven Epstein	Computer & Information Science Dept., University of Massachusetts, Amherst, MA 01003
Jörg-Peter Ewert	Neuro-ethology & Biocybernetic Laboratories, University of Kassel, Pf. 101380, 3500 Kassel, WEST GERMANY
Katherine Fite	Psychology Department, University of Massachusetts, Amherst, MA 01003
Stephen George	Biology Department, Amherst College, Amherst, MA 01002
Paul Grobstein	Dept. of Pharmacology & Physiological Science, University of Chicago, 947 East 58th St., Chicago, IL 60637
Donald House	Computer & Information Science Dept., University of Massachusetts, Amherst, MA 01003
David Ingle	Psychology Dept., Brandeis University, Waltham, MA 02254
Rolando Lara	Centro de Investigaciones en Fisiologia Celular, Universidad Nacional Autonoma, A.P. 70-600, 04510, MEXICO, D.F., MEXICO
Neil Montgomery	Psychology Department, University of Massachusetts, Amherst, MA 01003
D.P.M. Northmore	Institute for Neuroscience, University of Delaware, Newark, DE 19711
Kenneth Overton	Computer & Information Science Dept., University of Massachusetts, Amherst, MA 01003
Sansar Sharma	Dept. of Ophthalmology, New York Medical College, Valhalla, NY 10595
John I. Simpson	Dept. of Physiology, NYU Medical School, 550 First Avenue, New York, NY 10016
Susan Udin	Division of Neurobiology, 327 Cary Hall, SUNY at Buffalo, Buffalo, NY 14214

TABLE OF CONTENTS

Chapter 1: An Introduction to Modelling

Michael A. Arbib: MODELLING NEURAL MECHANISMS OF VISUOMOTOR COORDINATION IN FROG AND TOAD

ABSTRACT

Frogs and toads provide interesting parallels to the way in which humans can see the world about them, and use what they see in determining their actions. What they lack in subtlety of visually-guided behavior, they make up for in the amenability of their behavior and the underlying neural circuitry to experimental analysis. We provide an overview of problems involved in modelling neural mechanisms of frog and toad visuomotor coordination; and then present a number of background models "in search of the style of the brain." We then review three specific models of neural circuitry underlying visually-guided behavior in frog and toad. They form an 'evolutionary sequence' in that each model incorporates its predecessor as a subsystem in such a way as to explain a wider range of behavioral data in a manner consistent with current neurophysiology and anatomy. The models thus form stages in the evolution of Rana computatrix, an increasingly sophisticated model of neural circuitry underlying the behavior of the frog.+ Finally, we provide a quick tour of a number of studies which have developed from these basic models.

1. NEURAL SUBSTRATES FOR VISUALLY-GUIDED BEHAVIOR

Lettvin, Maturana, McCulloch and Pitts [1959] initiated the behaviorally-oriented study of the frog visual system with their classification of retinal ganglion cells into four classes each projecting to a retinotopic map at a different depth in the optic tectum, the four maps in register. In this spirit, we view the analysis of interactions between layers of neurons as a major approach to

---

* The research reported in this paper was supported in part by the National Institutes of Health under grant RO1 NS14971-03. My special thanks to Rolando Lara of Universidad Nacional Autonoma de Mexico with whom the recent modelling was conducted during his stay at the University of Massachusetts, 1978-1980. Portions of Sections 1 and 4 appeared in the earlier paper, Arbib (1982).

+ When both models and experiments are further advanced, the time will be ripe for the differential analysis of (different species of) frog and toad. In the present article, however, we conflate data gathered from both frog and toad studies to lay the experimental basis for the models that we discuss.

modelling "the style of the brain". In Section 3, we offer a general view of cooperative computation between neurons within a layer, and between layers within the brain. (The relation of "maps as control surfaces" to the general study of perceptual structures and distributed motor control is given in Arbib [1981].) In following sections, we shall then exemplify these general principles in three specific models of cooperative computation in neural circuitry underlying visuomotor coordination in frog and toad. The final section will then chart directions for further modelling.

Lettvin et al. found that group 2 retinal cells responded best to the movement of a small object within the receptive field; while group 3 cells responded best to the passage of a large object across the receptive field. It became common to speak of these cells as "bug detectors" (following Barlow [1953]) and "enemy detectors", respectively, though subsequent studies make it clear that the likelihood of a given frog behavior will depend on far more than activity of a single class of retinal ganglion cells (Ewert [1976], and Section 4 below). Given the mapping of retinal "feature detectors" to the tectum and the fact that tectal stimulation could elicit a snapping response, it became commonplace to view the tectum as, inter alia, directing the snapping of the animal at small moving objects -- it being known that the frog would ignore stationary objects, and would jump away from large moving objects. However, this notion of a simple stimulus-response chain via the tectum was vitiated by Ewert's observation that after a lesion to PT (pretectum-thalamus) a toad would snap at moving objects of all sizes, even those large enough to elicit escape responses in the normal animal. More detailed neurophysiological studies support the inference that the tectum alone will elicit a response to all (sufficiently) moving objects, and that it is PT-inhibition that blocks this response when the object is large, since tectal cells respond to visual presentation of large moving objects in the PT-lesioned animal [Ingle, 1973].

In Section 4a we present a model of local circuitry in the tectum (a 'tectal column') to explain certain facilitation effects in prey-catching behavior; then in Section 4b we study a linear array of such columns to model certain data on size-dependence of prey-catching activity in toads; and then, in Section 4c, we add PT-inhibition to such an array to model the behavior of an animal confronted with more than one prey-stimulus. These models form three stages in an evolutionary sequence for Rana Computatrix, our developing model of the neural circuitry underlying visuomotor coordination in frog and toad. Tectum and PT are but two of the many brain regions to be incorporated into the model during its further evolution. Section 5 provides a brief perspective of models discussed at greater length in later papers.

2. AN OVERVIEW OF MODELLING PROBLEMS

We may determine units in the brain physiologically -- for example, by electrical recording -- and anatomically -- e.g. by staining. In many regions of the brain, we have an excellent correlation between physiological and anatomical units -- we know which anatomical entity yields which physiological response. Unfortunately, this is not yet the case in many studies of visuomotor coordination in frog and toad. We have data on the electrophysiological correlates of animal behavior, and we have anatomical data. Often, though, we do not know which specific cell, defined anatomically, yields an observed electrophysiological response. For example, we have the Golgi anatomy of the frog tectum, shown in Figure 1a, and the physiological responses recorded from tectum during facilitation of prey-catching behavior shown in Figure 6d. However, our identification of the physiological responses with specific anatomically defined cells is still hypothetical. Nonetheless, such choices have to be made in formulating and testing our models.

Another problem that we confront in modelling is that we have both too much and too little anatomical detail: too much in that there are many connections that we cannot put into our model without overloading our capabilities for either mathematical analysis or computer simulation; and too little in that we often do not know which details of synaptology may determine the most important modes of behavior of a particular region of the brain. For example, in starting from the Golgi anatomy of frog tectum shown in Figure 1a, we can either follow Szekely and Lazar into the elaborate synaptology shown in Figure 1b, or we can rather accept their schematic view of a tectal column as the basic unit of structure, as shown in Figure 1c. In the modelling to be described in this paper, we have chosen the latter course, viewing the tectum as an array of interconnected columns each of which has the formal structure shown in Figure 1d, the behavior of the various neurons being described by coupled differential equations. In comparing the Golgi anatomy of Figure 1a with the model of Figure 1d, we see that a number of choices have been made. In Figure 1a we see that there are two types of output cells for the tectum, the pyramidal cell and the large tectal ganglionic neuron. Our model assumes that it is only the output of the former that is relevant to the phenomena that we are considering. Clearly, our models must be of such a kind that they are adaptable when we come to phenomena that in fact can be shown to depend upon the ganglionic output. Note, too, that we have ignored the bipolar neurons and amacrine cells, and that we have made certain assumptions about the connectivity between the neurons that are included in the model. However, an important point of our modelling methodology will be that we set up our simulation in such a way that we can use different connectivity on different simulations. In this fashion, we can generate hypotheses which can then be subjected to further experimental test.

Even if we have made a satisfactory choice of how to correlate physiological units with anatomical units, and of the appropriate connectivity, we still have the

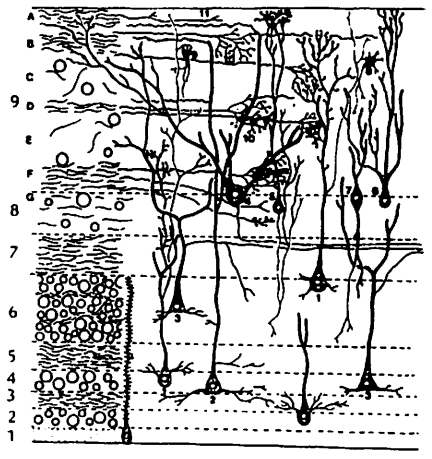

(a)

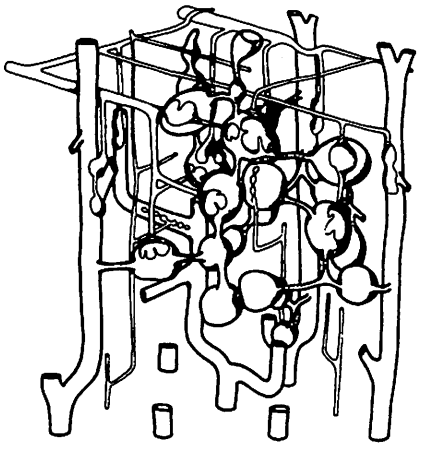

(b)

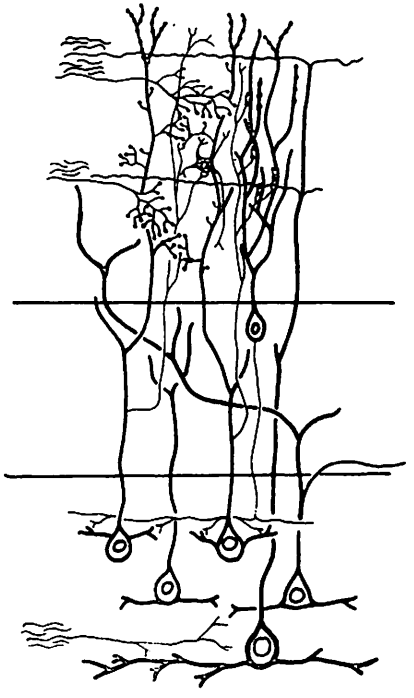

(c)

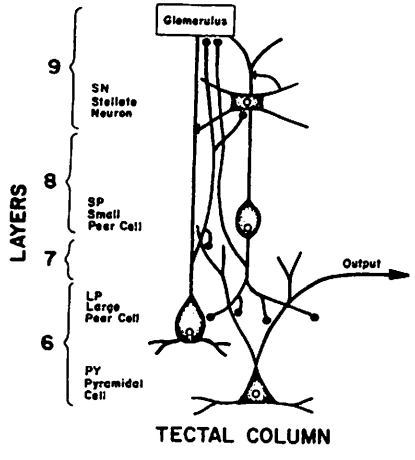

(d)

Figure 1.

Figure 1. (a) Diagramatic representation of the lamination and the representative types of neurons of the optic tectum. Numbers on the left indicate the different tectal layers. Numbered cell-types are as follows: (1) large pear-shaped neuron with dendritic appendages and ascending axon; (2) large pear-shaped neuron with dendritic collaterals; (3) large pyramidal neuron with efferent axon; (4) large tectal ganglionic neuron with efferent axon; (5-6) small pear-shaped neurons with descending and ascending axons respectively; (7) bipolar neuron; (8) stellate neuron; (9) amacrine cell; (10) optic terminals; (11) assumed evidence of diencephalic fibres [from Szekely & Lazar (1976)].

(b) Details of synaptic interaction of dendritic appendages, which exceed current models in intricacy [from Szekely & Lazar (1976)].

(c) Szekely and Lazar's schematic for a tectal column [from Szekely & Lazar (1976)].

(d) Neurons and synaptology of the model of the tectal column. The numbers at the left indicate the different tectal layers. The glomerulus is constituted by the LP and SP dendrites and recurrent axons as well as by optic and diencephalic terminals. The LP excites the PY, the SN, and the GL, and is inhibited by the SN. The SP excites the LP and PY cells, and it sends recurrent axons to the glomerulus; it is inhibited by the SN. The SN is excited by LP neurons and diencephalic fibres and it inhibits the LP and SP cells. The PY is activated by the LP, SP, and optic fibres, and is the efferent neuron of the tectum.

problem of correlating cellular structure and function with the animal's overall behavior. In the modelling to be described in this paper, for example, we have assumed that the activity of the pyramidal cells correlates with the orienting response of the animal. We have also assumed that when a population of pyramidal cells is active, the resultant orientation is to the mean position corresponding to that population, though there is not yet evidence to discountenance further hypotheses, such as that the orientation will be to the spatial locus corresponding to the peak of the pyramidal cell activity.

We have already spoken of the need to have a family of models which allows one to experiment with a number of different connectivities and parameter settings for the cells of the model. There still remains the question of what is the appropriately detailed model. Is it the fact that the overall behavior of a large collection of cells depends critically on the fine details of the response performance of each individual neuron, or can we hope to use relatively simple, computationally efficient, neuron models and still derive significant information about the behavior of the population? In the models to be described below, we have described the behavior of the neuron by a simple differential equation linear in terms of the synaptically weighted input values, and have assumed that the input from one cell to another is given by a simple non-linear transformation of the membrane potential of the source cell. We believe that with such models we can probe whether the neural networks of different kinds can yield overall classes of behavior. Future research will be both less detailed -- trying to provide quantitative analyses correlating classes of neural networks with classes of behaviors--and more detailed, as we try to establish detailed parametric specifications which can be subjected to experimental test in the laboratory. Section 3 will provide a survey of some of the conceptual models that enter into our

search for "the style of the brain," while Section 4 will present the first three stages of our attempts to model in some detail the experimental studies of visuomotor coordination in frog and toad.

Our modelling methodology must be based not on a single "take it or leave it" model, but rather on the exploration of a variety of different connectivities within some overall paradigm of brain function. Thus, the models to be described below are dominated by two main considerations: the visual system of the animal must be considered in the context of the ongoing behavior of the animal -- thus the stress on visuomotor coordination, rather than on vision per se; and the analysis will be in terms of the interaction between concurrently active regions of the brain, rather than in terms of any simple one-way flow of information in a hierarchically organized system. We use the term cooperative computation to refer to this style of concurrent neural processing.

In addition to our concern for embedding the brain within the ongoing cycle of the animal's action and perception, and studying the brain itself in terms of the cooperative computation of interacting subsystems, the three models to be exhibited in Section 4 exhibit a style of "evolutionary" modelling. As a first approximation, we continually try to localize the neural processes underlying some overt behavior of the animal within some relatively small portion of the brain. As we come to analyze more functions, though, we find that each function may require activity in many portions of the brain, and that each portion of the brain will be involved in many different activities. Thus, having successfully modelled several phenomena, one should try as far as possible, when modelling a new phenomenon, to do it by minor adaptations of the previous model, preserving the earlier successes, rather than introducing an ad hoc model of a new brain region specifically designed to achieve the new specified task. Thus, in Section 4 we shall start with the model of the single tectal column shown in Figure 1d, and show that it is able to account for certain behavioral and neurophysiological data on facilitation; we shall then show how a linear array of such columns (Fig. 10a) can account for data on worm pattern recognition, without losing the ability of the individual column to exhibit facilitation to a localized stimulus. Finally, as shown in Figure 11a, we shall introduce pretectal cells and newness interneurons in interaction with the linear array of columns of Figure 10a, and see how, again without losing earlier properties of the model, we can account for the certain aspect of prey facilitation. In Section 5, we shall briefly outline further developments which continue to increase the behavioral repertoire of our evolving model, Rana computatrix.

3. BACKGROUND MODELS: IN SEARCH OF THE STYLE OF THE BRAIN

Before turning, in Section 4, to the first three stages in the evolution of Rana computatrix, we devote the present section to a number of background models

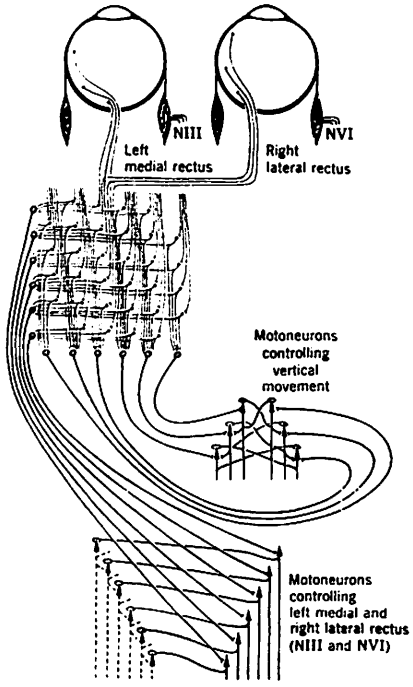

Figure 2. Pitts-McCulloch scheme for reflex control of eye position via superior colliculus. Eye can only be stationary when activity in two halves of colliculus is balanced. [Adapted from Pitts & McCulloch (1947).]

general scheme for distributed motor control into a specific model of a specific system. For example, the Pitts-McCulloch model does not give an account of ballistic movements. Again, it does not show us how, for increasing angles of deviation of the target, visual tracking might first evoke movement of eyes alone, then of eyes and head, and then of eyes, head, and trunk. It remains an important task in brain theory to explain how the output of a motor computer would control not a single pair of antagonist muscles, but rather a whole hierarchy of subcontrollers, in a distributed way.

3b. A Model of Frog's Snapping. Another problem is that in much visually guided behavior, the animal does not simply respond to "the center of gravity" of visual stimulation, but rather is responding to some property of the overall configuration. Consider, for example, the snapping behavior of frogs confronted with one or more fly-like stimuli.

Ingle (1968) found that in a certain region around the head of a frog, the presence of a fly-like stimulus elicits a snap; that is, the frog turns so that its midline is pointed at the stimulus and zaps it with its tongue. When confronted with two "flies," either of which is vigorous enough that alone it could elicit a

which establish the "style of the brain" with which we approach our modelling of visuomotor coordination in frog and toad.

Since we are concerned with motor control, we of course make use of such concepts as feedback and feedforward. In many treatments of these concepts in the literature on biological control systems, we see the use of lumped models. For example, the direction in which the animal should turn is encoded by a single angle variable. However, since we shall be concerned with the way in which patterns on the retina inpinge upon ongoing activity within the brain, we shall not consider it permissible to regard this angle as explicitly available in the brain as the value of, for example, firing of some neuron. Rather, we must consider it as encoded by the locus of the peak of activity within a neural array. Perhaps the first model of distributed motor control of this kind is that of Pitts and McCulloch (1947).

3a. Distributed Motor Control. Apter (1945, 1946) had shown that each half of the visual field of the cat maps topographically upon the contralateral superior colliculus. In addition to investigating this sensory map, she studied the motor map by strychninizing a single point on the collicular surface, flashing a diffuse light on the retina, and then observing which point in the visual field was affixed by the resultant change in gaze. She found that these sensory and motor maps were almost identical, and this basic finding has been replicated and extended in many recent studies. Starting from these data, Pitts and McCulloch developed the model shown in Figure 2. This outlined the reflex arc that extended from the eyes through the superior colliculus to the ocular-motor nuclei, thereby controlling the muscles that direct the gaze so as to bring the fixation point to the center of gravity of distribution of the visual input's brightness. (Our current knowledge of retinal preprocessing enables us to substitute for the term brightness such a term as contour information or an expression that describes some other feature of the input.) Pitts and McCulloch noted that excitation at a point on the left colliculus corresponds to excitation from the right half of the visual field and so should induce movement of the eye to the right; gaze is centered when excitation from the left is exactly balanced by excitation from the right. Their model is so arranged that each motor neuron controlling muscle fibers in the muscles that contract to move the eyeballs to the right, for example, should receive excitation summing the level of activity in a thin transverse strip of the left colliculus. This process provides all the excitation for muscles turning the eye to the right. Reciprocal inhibition by axons from nuclei of the antagonist eye muscles, which are excited similarly by the other colliculus, performs subtraction. The quasi-center of gravity's vertical coordinate is computed similarly. Eye movement ceases when and only when the fixation point is the center of gravity. Such a model leads to the idea that a plausible subsystem for vertebrate nervous system may be one in which position of the input on the control surface encodes the target to which the muscular control will be sent. Of course, much remains to be done in turning such a

snapping response, the frog exhibits one of three reactions: it snaps at one of the flies, it does not snap at all, or it snaps in between at the "average fly." Didday (1970, 1976) offered the simple model of this choice behavior shown in Figure 3a. It is presented not as the state of the art -- in fact, we shall see a more recent model built upon it in Section 4c -- but rather as a clear example of the processing of structured stimuli to provide the input to a distributed motor controller akin to that shown in Figure 2. Didday used the term foodness to refer to the parameter representing the extent to which a stimulus could, when presented alone, elicit a snapping response. The task was to design a network that could take a position-tagged "foodness array" and ensure that usually only one region of activity would influence the motor control system. The model maintains the spatial distribution of information, with new circuitry introduced whereby different regions of the tectum compete in such a way that in normal circumstances only the most active region provides an above-threshold input to the motor circuitry. To achieve this effect we first introduce a new layer of cells that is in retinotopic correspondence to the "foodness layer," and that yields the input to the motor circuitry. In some sense, then, it is to be "relative foodness" rather than foodness that describes the receptive field activity appropriate to a cell of this layer.

Didday's transformation scheme from foodness to relative-foodness employs a population of "S-cells" that are in topographic correspondence with the other layers. Each S-cell inhibits the activity that cells in its region of the relative-foodness layer receive from the corresponding cells in the foodness layer by an amount that augments with increasing activity outside its particular region.

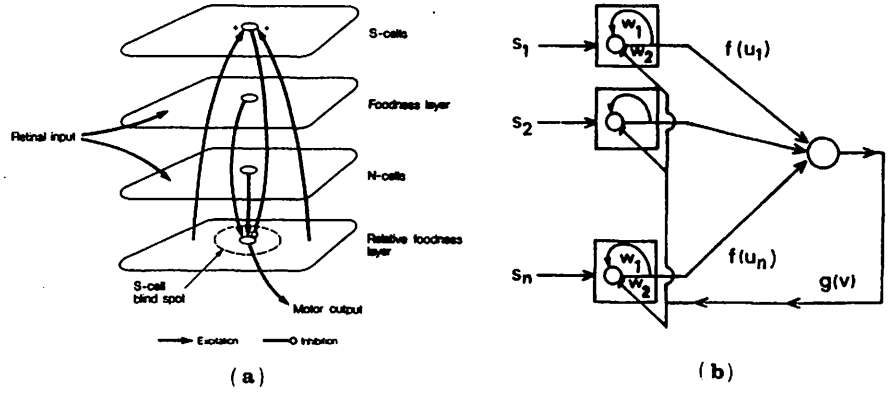

Figure 3. (a) Schematic view of Didday's model of interacting layers of neurons subserving prey-selection. (b) Primitive cooperation model in which the layer of S-cells of (a) is replaced by a single inhibitory neuron [from Amari & Arbib (1977)].

This ensures that high activity in a region of the foodness layer penetrates only if the surrounding areas do not contain sufficiently high activity to block it.

When we examine the behavior of such a network, we find that plausible interconnection schemes yield the following properties:

1. If the activity in one region far exceeds the activity in any other region, then this region eventually overwhelms all other regions, and the animal snaps at the corresponding space.

2. If two regions have sufficiently close activity then a) they may both (providing they are very active) overwhelm the other regions and simultaneously take command, with the result that the frog snaps between the regions; or b) the two active regions may simply turn down each other's activity, as well as activity in other regions, to the point that neither are sufficient to take command. In this case the frog remains immobile, ignoring the two "flies."

One trouble with the circuitry as so far described is that the buildup of inhibition on the S-cells precludes the system's quick response to new stimuli. If in case 2b above, for example, one of those two very active regions were to suddenly become more active, then the deadlock should be broken quickly. In the network so far described, however, the new activity cannot easily break through the inhibition built up on the S-cell in its region. In other words there is hysteresis. Didday thus introduced an "N-cell" for each S-cell. The job of an N-cell is to monitor temporal changes in the activity of its region. Should it detect sufficiently dramatic increase in the region's activity, it then overrides the inhibition on the S-cell and permits this new level of activity to enter the relative foodness layer. With this scheme the inertia of the old model is overcome, and the system can respond rapidly to significant new stimuli. Didday hypothesized that the S-cells and N-cells modelled the "sameness" and "newness" cells, respectively, that had been observed in the frog tectum. Regrettably, no experiments have been done to test this hypothesis.

3c. Competition and Cooperation in Neural Nets. The above model of prey selection is an example of a broad class of models dealing with competition and cooperation in neural nets. As one example of a model of such a kind, let us consider the problem of stereopsis, or segmentation on depth cues. Julesz (1971) has designed "random-dot stereograms" in which each eye receives a totally random pattern, but in which there are correlations between the inputs to the two eyes. Specifically, the different regions in the two inputs are identical save for a shift in position, yielding a different disparity in the two retina (Fig. 4a). Although such a pattern for a naive subject can initially appear to be nothing but visual noise, eventually disparity matching takes place and the subject perceives surfaces at different depths. Barlow, Blakemore and Pettigrew (1967) and Pettigrew, Nikara, and Bishop (1968) have found that cells in cat visual cortex are tuned for retinal disparity, and similar cells are posited in the human. What presumably causes the initial

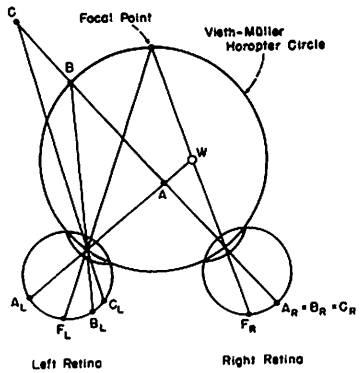

(a)

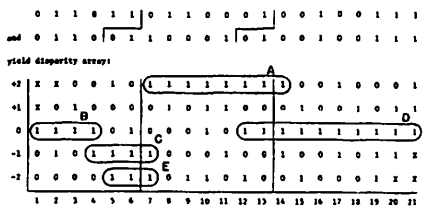

(b)

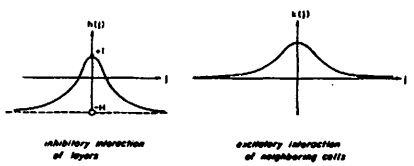

(c)

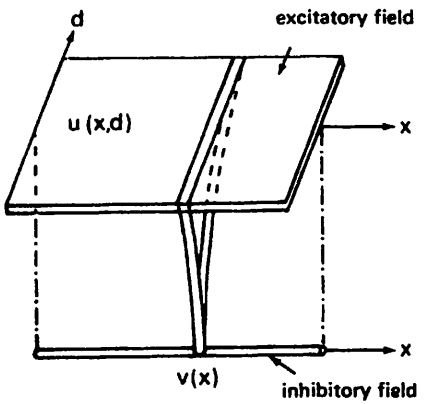

(d)

Figure 4. (a) Points projecting to the same point of one retina are projected to points with different disparities on the other retina. (b) The problem of resolving ambiguity: We conceptualize "layers" of cells (they are really in "columns"), one for each gross disparity. The aim is to segment the activity into connected regions. (c) Coupling coefficients for one approach to the problem: moderate local cross-excitation within layers; increasing inhibition between layers as difference in disparity increases. [From Arbib, Boylls & Dev (1974).] (d) The full model of competition and cooperation which allows the idea shown in (c) to be subject to mathematical analysis [from Amari & Arbib (1977)].

perception of visual noise is that in addition to the correct correlation of points in the two retinas, there are many spurious correlations, and computation is required to reduce them (Fig. 4b).

Dev (1975) [see also Sperling (1970), Arbib, Boylls and Dev (1974), Nelson (1975), and Marr and Poggio (1977)] has proposed that the cells of a given disparity be imagined as forming a population arrayed in a spatial map corresponding to the map of visual direction. Connections between cells could then be arranged so that nearby cells of a given disparity would be mutually excitatory, whereas cells nearby in visual direction but different in disparity would have inhibitory interaction (Fig. 4c). In this way, the activity of the array would organize into a pattern where in each region of visual direction, cells of only one disparity type would be highly active. As a result the visual input would eventually be segmented into a number of distinct surfaces.

In the stereopsis model, then, we have competition in the disparity dimension and cooperation in the other dimensions. The Didday model (Fig. 3a) can be regarded as the limiting case where there is only a competition dimension, namely that of prey location. Such informal observations have laid the basis for rigorous mathematical analysis of competition and cooperation in neural nets. For example, Amari and Arbib (1977) both offer the "primitive cooperation model" of Figure 3b which allows us to gain a mathematical handle on Didday's results, as well as a more sophisticated model, shown in Figure 4d, which allows us to provide a stability analysis of a model of the kind studied by Dev for stereopsis. Amari (1982) gives an up-to-date perspective on such models.

3d. Motor Schemas. We owe to the Russian school founded by Bernstein the general strategy which views the control of movement in terms of selecting one of a relatively short list of modes of activity, and then within each mode specifying the few parameters required to tune the movement. Where the Russians used the term synergy, we will use the term motor schema. The problem of motor control is thus one of sequencing and coordinating such motor schemas, rather than directly controlling the vast number of degrees of freedom offered by the independent activity of all the motor units. We have, to use the language of Greene, to get the system "into the right ballpark," and then to tune activity within that ballpark -- the dual problems of activation and tuning.

In the familiar realm of feedback control theory, a controller (which we will now think of as a motor schema) compares feedback signals from the controlled system with a statement of the desired performance of the system to determine control signals which will move the controlled system into ever greater conformity with the given plan. However, the appropriate choice of control signal must depend upon having a reasonably accurate model of the controlled system -- for example, the appropriate thrust to apply must depend upon an estimate of the mass of the object that is to be moved. Moreover, there are many cases in which the controlled system

will change over time in such a way that no a priori estimate of the system's parameters can be reliably made. To that end, it is a useful practice to interpose an identification algorithm which can update the parametric description of the controlled system in such a way that the observed response of the system to its control signals comes into greater and greater conformity with that projected on the basis of the parametric description. We see that when a motor schema is equipped with an identification algorithm (Fig. 5a) and when the controlled system is of the class whose parameters the algorithm is designed to identify, and when, finally, the changes in parameters of the controlled system are not too rapid, then in fact the combination of controller and identification algorithm within the motor schema provides an adaptive control system, which is able to function effectively despite continual changes in the environment.

3e. A Model of the Cerebellum. We have suggested that the problem of motor control is one of sequencing and coordinating motor schemas, rather than directly controlling the vast number of degrees of freedom offered by the independent activity of all the muscles. We have suggested that an "identification algorithm" can adapt a motor schema to changing conditions within some overall motor task. To see how this analysis can make contact with an interacting layers approach to neural circuitry, we now examine a model of the cerebellum (Arbib, Boylls, and Dev, 1974; Boylls, 1975, 1976). The model brings together the notion of a motor schema with the notion of maps as control surfaces, and is important in that it exhibits neural layers acting as control surfaces representing levels of activation for the coordination of muscles, complementing our study of retinotopic representations of visual input.

To provide neurophysiological data for the model, we consider cerebellar function in locomotion of the high decerebrate cat (Shik et al., 1966). Where Sherrington had noticed that stimulation of Deiter's nucleus in the standing animal would lead to extension of all the limbs, Orlovskii found that in the high decerebrate cat, stimulation of Deiter's nucleus during locomotion would not affect extension during the swing phase, but would increase extension during the support phase. Since the locomotory "motor schema" has been shown to be available even in the spinal cat (both in classical work by Sherrington (1910) and in modern studies (compare Herman et.al. 1976)), it seems reasonable to view the system in which the cerebellum and Deiter's nucleus are involved as providing an identification algorithm for the parametric adjustment of the spinal schema (Fig. 5b). We now turn to Boylls' model which shows how the adjustment of these parameters might be computed within the cerebellar environs.

As is well known (Eccles et al., 1967), the only output of the cerebellar cortex is provided by the Purkinje cells, which provide inhibitory input to the cerebellar nuclei. Each Purkinje cell has two input systems. One input is via a single climbing fiber which ramifies and synapses all over the Purkinje cell's

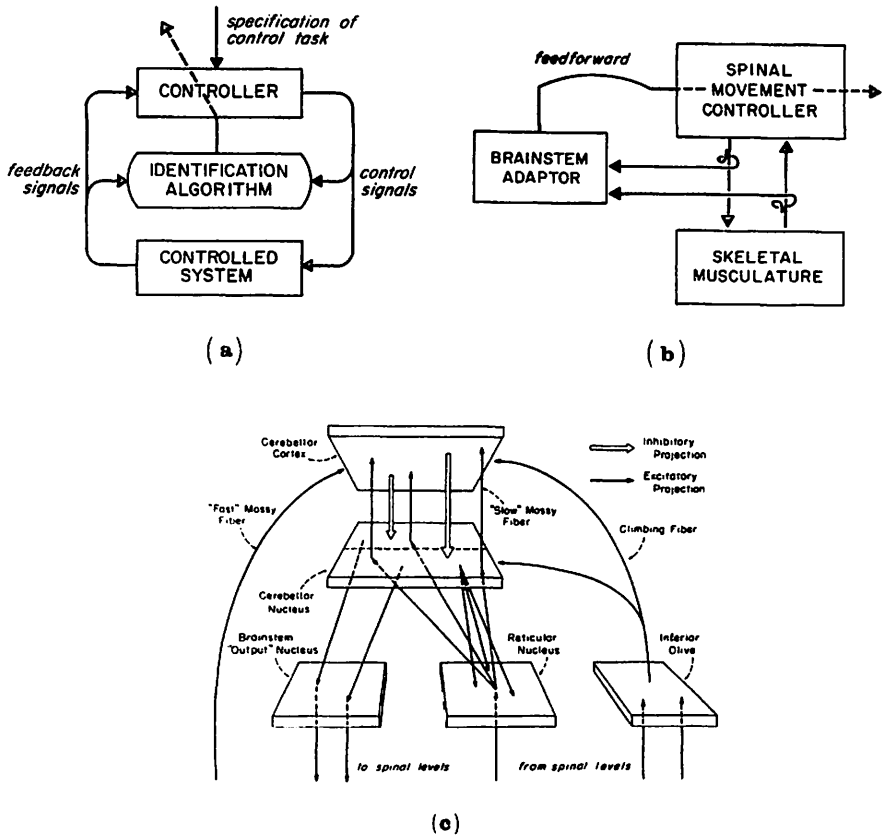

Figure 5. (a) An identification algorithm updates the parameters used to match the controller to the current properties of the system being controlled. (b) It is posited that the brainstem (cerebellum in interaction with various nuclei) serves as an identification algorithm for spinal movement controllers. (c) Schematic of the interacting control surfaces in the Boylls model of the tuning of motor schemas by cerebellum and related nuclei [from Arbib, Boylls & Dev (1974)].

dendritic tree. The other input system is via the mossy fibers, which activate granule cells whose axons rise up into the layer of Purkinje cell dendrites (which are flat, with the planes of all their dendritic trees parallel to one another) to form T's, whose crossbars run parallel to one another at right angles to the planes of the Purkinje dendritic trees. (There are a number of interneurons in the cerebellar cortex, but we shall not model these here, but shall instead concentrate on the basic cerebellar circuit of mossy and climbing fibers, and of granule and Purkinje cells.)

The climbing fiber input to a Purkinje cell is so strong that, when its climbing fiber is fired, a Purkinje cell responds with a sharp burst of four or five spikes, known as the climbing fiber response (CFR). Many authors have thought that the 'secret' of the climbing fiber is this sharp series of bursts, but Boylls suggested below that the true role of the climbing fiber input is to provide the suppression of Purkinje cell activity for as much as 100 milliseconds which has been found to follow the CFR (Murphy and Sabah, 1970).

The overall architecture of Boylls' model as played over an array of interacting control surfaces is shown in Figure 5c, which is an anatomical template of circuitry ubiquitous in cerebellar transactions. That is, specific labels could be given to, say, the 'brainstem output nucleus' as red or Deiters nucleus, the 'reticular nucleus' could be reticularis tegmenti pontis or paramedian, etc. From this architecture we gather that the output from the cerebellar nuclei via the brainstem 'output' nucleus results from the interaction between cerebellar cortical inhibition as supplied by the Purkinje cells and between drives from the reticular nucleus. Tsukahara (1972) has demonstrated the possibility of intense reverberation between the reticular and cerebellar nuclei following removal of Purkinje inhibition, and Brodal and Szikla (1972) and others have demonstrated the anatomical substrate for such loops, with a somatotopic mapping in both directions. We thus postulate that there will be explosively excitatory driving of the cerebellar nucleus by reticulo-cerebellar reverberation unless blocked by Purkinje inhibition.

The output of cerebellar tuning is expressed as a spatio-temporal neuronal activity pattern in a cerebellar nucleus, which can then be played out via the brainstem nuclei to spinal levels. A careful analysis of the anatomy enabled Boylls to predict that the agonists of a motor schema would be 'represented' along a saggital strip of the cerebellar cortex, while its antagonists will lie orthogonal to that strip (in the medio-lateral plane). Applications of this formula to cortical topography of the anterior lobe, as developed by Voogdt (1969) and Oscarsson (1973), allowed Boylls to identify particular cortical regions as associated with equally particular types of hindlimb-forelimb, flexor-extensor synergic groupings. This led to conclusions which are experimentally testable.

The Boylls model suggests that activity within the cerebellar nucleus is initiated through topically precise climbing fiber activity; the mechanism involves their direct cerebellar nuclear activation coupled with the suppression of the target Purkinje cell activity in the cortex via the above-mentioned 'inactivation response'. Once activity is installed in cortico-nuclear interactions via climbing fiber intervention, the underlying reverberatory excitation helps to retain or 'store' it. At the same time, this activity is transmitted to the cerebellar cortex on mossy fibers, eventually altering the inhibitory pattern in the nuclear region surrounding the active locus. The spread of parallel fibers yields a form of lateral inhibition which provides spatial 'sculpting' in a way depending on the elaborate geometry of cerebellar cortex and cortico-nuclear projections. Mossy

inputs of various types tune the resultant patterns to the demand of the periphery; and the program is spinally 'read out' as appropriate. Testing of the various hypotheses has required computer simulation of this neuronal apparatus. Simulation results corroborated the conjecture that cerebellar related circuitry could support the short-term storage of motor schema parameters initiated (and periodically refreshed) by climbing fiber activity.

4. THE FIRST THREE STAGES OF RANA COMPUTATRIX

4a. Facilitation of Prey-Catching Behavior. Frogs and toads take a surprisingly long time to respond to a worm. Presenting a worm to a frog for 0.3 sec may yield no response, whereas orientation is highly likely to result from a 0.6 sec presentation. Ingle [1975] observed a facilitation effect: if a worm were presented initially for 0.3 sec, then removed, and then restored for only 0.3 sec, the second presentation would suffice to elicit a response, so long as the intervening delay was at most a few seconds. Ingle observed tectal cells whose time course of firing accorded well with this facilitation effect (Fig. 6d). This leads us to a model [Lara, Arbib and Cromarty, in press] in which the "short-term memory" is in terms of reverberatory neural activity rather than in terms of the short-term plastic changes in synaptic efficacy demonstrated, for example, by Kandel [1978] in Aplysia. Our model is by no means the simplest model of facilitation -- rather, it provides a reverberatory mechanism for facilitation consistent with Ingle's neurophysiology and the known local neuroanatomy of the tectum. Unfortunately, the current knowledge of tectal circuitry is scanty, and much of the structure of the tectal column to be postulated below is hypothetical, and is in great need of confrontation with new and detailed anatomy and neurophysiology.

The model described in this section addresses facilitation at a single locus of tectum. Further developments address the interaction of a number of columns, and we shall discuss these in Sections 4b and 4c.

The anatomical study of frog optic tectum by Szekely and Lazar [1976] provides the basis for our model of the tectal column (Fig. 1a). In the superficial sublayers of tectum we see the thalamic input (which may also ramify in deeper layers), below which are the retinal type 1 and 2 inputs, with the retinal type 3 and 4 inputs deeper in turn. Deeper still, in layer 7, are the tectal efferents, which come from two cell types, the pyramidal cells and the so-called tectal ganglion cells. Our model of prey-catching will use only the pyramidal cells as efferents; we shall ignore the tectal ganglion cells which may (this is speculative) provide the output path for avoidance behavior. We incorporate the stellate cells as inhibitory interneurons, and ignore the amacrine interneurons. The other major components to be incorporated in our model are the large and small pear-shaped cells. Little of the anatomical connectivity of these cells is known,

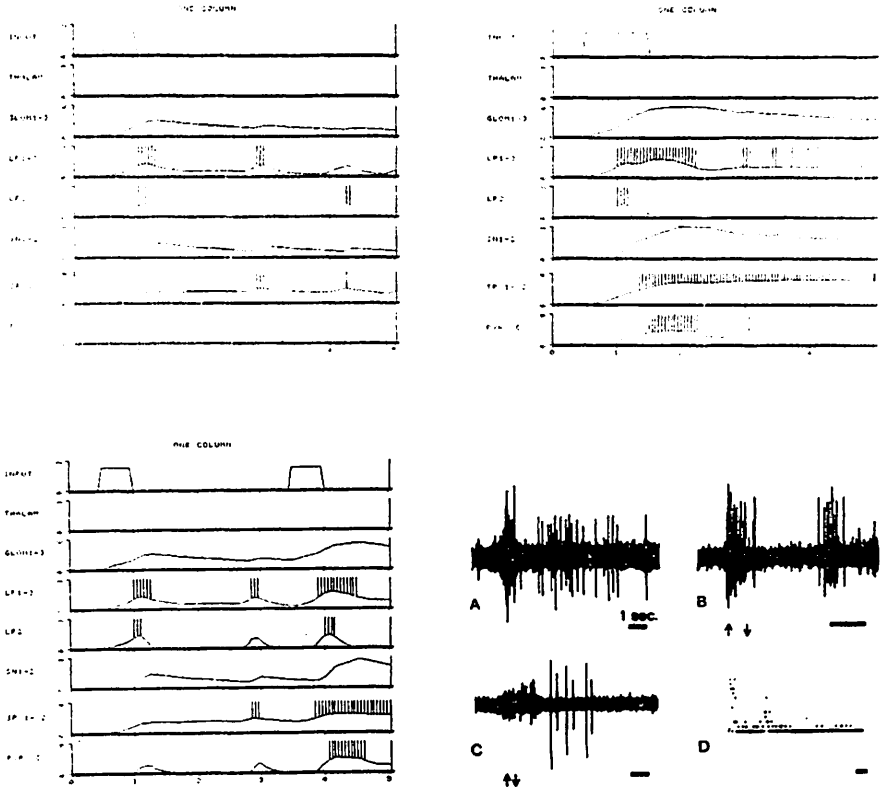

Figure 6. (a) Computer simulation of tectal cells response when a brief stimulus is presented. The onset of the stimulus produces a long lasting depolarizatin in the glomerulus which then fires the large pear-shaped cell (SP). This neuron in turn sends recurrent axons to the glomerulus and the stellate cell (SN) which acts as the inhibitory neuron in the column. When the inhibitory effect of SN releases the LP cell, a rebounding excitation occurs. The small pear-shaped cell is integrating the activity of GL, LP, and SN neurons to give a delayed short response. (b) If in the above situation we present a stimulus of longer duration then we show that now the pyramidal neuron fires. In (c) we show that when a second stimulus of the 'subthreshold duration' used in (a) is presented, the pyramidal cell (PY) responds. (The frequency of the spikes are a graphical convention. The spikes are drawn simply to highlight when the membrane potential of a cell is above threshold.) [From Lara, Arbib & Cromary (in press).]

(d) Physiological behavior of cells related to prey catching facilitation. A shows a brief class 2 burst followed by a delayed response of a tectal cell. In B the behavior of a tectal cell is shown, responding to the presentation of the stimulus and again with a delay. C shows a tectal neuron that produces a delayed response to the presentation of the stimulus. Finally, D shows the postimulus histogram of a tectal cell showing a delayed peak at 3 to 4 seconds. [From Ingle (1975).]

let alone the physiological parameters of their connections.

As we discussed in Section 2, the tectal column model (Fig. 1d) is abstracted somewhat crudely from the anatomy of Szekely and Lazar. It comprises one pyramidal cell (PY) as sole output cell, one large pear-shaped cell (LP), one small pear-shaped cell (SP), and one stellate interneuron (SN). (The simulation results of Figs. 6 and 7 were actually based on a larger column with 1 PY, 3 LP, 2 SP and 2 SN, but the results for the column of Fig. 1d are essentially the same.) All cells are modelled as excitatory, save for the stellates. The retinal input to the model is a lumped "foodness" measure, and activates the column through glomeruli with the dendrites of the LP cell. LP axons return to the glomerulus, providing a positive feedback loop. A branch of LP axons also goes to the SN cell. There is thus competition between "runaway positive feedback" and the stellate inhibition. (For a full presentation of the differential equations used in the simulation, see Appendix 1 of Lara, Arbib and Cromarty [in press].)

The role of SN in our tectum model is reminiscent of Purkinje inhibition of the positive feedback between cerebellar nuclei and reticular nuclei, a basic component of Boylls' model of cerebellar modulation of motor synergies outlined in Section 3. As mentioned above, Tsukahara [1972] found that reverberatory activity was indeed established in the subcerebellar loop when picrotoxin abolished the Purkinje inhibition from the cerebellar cortex. It would be interesting to conduct an analogous experiment by blocking inhibitory transmitters in the tectum.

Returning to the tectal model: glomerular activity also excites the SP cell which also sends its axon back to the glomerulus. The SP cell also excites the LP cell to recruit the activity of the column. The PY cell is excited by both SP cell and LP cell. Clearly, the overall dynamics will depend upon the actual choice of excitatory and inhibitory weights and of membrane time constants. It required considerable computer experimentation to find the weights that yielded the neural patterns discussed below. Further study was devoted to a sensitivity analysis of how weighting patterns affect overall behavior. It is our hope that our hypotheses on the ranges of the parameters involved in the model will stimulate more detailed anatomical and physiological studies of tectal activity.

Excitation of the input does not lead to runaway reverberation between the LP and its glomerulus; rather, this activity is "chopped" by stellate inhibition and we see a period of alternating LP and SN activity. The SP cell has a longer time constant, and is recruited only if this alternating activity continues long enough.

In one simulation experiment, we graphed the activity of the pyramidal cell as a function of the time for which a single stimulus is applied (Fig. 7a). There is, as in the experimental data, a critical presentation length below which there is no pyramidal response. Input activity activates the LP, which re-excites the glomerulus but also excites the SN, which reduces LP activity. But if input continues, it builds on a larger base of glomerular activity, and so over time there is a build-up of LP-SN alternating firing. If the input is removed too soon, the

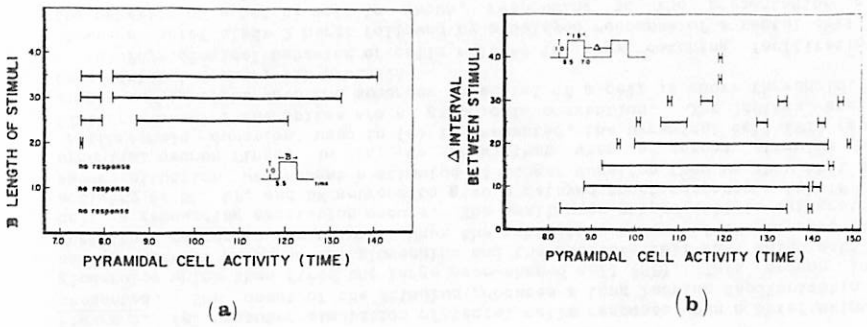

Figure 7. (a) Computer simulation of the PY behavior when stimuli are presented for different intervals. (b) Computer simulation of the temporal pattern of the facilitation process after the presentation of a brief stimulus.

reverberation will die out without activating the SP cells enough for their activity to combine with the LP activity and trigger the pyramidal output. However, if input is maintained long enough, the reverberation may continue, though not at a level sufficiently high to trigger output. However, a second simulation experiment (Fig. 7b) shows that re-introduction of input within a short time after cessation of this "subthreshold" length of input presentation can indeed "ride upon" the residual reverberatory activity to build up to pyramidal input after a presentation time too short to yield output activity on an initial presentation.

4b. A Simple Model of Pattern Recognition in the Toad. The facilitation model was 'local' in that it analyzed activity in a small patch of tectum rather than activity distributed across entire brain regions. We now outline Ewert's [1976, for a review] study of pattern recognition in the toad, analyzing what features of a single moving pattern will increase the animal's snapping responses. We then show how a one-dimensional array of tectal columns, of the type studied in the previous section, can model certain of these data. In Section 5, we briefly discuss our use of a two-dimensional array of such columns to model the whole range of Ewert's data on pattern recognition.

The toad is placed in a transparent cylinder. An object moves around a circular track concentric with, and on the floor outside, the cylinder. Some objects elicit no response. Other objects do elicit an orienting response (though the cylinder wall prevents the toad from actually snapping). Since the object keeps moving along its track, it can elicit a second response, and a third, and so on. Ewert's suggestion, then, is that the more 'attractive' is the object, the more frequently will the toad orient to it, so that the response rate is a measure of foodness. (Note a paradox here. The less attractive the object, the greater the

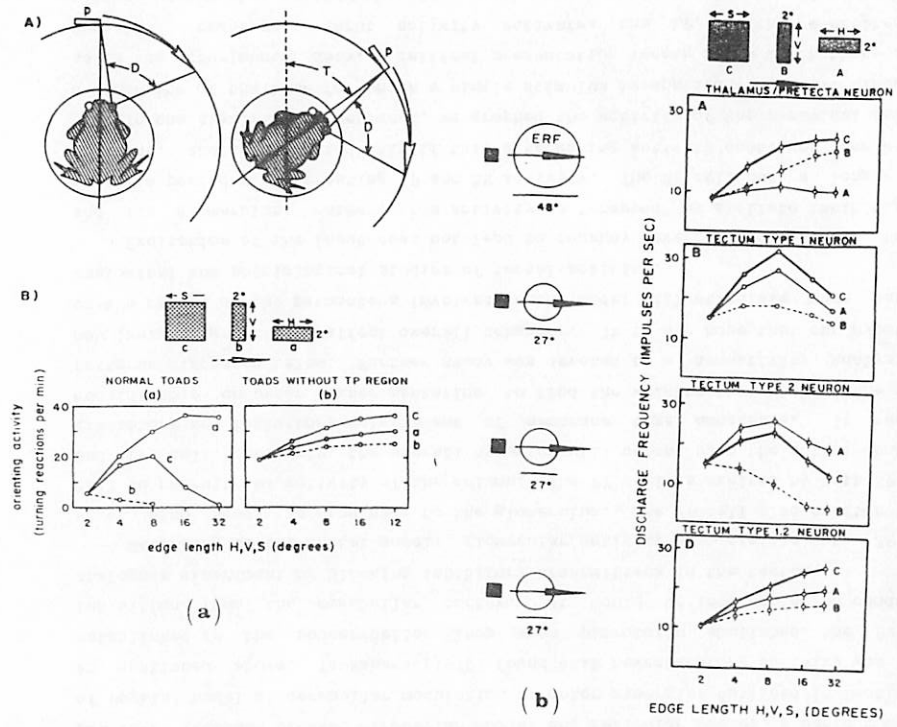

Figure 8. (a) Prey orienting behavior to different configuration of the stimulus. A) Turning reaction to the stimulus presentation. B) Orienting activity to three configurations (a,b,c): facilitation to stimulus a, inhibition to stimulus b, and an initial facilitation and then an inhibition to stimulus c. When pretectum ablation occurs this discrimination disappears.
(b) Tectal and pretectal cell activity to different configurations of the stimulus (a,b,c). A) Response of a pretectal neuron which is mostly sensitive to stimulus b and c. B and C show the response of two tectal cells to the three types of stimuli. Neuron C response is mostly sensitive to stimuli type a and c, and its response is greatly reduced for stimulus type b. This response is similar to the observed behavioral response. D shows the response of both tectal cells (B and C) without pretectum and how the discriminative abilities of these cells are lost. [From Ewert (1976).]

integration time to a response, and thus the greater the distance the animal has to move to orient towards the object if it orients at all.)

Ewert presented three types of rectangular stimuli: a "worm" subtending 2 degrees in the direction normal to the motion, and some d degrees in the direction of motion; an "antiworm" subtending some d degrees in the direction orthogonal to motion, and 2 degrees in the direction of motion; and a "square" subtending d degrees in both directions. The prey dummy was moved at 20 degrees per second at a distance of about 7 cm from the toad. Ewert studied the toad's response rate for

each stimulus for a range of different choices of d degrees (fixed for each trial) from 2 degrees to 32 degrees (Fig. 8). For d = 2, the three stimuli were, of course, the same. They elicited an orienting activity of 2 to 3 turning reactions per minute. For the "worm", the orienting activity increased to an asymptote of 35 turns per minute at d = 16; for the "antiworm", the orienting activity decreased rapidly to extinction at d = 8; while for the square the orienting activity reached a peak of about 20 turns per minute at d = 8, and then decreased to zero by d = 32. (The square gives the impression of a competition between "worm" excitation and "antiworm" inhibition.)

Ewert repeated this series of behavioral experiments in toads with PT-lesions, and found that for none of the stimuli was there decreased response with increased values of d. This more detailed evidence for PT inhibition of tectally-mediated orienting was further elaborated by neurophysiological recording of PT and tectal neurons in the behaving toads. In the intact toad, PT-neurons had a response rate insensitive to increasing d for "worms", but the response increased with d for "antiworms", and even more rapidly for squares. Tectum type 1 neurons were insensitive to changing d for "antiworms", but had a peak of response at d = 8 for both "worms" and squares; while the firing rate of tectum type 2 neurons was similar to the orienting activity of the intact toad -- monotonically declining with d for "antiworms", peaking at d = 8 for squares, and declining slightly after d = 8 for "worms". (Note the slight discrepancy here -- one would expect the response to "worms" to be non-decreasing if, as Ewert does, one takes tectal type 2 activity as the neural correlate of orienting behavior.)

On this basis, Ewert postulated a simple model: A filter in PT responds best to an antiworm stimulus; a tectum type 1 cell responds as a filter tuned to a worm

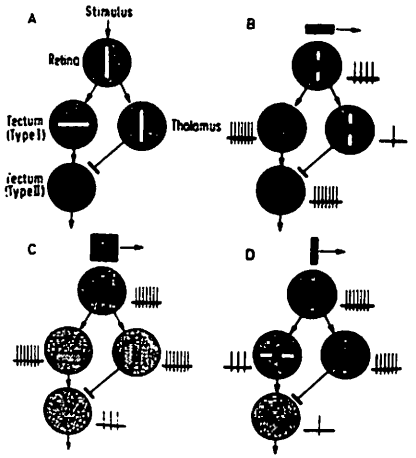

Figure 9. Schematic representation of the Ewert-von Seelen model of worm-'antiworm' discrimination. The tectum type II cell is excited by a tectal 'worm filter' and a thalamic-pretectal 'antiworm filter'.

stimulus; and a tectum type 2 cell is excited by the tectal type 1 cell and inhibited by a PT-cell (Fig. 9). Thus the type 2 cell responds with increased activity to increasing d for a worm stimulus; with decreased activity to increasing d for an antiworm stimulus; and with some tradeoff (dependent upon the actual parameters of the filters and the connectivity) for a square. Ewert and von Seelen [1974] fitted parameters to a linear formulation of this model to fit (part of) the response curves observed by Ewert. Note, however, that the domain of linearity is strictly limited; and that the model yields the average firing rate of the neuron: the model is thus lumped over time, and says nothing about the temporal pattern of neuronal interactions. Arbib and Lara [in press] have studied a one-dimensional array of tectal columns as in Figure 10a (without PT interaction) to provide a model of spatiotemporal neural interactions possibly underlying Ewert's "worm" phenomena. For example, in the Ewert study of the toad's response to an object moving along a track, we may regard the object's movement at one position as facilitating the animal's orientation to the object in a later position. The key question here is "How does the facilitation build up in the right place?" Part of the answer lies in noting the large receptive fields of the tectal columns; and analyzing how activity in a population of tectal columns can yield orientation in a particular direction. Thus, rather than analyzing activity in a single column, Arbib and Lara [in press] study the evolution of a waveform of activity in a one-dimensional array of columns (Fig. 10a). We show in Figs. 10b, c, d the response to a moving stimulus of various lengths. These reproduce Ewert's observations on the increasing attraction of a 'worm' with increasing length; Arbib and Lara also report a number of other computational experiments. The elaboration of this model to a two-dimensional array of columns (Lara, Cervantes and Arbib, 1982) is integrated with our model (Section 3c) of tectal-pretectal interactions in prey-selection to yield a model rich enough to extend an explanation of Ewert's data on pattern recognition into the temporal domain in a way which addresses the antiworm and square data, as well as the worm data.

4c. A Model of Prey-Selection. We saw in Section 3b that Ingle [1968] had studied the response of frogs to pairs of fly-like stimuli, each of which was such that when presented alone it would elicit a snapping response, and found that, under differing conditions, the animal would snap at one of the stimuli, snap between them, or not snap at all. We now turn to a model of such prey-selection which refines the Didday model discussed above (Fig. 3a) but differs in that -- in view of Ewert's study of PT-lesions -- it uses PT-tectal interactions, rather than positing that all the necessary circuitry is embedded in the tectum. Moreover, the new model extends the 'array of tectal columns' model of Section 4b to provide yet a third stage in the evolution of Rana Computatrix.

To make that transition from the Didday model, we now identify the "foodness layer" of Figure 3 with the retinal outflow to tectum and pretectum, and identify

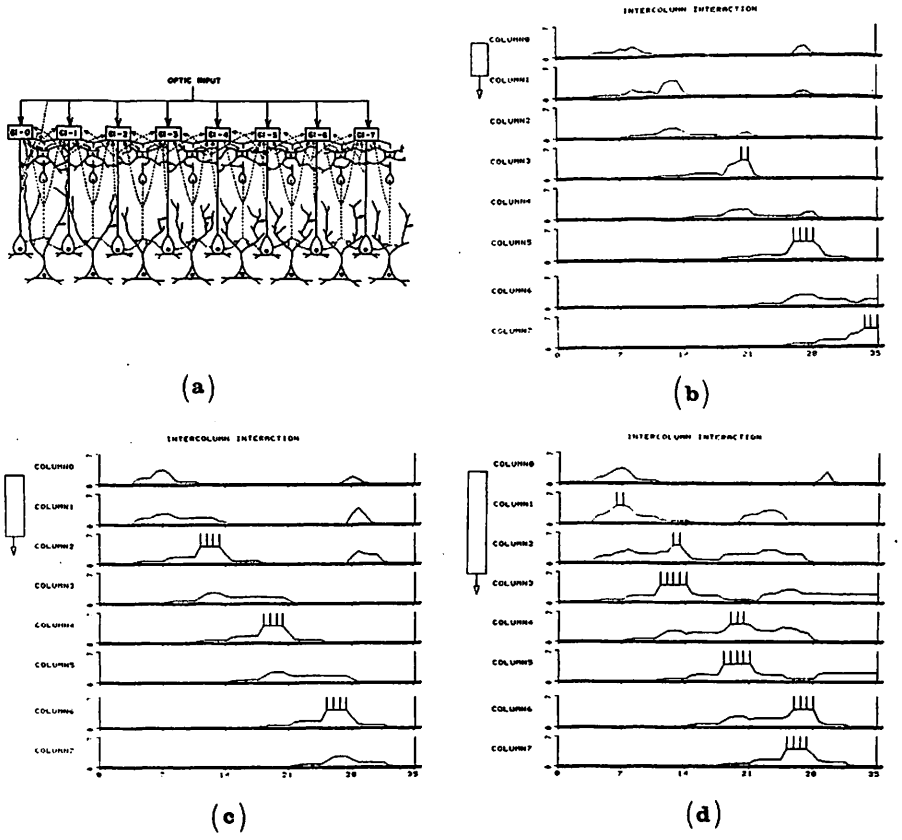

Figure 10. (a) Architecture of the model of the tectum. Each column is constituted by one GL (glomerulus), one LP (large pear-shaped) cell, one SP (small pear-shaped) neuron, one SN (stellate neuron), and one PY (pyramidal cell). The afferents are the optic fibres that arrive at the GL, LP, SP, and PY cells, and the efferents are the PY axons. LP cells are activated by the GL and the optic input, and they send recurrent axons to their own as well as neighboring glomeruli. The SN are activated by the LP cells, and they inhibit LP and SP neurons of their own as well as neighboring columns. The SP receive excitation from GL and are inhibited by SN; finally, PY receives afferents from the retina, the LP and SP neurons.

(b), (c) and (d) present a computer simulation of tectal response to a moving stimulus of different sizes. The graphs show the behavior of the 8 PY neurons of the tectal model of (a) to a moving stimulus. (b) Notice that in this case an alternate response is given in columns 3, 5, and 7 when the stimulus size only covers one glomerulus. (c) Here the stimulus covers 2 glomeruli simultaneously. The results show that the strength of activation increases when the size of the object is elongated. The latency of response is also shorter (column 2). (d) In this figure the stimulus covers 3 GL simultaneously. It can be seen that the latency of response is shorter and the total activity is greater than in (b) and (c). Notice that all columns fire with this stimulus. [From Arbib & Lara (in press).]

the "relative foodness layer" with the pyramidal cells of tectum. We now see that Figure 3a is too simple because it does not include other cells of the tectal column. The new model [Lara and Arbib, in press] interconnects a one-dimensional array of tectal columns with a layer of cells called S-cells, in retinotopic correspondence with the columns, which represent cells of the pretectum-thalamus (Fig. 11a). (In the 1970 model, the S-cells were identified with the sameness cells reported in the tectum by Maturana, Lettvin et al.) Each S-cell is excited by activity in the relative foodness layer, save for a blind spot centered at the locus corresponding to that of the S-cell. In the Didday model, the S-cell then provides an inhibitory input to cells within its blind spot on the relative foodness layer. Lara and Arbib [to appear], however, do not make the corresponding assumption that an S-cell must inhibit the PY cell in the corresponding tectal column. Rather they conduct a number of experiments on the dynamic consequences of choosing different sites for pretectal inhibition of columnar activity. The reader is referred to their paper for details.

The system described so far exhibits hysteresis. Should a new peak be introduced in the input array, it may not affect the output activity even if it is rather large, for it may not be able to overcome the considerable inhibition that has built up on the S-cells. The model thus follows Didday in postulating a further array of NE-cells (representing the newness cells of Lettvin et al.) which register sudden changes in input, and uses these to interrupt the ongoing computation to enable new input to affect the outcome.

Clearly, the detailed dynamics of the model will depend on the size of the blind spot, and the relative parameters of excitation and inhibition. We were able to adjust the coefficients in such a way that with several peaks in the foodness input array, the activity passed through to the tectal column would excite the S-cells in such a way that they would lower the corresponding peaks in tectal activity. However, if one peak were stronger than the others, it would be less inhibited, and would begin to recover; in doing so, it would suppress the other peak more, and thus be inhibited less; the process continuing until the stronger peak recovered sufficiently to control a "snap" in the corresponding direction (Fig. 11c). However, there were cases in which the mutual suppression between two peaks sufficed to hold each below a level sufficient to release behavior (Fig. 11b). We also showed that if the tectum became habituated to one of the stimuli, a standoff would be resolved in favor of the novel stimulus (Fig. 11d).

5. A PERSPECTIVE FOR FURTHER MODELLING

In Section 4, we exhibited an evolutionary sequence of models -- tectal column, one-dimensional array of columns; array with pretectal inhibition -- which explains an increasingly broad range of behavioral data on visuomotor coordination in frog

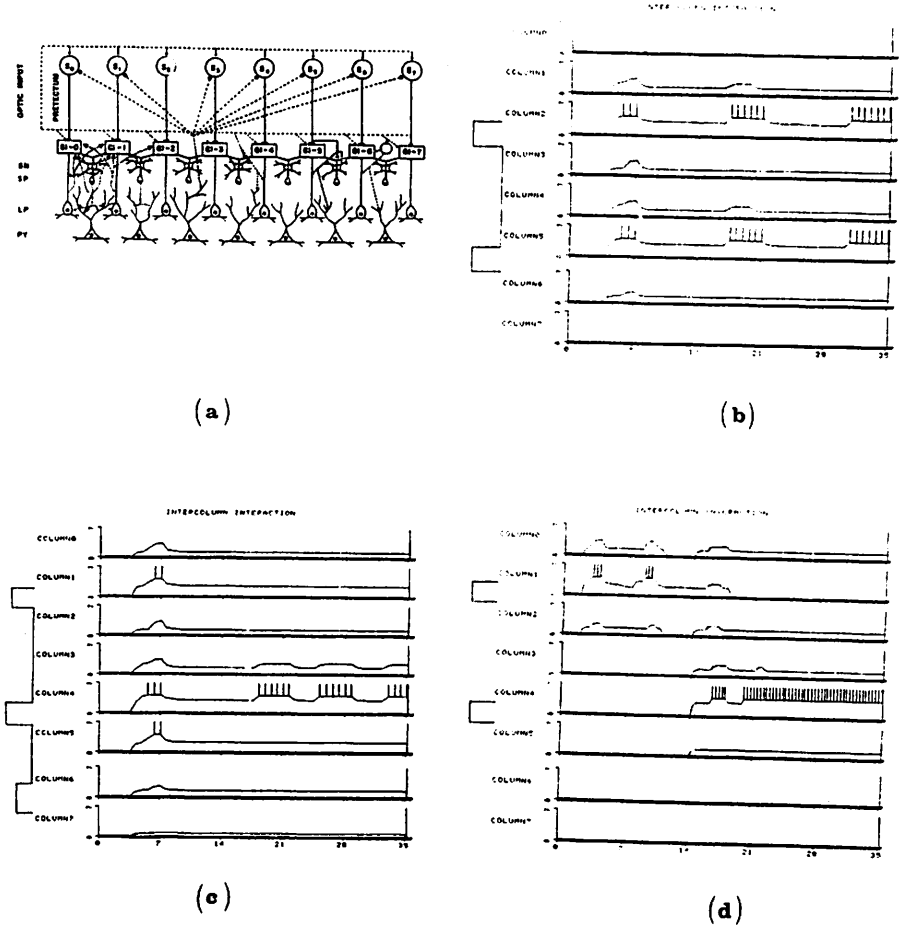

Figure 11. (a) Architecture of the model for the interactions between tectum and pretectum in prey selection. Each column receives the afferents from one sameness neuron; each PY (pyramidal) neuron excites all pretectal cells except the one whose blind spot is in its receptive field. The NE (newness) neurons arrive at the same site as the corresponding optic fibres. (b) Computer simulation of the behavior of PY neurons to two equally intense stimuli. The stimuli are presented in columns 2 and 5. Notice that an alternation of excitation and inhibition is present without convergence to any of the stimuli. (c) Computer simulation of the behavior of PY neurons to two equally intense stimuli to columns 2 and 5 biased by a third one. When the third stimulus is applied in column 7, then the response converges to the stimulus presented in column 5. (d) Computer simulation of habituation effects on PY activity. We first present a stimulus in column 1. After a period of rest, we present two equally intense stimuli in columns 1 and 4, the response converging to column 4, because the pathway of column 1 is habituated.

and toad. We note three important features of the style of modelling developed here.

1. New phenomena are addressed not by the creation of ad hoc models but by the orderly refinement and expansion of models already created. Of course, we expect that future development along this line will lead to redefinition and refinement of earlier models, rather than simple addition of new circuitry in each case. On the other hand, we would expect that the model, once sufficiently developed, will explain many data beyond those which specifically entered into its design.

2. Each 'model' in the sequence is in fact a 'model-family'. We design a family of overall models, and then conduct simulation experiments to see which choices -- of connectivity, synaptic weights, time constants -- yield neural dynamics, and input-output relations, compatible with available data.

3. The choices mentioned above are only loosely constrained by the experimental data presently available. To carry out simulations, we make choices which often must, perforce, go beyond these data. In making such choices, we form explicit hypotheses (whose details are spelt out in our papers cited in Section 4) which may serve to stimulate new experiments. These experiments in turn will stimulate more refined modelling. The continuing cycle will lead to an increasingly sophisticated understanding of the neural mechanisms of visuomotor coordination.

We close with a brief discussion of future directions for this modelling effort. We have already mentioned the transition from a one-dimensional to a two-dimensional array of tectal columns (and corresponding pretectal elements) as a further development of Rana Computatrix in Lara, Cervantes and Arbib (1982).

The models of Section 4 have nothing to say about the control of avoidance behavior, nor does the basic version described here address more than a few of the prey-predator discrimination phenomena discussed in Section 4b. A two-dimensional array of columns will allow us to study the full range of these phenomena.

Other developments in the modelling of frog brain visuomotor coordination will come as we try to take more and more regions of the brain into account -- for example, the cerebellum, the retina, and the forebrain. We will also want to look at more complex behaviors of the animal, not only prey-selection and predator avoidance, but also behaviors which require the integration of a number of motor schemas. For example, we are currently considering the way in which an animal will approach a worm when a vertical paling barrier is interposed. In this case, the animal's behavior can be analyzed in terms of the coordinated activation of three motor schemas: one for side-stepping, one for orienting, and one for snapping. The understanding of this behavior, then, reinforces our need to model the animal's behavior in terms of the cooperative computation of a number of brain regions. We have now adapted the Dev conceptual model of stereopsis, described above in Section 3c, to a model of depth perception in the frog, in which we take account not only of the disparity cues available in the binocular field of the animal, but also of

accommodation cues available in the monocular field (the animal can still strike with an accurate depth estimation if it has only one eye, and the worm is presented in the monocular field corresponding to that eye).

Clearly, then, developments in modelling will require both the generation of general concepts for vision and motor control, as well as specific studies which try to provide a variety of detailed models adapted to experimentation on different kinds of animals and different kinds of situations. We shall also need to get a better understanding of how regions of the brain are coordinated in complex behaviors. Finally, it will not be enough to understand how the adult brain behaves in any given situation; we must also understand the development of the brain (for example, by modelling the development of retinal-tectal connections), and by studying learning mechanisms.

There are further refinements not incorporated into the basic model. Increased motivation (due, e.g., to food odor or to hunger) will cause the animal to snap at larger moving objects than it would otherwise approach. Such an effect might be modelled by direct excitation of tectal columns, or by diffuse inhibition of the S-cells, probably under the control of telencephalic regions. Forebrain mechanisms allow the animal to learn simple discriminations. And there are habituation phenomena which we have begun to model (Fig. 11d). Habituation disappears when there is PT ablation. Moreover, the habituation is stimulus specific, and it appears that pattern recognition is necessary both for habituation and dishabituation to occur. For example, Ewert has studied habituation of a toad's snapping response to simple moving patterns and has discovered a hierarchy -- an ordering $A \leq B$ of patterns,such that if the toad habituates to A it will automatically be habituated to B, but not vice versa. Such data provide a continuing challenge to the theory-experiment interaction that will drive the future evolution of Rana Computatrix.

REFERENCES

Amari, S., 1982, Competitive and Cooperative Aspects in Dynamics of Neural Excitation and Self-Organization. In: Competition and Cooperation in Neural Nets (S. Amari and M.A. Arbib, Eds.), Lecture Notes in Biomathematics, Springer-Verlag (this volume).

Amari, S., and Arbib, M.A., 1977, Competition and cooperation in neural nets. In: Systems Neuroscience, (J. Metzler, Ed.), New York: Academic, p. 119-165.

Apter, J.T., 1946, Eye movements following strychninization of the superior colliculus of cats. J. Neurophysiol. 9: 73-85.

Apter, J.T., 1945, Projection of the retina on the superior colliculus of cats. J. Neurophysiol. 8: 123-134.

Arbib, M.A., 1981, Perceptual structures and distributed motor control. In: Handbook of Physiology: The Nervous System II. (V.B. Brooks, Ed.), Bethesda, Md.: Amer. Physiological Society, 1449-1480.

Arbib, M.A., 1982, Rana Computatrix: An Evolving Model of Visuomotor Coordination in Frog and Toad. In: Machine Intelligence 10 (J. Hayes and D. Michie, Eds.), Ellis Horwood.

Arbib, M.A., Boylls, C.C., and Dev., P., 1974, Neural models of spatial perception and the control of movement. In: Cybernetics and Bionics, (W.D. Keidel, W. Handler, and M. Spreng, Eds.), Munich: Oldenbourg, 216-231.

Arbib, M.A., and Lara, R. (in press), A neural model of the interaction of tectal columns in prey-catching behavior. Cognition and Brain Theory, 5.

Barlow, H., 1953, Summation and inhibition in the frog's retina. J. Physiol. (Lond.) 119: 69-88.

Barlow, H.B., Blakemore, C., and Pettigrew, J.D., 1967, The neural mechanism of binocular depth discrimination. J. Physiol. 193: 327-342.

Boylls, C.C., 1974, A Theory of Cerebellar Function with Applications to Locomotion. Ph.D. Thesis, Stanford University.

Dev, P., 1975, Computer simulation of a dynamic visual perception model. Int. J. Man-Mach. Stud., 7: 511-528.

Didday, R. L., 1970, The Simulation and Modelling of Distributed Information Processing in the Frog Visual System. Ph.D. Thesis, Stanford University.

Didday, R. L., 1976, A model of visuomotor mechanisms in the frog optic tectum. Math. Biosci. 30: 169-180.

Ewert J. P., 1976, The visual system of the toad: behavioral and physiological studies in a pattern recognition system. In: The Amphibian Visual System: A Multidisciplinary Approach. (K. Fite, Ed.), Academic Press, pp. 142-202.

Ewert, J. P. and von Seelen, W., 1974, Neurobiologie and System-Theorie eines visuellen Muster-Erkennungsmechanismus bei Kroten. Kybernetic 14: 167-183.

Ingle, D., 1968, Visual releasers of prey-catching behavior in frogs and toads. Brain Behav. Evol. 1: 500-518.

Ingle, D., 1973, Disinhibition of tectal neurons by pretectal lesions in the frog. Science 180: 422-424.

Ingle, D., 1975, Focal attention in the frog: behavioral and physiological correlates. Science 188: 1033-1035.

Ingle, D., 1976, Spatial visions in anurans. In: The Amphibian Visual System. (K. Fite, Ed.), Academic Press, New York, pp. 119-140.

Julesz, B., 1971, Foundations of Cyclopean Perception. Chicago: Univ. of Chicago Press.

Kandel, E.R., 1978, A Cell Biological Approach to Learning. Grass Lecture No. 1. Society for Neuroscience: Bethesda, MD.

Lara, R., and Arbib, M.A. (to appear), A neural model of interaction between tectum and pretectum in preytectum in prey selection.

Lara, R., Arbib, M.A., and Cromarty, A.S. (in press), The role of the tectal column in facilitation of amphibian prey-catching behavior: a neural model. J. Neuroscience.

Lara, R., Cervantes, F., and Arbib, M.A., 1982, Two-dimensional Model of Retinal-Tectal-Pretectal Interactions for the Control of Prey-Predator Recognition and Size Preference in Amphibia. In: Competition and Cooperation in Neural Nets (S. Amari and M.A. Arbib, Eds.), Lecture Notes in Biomathematics, Springer-Verlag (this volume).

Lettvin, J. Y., Maturana, H., McCulloch, W. S. and Pitts, W. H., 1959, What the frog's eye tells the frog brain. Proc. IRE. 47: 1940-1951.

Marr, D., and Poggio, T., 1977, Cooperative computation of stereo disparity. Science. 194: 283-287.

Nelson, J. I., 1975, Globality and stereoscopic fusion in binocular vision. J. Theor. Biol. 49: 1-88.

Pettigrew, J.D., Nikara, T., and Bishop, P.O., Binocular interaction on single units in cat striate cortex. Exp. Brain Res. 6: 391-410.

Pitts, W.H., and McCulloch, W.S., 1947, How we know universals, the perception of auditory and visual forms. Bull. Math. Biophys. 9: 127-147.

Rosenfeld, A., Hummel, R.A. and Zucker, S.W., 1976, Scene labelling by relaxation operations. IEEE Trans. Syst. Man Cybern. 6: 420-433.

Sperling, G., 1970, Binocular vision: a physical and a neural theory. Am. J. Psych. 83: 461-534.

Szentagothai, J. and Arbib, M. A., 1974, Conceptual Models of Neural Organization. NRP Bulletin vol. 12, no. 3: 310-479. (Also: The MIT Press, 1975.)

Tsukahara, N., 1972, The properties of the cerebello-pontine reverberating circuit, Brain Res. 40: 67-71.

Waltz, D.L., 1978, A parallel model for low-level vision. In: Computer Vision Systems (A.R. Hanson and E.M. Riseman, Eds.), New York: Academic, p.175-186.

Chapter 2: Pattern Recognition

Jorg-Peter Ewert: NEUROPHYSIOLOGICAL BASIS OF CONFIGURATIONAL PREY-SELECTION IN THE COMMON TOAD

Rolando Lara, Francisco Cervantes, and Michael Arbib: A NEURAL MODEL OF INTERACTIONS SUBSERVING PREY-PREDATOR RECOGNITION AND SIZE PREFERENCE IN ANURAN AMPHIBIAN

Jorg-Peter Ewert: NEUROPHYSIOLOGICAL BASIS OF CONFIGURATIONAL PREY-SELECTION IN THE COMMON TOAD

Prey Recognition

From quantitative experiments with rectangular moving stripes we know that toads Bufo bufo prefer "worm-like" prey objects (stripe axis oriented parallel to the movement direction) and avoid "antiworm-like" ones (stripe axis oriented perpendicular to the movement direction) (Ewert, 1976). The ability of toads to distinguish worms from antiworms is invariant to (i) the stimulus movement direction in the x,y,z-coordinates, (ii) the direction of the stimulus background contrast, (iii) the velocity of motion (within visible ranges), (iv) the stimulus distance (within behaviorally relevant limits (Ewert et al., 1979). Extracellular recordings from single axons of the three retinal ganglion cell classes demonstrate that the configurational area effects on prey-catching are not simply derived from the output of one of these neurons. Extracellular recordings from single visual "small-field" neurons of retinal central projection areas in the thalamic-pretectal (TP) region and the optic tectum in response to configurational parameters of moving contrast stimuli indicate for possible neuronal "gestalt filters" (Ewert, 1976). The TP small-field neurons (TH3) are sensitive to the whole stimulus area, mainly to its expansion perpendicular to the direction of stimulus movement. Tectum neurons of type T5(1) are sensitive to the whole stimulus area but mainly to its expansion in the direction of stimulus movement. There is a statistically distinct second neuronal population, tectum type T5(2) neurons, with response characteristics to configurational parameters, which reflect to a good approximation the probability that the stimulus fits the category prey. There is evidence that tectum T5(2) neurons receive excitatory inputs from tectum T5(1) neurons, and that they receive inhibitory inputs from TP-neurons (Ewert et al., 1979). It is thought that tectum T5(2) neurons are involved in a system which triggers the prey-catching orienting movement, once a particular level of neuronal activity has been reached. This is supported by the results from electrical point stimulation of the optic tectum in freely moving animals. Following lesions in the TP-region prey/predator recognition is abolished. Lesioned animals snap toward any moving object independent of its configuration. Hence, according to our hypothesis (Ewert, 1968; Ewert and v. Seelen, 1974; Arbib et al., 1982) prey-recognition is performed through excitatory and inhibitory connections between thalamo-tectal neuronal populations. Recording experiments from the same T5(2) neuron before and after injection of kainic acid (Cromarty et al., in prep. 1982) and microknife cut lesions (Laming et al., in prep. 1982) in the ipsilateral TP region have shown that these neurons lose their configurational response properties. The thalamic-pretectal-tectal framework appears to be modulated by telencephalic and related structures.

Comments on Approach and Avoidance Systems

Results from electrical brain stimulation and lesion experiments

confirm the concept that optic tectum and caudal thalamus are involved in mediating two classes of antagonistic behaviors (i) approach (mediated by the optic tectum and the caudal thalamus including the TP region). Moderate bilateral lesions of the TP region totally abolish escape avoidance behavior toward appropriate visual moving stimuli. However, following functional recovery of configurational prey selection after 6 weeks - TP lesioned toads and frogs regain some residual avoidance capacity in response to large looming objects. It seems likely that recovery of escape avoidance behavior is also subject to a process of functional recovery involving remaining thalamic areas, e.g., the LGN. If the entire forebrain is ablated bilaterally, just sparing optic tracts and hypothalamus, toads continue to catch prey, but escape avoidance behavior does not seem to recover after several months as far as has been investigated. Following ablation of the optic tectum both visual prey catching and visual predator avoidance behavior fail to occur, but barrier avoidance seems to be intact (Ingle, 1980). This suggests that the visual escape avoidance system resembles the properties of an AND gate, which requires inputs both from the TP region and the optic tectum. Electrical stimulation of the caudal thalamus in freely moving atectal toads still elicits directed escape responses, such as ipsilateral avoidance turns (Rehn, 1977). There is no evidence to show that in the intact toad visual escape avoidance behavior is elicited exclusively (!) via tecto-bulbar/spinal pathways as claimed by Ingle (1982).

Control of the Prey Catching Sequence

In connection with the concept of command systems we may assume that the output of several particular tectal neuron types,, each forming a command element ( ) , together constitute a command system [ ] , which itself activates a specific motor pattern. The entire sequence of motor patterns during prey-catching is released by different sequentially activated command systems that collectively belong to a multiple action system { } . In this sequence each executed command provides - so to speak - the stimulus situation of the next following command. It is assumed that operation of each command system requires simultaneous activation of all of its command elements, thus constituting an "AND gate" mechanisms. Command systems differ from each other by a distinct combination of command elements which can be shared by the different command systems, for example

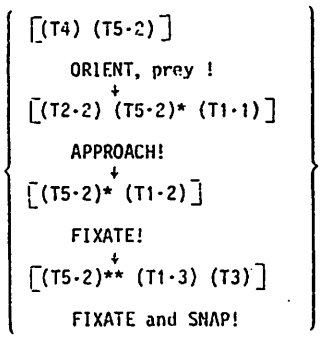

How could an AND gate system function? "Stimulus moving anywhere in the visual field" (T4) and "object recognized as prey, located n degrees outside the fixation area" (T5·2) yields the command ORIENT "Stimulus in the frontal visual field (T2·2) and "object recognized as prey located near the fixation area" (T5·2)* and "stimulus far afield" (T1·1) yields the command APPROACH→ "Prey near the fixation area"(T5·2)* and "stimulus close to the toad"(T1·2) yields the command FIXATE "Prey inside fixation area"(T5·2)** and "both retinae simultaneously stimulated" (T1·3) and "stimulus within snapping distance" (T3) yields the command FIXATE and S

If a predator crosses the visual field of the toad, then

[(T4) (T5·1) (TH3)]

AVOID!

Furthermore, the same command ORIENT for other goals - e.g., mate - may be issued by diferent combination of command elements, e.g.

[(T4) (T5·1)]

ORIENT, mate !

Of course, additional or alternative command elements of the above systems remain to be discovered. Whether or not these neurons correspond to "command elements" within such a proposed logical structure of command systems serving specific behavioral goals is as yet unknown. But this question can be answered by recording from these neurons in the behaving animal.

It is to some extent possible to test the proposed "AND" conditions. Thus, the command AVOID in response to a visual predator cannot be executed, if either T5·1 neurons (by tectal lesions) or TH3 neurons (by lesions of the caudal thalamic-pretectal region) are eliminated. Each motor command of the prey-catching sequence requires prey recognition as indicated by the output of T5·2 neurons. Reducing T5·2 activity by replacing the prey stimulus by an object with nonprey configuration decreases the probability of executing any command in the entire multiple action system of prey-catching. Elimination of visual input from one eye to binocular T1 neurons prolonges the execution and impairs the performance of the commands. However, the commands are not abolished, and this is obviously due to various kinds of functional neuroplasticity. For example and "AND" condition between two command elements subserving similar functions might be altered to an "OR" condition based on learning or due to the influence

of other modulatory elements (Kupferman and Weiss, 1978). Furthermore, after total elimination of the tectal visual neurons, cells sensitive to cutaneous input may mediate snapping. No command in the multiple action system of prey-catching can be issued when the motivation of the animal is not appropriate. Those influences might enter a command system at the level of a command element, e.g., the TS.2 neurons.

Neuroanatomical Considerations of the Circuitry

To repeat, the results from electrical brain stimulation experiments in freely moving toads have demonstrated in the optic tectum loci from which prey-catching responses were elicited in accordance with the topographical representation of the retina on the tectal surface (Ewert, 1967c and d). Furthermore, it was shown that stimulation points for snapping were mainly distributed at the lateral corner of the 3rd ventrical and below it in the subtectal region and the lateral torus semicircularis. Neurophysiological experiments have demonstrated that tectal neurons, which exhibit selectivity of response to the configuration of prey dummies, were exclusively distributed between the tectal layers 6 and 8 (Ewert and v.Wietersheim 1974b; v. Wietersheim and Ewert, 1978). Different strategies can be applied to investigate the descending connections of tectal neurons which are significant for the control of the motor systems that generate component of the pre-catching sequence: (i) Intracellular recording and staining of tectal neurons, which are supposed to be

command elements according to the nomenclature of Kupferman and Weiss (1978) and following the anterogradely labelled axons (Ewert, in preparation); (ii) injection of HRP into the behaviorally relevant premotor networks and motonerve nuclei and retrogradely tracing their afferent input (Weerasuriya and Ewert, 1981); (iii) Selective lesioning the cross and uncrossed tecto-spinal and tecto-bulbar projections in combination with behavioral observations and HRP studies (Ingle, 1982; Grobstein et al., 1982).

Motoneurons Controlling the Tongue Flip. The action pattern from strike at prey to swallowing requires coordinated activation of various muscles involved in movements of mouth, tongue and pharynx. The tongue flip is basically controlled by two extrinsic tongue muscles, the protractor (m. genioglossus and the retractor (m. hyoglossus), on each side. Following HRP injection into these muscles it could be shown that protractor and retractor motoneurons have a distinct topographical distribution within the hypoglossal nucleus (Weerasuriya and Ewert 1981), i.e., retractor motoneurons are rostral and protractor motoneurons are more caudal, which is simialr to that reported by Kramer et al. (1979) and Uemura-Sumi et al.(1981) in mammals. Since both anatomical (Cajal,1902) and physiological studies (Porter, 1965) failed to detect axon collaterals in mammalian hypoglossal motoneurons it seems likely that these are involved in preprogrammed activities requiring a minimum of feedback regulation. Because co-activation of protractor and retractor motoneurons would be extremely inappropriate, an inhibitory interaction between these

motoneuronal pools by non-propagated activity via dendro-somatic, dendro-dendritic or dendroaxonic synapses seems reasonable.

Afferent Connections of the Caudal Medulla Oblongata. Following injections of HRP into and around the hypoglossal nucleus, labelled cells were identified and ganglionic cells with their long axons coursing in layer 7 - project bilaterally to the medulla and most probably to the spinal cord as well, since the HRP injections may have damaged fibers of passage (Weerasuriya and Ewert, 1981). According to recent studies by Ingle (1982) neurons in and between tectal layers 6-8 are labelled following HRP injections into the medulla in areas of the tecto-bulbar and tecto-spinal pathways. In this context it is also interesting to note that turning behavior (e.g., prey-catching orienting) fails to occur after sectioning of the crossed descending tectal projection, whereas snapping remains intact. Prey-selective T5(2) neurons - which are considered as command elements with recognition properties - have been recorded from layers 6/7 and 8. Hence, like the ancient image of Janus' head these neurons look in two directions: toward the sensory side and the motorside.

Conclusions

In agreement with earlier results our current experimental investigations allow the following conclusions:

(1) The invariants prey, predator etc. are represented by certain combinations of stimulus features (e.g., configurations; cf. Ewert,

1968; Ewert et al., 1979c).

(2) Different sets of "simple neurons" (e.g., T5(1), TH3 neurons) are involved in the analysis of various stimulus features (Ewert and v. Wietersheim, 1974c; v. Wietersheim and Ewert, 1978; Schurg-Pfeiffer and Ewert, 1981).

(3) Innate recognition (configurational prey, prey/predator) is performed through weighted inhibitory and excitatory interactions among feature analyzing neuronal networks located in the diencephalon and the mesencephalon (Ewert et al., 1974; Ewert and v. Seelen, 1974; Lara and Arbib, 1981, 1982; Lara and Arbib, 1981; Arbib, 1981).

(4) There are sets of "complex neurons" (T5(2) neurons) which express the result of interacting neuronal networks and whose activation in response to a visual stimulus resembles the probability that the stimulus fits the prey category (Ewert, 1974; Ewert and v. Wietersheim, 1974c; Ewert et al., 1979a; Schurg-Pfeiffer and Ewert, 1981).

(5) According to the present state of our knowledge the innate pattern recognition system of toads (innate releasing mechanism for prey capture) contains no neurons that are specifically activated only be a certain kind of prey (Borchers and Ewert, 1979).

(6) The decision-making process (prey/nonprey) precedes goal oriented behavioral response (Ewert, 1968; Ewert and Kehl, 1978).

(7) Each motor command of the prey catching sequence requires activation of neurons subserving recognition (classification) and localization (e.g., strategy of catching) (Ewert, 1973; Ewert, 1980; Schurg-Pfeiffer and Ewert, 1981).

References

Arbib, M.A., Rana computatrix. An evolving model of visuomotor coordination in frog and toad. COINS Tech. Rep. (Univ. Mass. Amherst) 81-6 1-87.

Borchers, H.-W., and Ewert, J.-P., 1979. Correlation between behavioral and neuronal activities of toads Bufo bufo (L.) in response to moving configurational prey stimuli. Behav. Processes 4.99-106.

Ewert, J.-P., 1967a. Elektrische Reizung des retinalen Projektionsfeldes im Mittelhirn der Erdkröte (Bufo bufo L.). Pflügers Arch. 295:90-98.

Ewert, J.-P., 1967d. Aktivierung der Verhaltensfolge beim Beutefang der Erdkröte (Bufo bufo L.) durch elektrische Mittelhirnreizung. Z. vergl. Physiol. 54 455-481.

Ewert, J.-P., 1973. Lokalisation und Identifikation im Visuellen System der Wirbeltiere. In: Orientierung der Tiere im Raum (Vol. 1 (M. Lindauer, ed.) G. Fischer (Stuttgart) pp. 307-331.

Ewert, J.-P., 1974. The neural basis of visually guided behavior. In: Recent Progress in Perception (R. Held, ed.), Readings in Scientific American, W.H. Freeman Comp., San Francisco, pp. 96-104.

Ewert, J.-P., and Wietersheim, A.v., 1976. Musterauswertung durch tectale und thalamus-pretectale Nervennetze im visuellen System der Kröte (Bufo bufo L.). J. comp. Physiol. 92:131-148.

Ewert, J.-P., 1976. The visual system of the toad: behavioral and physiological studies in a pattern recognition system. In: The Amphibian Visual System. A Multidisciplinary Approach (K. Fite, Ed.), Academic Press, pp. 142-202.

Ewert, J.-P., 1980. Neuroethology. An Introduction to the Neurophysiological Fundamentals of Behavior. Springer-Verlag, Berlin, Heidelberg, New York.

Ewert, J.-P., and Kehl, W., 1978. Configurational prey-selection by individual experience in the toad Bufo bufo. J. Comp. Physiol. 126:105-114.

Ewert, J.-P., and Traud, R., 1979. Releasing stimuli for predator behaviour in the common toad Bufo bufo (L.). Behavior 68: 170-190.

Ewert, J.-P., and Wietersheim, A.v., 1974c. Der Einfluss von Thalamus Pretectum-Derektion auf die Antwort von Tectum-Neuronen gegenüber bewegten visuellen Mustern bei der Kröte (Bufo bufo L.). J. comp. Physiol. 92:149-168.

Ewert, J. -P. and von Seelen, W. (1974). Neurobiologie und System-Theorie eines visuellen Muster-erkennungsmechanismus der Kroten. Kybernetik 14: 167-183.

Ewert, J.-P., Hock, F.J., and Wiesenheim, A.v. (1974). Thalamus/Praetectum/Tectum: Retinale Topographie und physiologische Interaktionen bei der Krote (Bufo bufo L.). J. Comp. Physiol. 92: 349-356.

Ewert, J.-P., Borchers, H.-W., and Wiesenheim, A.v. (1979). Directional sensitivity, invariance and variability of tectal T5 neurons in response to moving configurational stimuli in the toad Bufo bufo (L.). J. Comp. Physiol. 131: 191-201.

Ewert, J.-P., Arend, B., Becker, W., and Borchers, H.-W. (1979). Invariants in configurational prey selection by Bufo bufo (L.). Brain, Behav. Evol. 16: 38-51.

Grobstein, P., Comer, Ch., and Kostyk, S.K. (1981). Frog prey-catching behavior: Between sensory maps and directed motor output. In "Advances in Vertebrate Neuroethology" (J.-P. Ewert, R.R. Capranica and D.J. Ingle, eds.), Plenum Press, London, New York.

Ingle, D., 1980. Some effects of pretectum lesions on the frog's detection of stationary objects. Behav. Brain. Res. 1: 134-143.

Ingle, D.J., 1982. Visual mechanisms of optic tectum and pretectum related to stimulus localization in frogs and toads. In Advances in Vertebrate Neuroethology (J.-P. Ewert, R.R. Capranica and D.J. Ingle, eds.), Plenum Press, London, New York.

Kramer, E.R., Rath, T., and Lischke, M.F., 1979. Somatotopic organisation of the hypoglossal nucleus - a HRP study in the rat. Brain Research 170: 533-537.

Kupferman, I., and Weiss, K.R., 1978. The command neuron concept. The Behav. and Brain Sci. 1: 3-09.

Lara, R., and Arbib, M.A., 1982. A neural model of interaction between tectum and pretectum in preytectum in prey selection. Biological Cybernetics (in press).

Lara, R., and Arbib, M.A., A model of the neural mechanism responsible for pattern recognition and stimulus specific habituation in amphibia. (in press.)

Porter, R., 1965. Synaptic potentials in hypoglossal motoneurones. J. Physiol. 180: 209-244. London.

Rehn, B., 1977. Cerebrale Repräsentation des visuellen Systems der Erdkröte (Bufo bufo L.). Ph.D. Thesis. Universität Darmstadt.

Schurg-Pfeiffer, E., and Ewert, J.-P., 1981. Investigation of neurons involved in the analysis of prey features in the frog Rana temporaria. J. Comp. Physiol. 141: 139-152.

Uemura-Sumi, M., Mizuno, N., Nomura, S., Iwahori, N., Takeuchi, Y., and Matsushima, R., 1981. Topographical representation of the hypoglossal nerve branches and tongue muscles in the hypoglossal nucleus of macaque monkeys. Neurosci. Lett. 22: 31-39.

Wiesenheim, A.v., and Ewert, J.-P., 1978. Neurons of the toad's (Bufo bufo L.) visual system sensitive to moving configurational stimuli: a statistical analysis. J. Comp. Physiol. 126: 35-42.

Rolanda Lara, Francisco Cervantes and Michael Arbib : A NEURAL MODEL OF INTERACTIONS SUBSERVING PREY-PREDATOR RECOGNITION AND SIZE PREFERENCE IN ANURAN AMPHIBIAN.

I. Introduction

In the present paper, we propose a two-dimensional model of the interactions among retina, optic tectum and pretectum in the anuran amphibian brain. The model analyzes neural processes subserving prey-predator recognition, with direction invariance of prey-predator recognition a consequence of tectal architecture, and size preference and latency of response of the animal depending on its motivational state. The model is an extension of the one dimensional model of the optic tectum, described elsewhere, [1-3] which takes into consideration anatomical, physiological and behavioral studies of the optic tectum, as well as earlier modelling efforts (Didday [19], Ewert and Von Seelen [17]).

Neuroethological studies [4-6] have shown that there are fixed action pattern in frogs and toads released by relatively simple key-stimuli. Innate mechanisms recognize the key-stimuli in the environment to elicit the proper response. It has been shown that both the size of a moving stimulus and its geometry in relation to the direction of motion play a prominent role in the prey-catching of the animal: small objects whose longest axis moves in the direction of motion ("worm-like") are considered as prey; if the same object is moved with its longitudinal axis perpendicular to the direction of movement ("antiworm-like") the animal do not elicit prey-catching orienting behavior, or may assume a freezing posture, or may give an avoidance behavior [4] (see Fig. 1). It has also been shown that this worm-antiworm recognition is invariant to both the direction and velocity of the stimulus [7].

Ingle [8-9] has shown that the preferred stimulus size and the latency of response to prey stimuli can change depending on the motivational state of the animal. He showed that animals highly motivated (i.e. with hunger or smelling worms) had low response thresholds and increase the response to prey stimuli, even to those normally uneffective. Ewert [20] showed that prey catching activity is greatly increased in these animals and Ingle showed that in these conditions animals prefer stimulus of 16 degrees to the normal prefered stimuli of 6 degrees.

A great deal of research has been aimed at trying to find the neuronal mechanisms responsible for these processes. Ewert [4] has shown that prey-catching orienting behavior is disrupted when the optic tectum is destroyed. Moreover, since the optic tectum receives information from the retina in a retinotopic way, it should be shown that electrical stimulation of a specific tectal region elicits the prey-catching orienting response to the corresponding retinal projection. This suggests that the optic tectum plays a prominent role in this sort of behavior. Ewert [10-11] has also shown that lesions of the dorsal pc/pl region within the thalamic-pretectal region (henceforth referred to as "pretectum" for short) disrupts the recognition abilities of the animal to the different

configurations of the stimuli (see Fig. 1B. b). Furthermore, he observed that toads with pretectum ablation snap indiscriminately to any object, they switched their preference from white to black moving visual stimuli, and they lost size selectivity. This suggests that the interaction among retina, optic tectum and pretectum may be responsible for the processes of prey-predator recognition, size preference and size constancy. These results have been confirmed by Ingle [25] , but Podufal claims that he did not observe these results in 4 of 20 animals which suggests that he could have made different lesions affecting other brain regions.

Trying to establish the role that each one of these brain regions may play in the control of these behaviors, Ewert studied the neuronal response in the retina, optic tectum and pretectum to the different configurations of the stimulus [4, 12-14]. He showed that in toads and frogs retinal ganglion cells of types R2, R3 and R4 do not change considerably their rate of response when a worm-like stimulus of different sizes was presented; whereas when an antiworm-like stimulus whose longest axis moves perpendicularly to the direction of motion was presented, ganglion cells of types R2 and R3 initially increased their rate of response up to the size of their respective excitatory receptive field and then the rate of response decreased when the object was larger than the excitatory receptive field (ERF). The inhibitory effect is stronger in ganglion cells R2 than ganglion cells R3. Class R4 ganglion cells increase their rate of response depending on the size of the object (see Fig. 2C). Ganglion cells of types R2, R3 and R4 increase their rate of response depending on the speed of the object, but they respond independently of the direction of motion.

There are class R2 and R3 ganglion cells exhibiting stronger response for a particular movement direction. However, almost no cells have been recorded showing "null-directions". Thus, directional sensitivity at this level may not significantly contribute to the processing of visual signals [12-13].

From the above results, Ewert concluded that the observed behavioral responses could not be explained simply by the retinal responses; thus he continued studying the response of tectal and pretectal cells to the different configurations of the stimuli. He found that some tectal cells, which he called T5(2), responded to moving configurational visual stimuli with overall firing level, resembling the probability that the stimulus under investigation fitted the prey category. That is, a facilitation of the firing rate, when the stimulus was elongated along the direction of motion, a decreased firing rate when the stimulus was elongated perpendicularly to the direction of motion, and a sort of summation of both responses when the stimulus was expanded in both directions (Fig. 3C). Moreover when pretectal ablation occurs, the overall response of this tectal cell (T5(2)) also resembled the behavioral response of the animal when the different stimuli were presented. Ewert also showed that this type of tectal cells could discriminate between prey and non-prey stimuli independently of the direction of motion while other tectal neurons, which he classified as T5(1), were directionally sensitive, and others which he called T5(3) responded more strongly to a predator-like stimulus [7]. For the above reasons, Ewert suggests that the tectal neuron type T5(2) may be responsible both for the discrimination between prey and non-prey stimuli and for indicating

the position to which the animal should orient. The tectal neuron performs this through combined activity with pretectal cells, possibly through an inhibitory effect [17]. Studies of the response of the pretectal cells [14] showed that most of these neurons had large receptive fields and that they were more sensitive to a predator-like stimulus (see Fig.3A). One of the pretectal cells, which Ewert called TH3, with a relatively small receptive field responded mostly to non-prey stimuli; for this reason, Ewert postulates that this cell inhibits the activity of tectal cells when a predator-like stimulus is present, thus allowing the animal to orient to the proper prey stimulus. In this way, Ewert sugests that the combined activity of retina-optic tectum and pretectum may control prey-predator recognition. With respect to the direction invariance recognition, Ewert argues that it must be a consequence of the tectal architecture rather than of a sophisticated "software"-like processing of information. Other hipothesis, however, claim that the correlation between behavioral and physiological data is arbitrary because different types of neurons have been found in the optic tectum which process differnt aspects of the stimuli, and the properties of prey orienting and prey catching behaviors cannot be explained by a single neuron [21-23] (see below); for these reasons these authors postulate that rather than by the activity of a single neuron, the mentioned behaviors are the result of the joint activity of several neurons. In latter works, however, Ewert [5,20] postulates a theory of coordination of motor schemas where there are recognition units for prey stimuli, but they need the activity of other neurons to control the prey catching orienting behavior, such as binocularity or depth perception neurons, which is in agreement with the argument that it is

needed the activity of several neurons to guide the motor response. Moreover, Ewert postulates that the other neurons found in the optic tectum may be related to predator recognition, depth perception, binocularity, etc., to which they might play a role for the control of different motor schemas. Therefore, the main argument against the correlation between the physiology and behavior can only be justified in the sense that we still need a theory which could relate the behavior of the cell with the actual motor pattern. In our model we have followed Ewert's hipothesis and in the discussion we propose a preliminary hypothesis of how the activity of several neurons, including the prey recognition units, could control prey-catching orienting behavior. However, further studies should clarify the real nature of these processes.

In relation to size preference, Ingle, following Ewert's hypothesis of pretectal inhibition over tectal activity, suggests that the changes in size, and latency of response could also be modulated by the pretectum [6,8-9]. He postulates that in normal conditions tectal cells are mostly guided by R2 ganglion neurons, and the effect over the optic tectum of the afferents from ganglion cell types R3 and R4 are normally inhibited by the pretectum. Ingle suggests that retinal R2 cells can overcome the pretectal inhibition through a facilitatory effect as a consequence of recurrent excitatory activity but the response has a long latency. In this way he explains why animals normally prefer small size stimuli. Whenever the pretectal inhibition is decreased, either by an increased motivational state or by a lesion, the tectal response is now controlled by ganglion R4 cells thus changing the receptive field size preference, and reducing

the latency of response.

II. The Model

The description of the model will be divided in four parts: a brief explanation of the proposed architecture for the two-dimensional model of the optic tectum, a description of the black box model of the retina, waiting for a more realistic retinal model, the description of the different pretectal cells and, finally, the proposed interaction among retina, optic tectum and pretectum.

II.1 Two-dimensional model of the tectum

In [1], we analized the anatomical data by Szekely and Lazar [18], which emphasized the vertical organization of the optic tectum, with a local 'vertical sample' of the optic tectum being referred to as a 'tectal column' with no suggestion of sharp transitions between properties of adyacent columns as has been suggested in some studies of mammalian cortex. We then offered a family of mathematical models of the tectal column. The two-dimensional model of the tectum shown in Fig. 4 is comprised of an 8x8 array of tectal columns, expanding the one-dimensional model of 8 tectal columns described elsewhere [2-3].

For the two-dimensional model the number of cells and their interactions is greatly increased. We will give a brief description of the most important considerations. Following [2-3], each column is constituted of one large (LP) and one small (SP) pear shaped cell, one stellate neuron (SN), one pyramidal (PY) cell, which correspond to

that neurons classified as T5(2) by Ewert (the efferent cell of the column), and one glomerulus (GL), for details of the construction of the tectal column refer to Lara et al. [1]. The interconnections among the cells of a column can be seen in Fig. 5, while the lateral connections among neighboring columns are all indicated in Table A :

a) The glomerulus is a synaptic complex comprising specific connections between axonal terminals, from retinal ganglion cells and diencephalic regions, and recurrent dendritic tectal terminals both from its own column as well as from neighbor ones.

b) Each LP cell receives afferents from retinal ganglion type R2 cells both through the glomerulus and through its dendrites along the length between glomerulus and cell body, from SP cells from its own column as well as from neighboring columns, and they are inhibited by the SN of its own column as well as by neighboring ones.

c) Each SP neuron is also activated by retinal ganglion R2 cells through the glomerulus and interglomerular dendrites both from its own column and from neighboring columns; this cell is inhibited by SN neurons from its own column.

d) The SN receives afferents from LP cells both from its column and from neighboring columns.

e) The PY cell, the efferent cell of the column, receives afferents from optic fibres of type R2, R3 and R4, from LP and SP cells of its own column and from LP cells of neighboring columns.

Table A. Lateral interactions among tectal columns.

	Cells of neighboring columns to (i, j)				
Cells of column (i, j)	GL	LP	SP	SN	PY
GL		+	+		
LP			+	+	
SP	+				
SN		+			
PY		+			

II.2 Black box model of the retina

As we have seen, retinal ganglion cells are sensitive to geometry in relation to the direction of motion, to contrast, and to the angular velocity function of the stimulus [4,15].

Our black box model of the different ganglion cells (types R2, R3, and R4) is based on the curves obtained by Ewert for the response of these cells to worm and antiworm-like stimuli (see Fig. 2) and the angular velocity function obtained by Grusser and Grusser-Cornehls [15] and Ewert [4].

The model simply defines the rate of response of type R2, R3 and R4 ganglion cells depending on the size and angular velocity of motion: the first with Ewert's graphs and the second with the following equation.

$R = kv\delta$, where k and δ are constants and v is the angular velocity function of the object. R is the frequency response of the retinal cell.

Each type of ganglion cell projects retinotopically to each tectal and pretectal column [18]. In the present model we have not considered the spatial representation of the different retinal receptive fields; we have only considered that the axon of each type of retinal cell projects to a specific column, and excites the surrounding neighbors with less intensity, either in the optic tectum or in the pretectum [15,18].

Each time a group of ganglion cells is stimulated, they will generate a response frequency R depending on the size, angular velocity, and direction of motion of the object. The parameters of the stimulus are specified by the modeller at the beginning of the simulation. We simulated the presence of a stimulus simply by a variable which defines when the stimulus should be present in a given zone and for how long it should rest there, depending on the speed and size of the object.

II.3 Pretectal cells

Because of the limited data about the anatomy of the pretectal region, in this model we simply modelled the pretectum as a two-dimensional array comprising two types of pretectal neurons :

The first type of pretectal neurons represents the TH3 cell of Ewert, which is mostly sensitive to antiworm-like stimuli and which he postulates to play a very important role, through its inhibitory

action, for prey-predator recognition of tectal neurons. This neuron only receives retinal afferents from ganglion cells of types R3 and R4. The second pretectal neuron is related to prey selection and has already been described elsewhere [3]. Briefly, this neuron is called a sameness cell, and receives the excitatory effects of all tectal pyramidal cells. These cells in their turn inhibit retinotopically the corresponding tectal column (see Fig. 6).

II.4 Interactions among retina, optic tectum and pretectum

Figure 6 shows the interactions among retina, optic tectum and pretectum. This figure shows that the retina projects retinotopically to both optic tectum (R2, R3 and R4) and pretectum (R3 and R4) [19,20]. Each pretectal cell inhibits the activity of LP, SP and PY neurons of its corresponding column (see inset Fig.6). The sameness cells receive its afferents from all the PY tectal neurons. Finally the PY cell activity defines the direction of the prey-catching orienting response and the prey-predator discriminative abilities of tectal neurons.

The mathematical description of the two-dimensional model of the interactions among retina, optic tectum and pretectum can be seen in the appendix.

It is important to notice that the final architecture proposed for the interactions among retina, optic tectum and pretectum was built, taking in count the anatomical data available untill now, with the purpose of obtaining the architecture that best reproduced the physiological and behavioral results. We have shown elsewhere [1] that the proposed architecture for a tectal column allow us to

simulate prey catching facilitation to a stimulus briefly presented; we then expanded this model to eight columns showing that this configuration permit us to simulate the facilitation of a stimulus elongated along the direction of motion [2]. Afterwards, we studied the interactions between the optic tectum and the pretectum both in prey catching facilitation and prey selection [3]. Now with the expansion of the model to two dimensions and including the interactions among optic tectum, retina and pretectum, we want to show the behavior of units that are sensitive to worm-like stimulus, and which pattern of response is independent of the direction of motion of the stimuli. Thus our choice for the final architecture was based on the following desired goals :

1) Simulation of worm-antiworm recognition independent of the direction of motion the stimulus; and 2) Changes in pretectal inhibition that increase the rate of response and reduce its latency.

For these reasons, we built a simetric architecture for the optic tectum with which for each direction there will be a facilitation if the stimulus is elongated along the direction of motion. We studied elsewhere [3] that for the inhibitory effect of pretectum to optic tectum, the best configuration, in terms of hysteresis effects and latency response, was that pretectal fibres arrive at LP, SP, and PY cells simultaneously. Finally, in order to simulate the change in the latency of response and the number of pulses discharged by the PY cells, we postulate that this neuron is excited, directly and through LP and SP cells, by ganglion cells R2, R3, and R4 and inhibited by the pretectum. Thus, our main problem was to adjust the weights from these cells to PY. The compromise was that without pretectum R4

should mostly control the response of PY, to simulate the preference for stimulus type c, while the sensitivity to stimulus type a was the effect of facilitation of tectal columns with recurrent activity, and finally R3 has a weak influence and both the architecture of the optic tectum and the activity of retinal ganglion cells yield to a poor response for stimulus type b. Moreover, this choice had also to include the effect of the inhibitory effect of TH3 over the tectal column to give the preference for stimulus type a, then to those type c, and a poor response to stimuli type b.

III. Computer Simulation

As mentioned above, the aim of the present model is to test the hypotheses both of prey-predator recognition and size preference through a model based on anatomical and physiological grounds. We shall also verify that this behavior is independent of the direction of motion, though this is, of course, an inmediate consequence of the symetry of the connections of each column. We will present the results of the computer simulation in two ways. First, graphs comprising the response of the pyramidal cell of each of the 64 columns of the two-dimensional model during the simulation of a specific computer experiment. Second, graphs with the same coordinates as those used to express the experimental data, that is, graphs that could be directly compared with phisiological and behavioral results. In the first case we divided the graph in 64 sections each one representing in the horizontal axis the time period of simulation and the vertical axis the PY activity. The PY activity is shown through its membrane potential and whenever the membrane potential reaches the threshold value we indicate it by an action

potential. We did not simulate the generation of the action potential in our neurons but it is simply a way of showing the results that could be easily compared with experimental results. Both ways of showing the actual behavior of the model allow us to make analogies and comparisons with experimental observations.

For the different simulations we used three types of stimuli: rectangles whose longest axis moves in the direction of motion (type a); rectangles whose longest axis moves perpendicular to the direction of motion (type b); and squares of different sizes (type c).

III.1 Behavior of pretectal cell TH3

Our purpose in simulating the response of TH3 to different stimuli is to show how the interaction of ganglion cells R3 and R4 could generate their properties. Trying different weights (see table 3 in the Apendix for the final values) the behavior of this cell to the different types of stimuli is shown in Fig. 7A. As can be seen in this figure, the response of this cell to the different types of stimuli is very similar to the behavior of the pretectal cell that Ewert suggests is related to prey-predator recognition (see Fig. 3A for comparison). This neuron responds more strongly to square stimuli (type c), then to "antiworm" (type b), while the response to "worm" stimuli (type a) does not change very much for different sizes of the object presented.

III.2 Behavior of tectal cells to different configurations of the stimulus without the inhibitory effect of pretectal cells.

It has been shown that tectal neurons without the inhibitory effect of pretectal cells respond better to stimuli of type c, then to stimuli of type a, while they give a weak response to stimuli of type b [4] (see Fig. 3D).

It is also known that axons of ganglion retinal cells R2, R3 and R4 project to the tectum [15,20]. It has been suggested that the facilitation effect for prey-catching orienting activity is mainly controlled by type R2 ganglion neurons [4,6], but anatomical studies and changes in the receptive field of the animal, latency of response etc., also suggest that tectal cells controlling prey-catching orienting behavior are also stimulated by ganglion cells R3 and R4.

As we mentioned earlier the final architecture proposed shows that the tectal column activity is mainly controlled by R2 ganglion afferents while the PY response is the combination of all three ganglion cell types.

The response of this neuron to the different types of stimuli is shown in Fig. 7D where it can be seen that it responds best to stimuli type c, then to those of type a, and lowest to those of type b. This behavior reproduces in general the experimentally observed behavior of tectal cells without pretectum (see Fig. 3D for comparison).

III.3 Model of the interaction among retina, tectum and pretectum for prey-predator recognition

As we mentioned above, there is a tectal neuron whose physiological response closely matches the prey-catching orienting response of the animal [4], its response is greater the longer the stimulus of type a, inhibited by longer stimuli of type b, while a combination of an initial facilitation and then an inhibition is observed for increasing size of stimuli type c.

The interaction among retinal cells, pretectum and optic tectum in our model, is shown in Fig. 6. Retinal ganglion cells project both to the pretectum and to the optic tectum. The pretectal cell then inhibits LP, SP and PY in the tectal column (see Lara and Arbib [3] for this configuration between optic tectum and pretectum).

In Fig. 7C we show the activity of the tectal columns through the response of the pyramidal neuron to the three types of stimuli. We have presented stimuli of different sizes starting with a 2x2 degrees and expanding it in three different ways ; expanding the dimension in the axis along the direction of motion (type a), expanding the dimension in the axis perpendicular to the direction of motion (type b), and expanding both dimensions (type c). We defined the speed of the stimulus as the time required to go from one column to the next, and the speed we used was 2 columns per unit of time of simulation which will be equivalent to 8 degrees per unit of time. We then counted the number of pulses of a given column (Fig. 7C) and the total activity in the optic tectum (Fig. 7B) to the presentation of the stimulus. It can be seen that the PY cells respond better to

stimulus type a, while for stimulus type c there is an initial facilitation and then an inhibition. These results reproduce in a general way the obtained physiological and behavioral observations (see Fig. 3C for comparison). Fig 7B shows a graph of the number of times the optic tectum is activated when a stimulus is presented, thus it is a better measure of the possible control by the optic tectum of the orienting response. This figure is equivalent to Fig. 7C.

In Fig. 8 we show the response of the 64 columns of the optic tectum to the three types of stimuli. The stimulus is presented from left to right with a speed of 8 degrees per unit of time and the abscisa shows five units of time of the membrane potential of each of the 64 PY neurons. Whenever the membrane potential reaches the threshold value, we showed it as a spike which is simply a graphical means to show the result, because we have not simulated how the action potential is generated nor the refractory period. This figure shows that the first column is activated at the beginning and the last column responds at the end with the respective latency. We have used in this case a stimulus of 8x2 degrees for stimulus type a, 2x8 degrees for type b, and 8x8 degrees for type c. It can be seen that the tectal activity is stronger for stimulus type a (Fig. 8A), than for type c (Fig. 8B) and the lowest activity is for stimulus type b (Fig. 8C).

III.4 Directional invariance for prey-predator recognition

It has been shown both behaviorally and physiologically [7] that prey-predator recognition is independent of the direction of motion of the stimulus. As a result, we used a symetric connection schema in

our models. Thus the direction invariance is to be expected in the response of the model. We report a simple test of this invariance, monitoring our model for prey-predator recognition to stimuli moved in eight different directions. We used a 12 x 2 stimulus which we know produces a very weak (almost no response in most tectal cells) response as an antiworm-like stimulus (type b) and a strong response as a worm-like stimulus (type a). We represent the results of this simulation in the same way that Ewert represented his experimental observations. We used the contrast formula:

$$D_{wa} = \frac{R_w - R_a}{R_w + R_a}$$

where D_{wa} is a measure of the discrimination between worm (w) and antiworm (a) stimuli. R_w is the response to worm-like stimuli and R_a is the response to antiworm-like stimuli. We then formed a circle divided by eight lines each one representing a given direction of the stimulus and the values of D_{wa} ranges between -1 (the origin) and +1 (the outer circle). The inner circle is when D_{wa} is equal to 0.

In Fig. 9 we show the response of tectal columns for worm and antiworm-like stimuli showing tht the discrimination is independent to the direction of motion.

Fig. 10 and 11 show the actual tectal response of the 64 columns to the presentation of worm (Fig. 10) and antiworm-like stimuli (Fig. 11) in different directions. It can be seen that the response to worm or antiworm stimuli is invariant to the direction of motion.

III.5 Size preference as a result of the interaction between tectum and pretectum

It has been observed that prey-catching orienting behavior and latency of response can be modulated depending on the motivational state of the animal [9]. It has been suggested that these changes are the result of a reduced inhibitory effect from pretectal neurons to tectal activity [4,9,20].

In order to test this hypothesis we used our model of prey selection described elsewhere, [2,3] where pretectal cells receive afferents from all tectal PY neurons.. Thus we postulate that when the animal is greatly motivated for prey catching orienting behavior the inhibitory effect of pretectal cells TH3 is greatly reduced (possibly increasing the threshold value of this neuron).

Based on this postulate we studied prey selection of the animal in the normal and motivated state. We represent our results in the same way that Ingle [8] and Ewert [20] did in their experimental observations ; we used a stimulus of a given size as a point of comparison; we then used stimuli of different sizes and studied which one of them was chosen when the animal was both in a normal or in motivated state. We also studied the latency of response in both cases.

Fig. 12 shows that a normal animal prefers smaller stimuli of 4 while the motivated animal always preferred larger stimuli. This figure also shows that the latency of response is greatly reduced in the motivated animal. These results reproduce in general terms the observed experimental results (see inset for comparison).

IV. Discussion

With the present model we have been able to simulate a great range of physiological, anatomical and behavioral observations. The present study builds on three earlier papers ; in [1], we simulated a single tectal column to reproduce the behavioral and physiological results obtained for prey-catching facilitation. This model was based on the anatomical and physiological studies of this region. We then in [2] analized an array of these tectal columns to provide a one dimensional model of the optic tectum which reproduced the facilitation of tectal response when the stimulus is elongated along the direction of motion as well as the facilitation to double stimuli moved along the direction of motion, with the preference of the animal being to orient to the leading of the two objects. In [3], we incorporated some notions of Didday [19] to form a one-dimensional model of the interactions among retina, optic tectum and pretectum for prey selection. With the expansion to two dimensions in the present paper we have here been able to reproduce prey-predator recognition and size preference depending on the motivational state of the animal, all this being independent of the direction of motion of the stimulus. This paper, then, offers the latest stage in the 'evolutionary development' of Rana Computatrix, a computational model, of increased hierarchical complexity, of how the different brain regions of anuran amphibians may interact to control the animal's behavior.

Our modelling studies in combination with the experimental evidence we have used suggest that the behavior of anuran amphibia is controlled by the cooperative activity among different brain regions. Each region itself has functional units for the processing of

information of specific properties of the stimulus. The retina evaluates different features of the stimulus. Then the pretectal neurons (and no doubt other thalamic cells) process features of the stimuli related to antiworm-like stimuli or static objects [6,15]. We know that in the optic tectum there are cells which seem to be very sensitive to worm-like stimuli; however, there is also evidence of cells which are mostly sensitive to antiworm-like stimuli as well as to other variables such as distance of the object, its position in the visual field, etc. [5,7]. This suggests that each region has different functional groups processing different properties of the stimulus whose integrative activity give the desired response.

With these modelling studies we suggest that the amphibian visual brain is organized in functional columns with a specific retinotopic configuration where the interactions between different brain regions yield the recognition of the stimulus and posteriorly the proper motor response. Each functional column, and we postulate a multifeatures column, extracts specific features of the stimulus which will then be combined with other functional columns to yield the motor response. The existance of functional columns have been described in several regions in the brain of higher vertebrates, which indicates that this type of organization must be crucial for the proper understanding of the nervous system. It has also been shown that a retinotopy is also present in the visual system of these animals and that there are different functional columns processing specific features of the stimulus, such as orientation, ocularity, etc. For this reason, the general principles of a distributive, joint, multifunctional cooperativity postulated in our model could be a general principle for

the processing of information of the visuomotor behavior in anuran amphibian.

The present modelling has, however, neglected the existance of other functional units with other processing of information which could be used by the animal to define the proper motor response. Our simulation has only considered a part of the integrative, more complex, activity of the optic tectum which controls the location and recognition of prey-predator stimulus. Further modelling should integrate other functional units in the optic tectum and other regions dealing with avoidance behavior, depth perception, binocularity, size constancy, etc., so we may have a clearer idea of how these function units interact among each other to give the proper motor response. Therefore, our model does not really deal with the problem of how the activity of the optic tectum or pretectum could yield the proper motor response. We have elsewhere [1,2] proposed a simplistic hypothesis that the activity of tectal PY cells (equivalent to T5-2 of Ewert) directly controls prey-catching orienting behavior; however, it is important to stress that motor behavior in the animal is really the coordination of several, possibly linked, motor schemas which are activated by a group of neurons which define a specific situation in the world. Therefore we first have to simulate how the animal has an internal representation of the world and how he uses it to coordinate its actions. Ewert [5,7] has specifically postulated that motor schemas, in cases such as detour, are activated by a group of cells and the action yields the activation of other neurons which then activate another motor schema. This hypothesis, however, does not take into consideration how the firing of neurons could control the

behavior nor how planning as a result of linked schemas or competition between schemas may occur. Arbib [24] has specifically postulated how cooperation and competition between schemas may occur, however not specifically applied to amphibians. Pellionisz [16], on the other hand, has postulated that the brain acts as a tensor like structure and then an internal representation of space, specifically on the cerebellum, can control motor behavior. This theory, again, does not really explain how coordination of motor schemas occur nor how the processing of information for the different features of the stimulus are used to guide the behavior.

The specific hypotheses of the present model can be listed as follows:

1) The tectal columns controlling prey-catching orienting behavior receive afferents from retinal ganglion cells of type R2, R3 and R4. The tectal column facilitates the response to retinal type R2 afferents; while retinal ganglion cells of type R3 and R4 control prey orienting behavior when the animal is in a motivted state or for the regulation of size constancy in the animal in combination with pretectal cells.

2) The inhibitory effect of pretectal cells gives tectal neurons the capacity for prey-predator recognition. The inhibitory effect of pretectal cells is mainly directed to the PY cell although a small effect can also be seen either on LP and SP or in the SN.

3) The directional invariance of prey-predator recognition is the result of the symetric connections posited in our model of tectal architecture.

4) Size preference is the result of a reduced pretectal inhibition of pretectal cells TH3 over the optic tectum. The change in the latency of response is also the result of this interaction. This effect may be controlled by the telencephalon.

The present model can be considered as a different way of simulating the ideas of Ewert and von Seelen for the relations among retina, optic tectum and pretectum for prey-predator recognition. Ewert and von Seelen [17] proposed a model of prey-predator recognition in which the retina, optic tectum and pretectum acted as filters for specific configurations of the stimulus. The inhibitory effect of the pretectum to the optic tectum enabled the latter to discriminate between worm and antiworm-like stimuli.

The limits of their model are : 1) they do not show how the architecture of the different brain regions will give rise to the properties of their postulated filters; 2) they only simulate prey-predator recognition with neither the possibility to reproduce other phenomena nor the capacity for expansion; 3) because of the linear nature of the model, it is only restricted to a given range of values; and 4) because the model is lumped both in space and time, it cannot be tested against the time course of response of specific cell types with specific retinotopic coordinates.

An alternative interpretation has been postulated for the mechanisms controlling prey-catching orienting behavior, where Ewert's idea of recognition units for prey and predators before the generation of the motor response is questioned. This hypothesis suggests, instead, that the motor response is the result not of a single recognition unit but the spatio-temporal pattern of several neurons acting simultaneously or serially (i.e. when a stimulus is present one cell will be activated, the movement will then induce the response of another neuron who will control other motor response). This postulate is based on the fact that there have been described neurons in the optic tectum which have different sensitivity to the configuration of the stimulus, some of them changing their preference depending on the speed of the stimulus [21-23]. Grusser and Grusser-Cornehls [15] and Roth [21] argue that because several neurons are activated in different ways with the same stimulus, prey catching orienting behavior could not be controlled by the activity of a single neuron. Moreover, these authors pose that the recognition units, if they exist, should have the following properties :

1) The all or nothing character of the different components of prey catching behavior; 2) They should respond to the real size of the stimulus and not to its angular size; 3) They should have a long latency of response; 4) They should change their response according to experience; 5) They should monitor the presence of the stimulus and the stationary world in detour behavior; and 6) They should respond to a specific location of space in avoidance behavior.

Because none of this properties have been found in the recognition units proposed by Ewert, they claim that the recognition units do not exist. This criticism is only valid if we identify the response of these units with the actual motor response; but if we consider, as Ewert does, that the response of the recognition unit only indicates that a prey or predator stimulus is present and its location in the visual field, and that the motor schema is activated by the joint activity of several neurons, possibly placed in different brain regions, these problems can be dealt as properties of integration of the motor schemas, as we propose below ; for example, we could think that the motor center is receiving information from several neurons one sensitive to specific configurations of the stimulus and others measuring depth perception of prey objects and of the stationary world, then the motor response could be elicited when the firing of these neurons reaches a certain value as an all or non-response (argument 1) with a latency depending on the frequency of response (argument 3), and at the same time, it could use this information in such a way as to give the size constancy effect (argument 2).

Similarly, changes in behavior could be related to the motor center rather than to units in the optic tectum, although plastic changes have been observed in these neurons. Finally, we think that detour behavior is not explained by Ewert's hypothesis nor by the hypothesis of Grusser and Grusser-Cornehls. In the case of Ewert, his hypothesis does not show how schemas simultaneously activated could yield to the proper sequential response, and Grusser and Grusser-Cornehls postulate a continuous feedback for the control of

the behavior which seems not to occur in these animals. In order to deal with these problems we postulate that there should be a group of motor schemas linked together, acting as a single schema, that are activated for a given situation, i.e. a group of neurons is activated with a given frequency to give the proper sequential response. This will allow us to explain detour behavior. However, for the final answer related with these topics further experimental research is needed.

Because of its anatomical and physiological bases, our model will be able to be tested against such experiments.

References

1. Lara, R., Arbib, M.A. and Cromarty, A.S. The role of the tectal column in facilitation of amphibian prey-catching behavior: a neural model. J. Neuroscience (to appear).
2. Arbib, M.A. and Lara, R. A neural model of the interaction of tectal columns in prey-catching behavior. Submitted to Biological Cybernetics.
3. Lara, R. and Arbib, M.A. A neural model of interaction between pretectum and tectum in prey selection. Cognition & Brain Theory (in press).
4. Ewert, J.P. The visual system of the toad: Behavioral and physiological studies on a pattern recognition system. In The Amphibian Visual System. (Fite, K. ed.) Academic Press, New York, pp. 142-202, 1976.
5. Schurg-Pfeiffer, E. and Ewert, J.P. Investigations of neurons involved in the analysis of gestalt prey features in the frog rana temporaria. J. Comp. Physiol. 141: 139-152 (1981).
6. Ingle, D. Spatial vision in anurans. In The Amphibian Visual System. (Fite, K. ed.) Academic Press, New York, pp. 119-141, 1976.
7. Ewert, J.P., Borchers, H.W., Wieterschein, von. Directional sensitivity, invariance and variability of tectal T5 neurons in response to moving configurational stimuli in the toad Bufo bufo (L). J. Comp. Physiol. 132:191-201, 1979.
8. Ingle, D. and Cook, J. The effect of viewing distance upon size preference of frogs for prey. Vision Res. Vol. 17, 1009-1013, 1977.
9. Ingle, D. Size preference for prey-catching in frogs: relationship to motivational state. Behav. Biol. 9:485-491, 1973.
10. Trachtenberg, M.C. and Ingle D. Thalamo-tectal projections in the frog. Brain Res. 79:419-430, 1974.
11. Scalia, F. The optic pathways of the frog: nuclear organization and connections. In Frog Neurobiology (Llinás, R. and Precht, W. eds.) Springer Verlag, 1976.
12. Ewert, J.P. and Hack, F.J. Movement sensitive neurons in the toad's retina. Exp. Brain Res. 16:41-59, 1972.
13. Ewert, J.P., Krug, H., Schnitz, G. Activity of retinal R3 ganglion cells in the toad. Bufo bufo (L.) in response to moving configurational stimuli: Influence of the movement direction. J. Comp. Physiol. 1979.
14. Ewert, J.P. Single unit response of the toad (Bufo americanus) caudal thalamus to visual objects. Z. Vergl. Physiol. 74: 81-102, 1971.
15. Grüsser, O.J., Grüsser-Cornehls, V. Neurophysiology of the anuran visual system. In Frog Neurobiology. (Llinás, R. and Precht, W. eds.). Springer Verlag, 1976, pp. 297-385.
16. Pellionisz, A. Modelling of neurons and neuronal networks. In The Neurosciences: Fourth Study Program (eds. Schmitt, F.O. & Worden, F.G.) MIT Press, Cambridge, pp. 525-546.
17. Ewert, J.P. and von Seelen, W. Neurobiologie und System-Theorie eines Visuellen Muster-Erkennungsmechanismus bei Kroten. Kybernetik. 14:167-183, 1974.
18. Szekely, G. and Lazar, G. Cellular and synaptic architecture of the optic tectum. In Frog Neurobiology (Llinas, R. and Precht, W. eds.). Springer Verlag, pp. 407-434, 1976.
19. Didday, R.L. A model of visuomotor mechanisms in the frog optic tectum. Mathematical Biosciences. 30 : 169-180, 1976.
20. Ewert, J.P. Neuroethology, an introduction to the neurophysiological fundamentals of behavior. Springer Verlag, 1980.
21. Roth, G. and Jordan, M. Response characteristics and stratification of tectal neurons in the toad Bufo Bufo (L.). Exp. Brain Res. 45 : 393-398, 1982.
22. Himstedt, W. and Roth, G. Neoronal responses in the tectum opticum of Salamandra to visual stimuli. J. Comp. Physiol. 135 : 251-257, 1980.
23. Luthardt, G. and Roth, G. The relationship between stimulus orientation and stimulus movement pattern in the prey catching behavior of Salamandra salamandra. Copeia (3), pp. 442-447, 1979.
24. Arbib, M.A. Segmentation, schemas and cooperative computation. In Studies in Mathematical Biology, Part I (S.A. Levin, ed.), MAA studies in mathematics, 15 : 118-155, 1978.
25. Ingle, D.J. Desinhibition of tectal neurons by pretectal lesions in the frog. Science, 180 : 422-424, 1973.

Appendix

We provide the mathematical definition of the two-dimensional model of the interactions between tectum and pretectum which complements the description of the one dimensional model of the interaction between tectum and pretectum given in Lara and Arbib.[3]

The specifications of threshold functions, membrane constants and weights is given in Tables 1, 2 and 3 respectively.

Glomerulus:

The equation defining the behavior of the glomerulus of the ith, jth unit column is given as follows:

$$\tau_{gl}\, \dot{gl}_{ij}(t) = -kl\, gl_{ij}(t) + U2_{ij}(t) + I_{ij}(t)$$

where τ_{gl} and kl are constants, U2 is the optic input from retinal ganglion cells type II, and I_{ij} are the recurrent inputs from LP and SP cells of the unit as well as those of neighboring columns, and are defined as:

$$I1(t) = w_{gl.sp}(SP_{i-1,\, j-1}(t) + SP_{i,\, j-1}(t) + SP_{ij}(t) + SP_{i+1,\, j-1}(t) + SP_{i+1,\, j}(t))$$

$$I2(t) = w_{gl.lp}(LP_{l-1,j-1}(t) + LP_{i-1,j}(t) + LP_{i-1,j+1}(t) + LP_{i,j-1}(t) + LP_{ij}(t) + LP_{i.j+1}(t))$$

$$I_{ij}(t) = I1(t) + I2(t) + LP_{i+1,j-1}(t) + LP_{i+1,j}(t) + LP_{i+1,j+1}(t)$$

where the values of w are given in Table 3.

Stellate Neurons: (SN)

The ith jth stellate neuron can be defined as follows:

$$A = LP_{i-1,j}(t) + LP_{i-1,j+1}(t) + LP_{ij}(t) + LP_{i,j+1}(t) + LP_{itl,j+1}(t)$$

$$\tau_{sn}\dot{sn}_{ij}(t) = -K2\ sn_{ij}(t) + w_{sn-lp}A$$

where τ_{sn} is the membrane constant of these neurons, K2 and $w_{sn.lp}$ are constants and can be seen in Tables 2 and 3 respectively.

Large pear shaped cells: (LP)

The behavior of the ith jth LP neuron can be defined as follows:

$$A1 = SN_{i-1,\, j-1}(t) + SN_{i,\, j-1}(t) + SN_{i\ j}(t) + SN_{i+1,\, j-1}(t) + SN_{i+1,\, j}(t)$$

$$A2 = SP_{i-1,\, j-1}(t) + SP_{i,\, j-1}(t) + SP_{i\ j}(t) + SP_{i+1,\, j-1}(t) + SP_{i+1,\, j}(t)$$

$$\tau_{lp}\dot{lp}_{ij}(t) = -lp_{ij}(t) - w_{lp.sn}A1 + w_{lp.th}TH_{ij}(t) + w_{lp.sp}A2 + gl_{ij}(t) + U2_{ij}(t)$$

where τ_{lp} is the membrane constant of these neurons; gl is the glomerulus input; U2 is the optic input from retinal ganglion type II cells; TH is the thalamic input; and w's are the weight factors shown in Table 3.

Small pear shaped cells: (SP)

The behavior of the ith jth SP neuron is defined as follows:

$$A3=gl_{i-1,j}(t)+gl_{i-1\ j+1}(t)+gl_{i,j+1}(t)+gl_{i+1,j+1}(t)$$

$$\tau_{sp}\dot{sp}_{ij}(t)=sp_{ij}(t)-w_{sp.sn}sn_{ij}+A3\ w_{sp.th}(IH_{ij}(t))+U2_{ij}(t)$$

where τ_{sp} is the membrane constant of these neurons; SN is the inhibitory effect of the stellate cells; TH is the inhibitory effect from thalamic neurons; and U2 is the optic input from fibres type II from the retina; w's are the weighting factors that can be seen in Table 3.

Pyramidal Neurons: (PY)

The ith jth PY cell is defined as follows:

$$A4=LP_{i-1,\ j}(t)+LP_{i-1,\ j+1}(t)+LP_{ij}(t)+LP_{i,j+1}(t)+LP_{i+1,j+1}(t)$$

$$A5=w_{py.u2}U2_{ij}(t)+w_{py.u3}U3_{ij}(t)+w_{py.u4}U4_{ij}(t)$$

$$\tau_{py}\dot{py}_{ij}(t)=-py_{ij}(t)+w_{py.sp}.SP_{ij}(t)+w_{py.lp}A4-w_{py.th}TH_{ij}(t)+A5$$

where τ_{py} is the membrane constant of these neurons; SP is the excitatory effect of small pear cells; TH is the inhibitory effect of both pretectal neurons; and U2, U3 and U4 is the optic input from retinal ganglion cells type II, III and IV respectively.

The w's are the different weight factors shown in Table 3.

Table 1

Threshold Functions

LP = f (lp - 1.0)
SP = f (sp - 2.0)
SN = h (sn - 0.2)
PY = h (py - 5.559)
TH = g (th - 3.7)

Table 2

Membrane Constants

τ_{gl} = 0.35, k1 = 0.15
τ_{sn} = 0.65, k2 = 0.4
τ_{lp} = 0.3
τ_{sp} = 0.9
τ_{py} = 0.12
τ_{th} = 1, k3 = 7

Table 3

Weights

$w_{gl.lp}$	= 1.0	LP to GL
$w_{gl.sp}$	= 0.1	SP to GL
$w_{lp.sp}$	= 0.8	SP to LP
$w_{lp.sn}$	= 8.0	SN to LP
$w_{lp.th,s}$	= 0.1, 0.4	TH to LP
$w_{lp.s}$	= 0.2	S to LP
$w_{sp.sn}$	= 20.0	SN to SP
$w_{sp.th,s}$	= .1, 0.4	TH to SP
$w_{sn.lp}$	= 2.1	LP to SN
$w_{sp.s}$	= 0.2	S to SP
$w_{py.lp}$	= 0.8	LP to PY
$w_{py.sp}$	= 1.0	SP to PY
$w_{py.th,s}$	= 0.9	TH to PY
$w_{py.u3}$	= 0.3	U3 to PY
$w_{py.u4}$	= 6.0	U4 to PY
$w_{py.u2}$	= 4.5	U2 to PY
$w_{th.u3}$	= 0.3	U3 to TH
$w_{th.u4}$	= 5.0	U4 to TH
$w_{py.s}$	= 0.4	S to PY

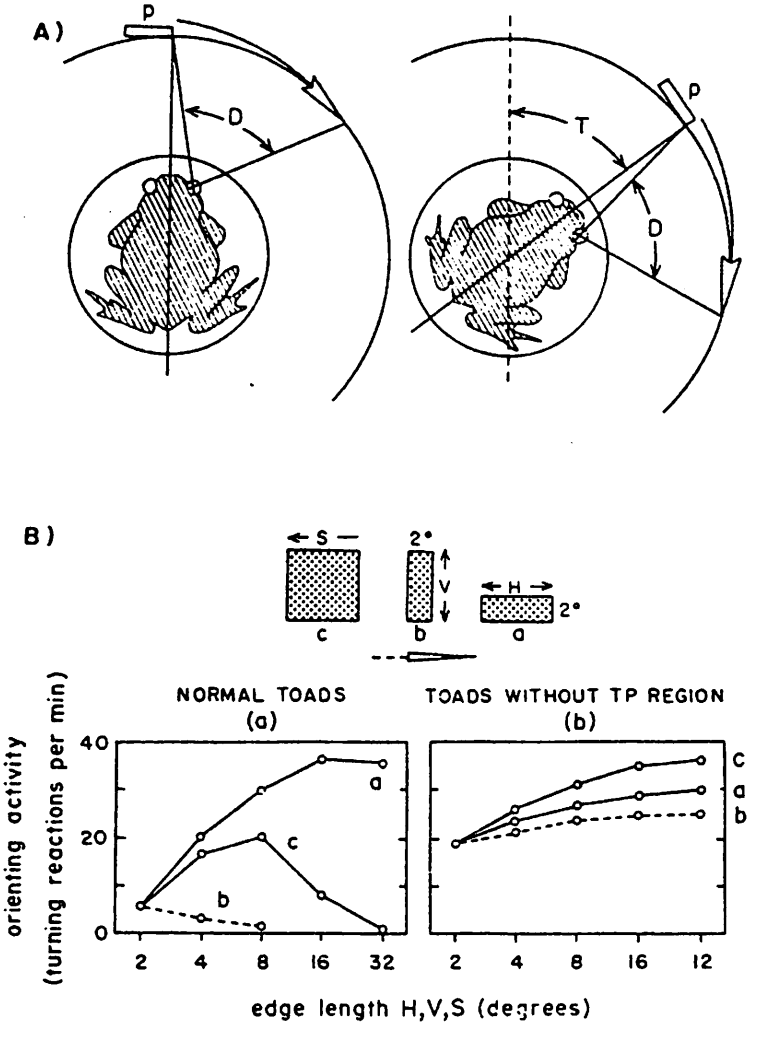

Fig. 1. Prey orienting behavior to different configurations of the stimulus. A) Turning reaction to the stimulus presentation. B) Orienting activity to three configuration (a,b,c): facilitation to stimulus a, inhibition to stimulus b, and an initial facilitation and then an inhibition to stimulus c. When pretectum ablation occurs this discrimination disappears. (From Ewert, 1976)

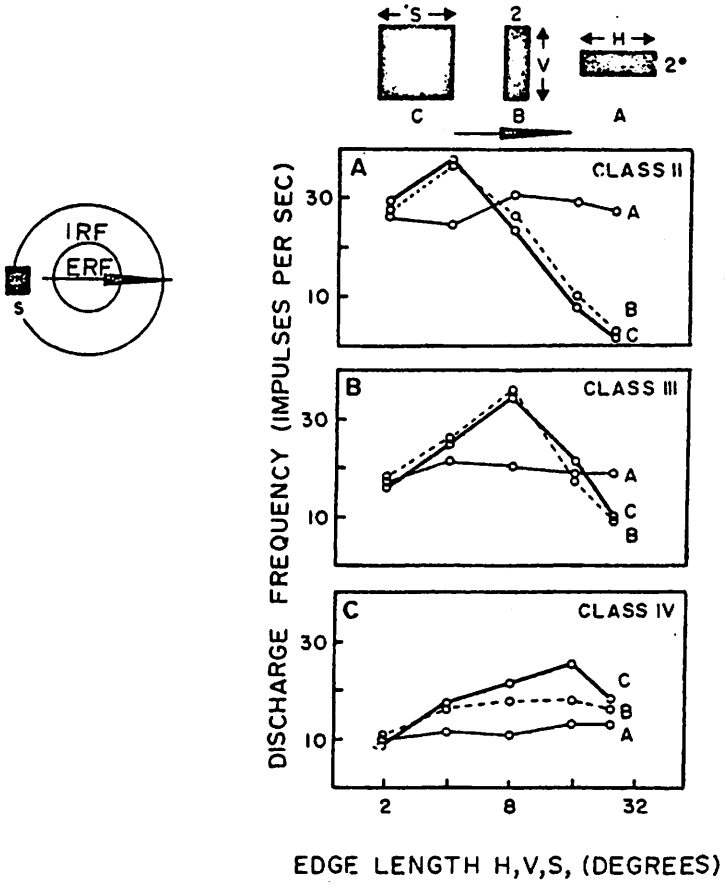

Fig. 2. Retinal ganglion cell response (II, III, IV) to different configurations of the stimulus (a,b,c). For stimulus type a the response of the three ganglion neurons is almost invariant for the different sizes of the stimulus. For stimulus type b and c, ganglion type II and III increase their rate of response up to their respective receptive field and then the response is reduced. For type IV ganglion cells the rate of response is proportional to the size of the stimulus. (From Ewert, 1976)

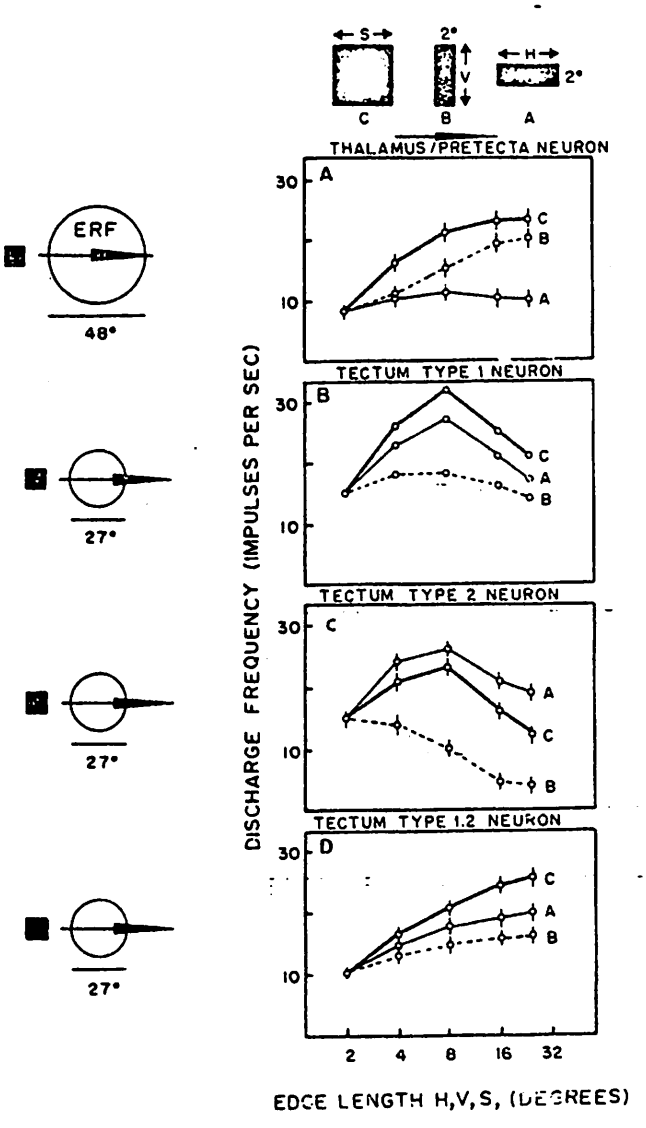

Fig. 3. Tectal and pretectal cell activity to different configurations of the stimulus (a,b,c). A) Response of a pretectal neuron which is mostly sensitive to stimulus b and c. B and C show the response of two tectal cells to the three types of stimuli. Neuron C response is mostly sensitive to stimuli type a and c and its response is greatly reduced for stimulus type b. This response is similar to the observed behavioral response. D shows the response of both tectal cells (B and C) without pretectum and how the discriminative abilities of these cells are lost. (From Ewert, 1976)

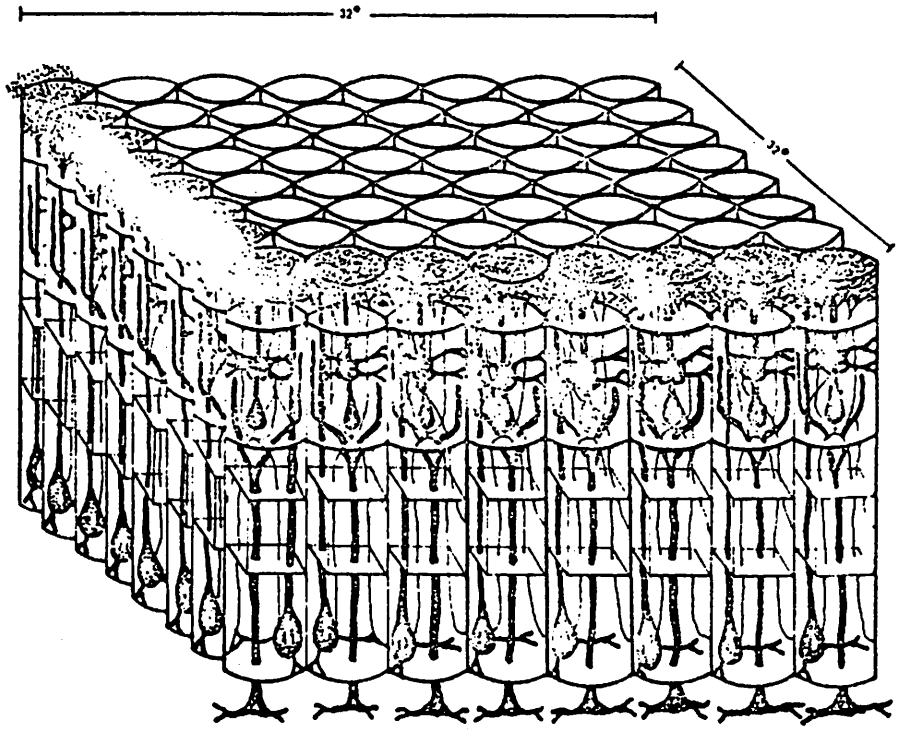

Fig. 4. Representation of the two-dimensional model of the tectum constituted of 64 columns.

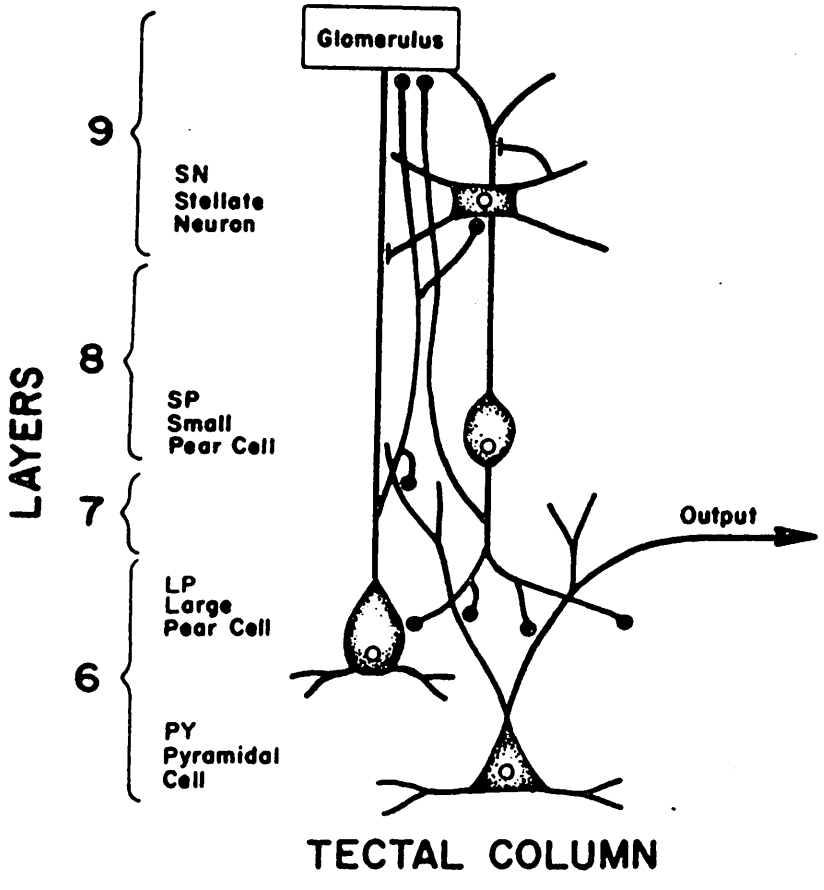

Fig. 5. Interconnections among the cells of a column. The PY cells is activated by LP and SP cells, and it also receives afferents from retinal ganglion cells type R2, R3 and R4. The SN neuron is excited by the LP cell. The SP cell receives excitatory afferents from the ganglion cells type R2 and from the glomerulus, and it is inhibited by the SN neuron. The LP cell is excited by retinal ganglion cells R2 and by both the SP cell and the glomerulus. The Glomerulus receives afferents from retinal ganglion cells type R2 and is excited by recurrent axons from LP and SP cells (from Lara and Arbib, 1982)

see Lara et al.[1-3]

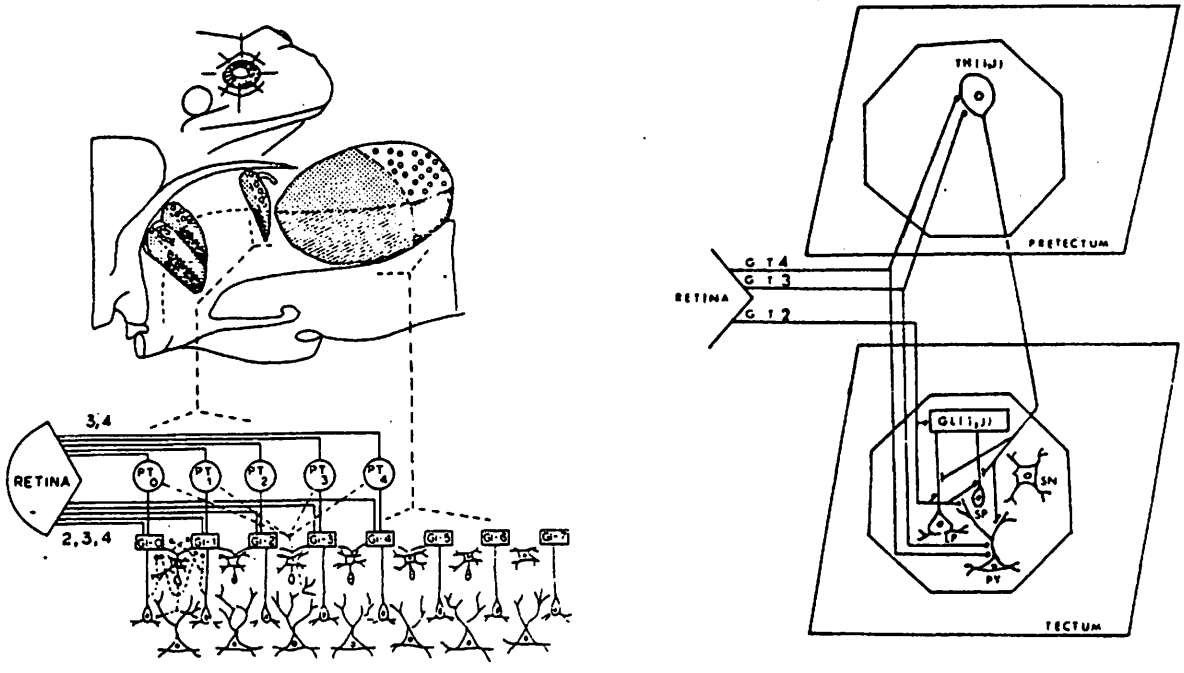

Fig. 6. Interactions among retina, tectum and pretectum. The retina sends fibres in a retinotopical way to both tectum (2, 3, and 4) and pretectum, TH3 (3, 4). The tectum PY cell excites all sameness cells (shown as PT for simplicity) except the one of its own column. Both pretectal neurons inhibit LP, SP and PY of the tectal column (right section).

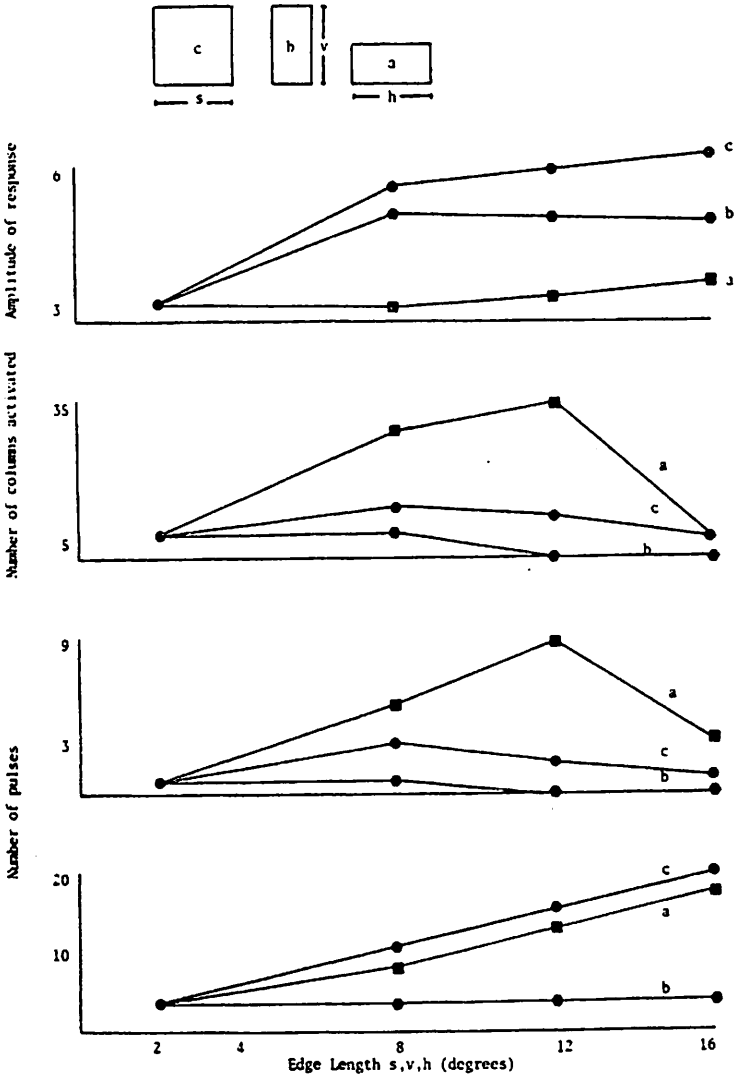

Fig. 7. Computer simulation of the response of pretectal and tectal cells to the different configurations of the stimulus (a,b,c). A) Pretectal cell response: it is mostly sensitive to stimulus type b and c. B) Response of the 64 PY cells to the three types of stimuli (a,b,c): the tectum is mostly sensitive to stimulus type a and it is inhibited by stimulus type b. C) PY response to the three configurations of the stimulus type a. D) PY response when pretectum ablation occurs: PY cells are mostly sensitive to stimulus type c, then to those of type a.

8c).

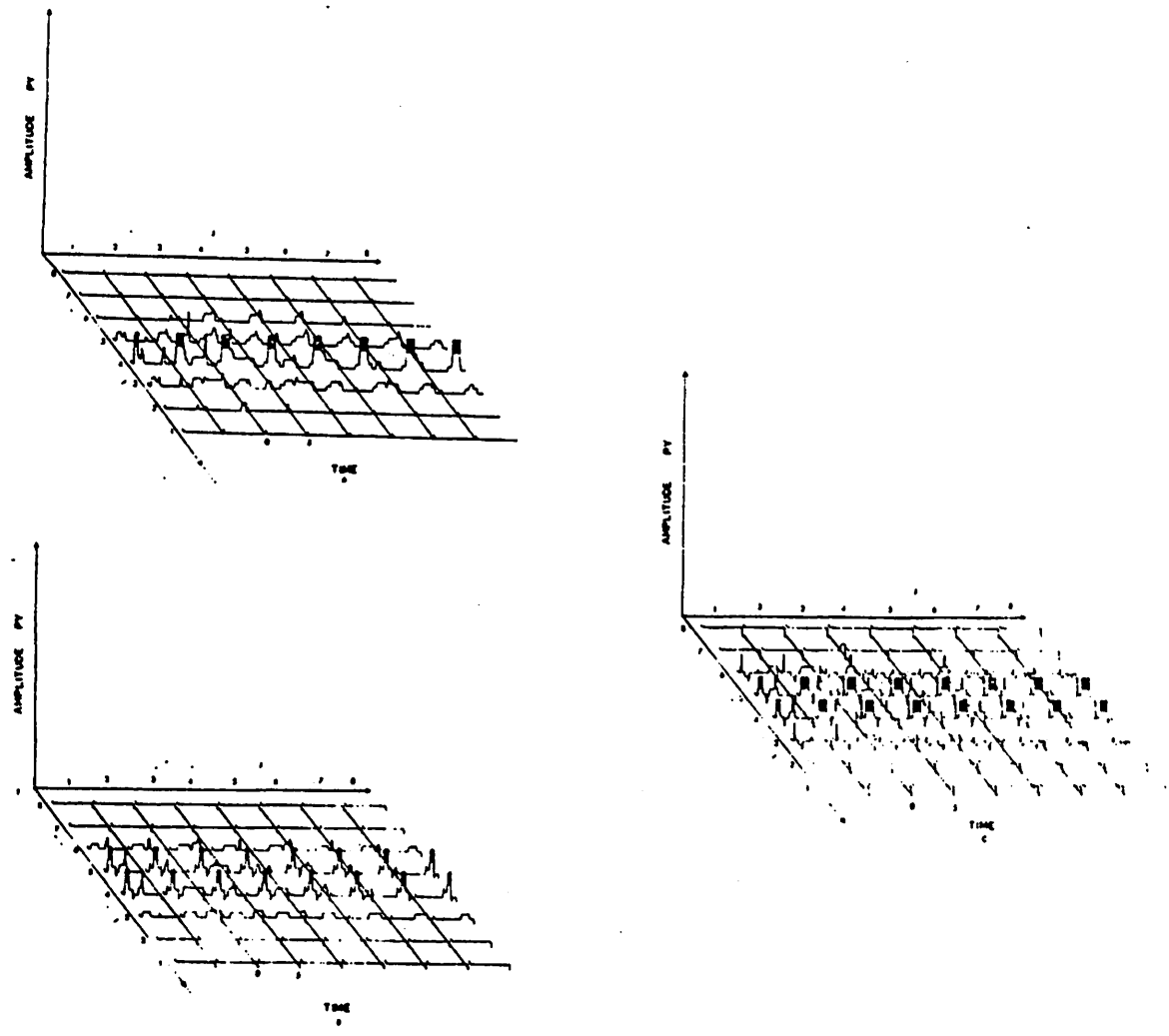

Fig. 8. Computer simulation of the PY response of the 64 columns of the tectum to the different configurations of the stimulus: (A = type a, B = type b, C = type C). The horizontal axis shows the temporal response of each of the 64 columns, while the vertical axis shows the PY cell response. Dark parts of the trace show the action potentials of PY cells. The response of the PY cells is stronger for stimulus type c, then to type a, and finally to type b.

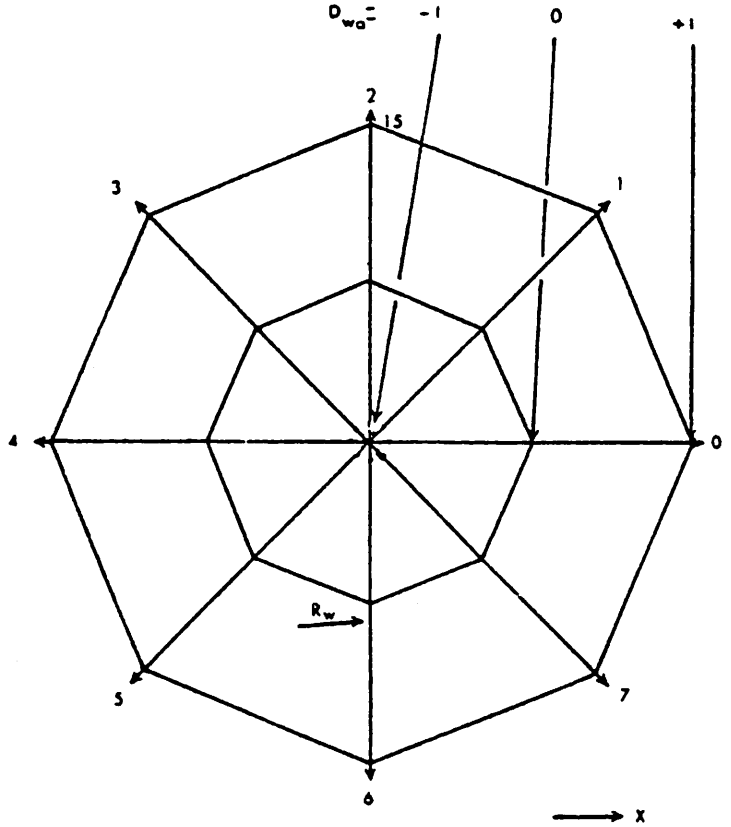

W – WORM

a – ANTIWORM

$$D_{wa} = \frac{R_w - R_a}{R_w + R_a}$$

Fig. 9. Computer simulation of PY cell response of the two-dimensional model of retina-tectum-pretectum for prey-predator recognition in eight different directions. The graph shows that the PY response is direction invariant. The formula shows how it has been quantified for the invariance of prey-predator recognition: R_w is the number of responses when a worm-like stimulus is presented and R_a is the response when an antiworm-like stimulus is shown. The outer circle is the value of D_{wa} of the PY cell response.

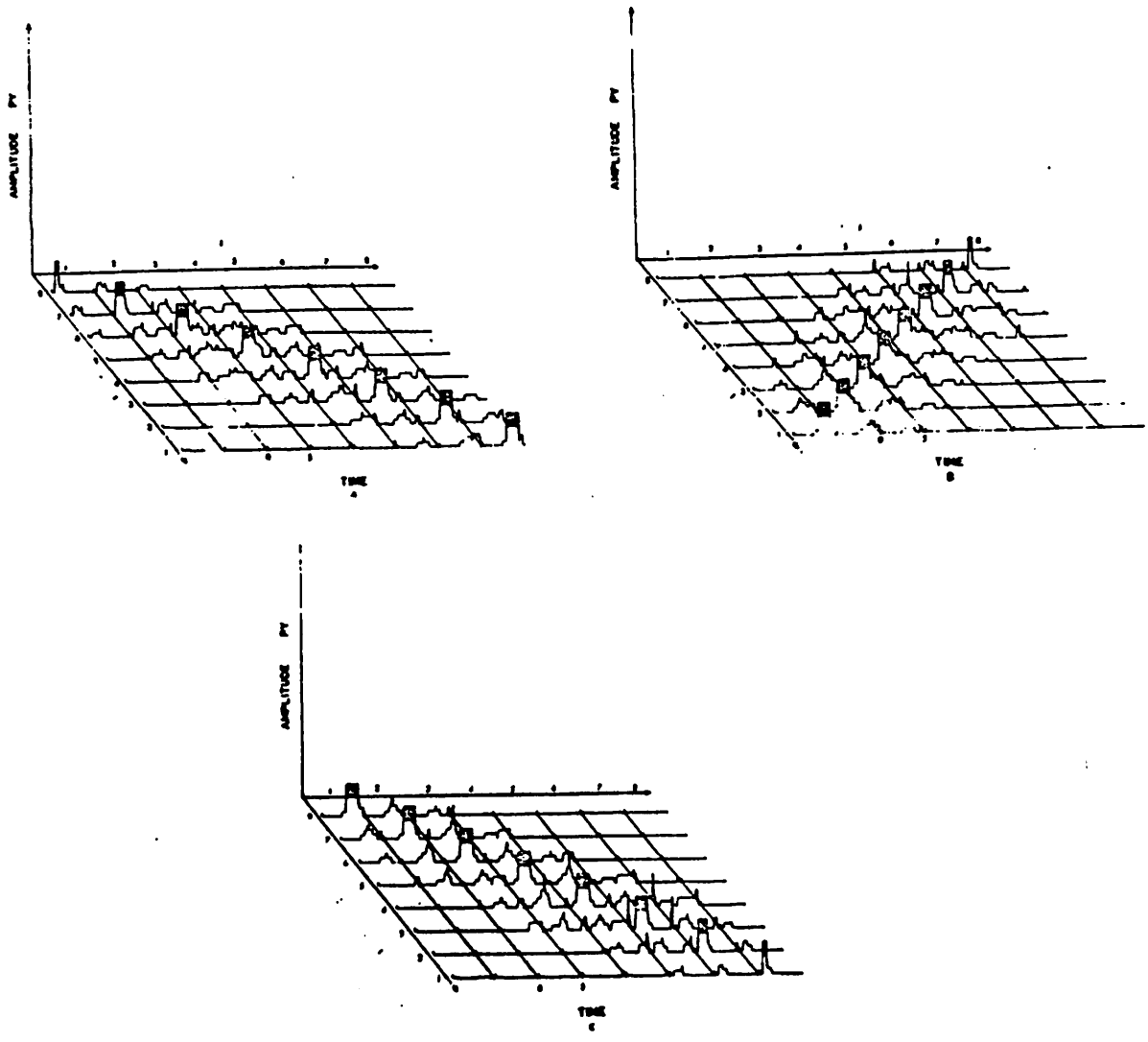

Fig. 10. Computer simulation of the 64 columns for prey-like stimulus in three different directions. The response is direction invariant.

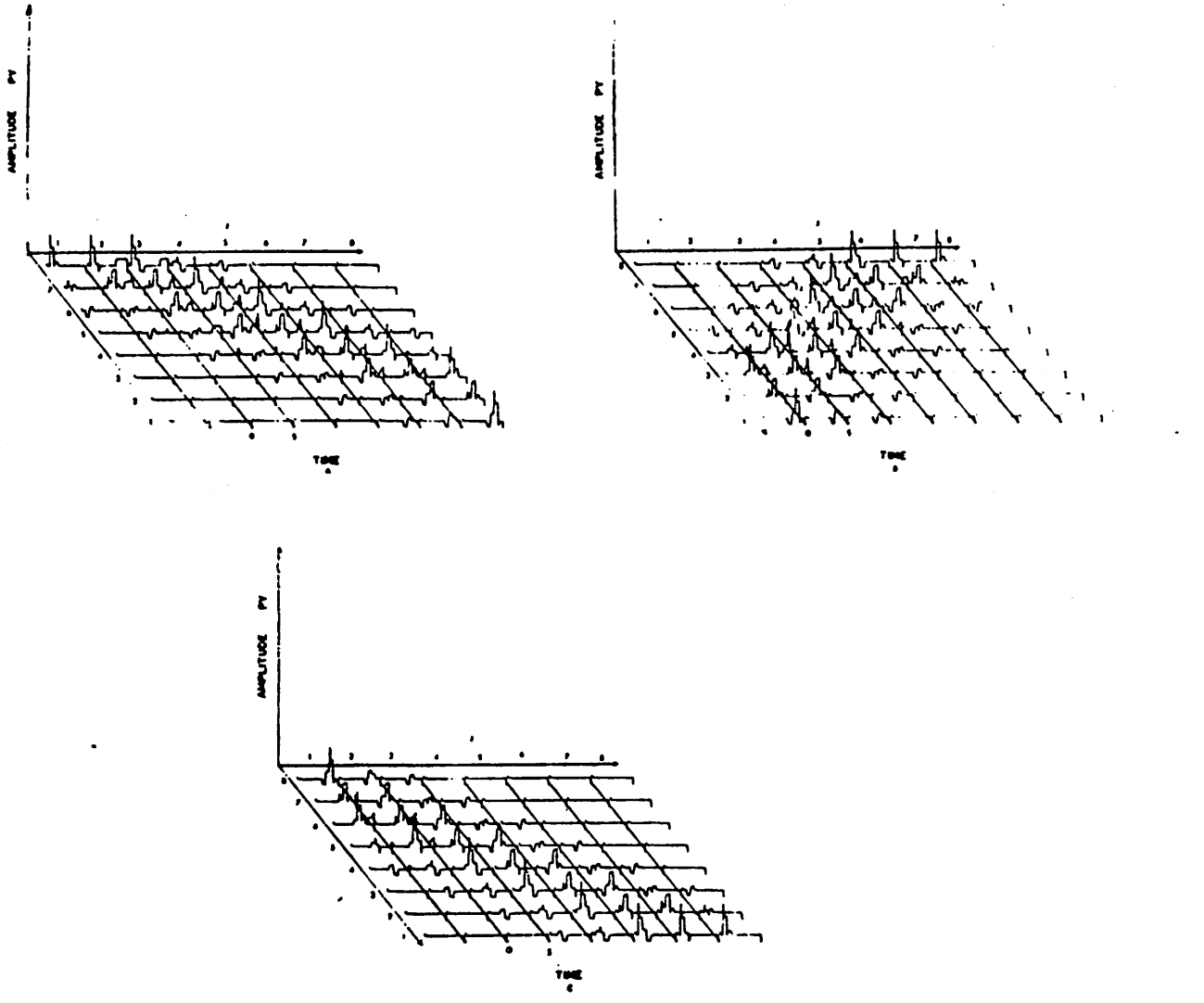

Fig. 11. Computer simulation of the 64 columns for predator-like stimulus in three different directions showing that it is direction invariant.

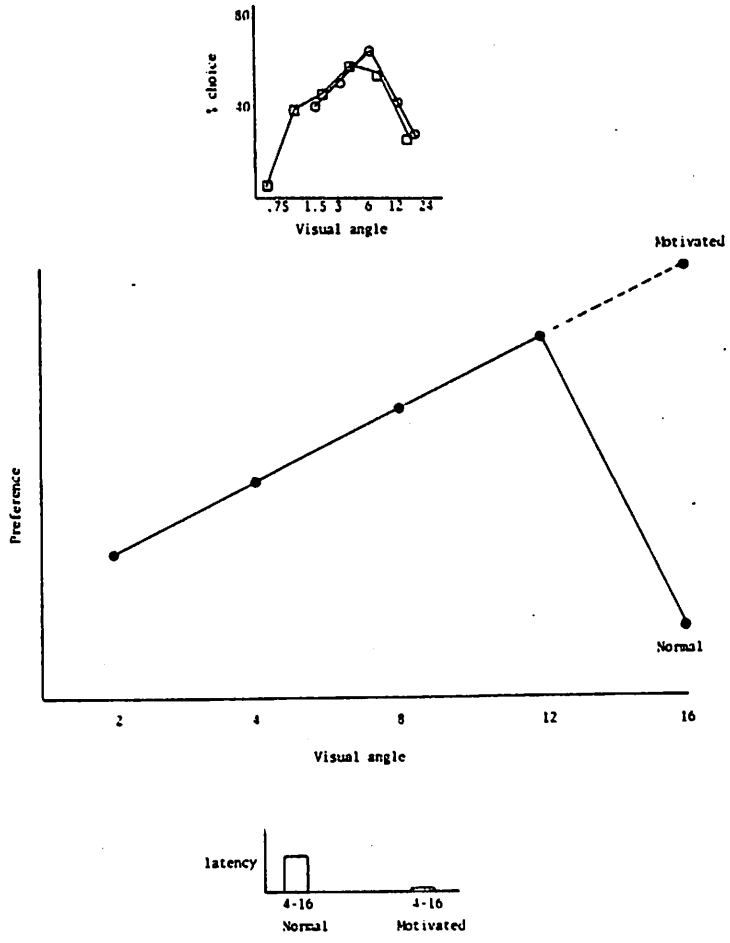

Fig. 12. Computer simulation of the response of the two-dimensional model of retina-tectum-pretectum to two stimuli of different sizes. The graph shows the hierarchy of preference in a normal and a motivated animal. In a normal animal the animal prefers the 4° high stimulus to the 16° high stimulus, while this preference is inverted in the motivated animal. In the lower part of the figure it is shown that the latency of response is also reduced in the motivated animal. See inset for comparison with experimental results. (From Ingle, 1977)

Chapter 3: Motor Control

Paul Grobstein, Christopher Comer, and Sandra K. Kostyk:
FROG PREY-CAPTURE BEHAVIOR: BETWEEN SENSORY MAPS AND DIRECTED MOTOR OUTPUT

H.W. Borchers: BEHAVIOR-CORRELATED NEURONS IN FREELY MOVING TOADS

D.P.M. Northmore: TECTAL MAPS AND VISUAL ORIENTING

John I. Simpson: THE COORDINATE SYSTEM OF VISUAL CLIMBING FIBERS TO THE CEREBELLAR FLOCULLUS

C.C. Boylls: CLIMBING FIBERS AND THE SPATIAL REFERENCE FRAME FOR MOTOR COORDINATION

Neil M. Montgomery and Katherine V. Fite: VISUOMOTOR CONNECTIONS IN ANURAN MESENCEPHALON

Paul Grobstein, Christopher Comer, and Sandra K. Kostyk:

FROG PREY-CAPTURE BEHAVIOR: BETWEEN SENSORY MAPS AND DIRECTED MOTOR OUTPUT

In frog prey capture behavior an appropriate sensory stimulus at a given location in space triggers a complex movement directed toward the stimulus. We are interested in how the frog brain is organized so as to yield such a spatial correspondence between a stimulus and the resulting movement. Initial stages of the neuronal circuitry underlying prey capture appear to involve topographic sensory representations in the midbrain. The prey capture outputs are triggered or ballistic, suggesting that they are based on pattern generating circuitry at some unknown location in the brain. Given these considerations, one approach to the problem of the spatial correspondence between stimulus and movement is to ask how topographic sensory maps are linked to pattern generating circuitry. In this paper we will discuss several experiments directed at exploring this linkage. We will focus particularly on how our ideas about the organization which brings about an appropriate correspondence between input and output have evolved during the course of these studies.

TACTUALLY ELICITED PREY CAPTURE BEHAVIOR: SEPARATION OF PATTERN-GENERATING CIRCUITRY AND TOPOGRAPHIC SENSORY MAPS

The frog, Rana pipiens, orients not only to visual stimuli but to tactile stimuli as well. Two aspects of these behaviors seem to us to have particular importance for understanding the neural basis of prey capture (Comer and Grobstein, 1981a). First, the movements are ballistic; once triggered, they proceed to completion independently of feedback from the target. Second, the outputs triggered by tactile stimuli appear to be the same as those triggered by near visual stimuli. These observations, plus the known dependence of visually elicited prey capture on the integrity of the optic tectum (cf. Sperry, 1944; Ingle, 1973) and the evidence for tactile inputs into the tectum (Fite, 1969; Grüsser and Grüsser-Cornehls, 1973), suggested the simple model of the

organization of the neuronal circuitry underlying prey capture which is shown in Figure 1. Besides the existence of superimposed topographic visual and somatosensory representations in the tectum (suggested by a variety of studies in mammals), the important aspect of the model is that each local tectal region receives sensory input corresponding to a particular stimulus direction and, in addition, also contains pattern generating circuitry which creates motor patterns appropriate for movements in that direction. The problem of the spatial correspondence between input and output was imagined to be solved by the existence of superimposed sensory and motor maps. The concept of multiple pattern generators each accessed appropriately by sensory input has precedent in studies on escape behavior in the crayfish (cf. Krasne and Wine, 1977). The medial and lateral giant fibers together with their respective sets of connections to motor neurons can be regarded as pattern generators for forwardly and backwardly directed escape movements respectively. Each receives sensory input from receptors located at the appropriate end of the animal.

The model of Figure 1 was tested by removing the optic tectum and asking whether atectal frogs continue to orient to tactile stimuli. The finding that they do suggested that the pattern generating circuitry for prey capture movements is not located in the tectum (Comer and Grobstein, 1978, 1981b). Electrophysiological recordings revealed the existence of tactile input to a second midbrain area, the lateral torus semicircularus (Comer and Grobstein, 1981c). Lesions in this area can abolish tactually elicited prey capture behavior while sparing prey capture movements triggered by visual stimuli (Comer and Grobstein, 1981b). These findings led to the revised model shown in Figure 2. In this model the pattern generating circuitry is located neither in the tectum nor in the lateral torus but rather at an unknown point of convergence of the outputs of the two structures. The spatial correspondence problem is solved in this

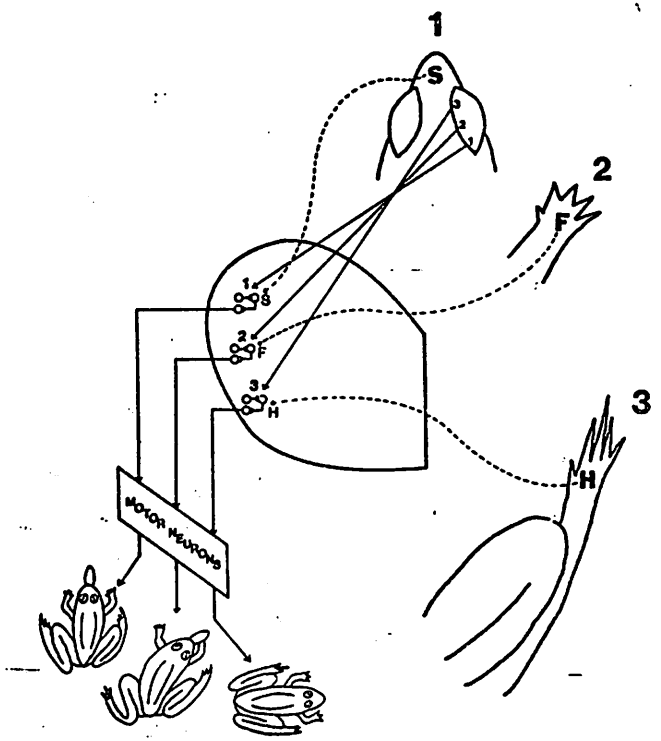

Figure 1. An early model of the neuronal organization underlying prey capture behavior in the frog. Illustrated are afferent and efferent pathways of the left tectal lobe. The three clusters of neurons are intended to suggest three sets of pattern generating circuitry which respectively cause activity in motor neurons yielding forward movement and two angles of rightward movement as illustrated in the sketches of frogs at the lower left. Each set of circuitry receives retinal input corresponding to a different stimulus direction (numbers) and also receives cutaneous input from a part of the body surface (S, snout; F, forelimb; H, hindlimb) where stimulation causes the same movement as that brought about by the retinal input.

model by a topographic pattern of connections between the two sensory maps and the elements of the output generating circuitry.

In hindsight, it is clear that several aspects of our observations in the course of these studies were not entirely consistent with such a topographic linkage. We attempted to produce tactile scotomas with small electrolytic lesions in the lateral torus but never observed these despite histological evidence of local damage (Comer and Grobstein, unpublished observations). The small lesions failed to abolish outputs in response to stimulation at any of the points on the body surface which we routinely tested; they did however sometimes alter the character of the outputs, producing "undershooting". We have observed a somewhat similar phenomenon in animals with partial tectal lesions. Such animals, as is well known, do exhibit a scotoma in the visual field. Frequently however they also exhibit a surrounding area where stimuli elicit orienting movements but the elicited movements are inaccurate, either overshooting or undershooting the target (Kostyk, Comer, and Grobstein, unpublished observations). Apparent alterations in the linkage between the location of a sensory stimulus and the direction of the resulting movement are subject to a variety of interpretations (cf. Ingle, 1970 on the effects of knife cuts in the tectum) and we did not systematically study them. They do however suggest the possibility that the direction of the motor output associated with stimulation of a given region in a sensory map is not so reliable and stereotyped as would be expected from a topographic linkage of the kind shown in Figure 2. A further anomaly was the finding that unilateral torus lesions not only abolished tactually elicited prey capture behavior in response to contralateral body stimulation, as would be expected from the fact that the opposite body surface is mapped in this region, but also caused inaccurate responses to ipsilateral body stimulation (Comer and Grobstein, 1981b). This observation is also subject to a variety of interpretations

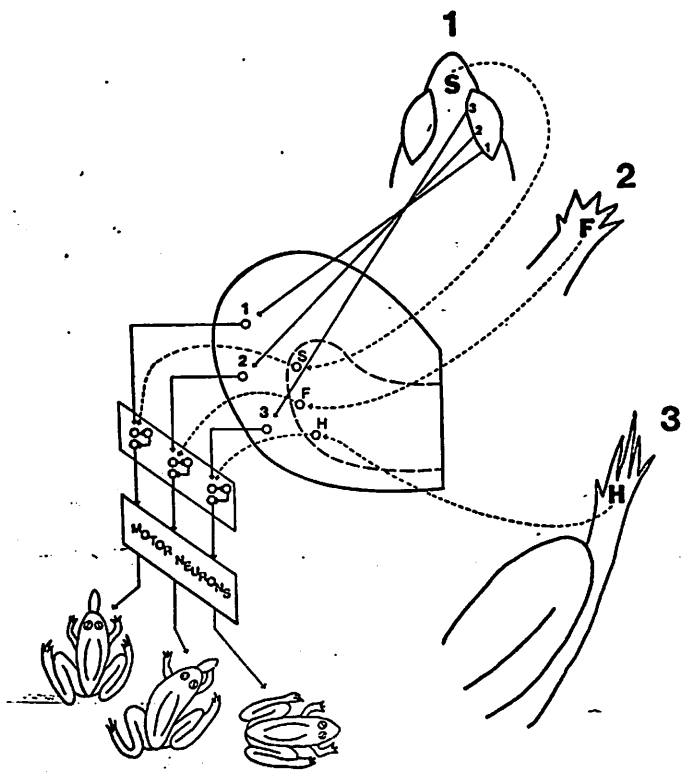

Figure 2. A modification of the model of Figure 1 based on the behavior of atectal frogs and on studies of the processing of cutaneous information in the midbrain. Cutaneous input is mapped not in the tectum but in the lateral part of the underlying torus semicircularus. The pattern generating circuitry is located not in the tectum but rather in an unknown structure which receives convergent topographic projections from the tectum and the lateral torus semicircularus.

but again suggests that the output resulting from activation of a given region in a sensory map is not simply related to the afferent input to this region. We will return to this issue below.

VISUALLY ELICITED PREY CAPTURE BEHAVIOR: SUBDIVISIONS OF PATTERN-GENERATING CIRCUITRY

The visual field of each eye in Rana pipiens extends to about 45° across the mid-sagittal plane in front of the frog and is mapped in its entirety on the opposite tectal lobe (Fite, 1973; Scalia and Fite, 1974; Grobstein et al., 1980). Hence, any location in the front 90° of visual space is represented twice, once in each tectal lobe. This redundant mapping raises the question of whether each tectal lobe is independently linked to the pattern generating circuitry responsible for prey capture movements towards rostrally located visual stimuli. Observations on frogs with unilateral tectal lobe ablation indicate that this is the case (Ingle, 1973; Kostyk and Grobstein, 1980, 1982). Such animals continue to exhibit typical prey capture movements toward stimuli located anywhere within the visual field of the eye ipsilateral to the lesion, including the 45° of visual field across the mid-sagittal plane. They fail to respond to stimuli at locations which are solely within the visual field of the eye contralateral to the lesion, as would be expected from the generalization that an intact sensory representation in tectum is necessary for visually elicited prey capture behavior.

Some years ago, Roger Sperry (1948) reported that in the newt a complete transverse hemisection of the neuraxis at a level between the optic tectum and the cerebellum disrupted prey capture movements towards visual stimuli located ipsilateral to the lesion, a result which he interpreted as suggesting that the efferent fibers from each tectal lobe which are involved in prey capture behavior cross shortly after leaving the tectum. We have repeated Sperry's experiment

in the frog with specific attention to the question of whether, as in the case of unilateral tectal lesions, normal orienting throughout the rostral 90° of visual field is spared (Kostyk and Grobstein, 1980, 1982). We have found that it is not. Hemisected animals fail to turn toward stimuli at any location to one side of the mid-sagittal plane, a result which indicates that the lesion in fact affects the outputs from both tectal lobes. The behavior of hemisected frogs also shows a significant dissociation of one component- horizontal turning - from the other components of the complex movements involved in prey capture (see Ingle, 1982, for a similar observation in frogs with midline lesions in the midbrain tegmentum). Our hemisected frogs exhibit well-directed prey capture movements for stimuli at any location to the side of the mid-sagittal plane contralateral to the lesion. For stimuli at any location on the side of the mid-sagittal plane ipsilateral to the lesion the animals fail to turn. They do however respond to such stimuli. The response, regardless of stimulus positon on the horizontal, is always a forwardly directed movement. Although the response does not vary with stimulus angle on the horizontal, it does vary with stimulus elevation and distance. Laterally placed stimuli near the animal elicit a forwardly directed snap. Distant laterally placed stimuli elicit forward movement without a snap. For elevated stimuli the forwardly directed movements include an upward component.

These observations led to the model illustrated in Figure 3, in which the pattern generating circuitry involved in prey capture behavior is regarded as consisting of several distinct sets of circuitry. Since a unilateral lesion abolishes turning toward the side of the lesion while leaving turning in the opposite direction unaffected, the model treats the turning-generating circuitry itself as being subdivided into two sets, one for leftward turns located on the left side of the brain and one for rightward turns located on the right. Such a lateralization of turn-generating circuitry may be characteristic of many animals and might help

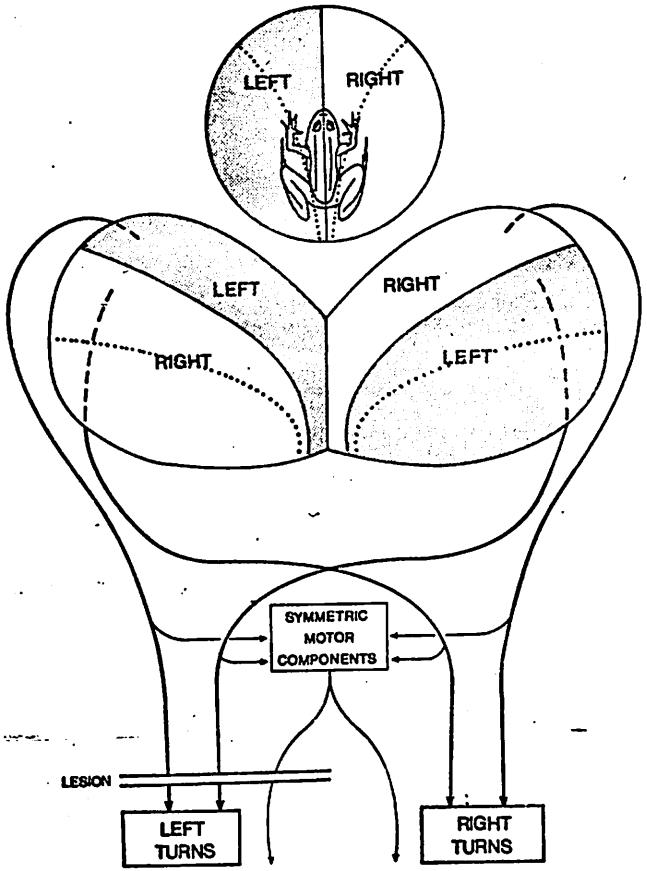

Figure 3. See legend next page

Figure 3. A model of the relation between the two tectal lobes and the pattern generating circuitry based on studies of visually elicited prey capture behavior in hemisected frogs. The figure illustrates the visual fields of the two eyes (above) and their mapping on the two lobes of the optic tectum (middle). Dotted lines define the edges of the binocular visual field and of its tectal representations. Since the visual field of each eye is represented in its entirety on the opposite tectal lobe, loci within binocular visual field are represented twice, once in each tectal lobe. Shading shows the parts of each tectal lobe which represent the left visual hemifield. The lower part of the figure illustrates the three sets of pattern generating circuitry which the studies suggest are involved in prey capture. These include sets of circuitry for left and for right turns, which are located respectively on the left and the right sides of the brain, as well as a third set of circuitry which generates the components of prey capture outputs which involve bilaterally symmetrical muscle activation. Lines show hypothetical pathways linking tectum with the several sets of pattern generating circuitry. The behavior of hemisected frogs can be understood in terms of an interruption of some of these pathways by a unilateral lesion as diagrammed to the left.

to explain some puzzling apparent deficits in orienting behavior consequent on abnormal early visual experience in cats (Gordon et al., 1979; see Kostyk and Grobstein, 1982). Since stimuli continue to elicit some components of prey capture movements even when turning is absent, the model includes a third set of pattern generating circuitry which generates components of prey capture outputs which are related to stimulus elevation and distance. Since such components involve largely bilaterally symmetric muscle activation we characterize this set of circuitry, which may itself ultimately be shown to be subdivided, as responsible for "symmetric motor components". The general notion of lateralized circuitry for horizontal movement components and distinct circuitry for components of movement occuring in other planes is not incompatible with the literature on the neuronal organization underlying saccade generation in primates (cf. Raphan and Cohen, 1978).

The model in Figure 3 also illustrates hypothetical pathways linking the two tectal lobes with the several sets of pattern-generating circuitry. Since activation of symmetric motor components by stimuli at any location in the visual field survives the unilateral lesion, the model shows bilateral paths from both tectal lobes to the "symmetric" pattern generator. Since each tectal lobe is capable of triggering turns both to the right and to the left, the model also shows a bilateral projection to the turn-generating circuitry. This is illustrated as a partial decussation, with those tectal regions representing visual field on the contralateral side of the mid-sagittal plane linked to turn-generating circuitry by a crossed pathway and those representing ipsilateral visual field linked by an uncrossed pathway. The suggestion that each tectal lobe may be able to trigger prey capture turns by an uncrossed pathway has not to our knowledge previously been made.

THE LINKAGE PROBLEM

In developing the model shown in Figure 3 we still had in mind the notion that the spatial correspondence between stimulus and movement seen in prey capture behavior is attributable to a topographic link between sensory maps and pattern generating circuitry, that is that each local region in a map is differently connected to pattern generating circuitry such that each causes a particular turn appropriate for the input to that region. This underlying assumption is explicitly represented on a large scale in Figure 3 in that we show the uncrossed path to the turn generating circuitry coming from rostro-medial tectum and the crossed path coming from caudo-lateral tectum. On a finer scale, not illustrated in the figure, we assumed that each output path consisted of a number of output fibers, each coming from a local tectal region and differently engaging the turn generating circuitry so as to cause a particular direction of turn. This might be because each fiber engages a different pattern-generating circuit in a fashion similar to the situation illustrated in Figures 1 and 2. Alternatively, and perhaps more probably, it might be because each output fiber engages a single pattern generating circuit in a slightly different way so as to cause it to produce different and appropriate patterns. The essence of our assumption of a fine scale topographic linkage was that activity in a single output fiber is produced by a stimulus at a given location and causes a motor output in that direction.

In experiments aimed at testing various aspects of the model of Figure 3 we have made observations which have caused us to question the assumption of a topographic linkage both on the large and on the fine scale. Hemisections of the neuraxis, in addition to cutting descending fibers from the midbrain, also destroy grey matter in the area between the tectum and the cerebellum. In an effort to eliminate the possibility that it is damage to structures in the grey matter rather than to descending tracts which is responsible for the behavior of

hemisected frogs we have explored the effects of smaller lesions (Kostyk and Grobstein, unpublished observations). We have found that large lesions in the region between the tectum and the cerebellum which spare the ventral white tracts (crossed-hatched area in Figure 4) have little or no effect on prey capture behavior while small lesions essentially restricted to the ventral white tracts (stippled area in Figure 4) produce the same behavioral results as a complete hemisection. The results are consistent with the existence of a population of fibers in the ventral white tracts which link the tectal lobes with turn-generating circuitry. More importantly however, in the present context, we have found that partial lesions in this region do not yield the results expected if this population consists of a number of fibers each causing a turn in a different direction. Were this the case, one would expect damage to a subset of the fibers to yield a syndrome of motor scotomas: normal turning toward stimuli in some areas of the visual field and an absence of turns for stimuli in others. What is in fact observed is that such frogs turn to stimuli at all locations but do so inaccurately, characteristically undershooting for stimuli located at any position throughout the affected hemifield. The partial lesions apparently do not destroy the linkage between any tectal region and the turn-generating circuitry but rather disturb the linkage for all tectal regions, causing each to activate turns different from those seen in normal testing.

A second aspect of the model in Figure 3 which we have been testing is the existence of an uncrossed path which links each tectal lobe with the ipsilateral set of turn-generating circuitry. Again we have obtained results which are consistent with the general form of the model but which raise questions about whether the linkage betwen the tectum and the turn-generating circuitry is topographic (Kostyk and Grobstein, unpublished observations). Animals with a combination of a unilateral tectal lobe removal and a hemisection on the same

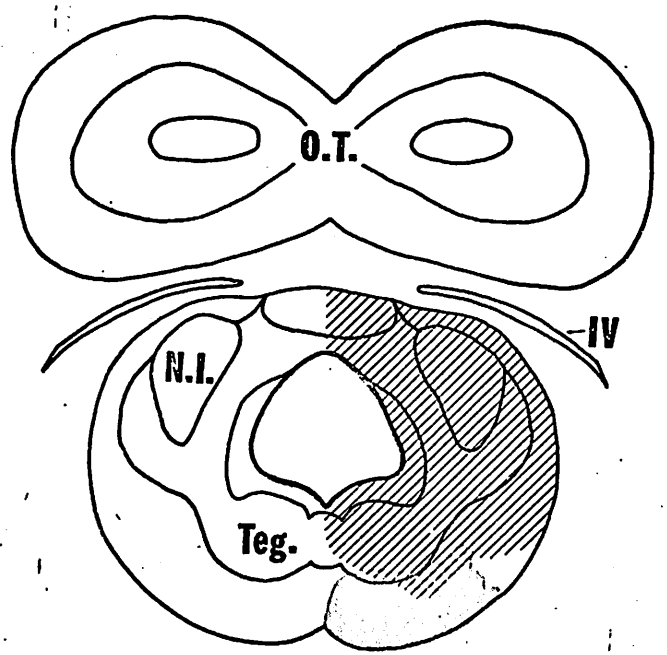

Figure 4. Schematic cross section of the frog brain at a level between the optic tectum and the cerebellum. A complete unilateral transverse hemisection at this level yields the behavioral results which led to the model of Figure 3. The same results are obtained with lesions essentially restricted to the ventral white tracts (stippling). We observed little or no change in prey capture behavior following large lesions which spare these tracts (cross-hatching).

side are left with only the hypothesized uncrossed pathway on one side of the brain. The model predicts that following such lesions done, for example, on the left, animals should continue to respond to stimuli at all locations represented in the right tectal lobe with either a turn or a forwardly directed movement; they should not turn to the left but should retain the ability to turn to the right. Initial observations on such animals confirm this general prediction; in particular, the animals do respond to stimuli with rightward but not with leftward prey capture movements. The anomalous finding is that the animals exhibit rightward movements not for stimuli presented to the right but rather for stimuli presented to the left; the farther around the animal to the left the stimulus is presented, the greater is the amplitude of the rightward turn. The implication of these results is that the more caudal parts of the right tectal lobe, which our model predicts should be linked only to the left turn-generating circuitry (see Figure 3), are connected to the right turn-generating circuitry as well. The anomalous behavior of multiply lesioned animals is not in conflict with the general suggestion, based on the behavior of hemisected animals, that there is an uncrossed pathway adequate to trigger prey capture turns; the observations conflict only with a model like that in Figure 3 which includes the additional assumption that the uncrossed pathway derives specifically and only from rostro-medial tectum. Again, the evidence suggests that the linkage between tectum and the pattern generating circuitry is not of a kind in which a given tectal region can activate only a particular turn but rather one in which a given tectal region activates different turns under different circumstances.

THE LINKAGE PROBLEM AND THE PROBLEM OF SPATIAL CORRESPONDENCE

The experiments we have discussed in some ways raise as many questions as they answer. The problem we began with is that of accounting in terms of nervous system organization for the spatial correspondence between stimulus and response seen in frog capture behavior. In addressing this problem we focused on the linkage between topographic sensory maps and the pattern generating circuitry responsible for elaborating the motor outputs. We began with the assumption that the spatial correspondence between input and output could be accounted for in terms of a simple topographic linkage between the sensory maps and the pattern generating circuitry, that is an arrangement such that each local region in a map receives input corresponding to a different direction in space and is connected to pattern generating circuitry in such a way as to cause the appropriate motor output. Our results on tactile behavior caused us to discard a model in which a linkage of this kind is a consequence of superimposed sensory and motor maps in one structure, the optic tectum, and to replace it with a model in which tectum projects topographically to pattern generating circuitry located elsewhere. Our observations on visual behavior resulted in an elaboration of the second model which involves several distinct sets of pattern generating circuitry each receiving input from the two tectal lobes via divergent and convergent paths. This version of the model requires substantially more testing but we suspect that it will prove in its broad outlines to be a more or less accurate characterization of the relations between the tectum and the pattern-generating circuitry. In the course of these studies however we have made a number of observations which make us doubt our assumption that the link between the sensory maps and the pattern-generating circuitry is in fact topographic.

As a result, our findings leave us with two distinct though related unanswered questions. The first is how is the linkage between the tectum and the pattern generating circuitry organized, if not topographically? We are currently attempting to develop models of this linkage based on the notion that a given tectal region is connected to pattern generating circuitry in such a way that activity in the region can potentially activate a variety of different output patterns. The models must account for the sorts of changes in the outputs associated with activation of a given tectal region which we have seen in our lesion experiments. They must also account for the fact that in a normal animal electrical stimulation of a given tectal region produces a motor output which corresponds reasonably with expectations based on the sensory input to that region (Ewert, 1967). We will suggest an additional desideratum of the models below.

The second question our findings leave us with is our original one: how is one to account for the spatial correspondence between stimulus and response seen in frog prey capture behavior? We began our studies with the implicit assumption that the key to the problem of spatial correspondence lay in understanding the brain organization which created a particular output for each tectal region. Our observations suggesting that the brain may in fact not be organized this way has caused us to question the validity of our initial assumption. It now seems clear to us that an organization in which a fixed output is associated with each tectal region would not, at least by itself, provide an adequate explanation of the observed behavior. Ingle (1970) has remarked on the fact that a frog strikes accurately at prey from a variety of different head postures and noted that this implies that the motor output associated with activation of a given retinal region and hence tectal region probably varies depending on head position. We have realized that even with head posture fixed there is still not

an invariant relation between the retinal and tectal region activated and the required motor output. As illustrated in Figure 5, stimuli located in a variety of different directions, and hence causing different turns, will all activate the same retinal region. This is a consequence of the fact that the spatial co-ordinate frame of the eye is displaced from that of the body, or, perhaps more correctly from the co-ordinate frame used in movement. Another way of saying the same thing is that the frog does not pivot around an axis centered in the eye and as a result a given line of sight does not correspond to a constant direction of movement. It is of some interest that in the case of saccadic eye-movements the spatial co-ordinates frames for input and movement do roughly coincide; one might then expect significant differences in the neuronal organization responsible for assuring spatial correspondence between input and output in the case of visually elicited saccades as opposed to the case of visually elicited orienting in the frog. The latter may however be quite similar to the situation for visually triggered head movements in mammals since the spatial co-ordinate frames for input and output are similarly displaced.

One can imagine a variety of ways in which the nervous system might be organized to deal with the fact that stimuli falling along a constant line of sight require different directions of movement. One class of hypotheses would retain the notion of a topographic linkage between the tectal lobes and the turn-generating circuitry. It would have additonal parallel circuitry which conveys the necessary information to go from the eye centered co-ordinate to the body-centered or movement coordinate frame (information about head position in the situation described by Ingle; information about target distance, derived perhaps from binocular cues and/or accomodative state in the situation we have described). Such circuitry would act to appropriately modify the particular output brought about by activation of a given tectal region.

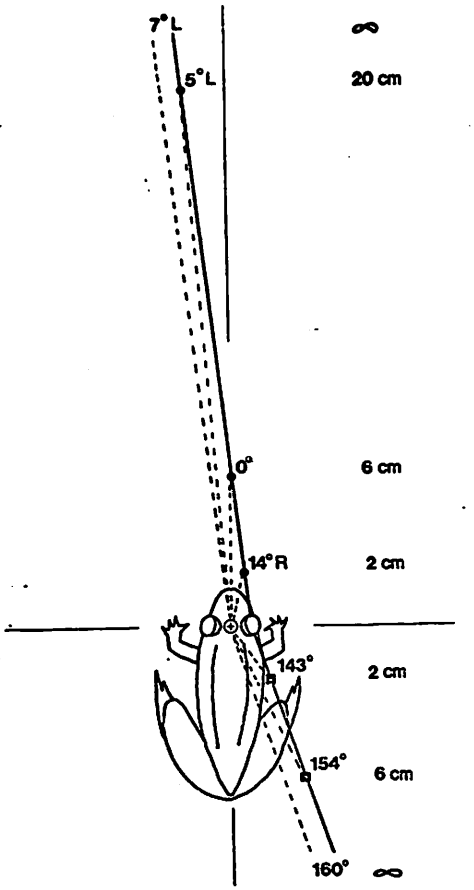

Figure 5: See legend next page

Figure 5. Diagram to illustrate the differences in the directons of stimuli when determined in a body-centered as opposed to an eye-centered co-ordinate frame. Heavier lines represent two lines of sight from a frog's right eye, one in rostral and the other in caudal visual field. All points along a given line of sight are imaged by the optics of the eye on the same position of the retina and hence are in the same direction in an eye-centered co-ordinate frame. For positions along each line of sight located at several distances from the eye (values to the right), the figure shows the directions as determined in a co-ordinate frame centered at a point between the frog's eyes. The directions are given as degrees to the left or right of the mid-sagittal line in the horizontal plane. The angles were calculated using a reasonable value for the inter-ocular separation (1.5 cm) in a medium sized Rana pipiens and are shown for distances within the range where stimuli elicit prey capture movements from such a frog. Angles given at the ends of the two lines of sight are those for positions at infinite distances from the eye. The caudal line of sight is well outside the limits of binocular field (see Grobstein et al., 1980); hence the physiological process by which turn angles for stimuli along this line of sight are determined cannot be based on binocular cues. The rostral line of sight is of interest in that it crosses the mid-sagittal line; hence stimuli along this line of sight may require turns either to the right or to the left. Given the existence of a caudal binocular field (Grobstein et al., 1980), a caudal line of sight crossing the mid-sagittal line could also be drawn.

The figure is intended to give a general feeling for the range of turn angles associated with stimulation of a given retinal point. The actual range is quite sensitive to interocular spacing as well as to the particular line of sight chosen. The range also depends on the position selected as the reference point of the body centered or movement co-ordinate frame. The position chosen for the figure seems the most likely point for a body-centered perceptual frame (a "cyclopean eye"). A more likely position for a movement frame might be the

point around which the animal pivots while turning. There is relatively little information on where this point is located and some evidence suggesting that its location may in fact vary in a complex way depending on the stimulus position (Comer and Grobstein, 1980a). In general however the pivot point is probably located somewhat more caudally than the reference point used in the figure. Moving the reference point caudally on the body will somewhat decrease the variation in angles along the rostral line of sight and increase it along the caudal line of sight.

We cannot at the moment totally exclude hypotheses which include both a topographic linkage and a parallel pathway as possible explanations for the spatial correspondence between input and output in frog prey capture behavior. It is possible that the abnormal orienting behavior we see in our lesioned animals and interpret as evidence that the linkage between the tectum and the pattern generating circuitry is not topographic is more properly to be understood in terms of disturbances in the parallel circuitry which modifies the particular output associated with stimulation of a given tectal region. On the other hand, we are struck by the parallelism between the more straight forward interpretation of our experimental studies, that the linkage between the tectum and the pattern generating circuitry is not in fact topographic, and the conclusion from a reconsideration of what is required to bring about spatial correspondence between input and output, that there is no compelling reason why the linkage should be. Our own inclination then is to explore hypotheses to account for the spatial correspondence between input and output which do not involve a topographic linkage between tectum and pattern-generating circuitry. Conversely, in our explorations of the variety of possible models of non-topographic linkages which could exist between the tectum and the pattern-generating circuitry, it may prove helpful to focus on those which not only account for our experimental results but which also have properties relevant to the problem of how the spatial correspondence between input and output seen in behavior is brought about.

A useful starting point for both explorations, we suspect, is the recognition that while a given retinal and tectal region corresponds to a single direction in an eye-centered co-ordinate frame, they in fact correspond to a set of directions in a body-centered or movement co-ordinate frame. Conversely, a given point in a movement co-ordinate frame in fact corresponds to a set of points in an eye-centered co-ordinate frame such as the retina or the tectum. We are

intrigued by the possibility that between the tectum and the pattern generating circuitry there may be an intermediate level of circuitry within which space is represented in a body-centered or movement co-ordinate frame. Because of the many to one and one to many character of the transformation in going from an eye-centered to a body-centered or movement co-ordinate frame, disturbances of circuitry involved in this transformation might be expected to result not in disconnection of particular tectal regions from pattern generating circuitry but rather in an alteration in the particular output associated with activation of given tectal regions.

In developing the argument for an intermediate level of circuitry involved in a co-ordinate transform we have focused on visually elicited prey capture behavior: on experimental observations suggesting that there is not a fixed output associated with each tectal region and on theoretical considerations suggesting that because the tectum is an eye-centered representation one should perhaps have expected that the output associated with a given tectal region would be variable. In closing, it seems appropriate to return to the problem of tactually elicited prey capture where, as mentioned earlier in this paper, there is some evidence that the motor output associated with activation of a given region of a second sensory map, the lateral torus semicircularus, is also variable. It is perhaps less obvious in this case why such a variability should exist, given that the co-ordinate frame of a cutaneous map is not in any clear sense displaced from a body-centered co-ordinate frame. In this regard however a recent study showing that frogs wipe accurately at a given point on the skin of the forelimb regardless of the actual position of the forelimb (Fukson et al., 1980) is of interest. Assuming that frogs also orient accurately to tactile stimulation of the forelimb regardless of limb posture, the situation is analogous to that which we have described for visual orienting: a given region of a receptor surface, in

this case the skin, and the coresponding region of a topographic sensory map, in this case the lateral torus semicircularus, should be capable of activating a variety of different movements; conversely, a given movement should be elicitable from a set of different points in the torus or on the forelimb. Hence circuitry yielding a one to many and many to one transformation may be required in going from cutaneous space to motor space just as it is in going from retinal space to motor space.

Acknowledgements

The research program of the senior author is supported by PHS EY 01658 and RCDA EY 00057, and by NSF BNS 7914122. S.K.K. has received support from PHS 1 T32 MH 14274.

Grüsser, O.-J., Grüsser-Cornehls, U. 1973, Neuronal mechanisms of visual movement perception and some psychophysical and behavioral correlations, In: "Handbook of Sensory Physiology, Vol. VII/3A," R. Jung, ed., Springer, Berlin.

Ingle, D. 1970, Visuomotor functions of the frog optic tectum, Brain Behav., Evol., 3:57-71.

Ingle, D. 1973, Two visual systems in the frog, Science, 181:1053-1055.

Ingle, D. 1982, The analysis of visuomotor organization in some vertebrates, In: "Advances in Analysis of Visual Behavior," D. Ingle, M. Goodale, and R. Mansfield, eds., M.I.T. Press, Cambridge. In press.

Kostyk, S.K., and Grobstein, P. 1980, Visual prey acquisition behavior in the frog: effects of various unilateral lesions, Soc. Neurosci. Abs., 6:75.

Kostyk, S.K., and Grobstein, P. 1982, Visual orienting deficits in frogs with various unilateral lesions, submitted Behav. Brain Res..

Krasne, F.B., and Wine, J.J. 1977, Control of crayfish escape behavior, In: "Identified Neurons and Behavior of Arthropods," G. Hoyle, ed., Plenum Press, New York.

Raphan, T., and Cohen, B. 1978, Brainstem mechanisms for rapid and slow eye movements, Ann. Rev. Physiol., 40:527-552.

Scalia, F., and Fite, K. 1974, A retinotopic analysis of the central connections of the optic nerve in the frog, J. Comp. Neurol., 158:455-478.

Sperry, R.W. 1944, Optic nerve regeneration with return of vision in anurans, J. Neurophysiol., 7:57-69.

Sperry, R.W. 1945, Restoration of vision after crossing of optic nerves and after contralateral transplantation of eye, J. Neurophysiol., 8:15-28.

REFERENCES

Comer, C., and Grobstein, P. 1978, Prey acquisition in atectal frogs, Brain Research, 153:217-221.

Comer, C., and Grobstein, P. 1981b, Involvement of midbrain structures in tactually and visually elicited prey acquisition behavior in the frog, Rana pipiens, J. Comp. Physiol., 142:151-160.

Comer, C., and Grobstein, P. 1981a, Tactually elicited prey acquisition behavior in the frog, Rana pipiens, and a comparision with visually elicited behavior, J. Comp. Physiol., 142:141-150.

Comer, C., and Grobstein, P. 1981c, Organization of sensory inputs to the midbrain of the frog, Rana pipiens, J. Comp. Physiol., 142:161-168.

Ewert, J.P. 1967, Aktivierung der Verhaltensfolge beim Beutefang der Erdkrote (Bufo bufo) durch elektrische Mittelhirnreizung, Z. Vergl. Physiol., 71:165-189.

Fite, K.V. 1969, Single unit analysis of binocular neurons in the frog optic tectum, Exp. Neurol., 24:475-486.

Fite, K.V. 1973, The visual fields of the frog and toad: a comparative study, Behav. Biol., 9:707-718.

Fukson, O.I., Berkinblit, M.B., and Feldman, A.G. 1980, The spinal frog takes into account the scheme of its body during the wiping reflex, Science, 209:1261-1263.

Grobstein, P., Comer, C., and Kostyk, S. 1980, The potential binocular field and its tectal representation in Rana pipiens, J. Comp. Neurol., 190:175-185.

Gordon, B., Moran, J., and Presson, J. 1979, Visual field deficits in cats with one eye rotated, Neurosci. Abstr., 5:626.

H.W. Borchers: COINCIDENCE BETWEEN NEURONAL ACTIVITY AND BEHAVIORAL PATTERNS IN FREELY MOVING TOADS

Our previous knowledge of information processing in neuronal networks of the toad's visual system is mainly obtained from investigations performed with paralyzed animals. In these experiments the response characteristic of single units in the visual pathway is analyzed by presenting precisely defined behaviorally relevant visual stimuli - such as little pieces of black or white cardboard on a contrasting background - to an awake immobilized animal sitting in a perimeter-like set-up (Ewert und Borchers 1971). However, coincidence between neuronal activity and corresponding behavioral patterns as well as the effect of the animal's behavior through possible feedback mechanisms on the ongoing neuronal activity can be analyzed only in the freely moving toad.

For these experiments a special micromanipulator has been devised according to the mechanical screw-axle technique to chronically record single unit activity extracellulary in the central visual pathway (Fig.1). Within a small piston etched twin stainless steel or tungsten microelectrodes are vertically fixed. The position of the electrode tips in the tissue of the brain can be adjusted in dorso-ventral direction by turning the screw which moves the piston up or down in a cylinder. The holder of the electrode positioner is firmly attached by means of dental cement to the dorsal surface of the skull above the exposed midbrain. It is possible to keep the recording electrode tip close to a fiber even when the toad jumps. A differential recording setup permits one to reject common,spurious,muscle potentials and part of the background noise. The electronic device is directly fixed to the headpiece (Fig.1). The action potentials are conducted to a storage oscilloscope with stepper. A video system consisting of camera, mixer and scan converter is designed to simultaneously record three kinds of events, namely (i) the toad's movement, (ii) a visual stimulus and (iii) the neuronal discharge. The composite video picture can be stored on magnetic tape for later analysis. Correlation between neuronal event, behavior and stimulus can be investigated in space and time by means of frame-by-frame analysis.

To demonstrate the temporal relationship between behavioral events and neuronal activity the interspike frequency time histogram can be utilized. The instantaneous interspike frequency f_i represents the reciprocal value of the interval duration t_i between two successive action potentials. This frequency is plotted on the ordinate as a function of time and is assumed to be constant during the corresponding interval t_i

$$f_i = 1/t_i$$

constant for $\sum_{1}^{i-1} t_i < t \leq \sum_{1}^{i} t_i$

The width of a column in the histogram is directly proportional to the interval duration. The area of each column is of constant size. Thus shorter intervals have larger values on the ordinate and vice versa. By this method variations of the discharge rate are emphasized by changes of the two parameters in the histogram.

The recording experiments showed different neuron types in the retino tectal projection system. The investigated neurons correspond to those of the following neuronal classes in the retina (ganglion cells, R) and optic tectum (T): R2, R3, R4, T2(1), T4 and T8 as described for the immobilized preparation (Ewert and Borchers 1971, Grüsser and Grüsser-Cornehls 1976, Borchers 1980, Ewert 1983). They can be classified into three groups depending on the correlation between their response characteristics and the behavior of the toad (Borchers 1980).

NEURONS OF GROUP 1 are activated by moving retinal images irrespective of whether the toad or the visual stimulus is moving. The neuronal activity is strongly influenced by the size, velocity, form and contrast of the stimulus. The neurons maintain their activity as long as the stimulus moves within their ERF. Neurons of group 1 generally exhibit response characteristics comparable to those of corresponding neuron classes in immobilized animals under similar stimulus conditions (Ewert and Borchers 1971). If the toad does not move, stationary objects within the ERF do not elicit any neuronal response. Since toads do not seem to have involuntary saccadic eye movements (for results in frogs see Autrum 1959) to produce moving retinal images from the static visual environment, the question as to whether there are eye movements by which a stationary stimulus pattern can be transformed into a moving pattern (Schipperheyn 1973, Pigarev et al. 1971) is of special interest. The normal respiratory movements of the buccal cavity are insufficient to elicit an activation of the investigated neurons. However, stronger eye movements correlated with deeper breathing indicated by stronger movements of the flanks or general motor

activity produce displacements of retinal images, which are sufficient to activate these neurons.

NEURONS OF GROUP 2 show activation in response to moving visual stimuli. However, activity is suppressed in the presence of certain movements initiated by the toad itself. For example, (i) a retinal class R3 neuron responds to sudden changes in the diffuse light level - such as switching off and on roomlights - with bursts of spikes at "off" and "on". The off-response, however, fails to occur if the animal closes the eye voluntarily (Ewert und Borchers 1974, Borchers and Ewert 1978). The off-activation is supressed by the toad's behavior. In this case the absence of spikes might be caused by efferent commands to the retina (v.Holst and v.Mittelstaedt 1950, Maturana 1958, Johnstone and Mark 1971, Byzov and Utina 1971, Miles and Rogers 1972, Ewert and Borchers 1974, Borchers and Ewert 1978, Tasaki et al. 1978). Together with the command for the movement (eye lid closure) possibly an "efference copy" is transmitted to inhibit the neuronal response. (ii) Some of the neurons recorded from the optic tectum which are strongly active in response to prey objects, are silent during any movement of the toad. E.g. a tectal large field unit is activated by a moving white disc (15 mm diameter) within its excitatory receptive field. However, the neuronal activity ceases, when the toad moves towards the disc even though the stimulus movement continues within the Excitatory Receptive Field. When the toad stops moving, the firing rate increases at least to its former level.

NEURONS OF GROUP 3 in contrast to those of other groups exhibit spontaneous activity. The mean spike rate is about 6/sec. However, the neuronal activity is strongly correlated with the toad's behavior. Two types have been identified. In both a change in the discharge rate precedes a subsequent behavioral pattern. For example turning and prey-catching is preceded either by an increase (class T8(1) neuron) or by decrease of the firing rate (class T8(2) neuron). Each time the toad initiates a movement the frequency of a T8(1) unit increases, and decreases later on at the end of the movement. Peaks of about 50-70/sec are reached just before the movements. These neurons have no "primary" receptive fields. Visual, tactile, vibratory or olfactory stimulation is unnecessary for their activation. The correlation between prey-catching behavior - a sequence of motor pattern which is typical for the toad - and the corresponding discharge of a class T8(1) neuron is demonstrated by frame-by-frame analysis in figure 2. In this behavioral sequence the toad responds to a small prey object, a mealworm which appears in the visual field with the following sequence of behavioral reactions (Fig. 2): a, b) the toad sits motionless, the mealworm moves within the visual field, the spike rate increases up to a maximum. c, d, e) the toad orients towards the worm, the neuronal activity decreases. f, g, h, i) just before the toad thrusts out its tongue j) and snaps at the worm, the spike

rate increases again strongly to a maximum. k, l, m, n) the toad swallows the prey, the spike rate decreases. A quantitative analysis of a spike train recorded during prey-catching is shown in the interspike frequency time histogram (Fig.3). In the same toad the prey catching behavior was elicited several times within few minutes. The question of whether there are certain motor patterns tightly coupled with corresponding "fixed" discharge patterns is of special interest. However, each recording occurs in a different experimental situation in which stimulus parameters may have changed e.g. by previous movements of the animal. Thus it is nearly impossible to create exactly reproduceable situations which allow a direct comparison among neuronal discharges in relation to corresponding behavioral processes, such as snapping at a worm (Fig.2). The analysis shows, that the neurons respond with greater increase of spike frequencies in connection with sudden and fast movements like snapping. Smaller increases of frequency are correlated with walking, stalking and turning. Repeated prey-catching experiments show common features in the discharge patterns (Fig.4). A change in the discharge rate generally precedes any kind of motor activity. We do not know the precise location of these neurons in the neural substrate of sensorimotor interfacing. It is possible that they receive the information about each imminent movement and then serve to converge the inputs back to an appropriate locus in the sensory system (Johnstone and Mark 1971). The enhanced discharge before movements may be related to an attention shift which facilitates subsequent behavioral activities (Wurtz and Goldberg 1972). Since the response of the neurons precedes and so to say predicts the movement, it could be that these neurons are related to elements of a command system (Kupfermann and Weiss 1978, Pearson 1976, Larimer 1976, Miles and Evarts 1979).

Further experiments in freely moving animals will help to elucidate the neuronal connections of the sensorimotor interface. The results can be used to extend and complete models for neuronal control of behavior which are until now supported by neurophysiological data obtained only from immobilized animals. Our future research is mainly concerned with localisation and characterisation of groups of neurons which participate in the control of paticular behavioral motor patterns.

REFERENCES

Autrum,H. 1959, Das Fehlen unwillkürlicher Augenbewegungen beim Frosch. Naturwiss. 46, 435.

Borchers,H.-W. 1980, Single unit responses from the optic tectum in freely moving toads related to behavioral patterns. In H.J.Jensen (Editor), Cybernetic 1980. R.Oldenbourg Verlag München,Wien, pp.

114-117.

Borchers,H.-W. and Ewert,J.-P. 1978, Eye closure in toads (Bufo bufo L.) does not produce off responses in retinal on-off ganglion cells: a question of efferent commands. J.Comp. Physiol. 125, 301-303.

Byzov,A.L. and Utina,I.A. 1971, Centrifugal effects on amacrine cells in the frog's retina. Neirofiziologiya 3 (3), 293-300.

Ewert,J.-P. 1983, Tectal mechanisms underlying prey-catching and avoidance behaviors in toads, in: "Comparative neurology of the optic tectum". (H.Vanegas, ed.), Plenum Press, New York,in press.

Ewert,J.-P. und Borchers,H.-W. 1971, Reaktionscharakteristik von Neuronen aus dem Tectum opticum und Subtectum der Erdkröte Bufo bufo L. Z. vgl. Physiol. 71, 165-189.

Ewert,J.-P. und Borchers,H.-W. 1974, Antwort von retinalen Ganglienzellen bei freibeweglichen Kroeten (Bufo bufo L.). J. Comp. Physiol. 92, 117-130.

Grüsser,O.-J. and Grüsser-Cornehls,U. 1976, Neurophysiology of the anuran visual system, in: "Frog neurobiology". (R.Llinas, W.Precht, eds.), Springer-Verlag, Berlin, Heidelberg, New York.

Holst,E.v. and Mittelstaedt,H. 1950, Das Reafferenzprinzip. Naturwiss.37, 474-476.

Johnstone,J.R. and Mark,R.F. 1971, The efference copy neurone. J.Exp.Biol. 54, 403-414.

Kupfermann,I. and Weiss,K.R. 1978, The command neuron concept. The Behavioral and Brain Sciences 1, 10-39.

Larimer,J.L. 1976, Command interneurons and locomotor behavior in crustaceans, in: "Neural control of locomotion".(R.M.Herman, St.Griller, P.S.G.Stein, D.G.Stuart, eds.) Plenum Publishing Corporation, New York, pp. 293-326.

Maturana,H.R. 1958, Efferent fibres in the optic nerve of the toad, (Bufo bufo L.). J.Anat. 92, 21-26.

Miles,F.A. and Rogers,L.J. 1972, Centrifugal control of the avian retina, I-V. Brain Res. 48, 65-156.

Miles,F.A. and Evarts,E.V. 1979, Concepts of motor organization. Ann. Rev. Psychol. 30, 327-362.

Pearson,K. 1976, The control of walking. Scientific American 235,

72-86.

Phillips,M.I. (ed.) 1973, Brain unit activity during behavior. Charles C. Thomas, Springfield, Ill.

Pigarev,I.N. and Zenkin,G.M., Girman,S.V. 1971, Activity of the retina detectors in unrestrained frogs. Physiol. J. of USSR, LVII (10), 1448-1453.

Schipperheyn,J.J. 1973, Respiratory eye movement and perception of stationary objects in the frog. Acta physiol. pharmacol. Neerl. 12, 157-159.

Tasaki,K., Tsukahara,Y. and Watanabe,M. 1978, Efferent system in the retina of the frog, Rana catesbeiana. Sensory Processes 2, 396-407.

Wurtz,R.H. and Goldberg,M.E. 1972, Activity of superior colliculus in behaving monkey. III. Cells discharging before eye movements. J. Neurophysiol.35, 575-586.

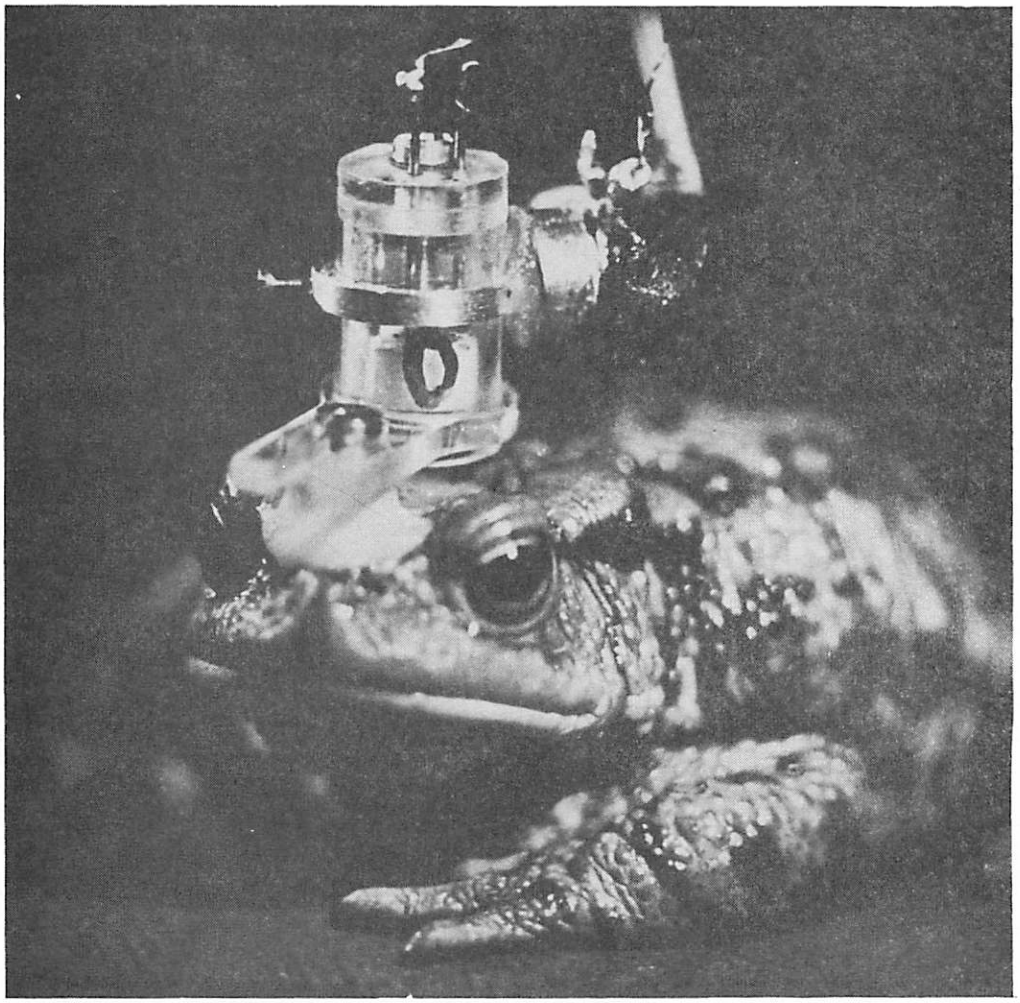

Figure 1: The micromanipulator assembly is mounted on the toad's skull.

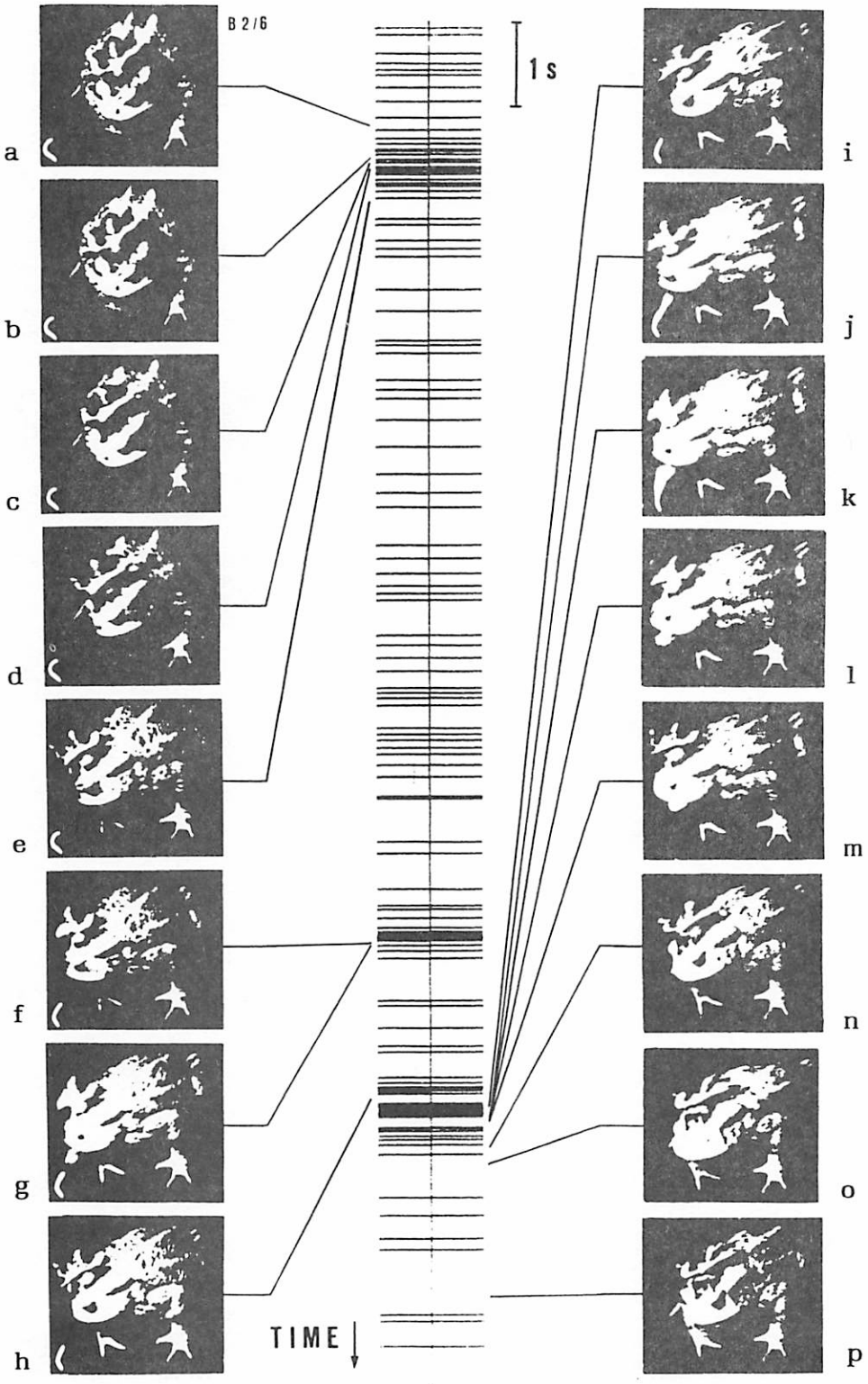

Figure 2: Frame-by-frame analysis of capture of a mealworm by the toad and corresponding discharge pattern of a behaviorally correlated neuron (group 3). For detailed description see text.

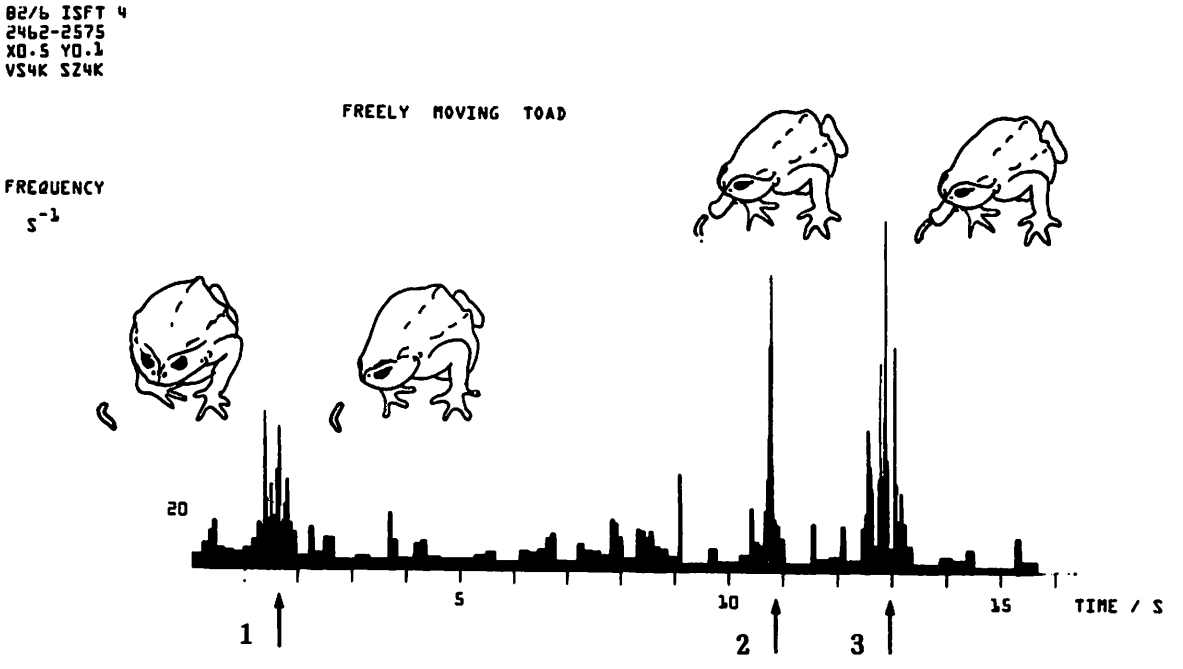

Figure 3: Interspike frequency time histogram. Spontaneous activity of a behavioral correlated neuron (group 3) during capture of a mealworm. Just before the toad starts to move, the discharge rate increases (1, 2, 3). The toad orients (1), snaps unsuccessfully (2) and then successfully (3).

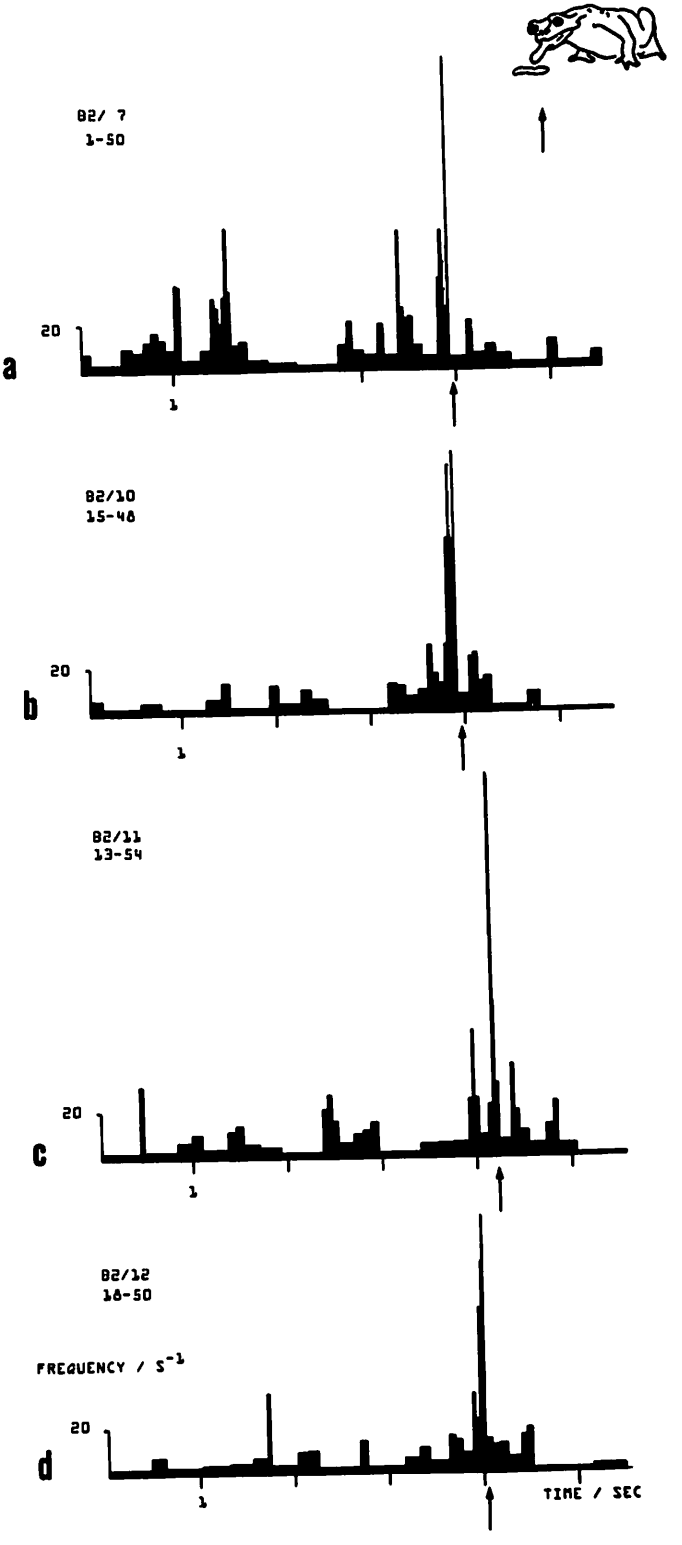

Figure 4: Interspike frequency time histogram. Spontaneous activity of a behaviorally correlated neuron (group 3). The toad snaps successfully at

D.P.M. Northmore: TECTAL MAPS AND VISUAL ORIENTING

In much of our thinking about prey capture, the assumption has generally been made that the amplitude of an orienting turn is determined by the locus of excitation in some form of "motor map." Since this motor map must derive its visual input from the retinotectal map, it is natural to suppose that it exists as a layer of cells underlying the retinotectal map in the tectum. A potential problem for this scheme is how the two maps are to be connected. If there are fixed topographic connections between the two, the excitation of a given point on the tectal surface should lead to an orienting turn of fixed amplitude. However, this would not work well for animals with sizeable eye movements. It would be necessary to postulate a relative shifting of the maps depending on eye position. A shifting between the sensory and motor maps is also implied by the ability of anurans to detour around a barrier. The following experiments on fish provide further instances of modifiability between the sensory or retinotectal map, and motor behavior, which taken together with other evidence, cast doubt on the usefulness of the motor map concept.

Retinotectal maps can be rearranged in fish by taking advantage of their remarkable neural plasticity. Thus, the removal of the caudal half of one tectum eventually leads to a compressed representation of most of the contralateral visual field (Sharma, 1972; Yoon, 1976). If excitation of a given

tectal locus invariably leads to a particular amplitude of orienting turn, one should expect a fish with a compressed tectum to turn about half way towards visual targets.

In order to be able to study orienting behavior in fish, a method was developed for obtaining a ballistic orientation to brief flashes of light (125 msec) presented at unpredictable positions on the walls of a circular tank (Northmore et al., 1981). Although this involves a training procedure, called autoshaping, the rewards used to maintain the behavior are not contingent upon the fish making any particular response. This has the advantage of encouraging the fish to point at the perceived position of a light, even in error. The following results were obtained with sunfish because, of several species tested, they oriented most consistently and accurately.

The caudal half of the left tectum was removed from 7 sunfish and 10-20 days later the right optic nerve was crushed. The latter operation was done because it promotes the formation of a compressed projection in goldfish (Yoon, 1976). In the case illustrated in Fig. 1, the recovery of orientation behavior was followed up to 421 days after the optic nerve crush (Northmore, 1981).

The first phase of recovery, which was accomplished relatively quickly (by 31 days post crush), consisted of a restoration of accurate orientation in the nasal right field. This result is to be expected on the basis of previous electrophysiological experiments showing that an optic nerve

regenerating into a rostral half tectum first establishes a map of the nasal field on the normally appropriate rostral tectum (Sharma, 1972; Yoon, 1976). Orienting to stimuli in the caudal half field recovered much more slowly, and in a nasal to temporal order. Figure 1A shows the orienting ability of a sunfish 421 days after crushing the optic nerve. The point to notice is that orienting in the nasal half of the right field (stimulus angles 0-90°) remained accurate, while it was generally inaccurate in the temporal half field. Although the fish did sometimes make large angle turns that were accurate, there was no evidence for the consistent undershooting alluded to earlier. The fish's retinotectal projection was then mapped electrophysiologically (Fig. 1B) to reveal that the nasal half of the right field projected in an orderly, but highly compressed fashion on the most rostral region of the tectal remnant, while the temporal field was represented on the remainder in a disorganized fashion. It appears then, that accurate orientation requires an orderly visuotopic map, but not necessarily one of normal magnification. Accurate orientation in the nasal field could not have been performed with the unoperated eye-tectum since it can only see some 25° of the contralateral field (Northmore et al., 1981). Orientation, then, is not immutably linked to excitation of a particular place on the tectum. Rather, there must be some reorganization of connections between the sensory map and the pattern generators responsible for orienting turns.

A possible form of reorganization might involve an expansion of projections from tectum onto the pattern generators outside the tectum, thereby tending to restore normal topographic relationships - if they exist - between the two. One way of testing whether such an anatomic rearrangement is necessary for the maintenance of normal orientation is to look at fish with an altered retinotectal map on an otherwise normal tectum. One such alteration is an expansion of the retinotectal map brought about by ablating half of the retina (Schmidt et al., 1978). Fig. 2A shows the orientation behavior of a sunfish about six months after the ablation of its most nasal right retina. As expected, this animal failed to orient or respond in any overt way to light flashes in its most temporal right field. Orientation over the rest of the right field, however, remained accurate. Subsequent electrophysiological mapping (Fig. 2B) showed that the intact visual field in this fish had projected over nearly the entire tectum. Despite the increased retinotectal magnification, there was no sign of the fish systematically overshooting the target. Since the tectum in this case remained intact, it seems unlikely that behavioral compensation could have been the result of any gross anatomic rearrangement of the tectal outputs. The mechanism of compensation is apparently more subtle, and may depend upon visual experience. Although the system can accommodate alterations in retinotectal magnification, it cannot deal with a scrambled mapping of its input.

If we are to retain the notion of a motor map, we must say that the projections to it from the sensory map are capable of being expanded or compressed. But how can this be done? Large scale neural rewiring such as occurs after surgery in fish would seem implausible, especially when no surgery is done to the brain. Even if this were the mechanism, the rewiring of many connections between the sensory and motor maps would have to be exact so as to preserve accurate behavior. The little data on the properties of intrinsic cells in fish tectum is not supportive of the motor-map-in-tectum idea either. These cells have large and diffuse receptive fields and so appear to be little concerned with preserving the topography so accurately provided by the retinotectal map (Guthrie and Banks, 1978; Niida et al., 1980).

It is worth considering an alternative to the motor map model. Suppose that the locus of excitation in the retinotectal map arising from the prey stimulus is converted into an intensity code, e.g. some combination of spike frequencies or numbers of active fibers. This code is then transmitted to the pattern generators controlling a turn. The site of this conversion could be tectum because Grobstein (this conference) has provided evidence from the frog that an orienting turn is not coded by a particular set of tectal output fibers. In other words, the output of tectum is non-topographic. The advantage in specifying orientation in terms of an intensity code is that it is simple to rescale. Thus, expansions and compressions of the retinotectal map could be readily accommodated by decreasing or increasing a gain control at some stage prior to the pattern generators.

It is also conceivable that the simple parameter, "gain," could be readily adjusted by the results of visuomotor experience: consistent undershooting a target would increase gain, overshooting decrease it. Such a mechanism would be valuable for keeping orienting behavior in proper calibration, especially in fish, whose eyes and brain grow throughout life (Easter et al., 1977; Meyer, 1978).

This work was supported by a grant (EY 02697) from the National Eye Institute.

REFERENCES

Easter, S. S., Johns, R. P. and Baumann, L. R. (1977). Growth of the adult goldfish eye - 1: Optics. Vision Res., 17, 469-477.

Guthrie, D. M. and Banks, J. R. (1978). The receptive field structure of visual cells from the optic tectum of the freshwater perch (Perca fluviatilis). Brain Res., 141, 211-225.

Meyer, R. L. (1978). Evidence from thymidine labelling for continuing growth of retina and tectum in juvenile goldfish. Exp. Neurol., 59, 99-111.

Niida, A., Oka, H. and Iwata, K. S. (1980). Visual responses of morphologically identified tectal neurons in the crucian carp. Brain Res., 201, 361-371.

Northmore, D. P. M., Skeen, L. C. and Pindzola, J. M. (1981). Visuomotor perimetry in fish: a new approach to the functional analysis of altered visual pathways. Vision Res., 21, 843-853.

Sharma, S. C. (1972). Reformation of retinotectal projections after various tectal ablations in adult goldfish. Exp. Neurol., 34, 171-182.

Schmidt, J. T., Cicerone, C. M. and Easter, S. S. (1978). Expansion of the half retinal projection to the tectum in goldfish: an electrophysiological and anatomical study. J. Comp. Neurol., 177, 257-278.

Yoon, M. G. (1976). Progress of topographic regulation of the visual projection in the halved optic tectum of adult goldfish. J. Physiol., 257, 621-643.

Northmore, D. P. M. (1981). Visual localization after rearrangement of retinotectal maps in fish. Nature, 293, 142-144.

Fig. 1

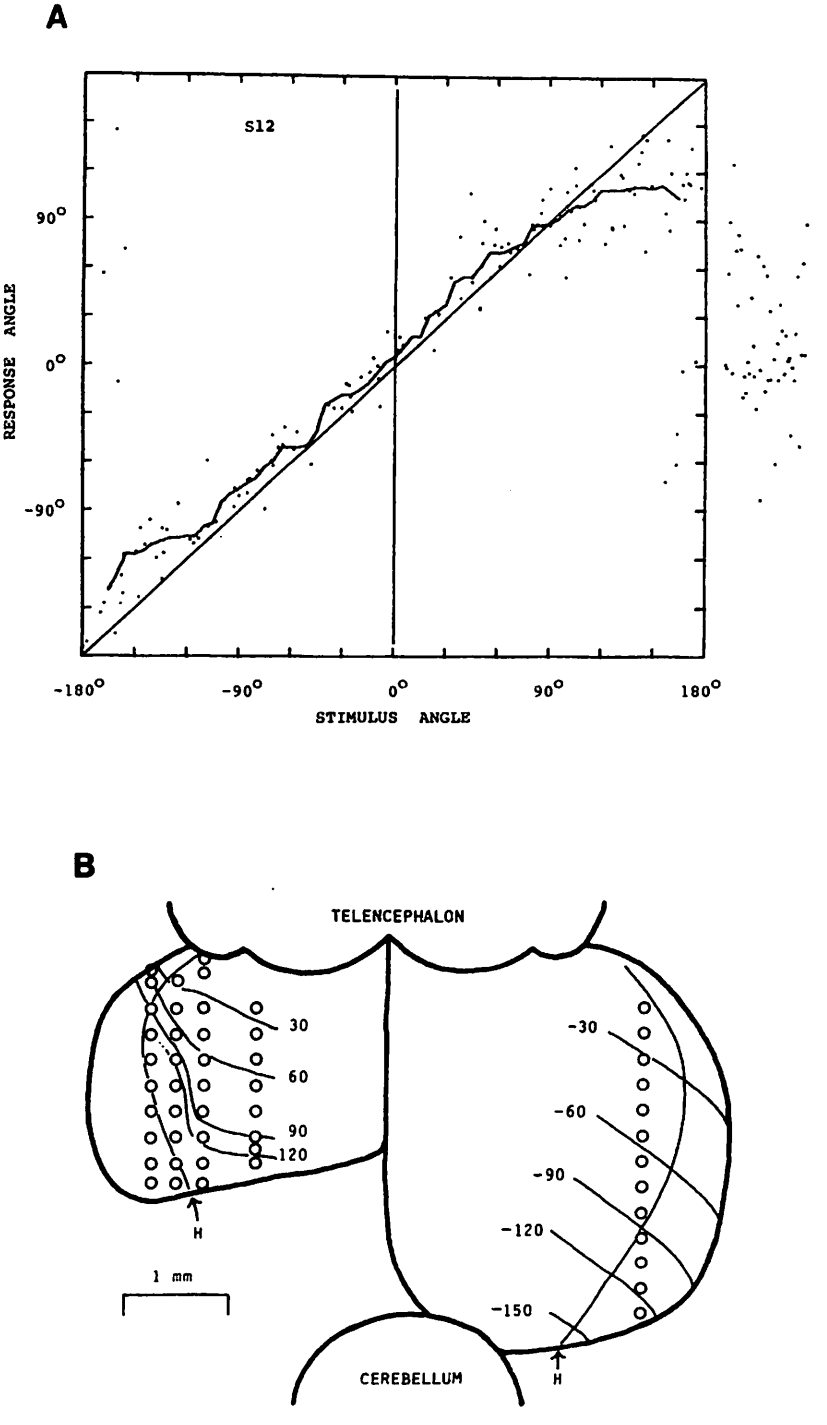
A
S12
90°
0°
-90°
RESPONSE ANGLE
-180°
-90°
0°
90°
180°
STIMULUS ANGLE
B
TELENCEPHALON
30
60
90
120
H
1 mm
-30
-60
-90
-120
-150
H
CEREBELLUM

Figure 1. A. Orientation data from a sunfish 414 days after ablation of its caudal left tectum, and 401 days after crushing its right optic nerve. Each point in the graph shows the fish's response angle 0.8 sec following a stimulus flash presented at an angle shown on the abscissa. The points to the right, outside the box show "response" angles on dummy trials in which no stimulus was flashed. The curve drawn through the points is a running median of response angle computed from a 30 deg-wide box car moved along the abscissa. This diagonal shows ideal responding (i.e. stimulus angle= response angle), and the vertical line separates left from right visual fields.

B. Results of electrophysiologically mapping the retinotectal projections in the same sunfish. Circles show microelectrode placements. The normal projection of the vertical meridia (-30 to -150°), and the horizontal meridian (H) of the left visual field are drawn on the right tectum. Similarly, meridia of the right visual field are drawn on the remnant of the left tectum. Note that the nasal 90° of this field is represented in highly compressed fashion on the rostral tectum. The temporal half of the field was represented more caudally in a disorganized fashion. The temporal vertical meridia could not, therefore, be plotted.

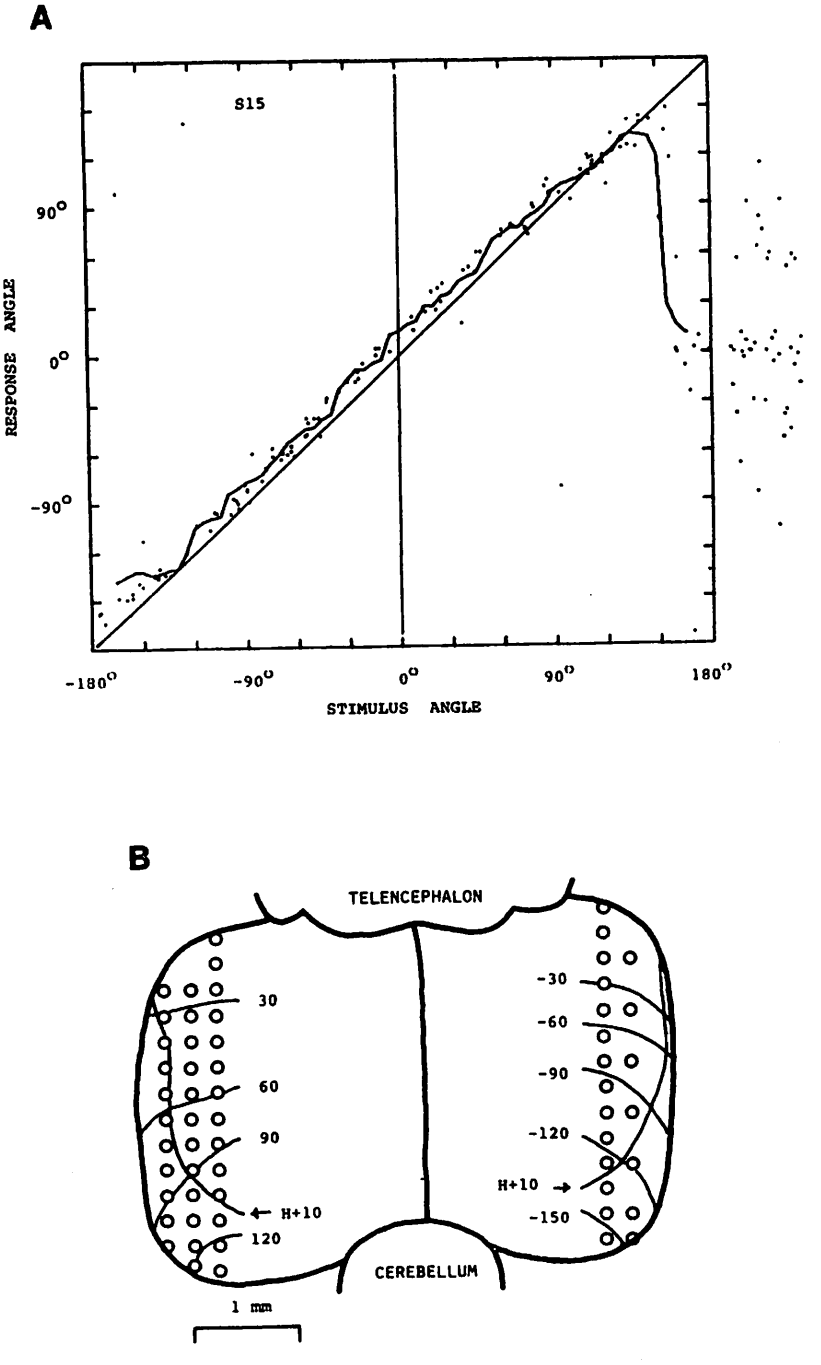

Figure 2. A. Orientation data from a sunfish 182 days after ablation of its most nasal right retina.

B. Results of electrophysiological mapping in the same sunfish. "H+10" shows the projection of the 10° parallel above the horizontal meridian. Note the expanded projection on the left tectum. Same conventions as for Fig. 1.

John I. Simpson: THE COORDINATE SYSTEM OF VISUAL CLIMBING FIBERS TO THE CEREBELLAR FLOCCULUS

How is the world around an animal, its external space, represented in the internal functional space of the brain? This question, which involves concepts of mapping and reference frames, has concerned us in our studies of how the flocculus of the cerebellum operates. To put cerebellar operations into the context of control of movement and posture, the language of mechanics is required. To use this language of positions, velocities and accelerations, spatial reference frames or coordinate systems must be employed, both by the experimenter and the brain. Any one of a number of reference frames may be used, but certain reference frames result in a simplicity in the experimenter's description of particular movements. Presumably a similar situation holds for the brain, simplifying the neuronal transformations performed in sensory-motor integration. The cerebellar flocculus, with its intimate relation to eye movements, seems a reasonable place for developing notions about coordinate systems, for while the eye is a "limb of only one joint", that joint has three degrees of freedom.

The cerebellar flocculus is particularly related to eye movements serving to stabilize the retinal image of the world when the head moves. These compensatory eye movements depend, in part, upon signals from the vestibular apparatus reporting the accelerations of the head, and these sensory signals have long been known to reach the flocculus as well as other parts of the brain. While vestibular signals are sufficient to initiate compensatory eye movements, the only measure of the adequacy of retinal image stabilization comes from signals arising from the retina itself. A particular type of retinal ganglion cell reports both the direction and speed of movement of discrete portions of the retinal image. We have previously shown in the rabbit that these local signals of retinal image slip are combined in the accessory optic system to create signals reporting the speed and directions of rotation of the entire visual world. Of course, in an animal's natural environment, rotation of the entire visual world occurs only as a result of movement of the animal itself. Therefore, the visual messages transmitted from the accessory optic system to the flocculus are about self-motion and are thus kindred to the signals of self-motion provided by the vestibular apparatus. Since both visual and vestibular signals reach the flocculus, might not these two sensory modalities share a common spatial organization facilitating their interaction in the control of compensatory eye movements? Indeed, they do.

Vestibular signals of head angular acceleration arise from the semicircular canals. Three canals are located on each side of the head and they form an approximately mutually perpendicular set. The orientation of each canal in space can be described by an axis perpendicular to its own plane. In general, when an animal holds its head in the position of alertness, one axis is oriented vertically while the other two axes are approximately in the horizontal plane and at 45° to the vertical plane of symmetry of the head. These axes establish a reference frame for describing head angular accelerations. Most interestingly, accessory optic system neurons respond best to rotation of the visual world about one of three axes whose orientations correspond closely to those of the three principal axes of

the semicircular canals. That is, one set of neurons responds best to rotation about the vertical axis while two other sets of neurons respond best to rotation about one or the other of the two horizontal axes at 45° to the vertical plane of symmetry. Thus, a reference frame remarkably similar to that of the vestibular system is established for describing rotations of the visual world.

The accessory optic system projects to the inferior olivary nucleus, which, in turn, gives rise to climbing fibers, one of the two major classes of input fibers to the cerebellum. Each of the three axes of rotational preference found for visual world movement is represented separately on neurons that are anatomically segregated within that part of the inferior olive projecting to the flocculus. This is of some consequence because the climbing fiber projection from the inferior olive to the cerebellar cortex has been shown both anatomically and physiologically to be organized into a number of termination zones oriented orthogonally to the folial pattern. Typically, each zone arises from a simply connected subdivision of the inferior olive. The significance of this zonal pattern extends beyond that of describing an afferent system for an apparently corresponding zonal pattern is delineated by the Purkinje cell efferent projection to the various deep cerebellar and vestibular nuclei. Since each Purkinje cell receives from only a single climbing fiber, each Purkinje cell in the flocculus can be assigned to one of three classes on the basis of the preferred axis of rotation of the climbing fiber that contacts it. In addition, we have found that the spatial organization of visual world movement yielding the three particular preferred axes of rotation of the climbing fiber input is also prevelant in the Purkinje cell responses associated with the second major class of cerebellar inputs, namely the mossy fibers. Thus, a given Purkinje cell responds best to rotation about one of the three preferred axes. Collectively, the three axes establish an internal or natural coordinate system, which presumably is used by the brain in signal processing and which, therefore, is likely useful to us in comprehending this signal processing.

C.C. Boylls: CLIMBING FIBERS AND THE SPATIAL REFERENCE FRAME FOR MOTOR COORDINATION

Introduction: Coordinate Systems for CNS Signals

A spinal frog can use its hindlimb to scratch an irritated patch of skin on the forelimb, irrespective of where that forelimb is positioned (27). From this demonstration, we can gather that spinal circuits have implicit "knowledge" of the forelimb state (e.g., position) and are able to transform that knowledge into a prescription for proportioned contraction of hindlimb muscles. For an engineer to coax a robot into a similar feat, limb states and effector actions would have to be expressed as concrete measurements within some form of coordinate system. Whether the spinal frog makes use of such systems in its calculations isn't yet known; but it does appear that other parts of the CNS contain internal, multidimensional yardsticks in whose units afferent and efferent signals are described. In particular, Simpson (this volume) provides evidence that visually-driven climbing fibers (cf) of the rabbit cerebellar flocculus encode movement of the visual world with reference to three axes of rotation. These not-quite-orthogonal axes thus constitute a coordinate system for whole-field retinal image motion (hereafter termed "retinal slip") to the same extent that the planes of the semicircular canals define a not-quite-orthogonal reference frame for angular accelerations of the head.

The similarity between the visual-cf and vestibular coordinate systems has resurrected a fundamental issue of sensorimotor integration: When vestibular and visual measurements are combined in, say, the cerebellum, how are their respective reference frames reconciled? We might predict that for "meaningful" visuovestibular interactions, the canal and cf rotational axes would have to coincide. But it is not clear that they do (Simpson, this volume). Furthermore, to finish the process of visuomotor coordination, the curvilinear, time-varying, overspecified control coordinates defining the actions of eye-muscle effectors must be added to this mix. How, therefore, are the correlations between signals expressed in such different reference frames to be computed, the correlations that presumably permit relevant sensory signals to modify effector commands? The spinal frog solves a version of this problem, as do, for example, humans interpreting signals from the labyrinths within the context of head position on the neck (45).

For the CNS to match up information expressed in differing coordinate frames might appear to require circuitry dedicated to translating between one frame and another. This has been the position of Pellionisz and Llinas (52,53), who have envisioned a motor rendition of such circuitry within the cerebellum (the abilities of spinal frogs notwithstanding). Their proposal, couched in tensorial taxonomy, is that the cerebellum does its translating as though it were an optical bench dealing with light: Image-like measurement vectors enter the cerebellum, encounter an appropriate series of tensorial mirrors, lenses, and prisms, interfere, and emerge scattered along a variety of novel axes. Pellionisz and Llinas have added dynamics to this process by having their cerebellum compute various time-derivatives of the intensity fluctuations in the incoming measurement-vectors. But the coordinate-translation procedure itself-- which specifies the orientation, as it were, of each tensorial mirror-- seems to lack dynamics of its own. It has no "memory". Hence, for any translations to have utility, cerebellar circuitry must encode accurate representations of the target coordinate systems (i.e., the coefficients of the "tensors"). The cerebellum thus would be remarkably well acquainted with its information sources and targets.

In theoretical (11,12) and experimental (14) studies of the cf apparatus, I also have also had occasion to discuss the cerebellar tuning of coordinate systems for motor control. Below I hope to extend some of these ideas to provide an alternative to the Llinas-Pellionisz scheme in the functioning of cf pathways. In particular, it will be suggested that the cf system could support continuously changing motor "reference frames" that allow conversations between heterogeneous sensorimotor coordinate systems (including those imposed by the external environment) without any emulation or modeling of those systems.

Climbing Fibers and Their Puzzles

The olivocerebellar, cf system pairs anatomical simplicity with physiological complexity. Anatomically, the cerebellar corpus appears to be composed of subzones of cerebellar cortex uniquely linked, by Purkinje cell axons, to matching subregions of the cerebellar and vestibular nuclei (19,65). Each such corticonuclear pairing is in turn supplied by cf from an equally unique subarea within the inferior olivary nuclei (1,15,62). Thus, the overall organization of the olivocerebellar pathway seems to be one of rather simple "private channels" associating olivary, cortical, and cerebellar nuclear subregions, with little or no overlap between them (Fig. 1). As if to reinforce this point-to-point arrangement, cf's bypass the interneuronal machinery of the cerebellar cortex to synapse directly and powerfully upon Purkinje cells, while also exciting, via collaterals, the targets of those cells among cerebellar nuclear neurons (1).

The physiological complexity of the cf apparatus quickly becomes apparent when

one tries to find out what is being transmitted within its private channels, and what the significance of each anatomically distinct channel is (50,51). Thus, for example, Fig. 2 illustrates the behavior of a neuron within the olivary complex in a precollicularly decerebrate cat capable of walking spontaneously upon a treadmill (48). The neuron projects to a region of the

cerebellar cortex (Zone A, lobule V, of the vermis) implicated in locomotor coordination by a variety of criteria (reviewed in ref. 14). Despite that, the cell does not seem particularly interested in the cat's stepping, discharging infrequently and apparently erratically as a function of the step cycle. It turns out that this particular neuron does have a greater probability of discharging at certain epochs during the step cycle (not shown here, but see ref. 14), as well as during locomotor speed changes (notice the slight increase of activity as the cat begins to walk in Fig. 2). But as a rule, cf activity recorded in either the olive or the cerebellar cortex (60) rarely gets beyond this probabilistic relationship to locomotor movement. Antedating the locomotor findings are similar results obtained with other motor paradigms (e.g., refs. 28,29,30,36,41,43,46,47,59,61), and the story can be further expanded (refs. 2,14,40,49 for further information) to allow the following short list of cf puzzles to be compiled:

WHY DO CF PATHWAYS EXHIBIT

Their Precise, Private-Channel Anatomical Organization?

Their Poor Activity-Correlation with Movement Events?

Their Low Discharge Frequencies?

Their Lengthy Conduction Delays?

Their Refractoriness to Peripheral Inputs?

There are, I think, plausible responses to these questions. Those responses will return us to the topic of the reference frames employed for motor coordination.

Puzzles Resolved: I.

Early experimental attempts to sort out what climbing fibers do entailed their chronic destruction by mechanical (44,64) or pharmacological (21,38) means. Cerebellar ataxia of varying severity ensues, suggesting that, puzzles aside, the cf do provide some continuing contribution to the cerebellum's coordinational task. However, these results are subject to the criticism that Purkinje cells chronically deprived of cf lose their ability to influence the

cerebellar nuclei (34,35). Removing the cf is thus tantamount to stripping off the cerebellar cortex, and probably reveals little about the cf per se.

A more recent approach to the cf influence has been to activate the fibers deliberately and to observe the behavioral results. An elegant way of doing that is to employ the MAO inhibitor harmaline to induce synchronous discharges of most (probably all) neurons within the accessory nuclear subdivisions of the inferior olive (10,20,32,37,58). This region includes most areas contributing cf to the "locomotor" cerebellum; and the outcome, as seen in a spontaneously swimming decerebrate rat, is illustrated in Fig. 3: A swimming "step cycle" is evident in the alternating activity of the two ankle antagonists. Interrupting

those activity periods, however, are high-frequency (approximately 12/sec), rhythmical pauses in the EMG. The interruptions are known to arise from the synchronous climbing fiber volleys that harmaline induces (63), and the phenomenon has prompted speculation that cf activity should aid transient, abrupt, stimulus-triggered, or "phasic" aspects of motor coordination (2,33,37, 56). The suggestion is retained by Llinas and Pellionisz in their speculations concerning reference frames for movement (52,53). Yet the proposal has always been difficult to reconcile with the time-delays and refractoriness of cf pathways, as well with the paucity of evidence associating cf activity with frankly "phasic" motor performances (e.g., saccades; 46,47). Furthermore, cf activity under harmaline does not respect the private channels of the olivocerebellar system (i.e., all the "channels" carry the same signal; 58), nor is there evidence that massive synchronization is a typical occurrence among olivary neurons (it is not apparent in multiunit recordings from the olive; 6,14).

One can employ microstimulation of subregions within the inferior olivary complex to accomplish the same deliberate activation of cf pathways while preserving their private-channel attributes. The motor outcome of this intervention differs greatly from that induced by harmaline, as is illustrated for the walking decerebrate cat of Fig. 4: Here we see that stimulation in a

given olivary subregion selects particular groups of muscles and alters the "tonic" EMG level upon which their cyclical, stepping-related activity is superimposed. In addition, that tonic biasing persists for tens of seconds following the cessation of the olivary stimulus; and, reflective of which muscle groups are affected, the animal's walking takes on a particular, enduring postural skew (hindlimb hyperextension or flexion in Fig. 4). Changing the locus of microstimulation within the olive, and thus the private channel through which the cf act, changes the "directionality" of the skew-- but preserves its lengthy time-course.

These findings (supported by others described below) resolve, I think, some of our puzzles about cf pathways: Their low discharge frequencies and lengthy

conduction delays seem mirrored in the equally lengthy duration of the postural biasing their activity appears to regulate. A different directional "sign" for that biasing appears to be encoded by each of the private channels into which the pathways are partitioned. Fig. 5, derived from an early mathematical model (11,12) used to predict Fig. 4's results, summarizes this view of the cf regime.

Animals treated with olivary microstimulation take on locomotor postures resembling those produced by Graham Brown using tonic labyrinthine and neck reflexes (39). Like the latter, the cf-induced postural skews can be created independently of whether the animal is stationary or locomoting (13). To me, this indicates that such skews could be employed to reference the directionality in space of an otherwise "spatially-neutral" stepping performance. The cf influence, in other words, joins those from labyrinths, neck, eye, and proprioceptors to mold generic locomotion into uphill or downhill, circling, sidling, or rectilinear, progression. Here, therefore, is the simple beginning of our association of the olivocerebellar system with the regulation of motor-coordinational reference frames.

To fill that last idea out, and to resolve our remaining cf puzzles, it will be necessary to augment the "locomotor" cf discussion above with data pertaining to the "visuomotor" cf reaching the cerebellar flocculonodular region. A commonality between these two arenas of cf function is suggested by the slow ocular nystagmus which results activating from activating, again by microstimulation, the visuomotor cf of awake rabbits (7). The nystagmus can persist for tens of seconds, and I deem it to be the oculomotor homolog of the sustained postural skews instituted by cf activation during locomotion (both phenomena may owe themselves to a protracted suppressive effect of cf volleys upon Purkinje activity; 16,54). The allure of visuomotor cf pathways is that we know a great deal about them within the context of "all" the circuitry required to elaborate a motor behavior. We will be exploiting that context to construct a qualitative, though explicit, model of cf paths and reference frames that may apply to visuomotor and locomotor processes alike.

Puzzles Resolved: II.

As schematized in Fig. 6, the visuomotor cf are embedded into a collection of interacting oculomotor reflexes concerned with stabilizing gaze (5,12). The basic oculomotor commands in this complex are typically instituted by head

rotations. These activate the semicircular canals and institute compensatory ocular counterrotation via the vestibuloocular reflex (VOR). The efficacy of the open-loop VOR in transducing these motor commands is evaluated by a retinal assessment of gaze stability. In a stationary visual world, that amounts to a comparison of eye versus head movement. Any mismatches appear as "retinal slip" to be transmitted in parallel to the optokinetic reflex (OKR) apparatus and to the visuomotor olivocerebellar pathways (Simpson, this volume). The response of the merged OKR/cf complex to such slip is then applied to outgoing VOR commands as a gaze-stabilizing modification (3).

Fig. 6's parallelism between OKR circuitry and the visuomotor cf (which we know about because optokinetic responses survive cerebellectomy; 55) resolves our remaining cf puzzles quite readily: At first approximation, the OKR is a simple negative feedback system which forever is attempting to reduce the "errors" (i.e., retinal slip) it detects. That same error signal is given to the cf. Thus, the normal action of the OKR is to disfacilitate those cf, which could leave the impression that the latter are "unresponsive" to ongoing movement events or peripheral input. Indeed, the better the OKR is at its job, the more pronounced is this "unresponsiveness". But if we assume that this deduction holds true for all types of cf paths (a test is currently underway for locomotor cf's), then we actually have come to another puzzle-- namely, what can the cf paths contribute to the performance of the circuitry they parallel?

We have already seen that activity in cf's seems associated with long time-course "postural biasing" in both the locomotor and oculomotor settings. That time-constant could be expected to appear as a substantial phase lag in the input-to-output transfer function of, for example, the OKR. The gain of the transfer function might also diminish with input frequency. As it happens, eye velocity in the OKR does lag retinal-image velocity considerably, and there is an accompanying reduction of gain with velocity in all response planes (3,25). Furthermore, the velocity response-lag in the OKR, when observed in neurons of the medial vestibular nucleus, almost wholly disappears immediately following an inactivation of visuomotor climbing fibers (8). The phase/gain characteristics of the OKR mark it as a "low-pass" system; and on the preceding evidence, I thus suspect that the visuomotor cf are employing their "postural biasing" potential to regulate those low-pass properties. It is interesting that other "low-pass" oculomotor reflexes, notably the utricular/otolithic (4) and cervico-ocular (9), also feature correlated cf activity (22,23,42). By contrast, eliciting the "high-pass" VOR results in somewhat equivocal cf correlations (e.g., refs 6,26,28,36).

As we've already described, the "directionality" of the postural biases associated with locomotor cf's are keyed to the private-channel organization of the cf pathways. There are anatomical hints of a similar private-channel partitioning of the visuomotor cf paths (65); and it is tempting, therefore, to associate with those channels Simpson's "directional" clustering of visuomotor cf's along rotational axes of retinal slip (57; see Introduction). We don't yet know, of course, whether this sensory directionality is mapped by those cf's into an analogous directional (or postural) bias applied to eye movement. However, as the model to follow illustrates, it may not be necessary to have such a matchup between sensory and motor "reference frames" in cf pathways-- or anywhere else in motor systems akin to Fig. 6: Instead, the private-channels

and the biasing dynamics associated with the olivocerebellar apparatus may improvise and skew the appropriate coordinate transformations as circumstances dictate.

Modeling the Olivocerebellar Tuning of Motor Coordinational Reference Frames

Fig. 7 sets forth our qualitative model, which is simply an abstraction of Fig. 6 above. Again, the efficacy of generic motor commands is evaluated by a comparison with the resulting motor outflow and the "environment" (here rendered more explicitly than in Fig. 6), with any "errors" signalling reflex

mechanisms and their associated cf paths to modify the actions of effectors. We are, however, interested in representating motor and sensory "coordinate systems" more explicitly. For clarity's sake, Fig. 7 does this using-- as an overall reference frame-- two orthogonal Cartesian coordinates, i and j. The hypothetical internal coordinate systems used by the motor-effector, reflex, and cf paths of Fig. 7 are represented by linear vector functions. Each of these functions twists i and j in the manner illustrated by a diagram at the site where that function resides. Thus, for example, if the motor-command/effector-action path in Fig. 7 were the VOR, then head rotation along the i dimension would yield eye movement in a plane tilted roughly 45 degrees relative to i; a more normal VOR (in terms of direction) would be produced by rotation in the j dimension.

I chose a rather pathological collection of "internal coordinates" for Fig. 7 to emphasize, again, the problem of meshing sensorimotor reference frames. If Fig. 7 represented the VOR/OKR system, would head movements ever yield compensatory eye movements in the appropriate direction? Pellionisz and Llinas (52,53) have advanced their "tensorial" cerebellum and its collection of coordinate transformations as a cure for problems of this sort (and as far as I know, a tensor is just a painful way of representing multilinear vector functions-- so we've already got a few, analgesically, in Fig. 7). There is, however, an alternative to Pellionisz' and Llinas' notions: It lies in the postural-biasing, "low-pass" properties of the cf private-channels. We have modeled these very simply in Fig. 7 with a stage of componentwise time-integration. If we represent the "comparison" stage of Fig. 7 with vector subtraction (as in the computing of retinal slip), and if the remainder of the system is, for the moment, similarly linear (see below), then the "outflow" vector of Fig. 7 is governed by:

$$(1+g)(\dot{\vec{v}}) + h(\vec{v}) = h(\vec{u} + \vec{w}) + (f+g)(\dot{\vec{u}}) + g(\dot{\vec{w}})$$

where

$\vec{v}$ is the "outflow" vector

$\vec{u}$ is the "command" vector

$\vec{w}$ is the "environment" vector

and f, g, and h are the vector functions describing the internal coordinates of the "effector-action", "reflex", and "cf" pathways, respectively.

To illustrate the typical behavior of this system, its reaction to a step-function "command" vector is illustrated in Fig. 8 (we will skip environment vectors for now): Here we have elected to switch in successively each pathway of Fig. 7 so that their separate influences on motor outflow can be seen. Initially only the "effector-action" path is active. When a command

vector appears, having a non-zero component only in the i dimension, this path twists that command into an inappropriate motor outflow along both i and j. When the "reflex" path is then enabled, it is able to suppress much of the inappropriate j-directed outflow-- but also kills a portion of the i-directed output in the process. Finally, we activate the "cf" path, which begins to integrate up a "postural bias" in each of its two private channels. When that integration ceases, we see that the outflow vector has come into both amplitude and directional accord with the original command. In other words, the cf apparatus has computed offsets between the differing reference frames of Fig. 7 to allow efficacious information exchange between them. If our "command" vector now suddenly disappeared, the "animal" to which Fig. 7 corresponded would be left with a directional/postural skew proportional to the slowly decaying activity in its cf channels. Like the gyroscopes of an inertial guidance system, these activity residues form implicit reference frames in their own right.

The phenomena of Fig. 8 should not be too surprising, since Fig. 7 is but a generalization of the familiar "proportional-plus-integral" controller of classical system theory. Because the integrator in the system receives only an "error" signal, it cannot rest until that signal is zero. There is thus the propensity for instability; and the internal coordinates of Fig. 7 cannot skew measurements in just any direction (to wit, the crossed optic wiring of the anterior visual field in albino rabbits, which leads to an unstable OKR; 18). The system also responds more quickly if f, g, and h are already in reasonable accord to begin with-- perhaps explaining the fair congruence of semicircular canal planes and visuomotor cf response axes (Simpson, this volume); the spinal frog might be recalled in that regard.

To provide this working alternative to the cerebellum of Pellionisz and Llinas (52,53), I have emphasized their concern for the reconciliation of internal sensorimotor reference frames. However, it could eventually prove more utilitarian to see the cf system as matching up those frames with references imposed by the outside environment-- computing how to deal with a slewing visual, auditory, or proprioceptive topography that we hadn't anticipated. There the residuum of activity in cf channels might be called "vection".

Conclusions

I have tried to argue that the olivocerebellar apparatus contributes to a CNS faculty that creates postural or directional reference frames for motor coordination; and that the cf have the particular task of continuously updating these frames. The basis for that updating may stem from attempts to reconcile the internal coordinate systems of different sensorimotor modalities-- or, more probably, from the weighted history of directional congruence or correlation between motor commands and environmental conditions. Hay (31) and more recently, Collewijn (17), have stressed the importance of command/feedback correlation in modifying oculomotor responses. My guess is that the subtractive "comparator" and the cf "integrator" of Figs. 6 and 7 will evolve into such a correlator. At the same time, perhaps, the linearity of our qualitative model-- which poses clear limitations-- will give way to circuitry that can produce dynamic coordinate transformations using some form of controllable multiplication. Present investigations into the cf's ability to regulate Purkinje responsivity (24) may supply the requisite details.

References

1. Andersson, G., and Oscarsson, O. Climbing fiber microzones in cerebellar vermis and their projection to different groups of cells in the lateral vestibular nucleus. Exp. Brain Res., 1978, 32: 565-579.

2. Armstrong, D.M. Functional significance of connections of the inferior olive. Physiol. Rev., 1974, 54: 358-417.

3. Baarsma, E.A., and Collewijn, H. Vestibulo-ocular and optokinetic reactions to rotation and their interaction in the rabbit. J. Physiol. (Lond), 1974, 238: 603-625.

4. Barmack, N.H. A comparison of the horizontal and vertical vestibulo-ocular reflexes of the rabbit. J. Physiol. (Lond), 1981, 314: 547-564.

5. Barmack, N.H. Immediate and sustained influences of visual olivocerebellar activity on eye movement. In: Talbott, R.E., and Humphrey, D.R. (Ed.), Posture and Movement, Raven (New York), 1979: 123-168.

6. Barmack, N.H., and Hess, D.T. Multiple-unit activity evoked in dorsal cap of inferior olive of the rabbit by visual stimulation. J. Neurophysiol., 1980, 43: 151-164.

7. Barmack, N.H., and Hess, D.T. Eye movements evoked by microstimulation of dorsal cap of inferior olive in the rabbit. J. Neurophysiol., 1980, 43: 165-181.

8. Barmack, N.H., and Pettorossi, V.E. Influence of visual olivocerebellar inactivation on the optokinetic properties of neurons in the vestibular nuclei of rabbits. Progress in Oculomotor Research, 1981, 12: (in press).

9. Barmack, N.H., Pettorossi, V.E., and Nastos, M.A. The cervicoocular reflex of the rabbit and its linear summation with the vestibuloocular reflex. Neurosci. Abstr., 1980, 6: 694.

10. Batini, C., Bernard, J.F.,Buisseret-Delmas, C., Conrath-Verrier, M., and Horcholle-Bossavit, G. Harmaline-induced tremor. II. Unit activity correlation in the interposito-rubral and oculomotor systems of cat. Exp. Brain Res., 1981, 42: 383-391.

11. Boylls, C.C. A theory of cerebellar function with applications to locomotion. I. The physiological role of climbing fiber inputs in anterior lobe operation. In: COINS Technical Report 75C-6, Dept. of Computer & Information Sciences, Univ. of Massachusetts (Amherst), 1975.

12. Boylls, C.C. A theory of cerebellar function with applications to locomotion. II. The relation of anterior lobe climbing fiber function to locomotor behavior in the cat. In: COINS Technical Report 76-1, Dept. Computer & Information Sciences, Univ. Massachusetts (Amherst), 1976.

13. Boylls, C.C. Prolonged alterations of muscle activity induced in locomoting premammillary cats by microstimulation of the inferior olive. Brain Res., 1978, 195: 445-450.

14. Boylls, C.C. Contributions to locomotor coordination of an olivocerebellar projection to the vermis in the cat: Experimental results and theoretical proposals. In: Courville, J., Lamarre, Y., and de Montigny, C. (Ed.), The Inferior Olivary Nucleus: Anatomy and Physiology, Raven (New York), 1980: 321-348.

15. Brodal, A., and Walberg, F. The olivocerebellar projection in the cat studied with the method of retrograde axonal transport of horseradish peroxidase. IV. The projection to the anterior lobe. J. Comp. Neurol., 1977, 172: 85-108.

16. Colin, F., Manil, J., and Desclin, J.C. The olivocerebellar system. I. Delayed and slow inhibitory effects: An overlook salient feature of cerebellar climbing fibers. Brain Res., 1980, 187: 3-27.

17. Collewijn, H. The Oculomotor System of the Rabbit and Its Plasticity. In: Studies of Brain Function, Springer-Verlag (New York), 1981, 5.

18. Collewijn, H., Winterson, B.J., and DuBois, M.F.W. Optokinetic eye movements in albino rabbits: inversion in anterior visual field. Science, 1978, 199: 1351-1353.

19. Courville, J., and Diakiw, N. Cerebellar corticonuclear projection in

the cat. The vermis of the anterior and posterior lobes. Brain Res., 1976, 110: 1-20.

20. de Montigny, C., and Lamarre, Y. Rhythmic activity induced by harmaline in the olivo-cerebello-bulbar system of the cat. Brain Res., 1973, 53: 81-95.

21. Denk, H., Haider, M., Kovac, W., and Studynka, G. Verhaltensänderung und Neuropathologie bei der 3-Acetylpyridinvergiftung der Ratte. Acta Neuropath., 1968, 10: 34-44.

22. Denoth, F., Magherini, P.C., Pompeiano, O., and Stanojević, M. Responses of Purkinje cells of the cerebellar vermis to neck and macular vestibular inputs. Pflügers Arch. Ges Physiol., 1979, 381: 87-98.

23. Denoth, F., Magherini, P.C., Pompeiano, O., and Stanojević, M. Responses of Purkinje cells of cerebellar vermis to sinusoidal rotation of neck. J. Neurophysiol., 1980, 43: 46-59.

24. Ebner, T.J., and Bloedel, J.R. Role of climbing fiber afferent input in determining responsiveness of Purkinje cells to mossy fiber inputs. J. Neurophysiol., 1981, 45: 962-971.

25. Erickson, R.G., and Barmack, N.H. A comparison of the horizontal and vertical optokinetic reflexes of the rabbit. Exp. Brain Res., 1980, 40: 448-456.

26. Ferin, M., Grigorian, R.A., and Strata, P. Mossy and climbing fibre activation in the cat cerebellum by stimulation of the labyrinth. Exp. Brain Res., 1971, 12: 1-17.

27. Fukson, O.I., Berkinblit, M.B., and Feldman, A.G. The spinal frog takes into account the scheme of its body during the wiping reflex. Science, 1980, 209: 1261-1263.

28. Ghelarducci, B., Ito, M., and Yagi, N. Impulse discharges from flocculus Purkinje cells of alert rabbits during visual stimulation combined with horizontal head rotation. Brain Res., 1975, 87: 66-72.

29. Gilbert, P.F.C., and Thach, W.T. Purkinje cell activity during motor learning. Brain Res., 1977, 128: 309-328.

30. Harvey, R.J., Porter, R., and Rawson, J.A. The natural discharges of Purkinje cells in paravermal regions of lobules V and VI of the monkey's cerebellum. J. Physiol. (Lond), 1977, 271: 515-536.

31. Hay, J.C. Visual adaptation to an altered correlation between eye movement and head movement. Science, 1968, 160: 429-430.

32. Headley, P.M., Lodge, D., and Duggan, A.W. Drug-induced rhythmical

activity in the inferior olivary complex of the rat. Brain Res., 1976, 101: 461-478.

33. Houk, J.C. Motor control processes: New data concerning motoservo mechanisms and a tentative model for stimulus-response processing. In: Talbott, R.E., and Humphrey, D.R. (Ed.), Posture and Movement, Raven (New York), 1979: 231-241.

34. Ito, M. Roles of the inferior olive in the cerebellar control of vestibular functions. In: Courville, J., Lamarre, Y., and de Montigny, C. (Ed.), The Inferior Olivary Nucleus: Anatomy and Physiology, Raven (New York), 1980: 367-377.

35. Ito, M., Nisimaru, N., and Shibuki, K. Destruction of inferior olive induces rapid depression of synaptic action of cerebellar Purkinje cells. Nature, 1979, 277: 568-569.

36. Lisberger, S.G., and Fuchs, A.F. Role of primate flocculus during rapid behavioral modification of vestibuloocular reflex. I. Purkinje cell activity during visually guided horizontal smooth-pursuit eye movements and passive head rotation. J. Neurophysiol., 1978, 41: 733-763.

37. Llinás, R., and Volkind, R.A. The olivocerebellar system: Functional properties as revealed by harmaline-induced tremor. Exp. Brain Res., 1973, 18: 69-87.

38. Llinás, R., Walton, K., Hillman, D.E., and Sotelo, C. Inferior olive: Its role in motor learning. Science, 1975, 190: 1230-1231.

39. Lundberg, A., and Phillips, C.G. T. Graham Brown's film on locomotion in the decerebrate cat. J. Physiol. (Lond), 1973, 231: 90P-91P.

40. MacKay, W.A., and Murphy, J.T. Cerebellar modulation of reflex gain. Progress in Neurobiology, 1979, 13: 361-417.

41. Mano, N-I Simple and complex spike activities of the cerebellar Purkinje cell in relation to selective alternate movement in intact monkey. Brain Res., 1974, 70: 381-393.

42. Marini, G., Provini, L., and Rosina, A. Gravity responses of Purkinje cells in the nodulus. Exp. Brain Res., 1976, 24: 311-323.

43. McElligott, J.G. Cerebellar neuronal firing patterns in the intact and unrestrained cat during walking. In: Herman, R.M., Grillner, S., Stein, P.S.G., and Stuart, D.G. (Ed.), Neural Control of Locomotion, Plenum (New York), 1976: 781-784.

44. Murphy, M.G., and O'Leary, J.L. Neurological deficit in cats with lesions of the olivocerebellar system. Arch. Neurol., 1971, 24: 145-157.

45. Nashner, L.M., and Wolfson, P. Influence of head position and proprioceptive cues on short latency postural reflexes evoked by galvanic stimulation of the human labyrinth. Brain Res., 1974, 67: 255-268.

46. Noda, H., and Suzuki, D.A. The role of the flocculus of the monkey in saccadic eye movements. J. Physiol. (Lond), 1979, 294: 317-334.

47. Noda, H., and Suzuki, D.A. Processing of eye movement signals in the flocculus of the monkey. J. Physiol. (Lond), 1979, 294: 349-364.

48. Orlovsky, G.N., and Shik, M.L. Control of locomotion: a neurophysiological analysis of the cat locomotor system. In: Porter, R. (Ed.), Neurophysiology II, International Review of Physiology, 1976, 10: 281-317.

49. Oscarsson, O. Functional organization of spinocerebellar paths. In: Iggo, A. (Ed.), Handbook of Sensory Physiology, Springer (New York), 1973, 2: 339-380.

50. Oscarsson, O., and Sjölund, B. The ventral spino-olivocerebellar system in the cat. I. Identification of five paths and their termination in the cerebellar anterior lobe. Exp. Brain Res., 1977, 28: 469-486.

51. Oscarsson, O., and Sjölund, B. The ventral spino-olivocerebellar system in the cat. III. Functional characteristics of the five paths. Exp. Brain Res., 1977, 28: 505-520.

52. Pellionisz, A., and Llinás, R. Brain modelling by tensor network theory and computer simulation. The cerebellum: Distributed processor for predictive coordination. Neuroscience, 1979, 4: 323-348.

53. Pellionisz, A., and Llinás, R. Tensorial approach to the geometry of brain function: Cerebellar coordination via a metric tensor. Neuroscience, 1980, 5: 1125-1136.

54. Rawson, J.A., and Tilokskulchai, K. Suppression of simple spike discharges of cerebellar Purkinje cells by impulses in climbing fibre afferents. Neuroscience Lett., 1981, 25: 125-130.

55. Robinson, D.A. Adaptive gain control of vestibuloocular reflex by the cerebellum. J. Neurophysiol., 1976, 39: 954-969.

56. Rushmer, D.S., Roberts, W.J., and Augter, G.K. Climbing fiber responses of cerebellar Purkinje cells to passive movement of the cat forepaw. Brain Res., 1976, 106: 1-20.

57. Simpson, J.I., Soodak, R.E., and Hess, R. The accessory optic system and its relation to the vestibulocerebellum. In: Granit, R., and Pompeiano, O. (Ed.), Reflex Control of Posture and Movement. Prog. Brain Res.,

Elsevier/North-Holland (New York), 1979, 50: 715-724.

58. Sjölund, B., Björklund, A., and Wiklund, L. The indolaminergic innervation of the inferior olive. 2. Relation to harmaline induced tremor. Brain Res., 1977, 131: 23-37.

59. Thach, W.T. Discharge of Purkinje and cerebellar nuclear neurons during rapidly alternating arm movements in the monkey. J. Neurophysiol., 1968, 31: 785-797.

60. Udo, M., Matsukawa, K., Kamei, H., Minoda, K., and Oda, Y. Simple and complex spike activities of Purkinje cells during locomotion in the cerebellar vermal zones of decerebrate cats. Exp. Brain Res., 1981, 41: 292-300.

61. Viala, G., Coston, A., and Buser, P. Participation de cellules du cortex cérébelleux aux rythmes "locomoteurs" chez le lapin curarisé, en absence d'informations somatiques liées au mouvement. Soc. Biol. Comptes Rendus, 1970, 271: 688-691.

62. Voogd, J., and Bigaré, F. Topographical distribution of olivary and corticonuclear fibers in the cerebellum: A Review. In: Courville, J., Lamarre, Y., and de Montigny, C. (Ed.), The Inferior Olivary Nucleus: Anatomy and Physiology, Raven (New York), 1980: 207-234.

63. Weiss, M. Influence du systeme olivo-cérébello-bulbaire sur les neurones moteurs de la moelle lombaire chez le chat aprés administration d'harmaline. Arch. ital. Biol., 1978, 116: 1-15.

64. Wilson, W.C., and Magoun, H.W. The functional significance of the inferior olive in the cat. J. Comp. Neurol., 1945, 83: 69-77.

65. Yamamoto, M. Localization of rabbit's flocculus Purkinje cells projecting to the cerebellar lateral nucleus and the nucleus prepositus hypoglossi investigated by means of the horseradish peroxidase retrograde axonal transport. Neuroscience Lett., 1978, 7:197-202.

Figure Captions

Fig. 1 (from ref. 14): The private-channel organization of cf pathways from the inferior olivary nucleus to the cerebellum. Schematized in (A) is the partitioning of cerebellar cortex into discrete subzones, each of which has a demarcated projection area within the cerebellar (or vestibular) nuclei. How these associated corticonuclear groupings are bound together by a cf private-channel projection is illustrated in (B). A given channel ultimately allows inputs to a small region of olive to oversee outflow from a correspondingly circumscribed subdivision of the cerebellum. Examples of such inputs are peripheral receptors or spinal interneuronal networks (SIN's) arriving via the ventral spino-olivocerebellar pathway (VF-SOCP; 50,51). Outflow can exit on the lateral reticulospinal tract (LRST)-- among a host of others-- to arrive at SIN's and/or motoneurons (MN's). Other abbreviations: v.IV = fourth ventricle; P-axon = axon of a Purkinje neuron.

Fig. 2 (ref. 14 and unpublished): Reactions of an olivary neuron to the onset (lefthand traces) and maintenance (righthand traces) of spontaneous treadmill locomotion (0.22 m/sec) in a precolliculary decerebrate cat. The cell was located in the caudal portion of the medial accessory olivary nucleus contributing cf to zone A of the contralateral cerebellar vermis (verified antidromically and histologically; 13,14). Locomotor measurements consist of hip joint-position trajectory of the contralateral hindlimb, and EMG's from selected muscles (both raw and "integrated"-- rectified/filtered-- signals are shown; the latter are inverted for lateral gastrocnemius and tibialis anterior). Note the discharge frequency of the cell relative to the time scale, and the erratic relationship of those discharges to the step cycle. See text and ref. 14 for further remarks.

Fig. 3 (unpublished): Effect of harmaline-elicited cf volleys upon spontaneous locomotor muscle activity in a precollicularly decerebrate rat. The animal is swimming freely while suspended in a tank of water. See text for details.

Fig. 4 (from ref. 14): Prolonged postural alterations initiated by olivary microstimulation in a locomoting, precolliculary decerebrate cat. Stimulation (4.5 sec cathodal train of 0.2 msec pulses, 20 microamperes, 20/sec) was delivered at sites (black circles and "target" symbols) along a dorsoventral electrode penetration through the caudal medial accessory olivary nucleus (shown shaded in parasagittal cross-section with stereotaxic levels; NC = cuneate nucleus). Microstimulation effects were assessed using contralateral hindlimb hip-joint trajectories and rectified/filtered EMG's (see Fig. 2 above; lateral gastrocnemius EMG inverted). Stimulation in the caudorostral portion of the nucleus yields "extensor" EMG biasing, which shifts to "flexor" at the rostroventral margin. Few effects appear outside the olive (a correlation between biasing and the appearance of cf field potentials in the cerebellum has been shown elsewhere; 13). Note that the biasing survives the microstimulation interval for a protracted period, sometimes exceeding 1 minute.

Fig. 5 (from ref. 14): Theoretical mechanism relating private channels of the cf system to the regulation of postural/directional biases applied to movement. On the left are 3 cerebellar subzones, each serviced by a cf private channel. The quasi-periodic outflow from each of these zones during a motor performance (locomotion, in this instance) is graphed against time at the right, along with the cf activity in the private channel serving one of the subzones. During the interval marked "STIM", some outside event raises the overall traffic in that channel. In response, there is a gradual elevation in the activity baseline of outflow from the targeted cerebellar subregion. This "DC" bias is translated into a postural or directional bias applied to ongoing movement (illustrated in before/after fashion by two snapshot diagrams of a stepping limb).

Fig. 6: The context of the visuomotor cf within the visuovestibular apparatus. Details in text.

Fig. 7: A qualitative model, based upon Fig. 6, for illustrating the reconcilitation of internal (or, alternatively, environmentally-imposed) reference coordinate frames by the cf system. All signal flows through the network are vectors referenced to a single Cartesian coordinate scheme, while the internal references for those signals are captured in vector functions mapping Cartesian coordinates into other orientations (described in text). Notice that the "reference frames" of the cf, reflex, and effector-action pathways are neither orthogonal, nor in agreement; and we could overspecify them without loss of generality (though that hasn't been done here).

Fig. 8: Behavior of the model to a step-function "motor command" vector, where the system vector functions are specified as the pre-multiplying matrices

$$f = \begin{bmatrix} 0.6 & 0.2 \\ 0.7 & 0.9 \end{bmatrix} \qquad g = \begin{bmatrix} -0.17 & 0.98 \\ -0.98 & 0.17 \end{bmatrix} \qquad h = 0.1 * \begin{bmatrix} 0.98 & -0.17 \\ -0.17 & 0.17 \end{bmatrix}$$

and all resulting signals are resolved into their (i,j) coordinates. As described in the text, the pathways of Fig. 6 are switched in sequentially, with the "effector" path initially active, the "reflex" path awakening at the small black arrow, and the "cf" path following at the large open arrow. The traces represent 1000 time-units of duration 0.1 (arbitrary scaling). Details in text.

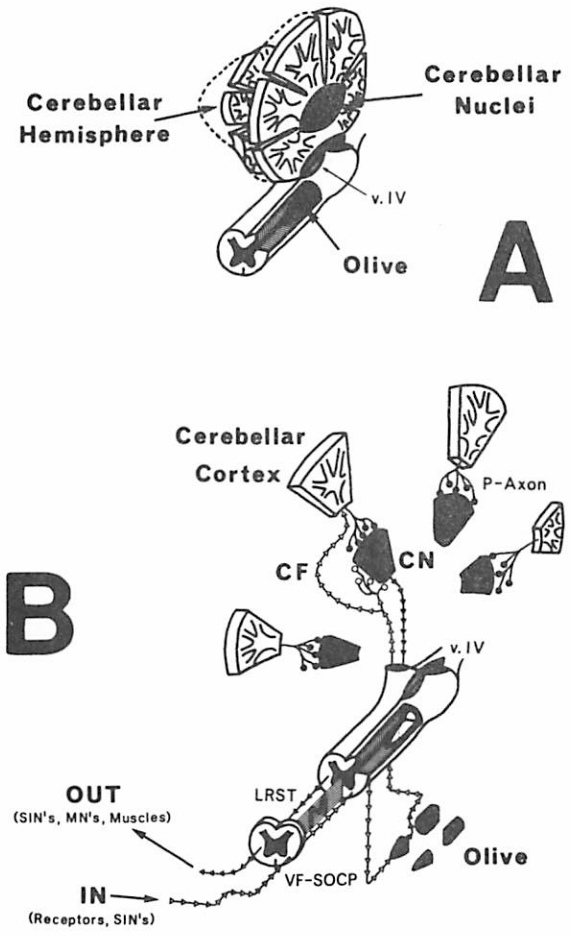
Cerebellar
Hemisphere
Cerebellar
Nuclei
v. IV
Olive
A
B
Cerebellar
Cortex
P-Axon
CF
CN
v. IV
OUT
(SIN's, MN's, Muscles)
LRST
Olive
VF-SOCP
IN
(Receptors, SIN's)

Fig. 1

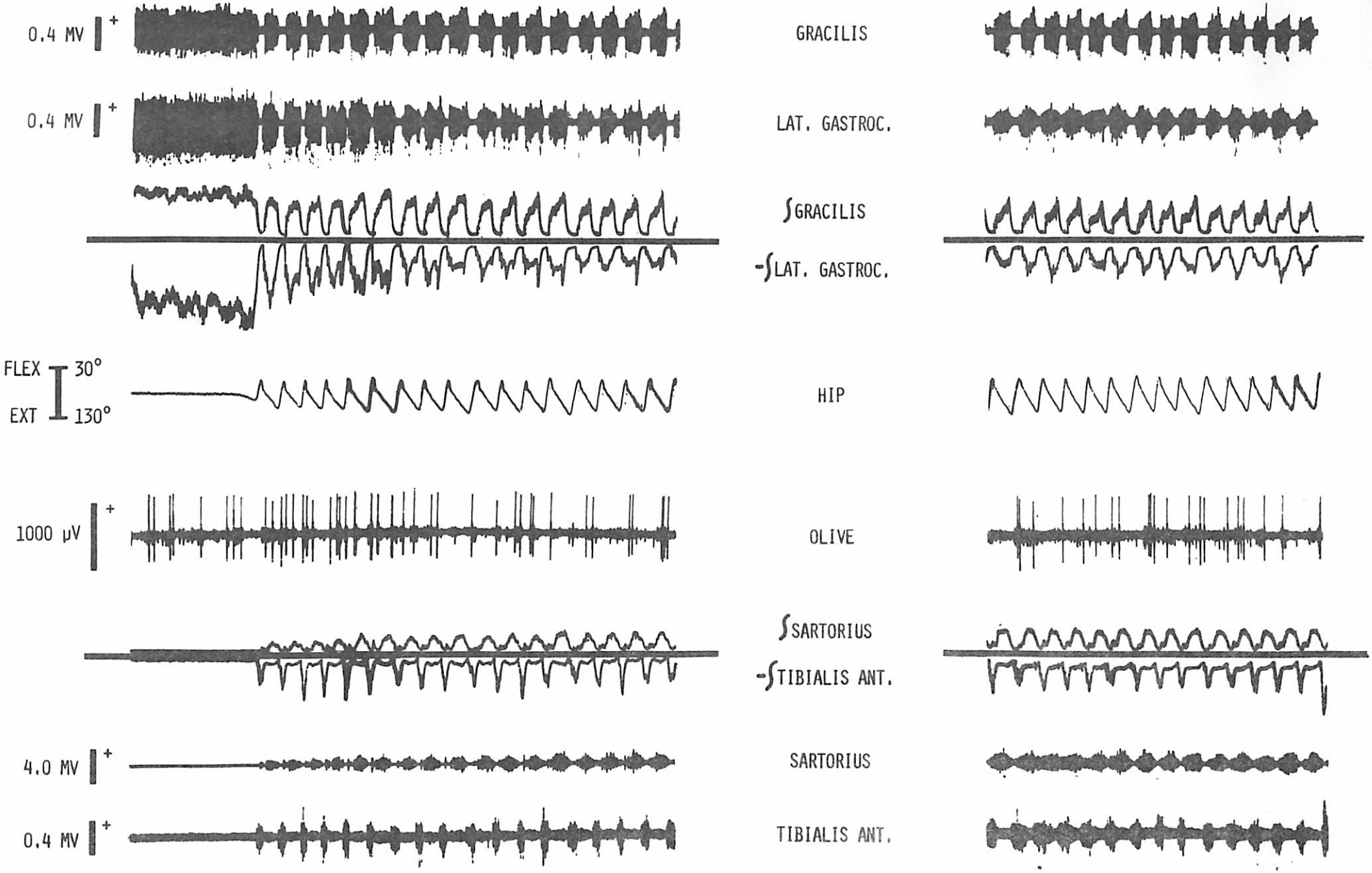
0.4 MV
+
GRACILIS
0.4 MV
+
LAT. GASTROC.
∫GRACILIS
-∫LAT. GASTROC.
FLEX
30°
EXT
130°
HIP
1000 μV
+
OLIVE
∫SARTORIUS
-∫TIBIALIS ANT.
4.0 MV
+
SARTORIUS
0.4 MV
+
TIBIALIS ANT.
8 SEC

Fig. 6

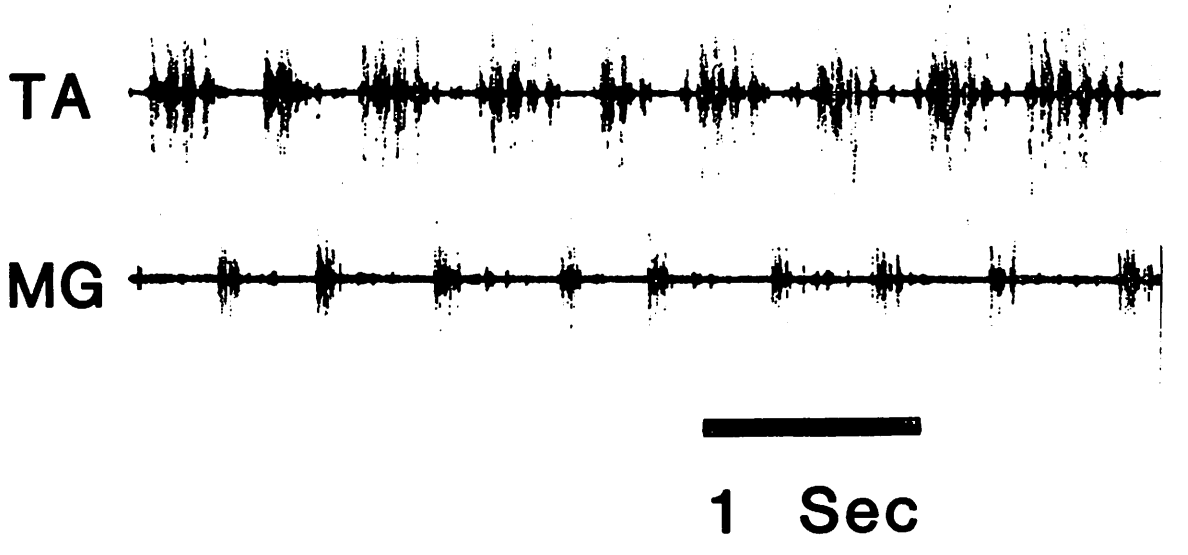

Fig. 3

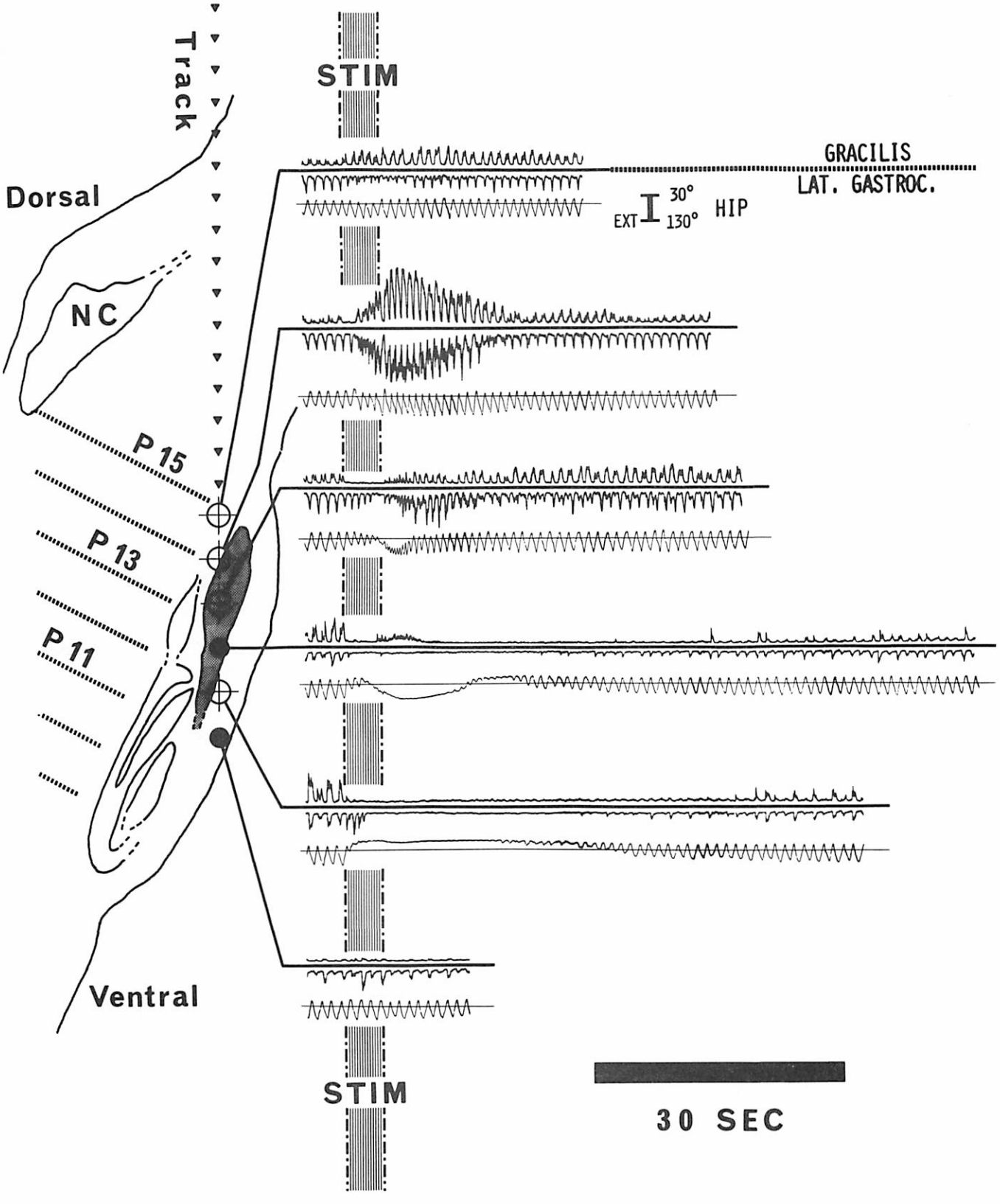
Track
STIM
GRACILIS
LAT. GASTROC.
Dorsal
EXT
30°
130°
HIP
NC
P 15
P 13
P 11
Ventral
STIM
30 SEC

Fig. 4

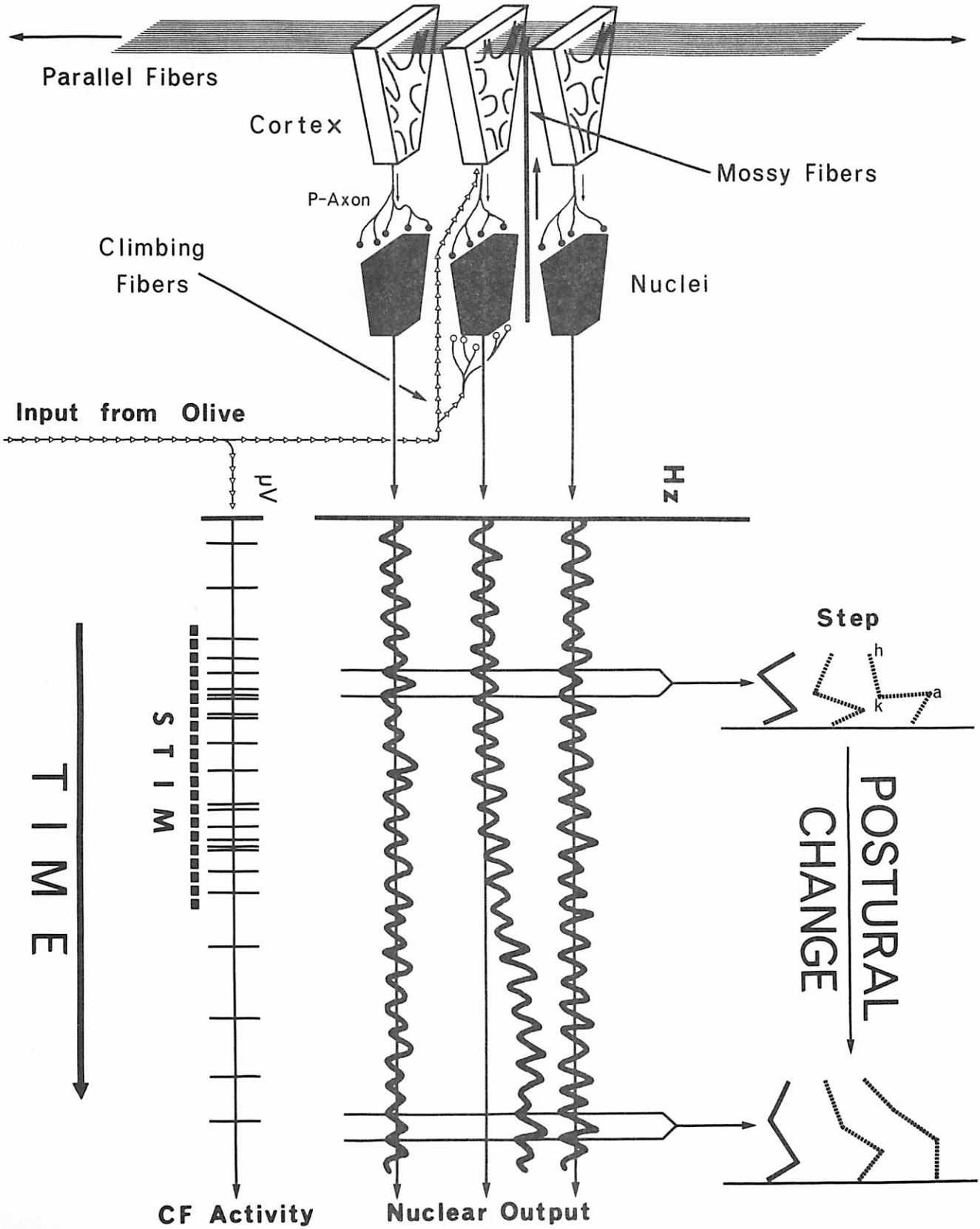
Parallel Fibers
Cortex
Mossy Fibers
P-Axon
Climbing
Fibers
Nuclei
Input from Olive
μV
Hz
Step
h
k
a
TIME
STIM
POSTURAL
CHANGE
CF Activity
Nuclear Output

Fig. 5

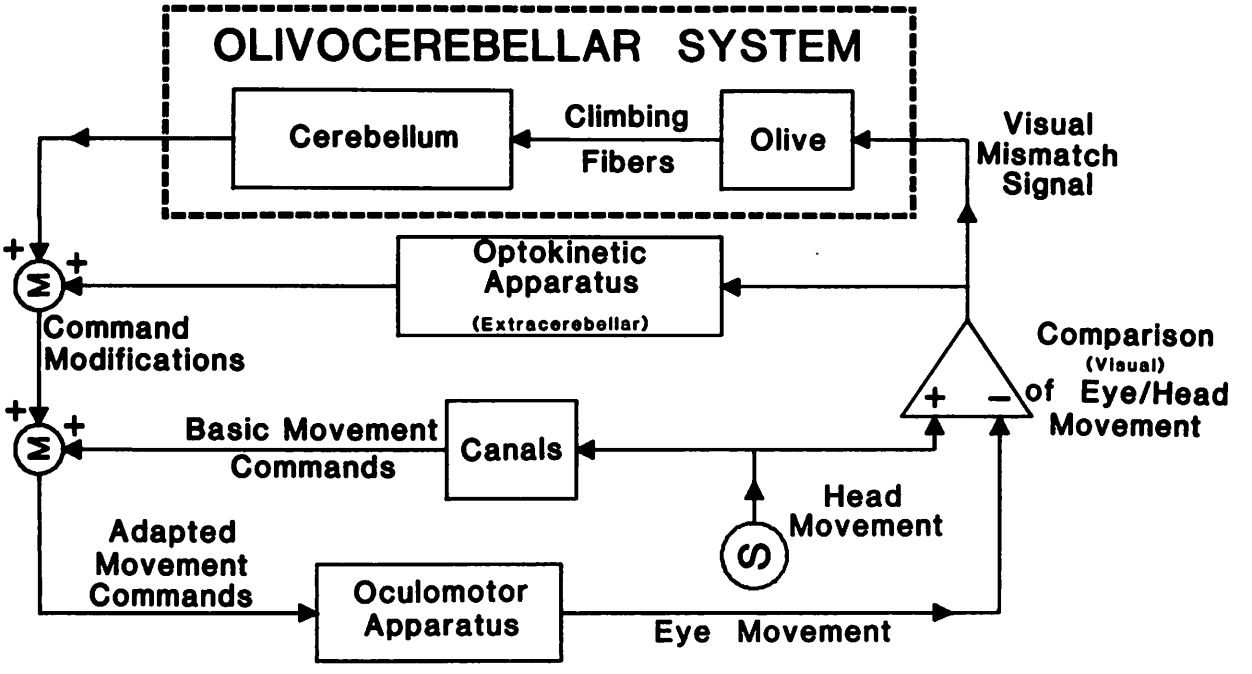
OLIVOCEREBELLAR SYSTEM
Cerebellum
Climbing Fibers
Olive
Visual Mismatch Signal
Optokinetic Apparatus
(Extracerebellar)
Command Modifications
Comparison (Visual) of Eye/Head Movement
Basic Movement Commands
Canals
Head Movement
Adapted Movement Commands
Oculomotor Apparatus
Eye Movement

Fig. 6

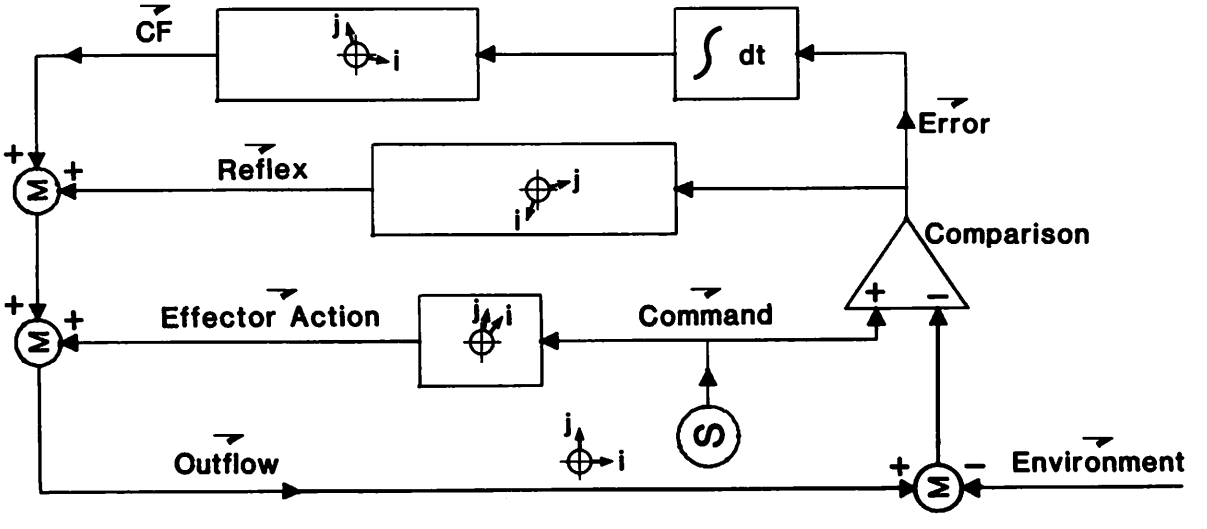
CF
dt
Error
Reflex
Comparison
Effector Action
Command
Outflow
Environment

Fig. 7

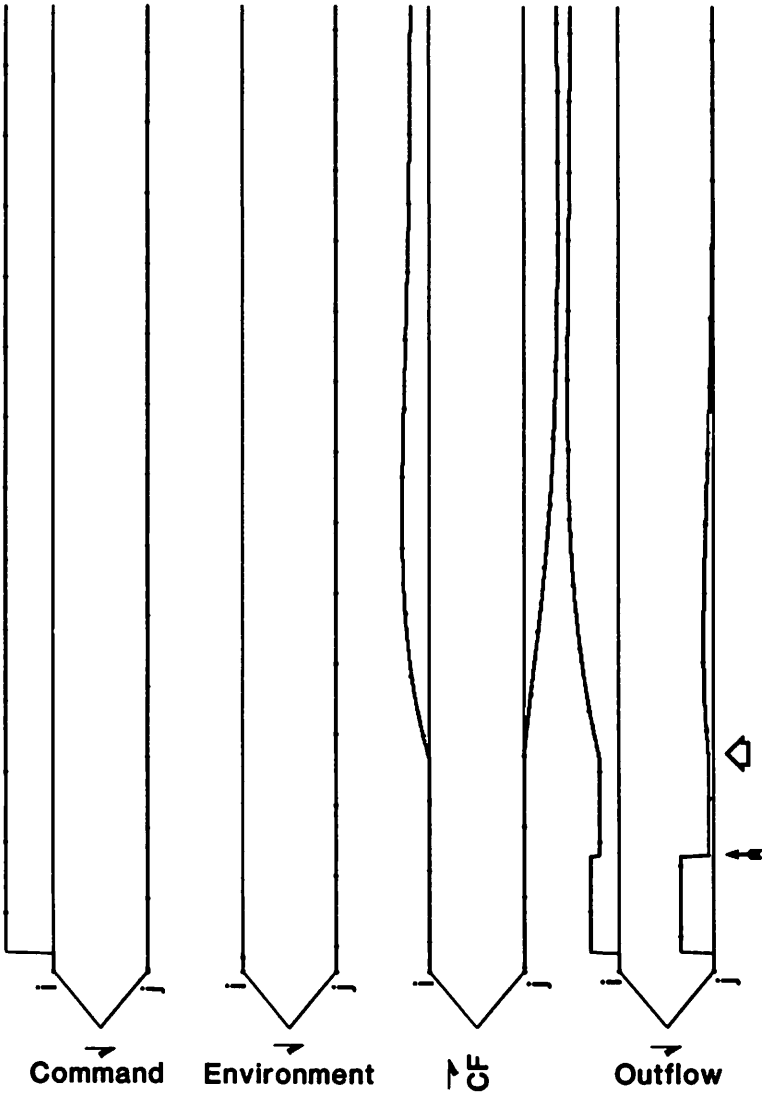

Fig. 8

Neil M. Montgomery and Katherine V. Fite: VISUOMOTOR CONNECTIONS IN THE ANURAN MESENCEPHALON

Understanding the structural and functional correlates of the anuran accessory optic system has been the subject of investigation in our laboratory for the last few years (Montgomery, et al., 1979, 1981a; Fite, et al., 1980). The results thus far indicate that this system may ultimately be amenable to computer simulation. Although many fundamental relationships concerning its basic neuroanatomical organization remains to be clarified.

Neuroanatomical Constituents

The cellular constituents of the nucleus of the basal optic root (nBOR) closely resemble those previously described for the superficial layers of the optic tectum (Szekely and Lazar, 1976). Four morphologically distinct cell types were identified within the terminal field of nBOR: 63% stellate, 19% amacrine, 14% elongate and 4% ganglionic cells. Both the stellates and amacrines appear to be intrinsic neurons. In addition, pyriform neurons located in the region medial to nBOR send their dendrites into the retinal terminal field and their axons to central grey and oculomotor column n.III and n.IV. This medial region has been termed the 'peri-nBOR' region. Also found within peri-nBOR are commissural neurons which send axons through the posterior commissure to the opposite anterior ventral mesencephalon. The nBOR also receives afferents from another source located in the anterior thalamus from cells postsynaptic to the thalamic retinal terminal fields (n.Bellonci and corpus geniculatum). Optic and thalamic afferents, as well as the dendritic and axonal processes of stellates appear to converge upon the dendrites of both ganglionic and pyriform neurons in a glomerular configuration. Ganglionic neurons within nBOR project dorsally to the 'dense core' region of the large-celled pretectal nucleus.

The organization of the anuran anterior ventral mesencephalon appears somewhat similar to that of the tectal columns described by Szekely and Lazar (1976). This column is organized along the lateral-to-medial axis of the brain with optic afferents arborizing in the superficial portions of the column, in nBOR. Medial to nBOR is the peri-nBOR region which may be conceptualized as representing the central portion of the column. The central grey and oculomotor nuclei would then represent the deep layers of such a column (Figure 1). Cells in peri-nBOR (in addition to being postsynaptic to nBOR) also receive a projection from the nucleus of the cerebellum which may contain somatic information. The central grey and oculomotor nuclei n.III and n.IV receive a dense projection from the vestibular nuclei. Thus, within this single 'column', information is present from the visual and vestibular systems and perhaps also from the somatosensory system. Neurons within the central grey also send dendrites through peri-nBOR and into the primary retinal terminal field of nBOR. These neurons appear similar morphologically to the pyramidal neurons of the deep tectal layers. All of these observations strongly imply that the anuran accessory optic system may play an important role in visuo-ocular behaviors as has been suggested previously by Herrick (1948), Shanklin (1933) and a number of subsequent investigators.

Functional Correlates

Several studies have suggested that the accessory optic system mediates horizontal optokinetic nystagmus (OKN) (Lazar, 1973; Fite, et al., 1979). In order to further evaluate the role of the accessory optic

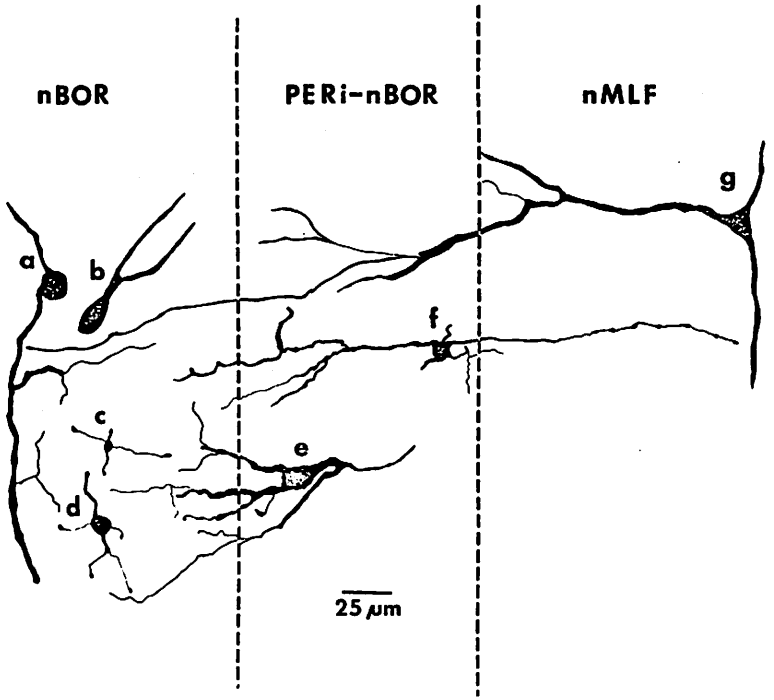

Figure I. Cell types occurring in each of 3 regions associated with the accessory optic system as determined from Golgi and HRP material (camera lucida drawings). nBOR region: a - ganglionic neuron, b - elongate neuron, c - amacrine cell, d - stellate neuron; peri-nBOR region: e - commissural neuron, f - pyriform neuron; nMLF (nucleus of medial longitudinal fasciculus): g - reticular neuron.

system in OKN, extensive pre- and post-lesion response baselines[1] were established using OKN response frequences (saccadic eye and head movements) over a wide range of effective pattern velocities for thirty Rana pipiens. Selective and localized electrolytic lesions were produced in nBOR, peri-nBOR, the large-celled pretectal nucleus, the dorsal tegmental grey adjacent to the uncinate neuropil and the optic tectum. Localized lesions of nBOR, the large-celled pretectal nucleus and the dorsal tegmental grey all substantially reduced OKN response frequences, however, the specific effects varied according to lesion site. Lesions restricted to nBOR produced a reduction in OKN frequences of response only at the higher range of pattern velocities. Lesions of the large-celled pretectal nucleus or the dorsal tegmental grey produced a reduction in horizontal OKN response frequences across all pattern velocities but did not totally abolish OKN in any of the animals tested. Lesions of peri-nBOR totally abolished OKN in all animals tested. These lesions did not invade nBOR, the central grey, or the oculomotor nuclei or tracts.

Three neural systems are known to exist in the peri-nBOR region: the neurons of peri-nBOR, the tecto-bulbar pathway and the descending projections from the dorsal tegmental grey. Neurons of peri-nBOR, as we have seen, are postsynaptic to nBOR and project directly to the oculomotor nuclei and related central grey. The tecto-bulbar pathway also passes through peri-nBOR as it ascends to the region of the nucleus profundus lateralis. In peri-nBOR, small collaterals of the tecto-bulbar pathway leave the main bundle and arborize in and around the cranial nerve nucleus n.III (Montgomery, et al., 1981b). Descending fibers from the dorsal tegmental grey also pass through peri-nBOR on the way to the brainstem and some of these fibers arborize in the peri-nBOR region. Thus

peri-nBOR contains pathways by which information from nBOR, the dorsal tegmental grey and the tectum reach the oculomotor nuclei n.III and n.IV. As this region represents the final common pathway by which visual information is relayed to the oculomotor system, it is not surprising that ocular nystagmus can be abolished by lesions in this region. In another series of experiments, the cranial nerves n.III and n.IV were bilaterally transected. These transections produced a decline in the frequence of OKN responses but did not abolish the behavior. It appears that lesions of peri-nBOR have a more drastic effect on OKN response than transection of either n.III and n.IV. We believe that the lesions reported by Lazar (1973) in which OKN was abolished by lesions of nBOR may have also involved the peri-nBOR region. If so, discrepencies which currently exist between his findings and those of the present study might thus be reconciled.

Several recent electrophysiological studies have indicated that nBOR and the surrounding region contains wide-field directions sensitive units (Cochran, et al., 1982; Grunberg and Grasse, 1981). These units have been recorded from nBOR, peri-nBOR and the central grey surrounding the oculomotor nuclei. Based on our anatomical observations, information from nBOR could be relayed to the large-celled pretectal nucleus, which also contains wide-field directions sensitive units and from there to the dorsal tegmental grey and tectum. The weight of evidence today indicates that nBOR and its homologs in a number of different species are involved in both horizontal and vertical optokinetic responses, however, the majority of responses reported in electrophysiological studies indicate a predominance of vertical units. Units responding to horizontal OKN stimuli appear to be localized predominently in the pretectum, particularly in the nucleus of the optic tract (NOT) of mammals and avians.

The NOT may be homologous to the large-celled pretectal nucleus of anurans.

In summary, our studies have indicated that the anuran anterior mesencephalon is composed of small, relatively undifferentiated groups of neurons which undoubtedly subserve a number of visuomotor functions which are mediated by larger and more specific neural populations in amniotes.

[1]We thank Micheline D. Taylor for extensive behavioral testing and Lynn Bengston for histological assistance.

References

Cochran, S. L., W. Precht, and N. Dieringer (1980) Direction-selective neurons in the frog's visual system. Neurosci. Abstracts 6:121.

Fite, K., N. Montgomery, C. Wojcicki, and L. Bengston (1980) Visuomotor correlates of the anuran accessory optic system. Neurosci. Abstracts 6:839.

Fite, K. V., A. Reiner, and S. P. Hunt (1979) Optokinetic nystagmus and the accessory optic system of pigeon and turtle. Brain Behav. Evol. 16:192-202.

Grunberg, E. R., and K. L. Grasse (1980) Basal optic projection in the grog, Rana Pipiens. Neurosci. Abstracts 6:121.

Herrick, C. J. (1948) The Brain of the Tiger Salamander. Chicago: University of Chicago Press.

Lazar, G. (1973) Role of the accessory optic system in the optokinetic nystagmus of the frog. Brain Behav. Evol. 5:443-460.

Montgomery, N. M., K. V. Fite, and L. Bengston (1981a) The Accessory Optic of Rana Pipiens: Neuroanatomical Connections and Intrinsic Organization. J. Comp. Neurol. 203:595-612.

Montgomery, N. M., K. V. Fite, and L. Bengston (1981b) The anuran oculomotor complex (n.III and n.IV). Anat. Rec. 199:176.

Montgomery, N. M., K. V. Fite, and L. Bengston (1979) The anuran accessory optic system: A neuroanatomical analysis. Neurosci. Abstracts 5:798.

Shanklin, W. M. (1933) The comparative neurology of the nucleus opticus tegmenti with special reference to Chameleon vulgaris. Acta Zool. 14:163-184.

Szekely, G., and G. Lazar (1976) Cellular and synaptic architecture of the optic tectum. In R. Llinas and W. Precht (eds): Frog Neurobiology. Berlin: Springer-Verlag, pp. 407-434.

Chapter 4: Detour Behavior and Depth Perception

David J. Ingle: INTERACTIONS BETWEEN TECTUM AND PRETECTUM: NEW LEVELS OF COMPLEXITY

T.S. Collett: PICKING A ROUTE: DO TOADS FOLLOW RULES OR MAKE PLANS?

Donald H. House: THE FROG/TOAD DEPTH PERCEPTION SYSTEM -- A COOPERATIVE/COMPETITIVE MODEL

David J. Ingle: INTERACTIONS BETWEEN TECTUM AND PRETECTUM: NEW LEVELS OF COMPLEXITY[1]

Some of the complexities of the decisions that frogs and toads make in real life situations have already been modelled in laboratory situations. It has been shown that frogs and toads have at least rudimentary capacities for selective attention (Ingle, 1975); size-distance constancy (Ingle, 1968; Ingle & Cook, 1977; Ewert & Gebauer, 1973) and are able to plan efficient routes around barriers in pursuit of prey (Ingle, 1971b; 1982a) see also Collett's chapter in this volume). I will propose in this section that these three phenomena each depend upon subtle modes of interaction between pretectum and tectum: I will argue that pretectal input to tectum in modulates the excitability of certain tectal neurons and "switches" dominance among pairs of alternative pathways.

The first hypothesis makes use of the model developed by Ewert (see chapter) in which pretectal neurons tonically inhibit the "worm-detection" neurons (T5-2 cells) in layers 7 and 8 of the tectum. Some additional considerations are required to formulate an explanation of size-distance constancy in terms of changing size-selection by the T5-2 neurons. In this model, I propose that pretectal inputs to tectum alter the weighting of different sensory inputs to the prey-catching system, as a function of viewing distance. In case of detour behavior, I propose that a second set of pretectal neurons modulates the excitability of tectal cells so as to alter the usual topographic relationship between stimulus location and motor output. The switching of sensory or motor patterns originates in different pretectal cell groups (lateral and posterior nuclei, respectively) and the sites of modulation underlying the two types of decision are proposed as layers 7+8 and layer 6, respectively. There is a

[1]Most of the author's recent research described in this chapter was supported by an N.I.H. research grant (NS 13, 592).

significant amount of evidence available to support the first hypothesis regarding size-constancy, although critical experiments still need to be done to move from plausibility to proof. The second model is but one of two equally plausible alternatives, and relies upon indirect evidence and the esthetic appeal of "parallism" for present support. I present the first model because I think it likely to be largely correct, and include the second as an example where reasoning by analogy can lead to an interesting and testable model of behavior. Without exploring the model as a "gedanken experiment" certain behavioral details might never be sought.

SIZE-DISTANCE CONSTANCY: SOME FACTS AND AN EXPLANATION

Fortunately, independent studies of size-selection by frogs and toads during variations of prey-distance (Ingle & Cook, 1977; Ewert & Gebauer, 1973 provide closely comparable data. When we compare prey-size preference in frogs at distances of 7.5 vs 15 cm, the optimal angular size for elicitation of orienting responses is reduced by about half. For distances up to 18 cm, both Ewert and I have found that animals' preferences are linked to the prey-objects' real size, although beyond that distance stimuli of a 2^{o} angular height remain prepotent. Because, these effects are found within the frog's monocular fields, it is likely that optical accommodation cues are critical for size estimation. This hypotheses (Ingle, 1968) was later confirmed by Collett (1977) for Bufo marinus in my laboratory. The simplest (but unproved) assumption is that a corrollary discharge is initiated during the frog's effort to accommodate upon a prey object, such that increased corrollary discharge bias the tectum toward response to larger objects. The next problem would be to link effects of corrollary discharge to a neural system with access to the tectum. While it is possible that this might be done through the giant neurons of lateral tegmentum whose axons enter the tectum (Wilczynski & Northcutt, 1977), it is more probable that the robust projections from neurons of pretectum or rostral thalamus (Ingle

& Trachtenberg, 1974; Ingle & Quinn, 1982b)influence the size-selectivity of tectal neurons. In fact, studies by Ewert and colleagues (see chapter) have demonstrated a direct inhibitory effect of pretectum activation upon visual sensitivity of tectal neurons (Ewert et al. 1974a). Moreover removal of pretectum inputs via lesions or knife cuts abolishes the usual selective response of T5-2 neurons to small prey-like objects (Ewert et al. 1974b). It is also important to note that pretectum lesions abolish the size-distance constancy effect in toads, at least when tested soon after surgery (Ewert & Gebauer, 1973).

The model developed by Ewert & vonSeelen (1974) accounts well for the effects of large objects in increasing pretectal input to tectum, and hence their suppressive effect on feeding behavior. But additional dynamic changes must be postulated to explain how an increase in tonic inhibition (while viewing more distant objects) can switch the bias of T5-2 cells to smaller objects. Let us consider first the cell's response to prey when inhibition is very low (the object is very close, or prey-odor has excited the animal). Here the preference for large objects must reflect dominance of class-3 inputs to T5-2 cells, since class-2 fibers respond little or not at all to 20^{o} objects. If class-3 fiber input outweighs that of class-2 upon T5-2 neurons during the low-inhibition state, how can increased inhibition from pretectum reverse the dominance during distant viewing of prey? Unless we invent a new class of interneurons which are only active during distant viewing, we must postulate a facilitatory mechanisms which amplifies the effects of class-2 input to tectum, without affecting class-3 inputs.

Such a facilitatory mechanism has been inferred from behavioral studies (Ingle, 1975, 1982c)in which it is found that the second of two brief prey movements is much more effective in eliciting prey-strikes (e.g. 11% vs 85% probability). Furthermore, I have reported that many neurons in layers 7 and 8

will show the enhancement effect if a small spot is moved twice within their ERF (Ingle, 1982c). The physiological basis of this temporal summation effect, which lasts up to 4 sec (Ingle, 1982c),is thought to involve the after-discharge properties of a unique class of non-retinal units in the frog's superficial tectum (Ingle, 1975). These units are selective for small objects (as are class-2 retinal fibers) and typically show peak discharge at 3-4 sec following brief incursions into their small ERF's (Ingle & Naylor, in preparation). I have presented a model in which these after-discharging units are identified with recurrent axons from deeper tectal soma, frequently seen in Golgi preparations (Lazar & Szekely, 1967). According to this model (see Fig. 1) the recurrent axon depolarizes dendrites of T5-2 cells for 2-4 sec following a brief movement, and so lowers the threshold of cell activation for a second burst of class-2 input fibers within the critical 4 sec interval. Additional support for this model comes retrospectively from an earlier study (Ingle, 1971c) in which toads showed delayed snapping at stopped dummy prey stimuli, which peaked in frequency after a delay of 3-4 seconds.

Since pretectal inhibition must delay the response of T5-2 cells to initial stimulus motion, the initial dominance of large object excitation will soon give way to dominance of smaller stimuli in 2-3 sec because only the latter can activate the recurrent-axon loop. We find confirmatory support for this explanation in an earlier study (Ingle, 1973c) which showed that frogs with short response latencies (less than 1.5 sec) preferred as prey 16^{o} to 6^{o} high objects, while those with latencies averaging more than 2.5 sec preferred the smaller stimulus as prey. A final observation (Ingle, 1973a) should also be quoted in support of the model: frogs disinhibited in feeding by pretectal lesions show ERF's for layer 7 and 8 cells to be about twice the average size of cells recorded at this level in normal frogs. An unpublished experiment by Cromarty & Ewert has replicated this effect in a more satisfactory manner: the same

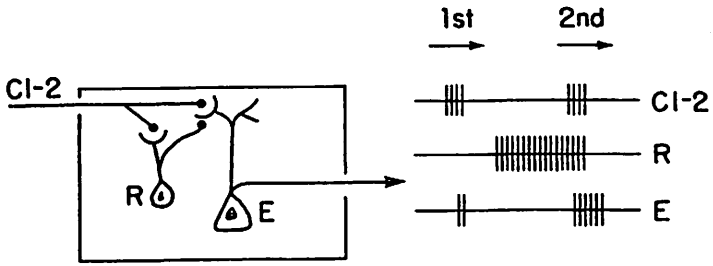

Fig. 1

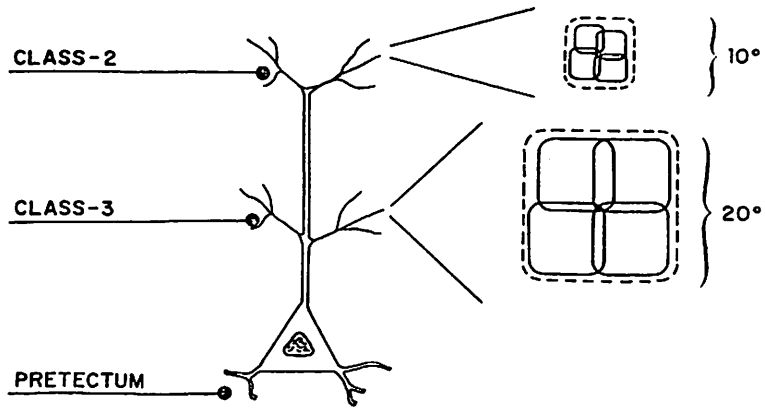

Fig. 2

neuron shows an expanded ERF following a pretectal lesion induced by injection of kainic acid. Fig. 2 shows how this size change could reflect a switch in dominance from class-2 input (with more restricted ERF spread) to dominance of class-3 inputs with larger ERF's.

I conclude that studies of tectal neurons in the paralyzed animal, plus observations on time-related changes in feeding activity support the idea that size-constancy can result from an interaction of extrinsic inhibition of tectal cells by pretectum and intrinsic self-exciting loops. A proof of the model, however, will depend upon rather difficult chronic recording experiments in the behaving animal to establish the link between object distance and ERF changes of tectal neurons. Are there less arduous ways to test the model as presented here? One critical test would be based upon the assumption that changes in stimulus-size election of T5-2 neurons depends upon a switch in relative efficacy of class-2 and class-3 inputs upon prey-catching activity. If either class of input could be selectively removed, there should be no substantial shifts of prey-angle preference with viewing distance, only changes in response rate.

A recent study in our lab (Glasser et al., 1982) has shown that shallow burns or cuts of the tectal surface, made orthogonally to the course of retinal fiber projections, can selectively denervate the upper tectal lamine of class-2 input, leaving robust activity of class-3 axons which travel below the cut. After 3-4 weeks time, the class-3 fibers have sprouted or regenerated terminals into the formerly denervated zone and have begun to activate some types of tectal neurons normally associated with class-2 dominance (i.e. the afterdischarge units at the surface, and the ipsilateral tectal projection relayed via the nucleus isthmus). We have seen the incidence of prey catching in the upper visual field increase significantly during this period of "filling in" with aberrant class-3 fibers. It now remains to test such "compensated" frogs for the size-constancy phenomenon: according to the proposed model no constancy

effect will be possible until class-2 axons have regenerated to their rightful receptors and restored the status quo.

DETOUR BEHAVIORS TOWARD OCCLUDED PREY

When frogs or toads view attractive prey that is partially occluded by a semitransparent barrier, they will attempt a detour response if there is a sufficient depth disparity between the prey and the barrier (Locke & Collett 1979; Ingle, 1982a). The attempt to jump through a striped barrier or a fence when the prey is close behind should not be regarded as an "error" since natural barriers are likely to bend under the animal's impact. Three types of detours can be elicited, depending upon the height or width of the barrier: jumping over a low fence, crawling under a fence with a low gap, or jumping to the side of the barrier. The latter response is especially interesting since a toad or frog will re-orient to the initial prey position on clearing the barrier (Fig. 3) even when the prey has been removed before the first jump has been completed (Ingle, 1971b). At present we have no ideas as to how the toad's brain programs the second reverse turn, although our unpublished experiments show that this response is intact in frogs after bilateral removal of telencephalon. The current task is to explain how tectum and pretectum collaborate in producing an integrated sequence of action from primary tendencies to approach prey and avoid barriers.

Detailed film records show that toads achieve a detour by combining two kinds of movement: they rotate the body toward the barrier edge, but sidestep as well during the sequence (Fig. 3). Because a transation movement is added to a rotary movement, the change in head angle is typically less than the angle of the barrier edge in respect to the initial head direction. On the other hand, for objects located within 60^{o} from the frontal midline, the change in head angle (or change in the direction of regard) is significantly greater than would be the case were the prey not occluded. That is to say, the presence

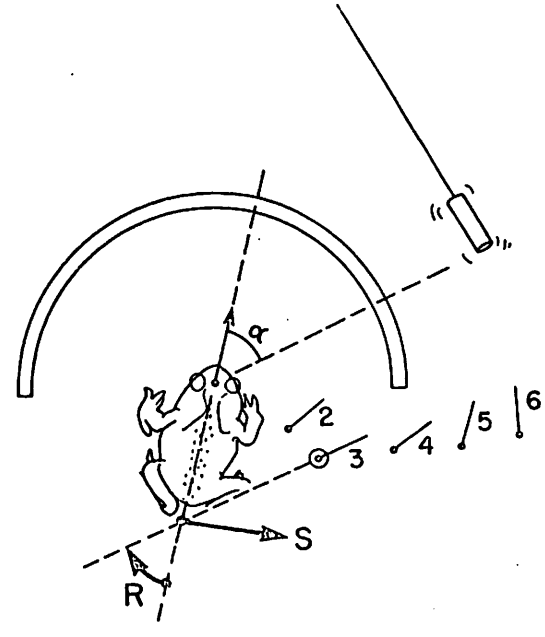

Fig. 3

A diagram of the movements underlying detour behavior in frogs and toads, based upon single frame film drawings from a marine toad (Bufo marinus). The successive changes of head orientation and position are indicated by a dot at the center of the head and a line from this point through the center of the snout (indicating the so-called direction of regard). During the barrier detour sequence, the change in the toad's direction-of-regard is achieved mainly by rotation of the body (R) but also by side-stepping (S). After the animal clears the barrier it re-orients toward the initial prey location (even if the prey has been removed during the detour). Thus the maximal change in direction-of-regard is much larger than the angle of the prey in respect to the toad's initial direction. While the stimulus angle and the final response angle usually coincide in absence of a barrier, its presence induces a considerable overshoot.

of the barrier increases the amplitude of the body rotation such that it "overshoots" the actual position of prey. It is assumed that retinotectal activity initiates the detour sequence (since the response closely follows a sudden prey motion) and we continue to assume that the barrier itself is detected via a retinopretectal mechanism. How then does activity in pretectum initiate a sidestep response, and how does it modify the tectal efferent command so as to produce a stimulus overshoot?

There are at least three first order explanations of detour behavior. One postulates that tectum and pretectum send information to regions of telencephalon where a "higher level" integration of perceptual information occurs and a complex motor program is formulated. While this explanation might be true for mammals, it seems to be negated for frogs by our observations of efficient detour behavior in animals with telencephalon ablated. However, thus far no critical tests have been made for the possibility that the "high level" integration is carried out within rostral thalamus, to which tectum and pretectum both project (Rubinson, 1968; Neary & Wilczynski, 1977). A second alternative, which remains plausible, is that the two retinal-recipient structures project downstream to a brainstem regions where integration of different response tendencies occurs. Thus tonic efferent activity derived from pretectal neurons could "reflect" the tectofugal discharge into a different motor pattern. Third, I advance the notion that the new output pattern is determined within the tectum via modulation from pretectal efferent fibers (demonstrated anatomically by Trachtenberg & Ingle, 1974; Wilczynski & Northcutt, 1977, and Ingle & Quinn, 1982b).

Studies of behavior of split-pons frogs provide relevant information as to neural mechanisms of detour behavior. These animals consistently fail to make side-steps around frontal barriers (45^{o} wide) set on the frontal midline, when a prey object is placed directly behind (Fig. 4 , while split-tegmentum frogs continue to sidestep. The side-step is thus dependent upon the crossed pretectal-

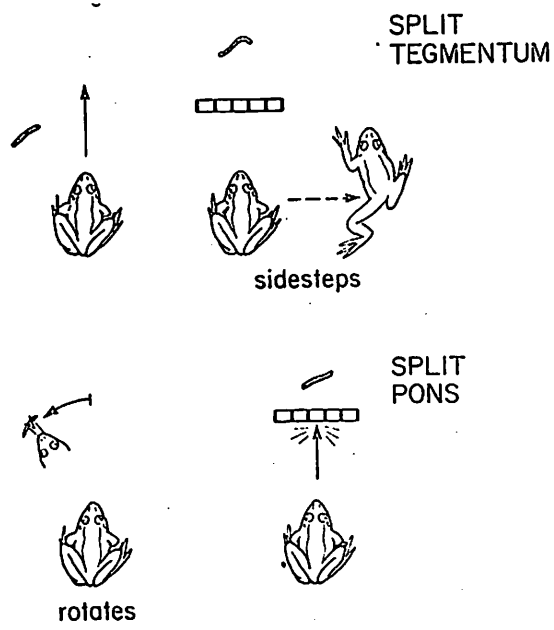

Fig. 4

A summary of some behavioral comparisons between frogs with midline splits of the tegmentum and those with more caudal splits of the isthmic region, here labelled as "split pons" animals. The first group fail to turn toward prey but are able to make a sidestep detour when a frontal worm is occluded by midline barrier. By contrast the second group (below) can rotate the body toward prey but fail to sidestep when a prey is blocked by a small barrier. If the motivation is high and the "split pons" frog finally strikes at the prey, he will always collide with the barrier. The implication of this summary is that tectum initiates and directs turns toward prey via crossed pathways, while pretectum governs turns around barriers via crossed efferent pathways. However, the latter pathway from pretectum to opposite medulla is not necessarily via direct pretectal efferent axons, since other tegmental and medullary groups have commissural connections at the same level.

pontine route, but could not reflect changes of activity in the crossed tectofugal route. These observations strongly suggest that the side-step is independently programmed by the pretectum, but we can only guess how prey-motion initiates this response. It is possible that tectal projections to pretectum activate a sidestep command. It is also possible that descending tectofugal activity in ipsilateral pons interacts there with an ipsilateral projection from the pretectum. This would not contradict evidence from tests of split-pons frogs if that deficit resulted from transection of (unknown) crossed projections from the ipsilateral pons.

The second problem concerns the origin of the turn-overshoot. Because the barrier-detecting region of pretectum (posterior nucleus) projects directly into tectum with a topographic order (Ingle & Quinn, 1982b) we must consider the possibility that this cross-talk between pretectum and tectum serves to re-program the amplitude of prey-orientation by re-organizing the tectal efferent pattern. While there is no direct evidence for this proposition, two unpublished studies do indicate that shifts from normal input-output topography can occur as a result of brain lesions. I earlier observed that a small lateral undercut of the optic tectum, which cut efferent but not afferent fibers, would render frogs unable to orient normally toward stimuli impinging upon that part of tectum deprived of efferent fibers. The consequence of this disconnection was that frogs would either overshoot or undershoot the stimulus position by 20-30^{0}, as judged from film records (Ingle, 1970). This means that excitation derived from prey-motion had "detoured" around the cut by activating neighboring output neurons with intact axons. This "rerouting" of the visuomotor pathway might depend upon short intratectal axons or upon the activity of large-field efferent neurons (see below). A second relevant finding is that frog and toads with large pretectal lesions are unable to orient selectively toward one of two prey stimuli moved synchronously within the lateral field,

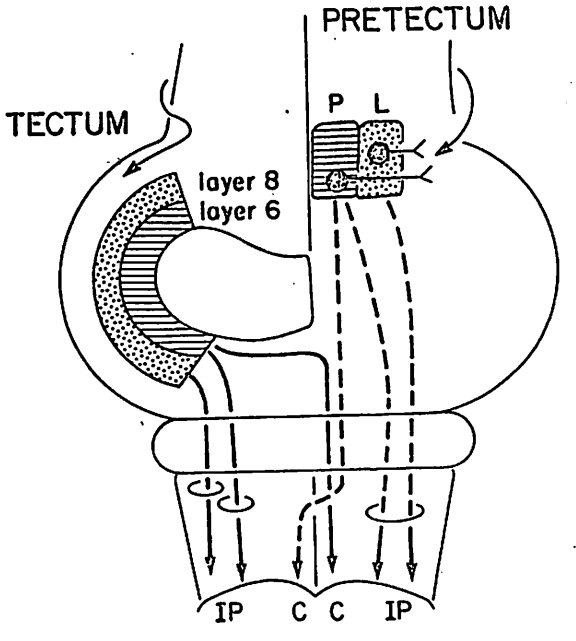

Fig. 5

A schematic view to compare tectal and pretectal efferent projections to the medulla, as seen from an overhead view of a horizontal section of the brain. For clarity, the two different systems are placed on opposite sides of the brain. As reviewed in the text, the more medial tectal layer 6 sends efferents to both sides of the brainstem, while the more lateral laminae (layer 8) sends decending fibers only ipsilaterally. Not shown in the crossed projection to tegmentum via the postoptic commissure which may carry layer 8 axons. The medial pretectal cell group (posterior nucleus) also projects to both sides of the brainstem, while the lateral nucleus projects only ipsilaterally.

although these are separated by as much as 50°. Unlike normal frogs who usually respond cleanly to one or the other target (Ingle, 1973d) these lesioned animals turn repeatedly toward a position half-way between the two stimuli. The best explanation of this syndrome is that the "functional columns" within the tectum are expanded in absence of pretectal inhibition, such that excitation from two foci of input summate upon efferent neurons whose "visual fields" include both stimuli.

In order to explain detour behavior, we assume that the usual motor outputs via small-field neurons are blocked via inhibitory inputs from barrier-detecting pretectal neurons. If the disparity of prey and barrier-edge are not too great, some efferent neurons which normally represent a more lateral input locus will eventually reach threshold and initiate an overshoot turn. These motor elements could be large-field neurons, frequently seen in layer 6 of the tectum after implants in the opposite medial pontine region. The filled dendrites of these so-called "ganglionic cells" (Lazar & Szekely,1967) extend far laterally in each direction for up to one-third the length of the tectum but terminate near the surface. We have recently studied a type of tectal neuron which may correspond to the ganglionic cell, since it has a wide field (60-90°) and responds selectively to small moving spots. These units, which can be best obtained when the frog is under a light paralysis, seem to correspond to the so-called "sameness cells" of Lettvin et al. (1961) in that two or three short stimulus movements are needed before vigorous cell discharge is elicited. Such a long-latency response would normally eliminate these cells from participating in the quick response to non-occluded prey; the small field efferent cells would promptly initiate direct turns toward the prey. However, when the barrier inhibits this direct response, some large-field cells would gradually begin to respond to movement in the periphery of their ERF's and activate an overshoot turn corresponding to the retinotopic

location of their own soma. In support of this model, we have noted that with prey-barrier disparities greater than 35-40° frogs typically move toward the prey, rather than attempting detour movements. Additional behavioral data is needed to define these limits of prey-barrier integration and this value must be compared with ERF size range of the large-field cells. Since frogs do not seem to make overshoot responses to partly occluded prey located more than 90° from the midline, we predict that large-field prey-selective units with caudal ERF's will be rare or absent. This model of tectum-pretectum collaboration has a few virtues, in the author's opinion, which justify the effort here devoted to its elaboration. (1) It accounts for the existence of a strong pretectal-input to tectum, which does not seem to be involved in modulation of prey-selection (according to the knife-cut experiment quoted above); (2) It accounts for the existence of large-field cells which receive class-2 input and project into the efferent channel implicated in regulation or turning amplitude. It is not otherwise clear why large-field cells should aid the accurate localization of prey. (3) It postulates a mode of plasticity in determination of orienting direction which parsimoniously accounts for the effects of small tectal undercuts, and the loss of selective choice between twin prey-stimuli after pretectal lesions. (4) The model is subject to clear experimental refutation, if it is discovered that appropriate cuts between tectum and pretectum (which preserve retinal input to each center) do not eliminate the overshoot turns produced by barriers. (5) Finally, as I have argued elsewhere (Ingle, 1982a), the analagous operation of tectal wide-field neurons can account for other types of variation in orientation amplitude documented in mammals. While such a model should not be taken too seriously until the critical test experiments have been done, we have reached the point in our physiological and anatomical technique where thinking out the implications of such models can help us decide upon critical experiments at each logical junction.

Collett, T., 1977. Stereopsis in toads. Nature 267:349-351.

Ewert, J.-P., and Gebauer, L., 1975. Grossenkonstanzphanomene in Beutefangverhalten der Erdkrote (Bufo bufo L.). J. Comp. Physiol. 85:303-315.

Ewert, J. P. and von Seelen, W., 1974. Neurobiologie und System-Theorie eines visuellen Muster-Erkennungsmechanismus bei Kroten. Kybernetic 14: 167-183.

Glasser, S., Fraser, J. and Ingle, D. 1983. Vertical migration of retinal axons in the frog's optic tectum following laminar denervation. (Submitted)

Ingle, D., 1968. Visual releasers of prey catching behavior in frogs and toads. Brain, Behav., Evol. 1:500-518.

Ingle, D., 1970. Visuomotor functions of the frog optic tectum. Brain Behav. Evol. 3:57-71.

Ingle, D., 1971c. Prey catching behavior of anurans toward moving and stationary objects. Vision Res. Supp. 3, 447-456(1971).

Ingle, D., 1971c. A possible behavioral correlate of delayed retinal discharge in Anurans. Vision Research 11:167-169.

Ingle, D., 1973a. Disinhibition of tectal neurons by pretectal lesion in the frog. Science 180, 442-444 (1973).

Ingle, D., 1973d, Selective choice between double prey objects by frogs, Brain Behav. Evol. 7:127-144.

Ingle, D., 1975, Selective visual attention in frogs, Science 188:1033-1035.

Ingle, D., 1975. Selective visual attention in frogs. Science 188:1033-1035.

Ingle, D., 1982a. The organization of visuomotor behaviors in vertebrates. In: The Analysis of Visual Behavior (D. Ingle, M. Goodale, and R. Mansfield, Eds.), MIT Press.

Ingle, D., and Cook, J., 1977. The effect of viewing distance upon size preference of frogs for prey. Vision Res. 17: 1009-1014.

Ingle, D., and Quinn, S., 1982a. Efferent functions of the frog's tectum: identification vs. localization of prey. (Submitted)

Ingle, D., and Quinn, S., 1982b. Topographic order in tectal and anterior thalamic afferents to the frog's optic tectum. (In preparation)

Lazar, G., and Szekely, G., 1967. Golgi studies on the optic center of the frog. J. Morphology 4: 329-341.

Lettvin, J.Y., Maturana, H.R., Pitts, W.H., and McCulloch, W.S., 1961. Two remarks on the visual system of the frog. In: Sensory Communication (W.A. Rosenblith, ed.), M.I.T. Press, Cambridge, Mass.

Lock, A., and Collett, T., 1979. A toad's devious approach to its prey: A study of some complex uses of depth vision. J. Comp. Physiol. 131:179-189.

Neary, T.J., and Wilczynski, W., Anterior and posterior thalamic afferents in the bullfrog. Neurosci Abstr. 5:144.

Robinson, K., Projections of the tectum opticum of the frog. Brain Behav. Evol. 1: 529-561. 1968.

Trachtenberg, M.C., and Ingle, D., Thalamo-tectal projections in the frog. Brain Res. 79: 419-430 (1974).

Wilczynski, W., and Northcutt, R.G., 1978. Afferents to the Optic Tectum of the Leopard Frog: An HRP Study. J. Comp. Neurol. 178: 219-229.

higher proportion of approaches was aimed at it. The results obtained for the two closer starting distances were very similar when the percentage of trials aimed at the gap was plotted against gap-width measured in cms. But the plots were significantly different when width was measured in degrees subtended by the gap from the starting position. Thus over this range of starting distances toads seem to be guided by the real width of the gap. However, when the starting distance was increased to 30 cm constancy broke down. The results for the 15 and 30 cm starting distances were similar when gap-width was measured in terms of its angular extent and different when measured in cms.

Size constancy is also shown for much larger objects like the fence itself. As the length of an unbroken picket fence is increased toads become reluctant to detour round the end, they prefer instead to aim straight at the prey, as though the fence were not there. The toads' choice between detour and direct approach was measured for different starting distances and fence-widths. Again the results suggest toads measure real size. The percentage of trials on which the toad detours is independent of starting distance over the range tested, provided that width is measured in cms (Fig. 1c).

Analogous tests demonstrate that toads also appreciate the absolute distance between fence and prey. When the prey is in front of the fence, or so close behind it that it can be reached through the bars, there is no need for the toad to make a detour. And indeed toads only make detours on a high proportion of trials when the prey does lie well behind the fence. Furthermore, within limits, the separation between fence and prey at which toads switch to a detour from a direct approach depends on the prey does not depend on their initial distance from the fence (Look and Collett, 1979, 1983).

How do toads use this three-dimensional information about their immediate surroundings when planning routes? To answer this question toads were challenged with slightly more complex spatial problems (Collett, 1982). Fig. 2 shows the animals' (Bufo viridis) behaviour when meal worms were placed behind an obstacle composed of two parallel fences. When both fences were unbroken, the toads mostly detoured round the structure. However, when a gap was placed in the front fence this attracted the toads' approach even though the rear fence continued to block their subsequent path. In this case the route the animals chose was merely suboptimal, for the prey could still be reached by detouring round the rear fence. But with sides added the double fence is transformed into a kind of lobster pot and it becomes pointless for the toads to pass through the gap. Then their only way out is by retracing their steps. Nonetheless, as Fig. 3a shows, they continue to aim for the gap on the majority of trials. In this situation the toads do not select a path they know will lead to the prey, they seem to be doing no more than aiming for the nearest gap.

As they do with single fences, when the gap in the front fence is made wider toads approach the gap more readily. Somewhat surprisingly, the gap continued to draw the toads' approach when it was so wide that the front fence was nothing more than a pair of pillars at each end (Fig. 3b). Thus a very skeletal fence is enough to suppress in part the toads' reactions to the one behind.

Is the toads' seemingly maladaptive behaviour a consequence of their faulty perceptions of a complex obstacle, or is it because of the limitations of their procedures for dealing with barriers? This question was approached by getting [illegible] toads are aware of the three-dimensional structure

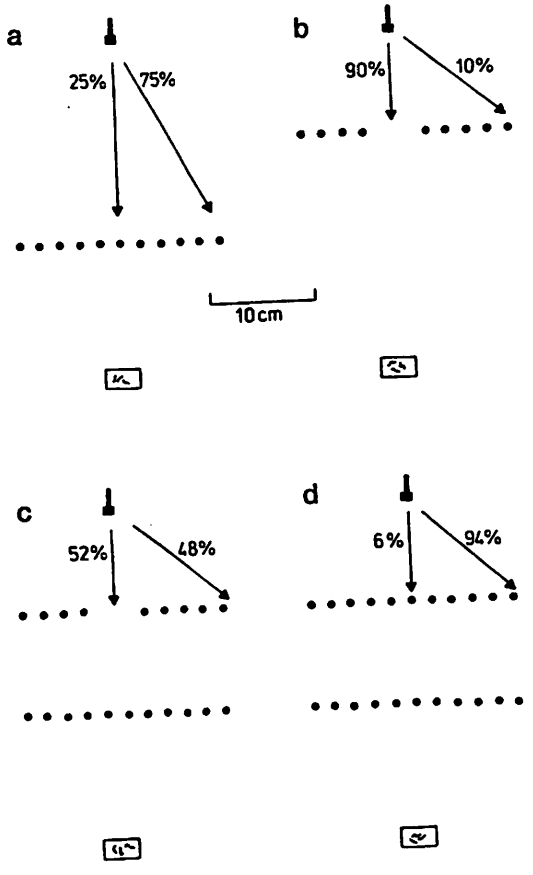

Fig. 2

Fig. 2. Approaches to prey with single and double barriers interposed. In each case, the "hammer" indicates the toad's starting position and orientation, the filled circles show the fence, and the arrows summarise the directions of the approaches. For this and the following figs, the results are given in terms of the percentage of approaches made in a particular direction. (a) Single fence with prey 12 cm behind. (b) Single fence with 6 cm gap and with prey 22 cm behind. (c) Double fence composed from single fences of (a) and (b). (d) Double fence with no gap. In (c) toad makes for gap on about half of the trials, even though rear fence still blocks approach. Directions of approach in (c) differ significantly from those of (a), (b) and (d) ($p < 0.001$ in each case). From Collett, 1982.

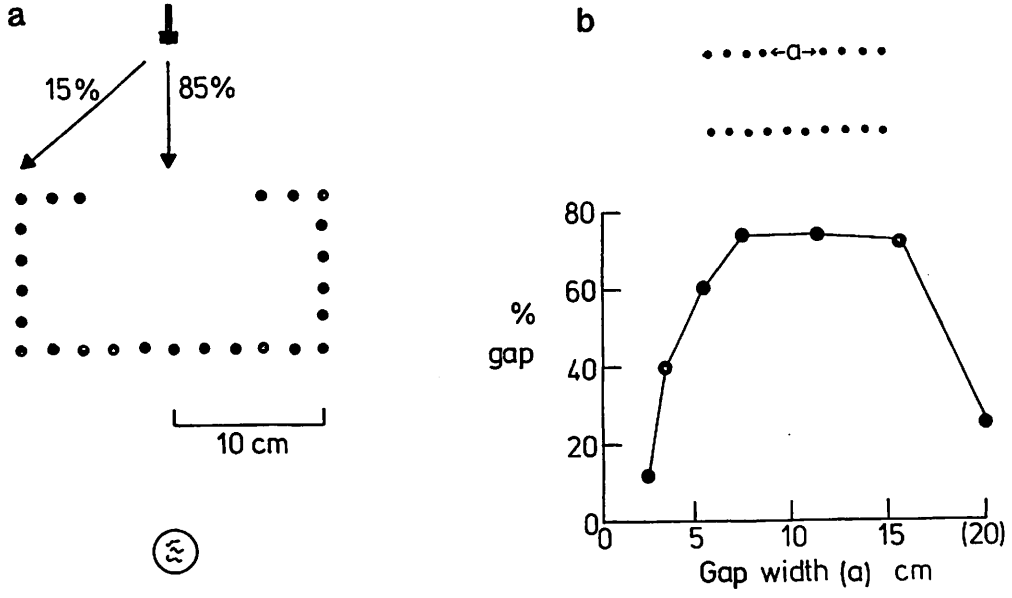

Fig. 3 (a) Approaches to prey behind "lobster pot". Lobster pot is formed from double fence with palings connecting the ends. Toads still aim for gap in front fence. This suggests that toads do not work out the consequences of a particular approach, but are simply attracted toward certain local features in their environment.

(b) Double fences with varying gap-widths. % trials scored at gap is plotted against the width of the gap in the front fence. Fences are 20 cm wide and separated by 10 cm with the prey 12 cm behind rear fence. From Collett, 1978.

of the obstacle, and secondly whether they see the rear fence as a distinct entity.

When projected on to the retina, the arrangement of fences with a gap in the front one is equivalent to a change in the density and thickness of the palings. To be sure that the toad is reacting to the three-dimensional situation and not to its two-dimensional projection, animals were tested with single fences in which the thickness and spacing of the palings was arranged so as to mimic the retinal projection of various gaps in double fences. The toads never responded to these two-dimensional analogues as though they were the real thing. It appears then they have no problem in segregating the information they obtain from different depth planes: the rear fence does not interfere with the detection of a gap in the front one.

Although toads seem largely to ignore the rear fence in the situation of Fig. 2 they are nonetheless aware of many of its features. Thus it can be shown that they probably appreciate the distance of the prey from the rear fence (Collett, 1982) and that they also detect the presence of gaps in the rear fence. The latter point is demonstrated in Fig. 4a by the way a gap in the rear fence biased a toad's choice between two symmetrically placed gaps in the front fence. On the majority of trials toads chose the gap lying on the same side as the gap in the rear fence. When the front and rear gaps were aligned, that is, the toad's viewpoint they fell on the same line of sight, the rear gap acted very powerfully in drawing the toad's approach (Fig. 4b). At first it might seem in such situations the toad is selecting the prey [illegible]. This is not so, since, when the rear fence was [illegible] in front of it, toads [illegible] at gaps in front of it.

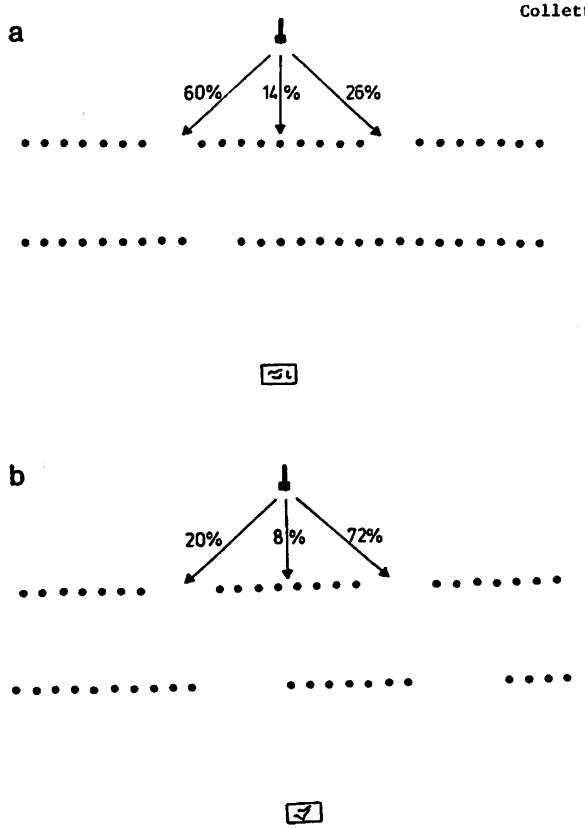

Fig. 4. Approaches to double fences with symmetrically placed gaps in front fence and one or two gaps in rear fence. (a) Single offset gap in rear fence. Prey in line with long axis of toad, 12 cm behind rear fence. Toads tend to approach gap in front fence on same side as gap in rear fence, indicating that they see the rear gap. Note toads were tested with asymmetrical gap positioned to left on some trials and to right on others. (b) Two gaps in rear fence. On one side the toad views gap in rear fence through the gap in the front fence and, on the other side, the rear gap is seen through the palings. Prey 12 cm behind rear fence. Approaches are strongly biased to side on which gaps in two fences are aligned. From Collett, 1982.

reduces but does not abolish a gap's attraction.

The results so far suggest that toads perceive many of the three-dimensional features of the arrangement of barriers, and that they make mistakes because of the very simple strategy they use to deal with such obstacles. They just aim for the most "attractive" gap, where a gap's attraction is specified by a number of simple attributes like its width, its proximity, and how far it extends in depth. (One quality that is apparently not assessed is the destination to which the gap leads.) If this hypothesis is true, it should be possible to manipulate a toad's approach by altering these attributes.

Such an experiment is illustrated in Fig. 5. Given a choice toads generally select the gap closest to their midline and their prey. In Fig. 5a a pair of fences is shown with two gaps in the front fence placed to one side of the midline. Approaches were then mostly aimed at the nearer of the two. This bias was significantly reduced by the insertion of a gap in the rear fence in line with the more peripheral gap in the front fence (Fig. 5b). But the preference though lessened was not reversed. The two gaps were now almost equally attractive.

At the beginning it was stressed that toads have rather precise three-dimensional information about their surroundings. It can now be seen that this enables them to make decisions about local features of their environment, such as whether a gap is wide enough to pass through, or how far prey lies behind a barrier. These experiments suggest toads do not plan routes in the same way we do. Rather they are equipped with a set of sensorimotor rules of the kind "make for the nearest gap" or "jump over that which lies in the way". If the short term these rules [illegible]

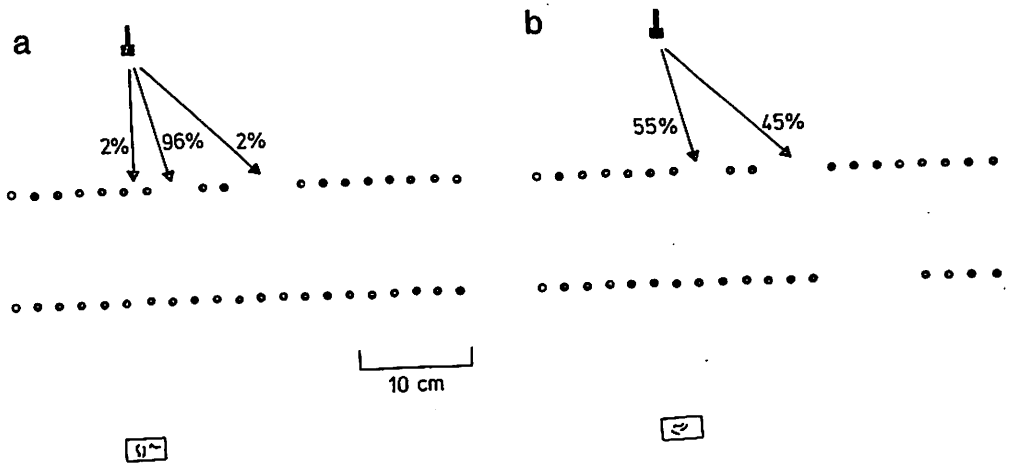

Fig. 5. Approaches to double fence with two gaps in front fence, to one side of midline. Prey positioned in line with toad's long axis, 12 cm behind rear fence. (a) No gap in rear fence. (b) Gap in rear fence viewed through more peripheral of two gaps in front fence. Fences continue for 14 cm to left of open circles. In (a), toads approach the nearer gap on almost all trials, indicating that the proximity of the gap to their long axis and/or prey is a powerful influence. In (b) rear gap has considerably reduced this bias. From Collett, 1978.

these rules, but it is not used to tell them whether a rule will work in any particular instance.

It must be rare that a toad's environment contains no more than the features pertinent to one sensori-motor rule. Consequently, natural selection, as well as shaping individual rules, will also have designed appropriate ways of linking them together. For instance, if there is no barrier toads approach prey directly, but as we have seen, obstacles modify this direct approach as when toads make detours or jump over holes. An obstacle may also cancel an approach altogether, as when a very wide chasm causes a toad to turn away and abandon its attempt (Lock & Collett, 1979). Similarly, when frogs jump to avoid an approaching object, the direction of their leap is biased away from a stationary barrier placed in their expected trajectory (Ingle, 1976). It is too soon to guess how generally applicable is this description of a toad's spatial behaviour in terms of a network of rules for which the underlying neural machinery is hard-wired.

ACKNOWLEDGEMENTS

The experimental work described here was supported by the U.K. Science Research Council and the Nuffield Foundation.

REFERENCES

Collett, T.S. 1982. Do toads plan routes? A study of the detour behaviour of Bufo viridis. J. comp. Physiol. In press.

Ewert, J.-P., Gebauer, L. 1973. Grössenkonstanzphänomene im Beutefangverhalten der Erdkrote (Bufo bufo L.). J. comp. Physiol. 85, 303-315.

Ingle, D.J. 1971. Prey-catching behaviour of anurans toward moving and stationary objects. Vision Res. (suppl.) 3, 447-456.

Ingle, D. 1976. Spatial vision in anurans. In: "The amphibian visual system - a multidisciplinary approach", Fite, K.V. (ed.). Academic Press, New York.

Ingle, D., Cook, J. 1977. The effect of viewing distance upon size preference of frogs for prey. Vision Res. 17, 1009-1013.

Lock, A., Collett, T. 1979. A toad's devious approach to its prey: a study of some complex uses of depth vision. J. comp. Physiol. 131, 179-189.

Lock, A., Collett, T. 1980. The three-dimensional world of a toad. Proc. R. Soc. Lond. B 206, 481-487.

Thomson, J.A. 1980. How do we use visual information to control locomotion? Trends in Neurosci. 3, 247-250.

von Uexkull, J. 1957. A stroll through the worlds of animals and men. In: "Instinctive behaviour" ed. C.H. Schiller. Methuen, London.

THE FROG/TOAD DEPTH PERCEPTION SYSTEM - A COOPERATIVE/COMPETITIVE MODEL

DONALD H. HOUSE

Center for Systems Neuroscience and Computer and Information Science Department, University of Massachusetts, Amherst, Mass. 01003 (U.S.A.)

Key words: frog - toad - depth perception - neural model - tectum - nucleus isthmus - stereopsis - accommodation - cooperative computation

---

SUMMARY

A model of the frog/toad depth perception system is developed. The model draws upon both monocular and binocular depth cues in order to build a spatial map of the animal's visual environment by utilizing the techniques of cooperative computation. It is assumed that the monocular cues are derived from lens accommodation and that the binocular cues are derived from disparity matching. The model is constructed so that monocular information is sufficient for building an adequate depth map. However, if binocular information is available it is used for further refinement of the otherwise monocular depth estimation.

The model is offered as a possible explanation for some of the physiological data concerning the optic tectum and nucleus isthmus. Further physiological and behavioral studies are suggested.

INTRODUCTION

Background

The work described in this paper grew out of attempts to develop a model of depth perception in frog and toad adequate to be used as a basis for simulating behavioral experiments conducted by Lock and Collett [20, 21], Ingle [16], and more recently by Collett [5]. These experiments involved observations of prey catching and predator avoidance behavior in the presence of barriers. Although modeling work concerning this problem had been done in this laboratory [8], no effort had been made to date to either include depth information in the model or determine mechanisms by which this information could be inferred. Although anatomical, physiological, and behavioral data concerning depth perception are available it remained a significant challenge to synthesize this information into a coherent model.

Several behavioral studies pointed to the ability of frogs to do an adequate job of prey catching with only one eye intact, even though they appear to rely heavily upon binocular depth perception when both eyes are usable. Thus it became a major modeling goal to produce appropriate binocular results while also replicating the monocular data.

It was desired that the model also be one which utilized mechanisms that could be supported by existing anatomical structures. As the model developed, it was hoped that it would in turn begin to provide a theoretical framework within which to interpret previously unexplained details of the structural as well as the behavioral data.

Review of the Problem

Frog and toad experiments have revealed that the visual system of these animals is able to discriminate depth information using both monocular and binocular cues. In particular, work by Ingle [16] with monocular frogs demonstrated that information from a single eye was sufficient for consistent depth estimation (albeit less accurate than in the binocular frog) during prey catching behavior (Fig. 1). On the other hand Collett [4] showed by experiments using lenses and prisms that toads depend heavily upon binocular disparity information for targets within the binocular field (Fig. 2). He was able to closely match experimental data with a formula which gave a 94% weighting to binocular cues and 6% to monocular cues. However, he too found that when the animals were monocularly bound they were able to shift to total dependence on information from their single eye.

In support of Collett's data concerning binocularity, important cross-tectal neural pathways have been studied by Fite and Scalia [10], Gruberg and Udin [13], and Gruberg and Lettvin [14] which seem to connect the tectal projections of the visual fields of the two retinas. Some of the efferent fibers from the pyramidal cells of the tectum project to the ipsilateral nucleus isthmus. The isthmus in turn sends its fibers to both the ipsilateral and the contralateral tecta. The resulting connections yield the retino-topic mappings shown in Fig. 3. A block-diagram of the connections themselves is presented in Fig. 4.

The Monocular Mechanism - Lens Accommodation

The nature of the error in monocular depth estimation (Fig. 1) found by Ingle led him to conclude that lens accommodation is an important depth cue in the frog's visual system. Collett's use of lenses also pointed to the utilization of accommodation information by these animals. Further, behavioral data support the building of a depth map by the relatively slow, partially mechanical, mechanism of accommodation. It may be due to the inability to derive depth information at the rate one would expect from entirely neural mechanisms which mediates the frog's relatively long latency between encountering a prey and the ensuing snapping or orienting response. What may be another indicator is the animal's apparent lack of use of size constancy (and thus depth) information for barrier avoidance during escape behavior [16] although it exhibits sophistication in the use of depth information to navigate around barriers during prey catching behavior [20].

Lens accommodation by its nature must be a rather coarse measure of depth. Accommodative data might well be viewed as a relatively broad distribution describing the likelihood of a certain depth being the true depth of a portion of the visual field. To be useful this distribution would have to be estimated at each local region of the visual field or at least for each such region which seems to contain "interesting" stimuli. The likelihood of a particular depth would then most probably be a function of the amount of edge information or contrast in the image when the lens is accommodated to that depth. (For an interesting example of a self focusing system built upon this principle see Selker [24])

For the purposes of this research it was decided to ignore the problem of the design of a control system for inferring the distributions of depth likelihood. Rather, the concentration was upon how such a collection of distributions might be refined into a consistent depth map. It is sufficient to note that if accommodation is being used to build a depth map there must be some mechanism for varying the accommodative state of the lens, and simultaneously determining and holding the most probable depth at each region of the retinal image. Thus, the model must be one which can make this selection and which also exhibits a hysteresis effect capable of maintaining a short-term memory of this selection.

The Binocular Mechanism - Stereopsis via Disparity Matching

The availability of binocular information over a portion of the visual field makes it likely that some form of the disparity matching process is being used to derive depth estimates. In hypothesizing how this may be implemented in the nervous system one notes arguments by Arbib [2] that neurally based perceptual processes are essentially cooperative in nature. (For an argument against cooperativity in stereopsis, see Marr & Poggio [23]. For a counterargument see Frisby & Mayhew [11]). However, Burt [3] showed that the most important cooperative models of stereopsis (Dev [7], Marr and Poggio [22]) are not by themselves adequate for determining depth in visually sparse scenes or scenes containing ambiguous disparity information (Fig. 5) He proposed that in foveate animals vergence is an additional depth cue which could be used to bias the disparity models enough to remove most ambiguity.

In a foveate animal which also exhibits vergence eye movements the problem of disparity matching is reasonably well constrained (Fig. 6). In this case, due to vergence the images on the two fovea can be assumed to be nearly identical. Exceptions to this will be due to small shifts which are geometrically related to the separation of the two eyes and the depth of the viewed object relative to the spatial location of the visual fixation point. Disparity matching can then be summarized as the process of determining the amount of shift (disparity) at each point of the foveal image and then directly computing the depth of the point from geometrical considerations. Local ambiguities which naturally arise in this process can be resolved in favor of the smaller disparity since vergence maximizes the likelihood of zero disparity within the local region fixated on the foveas

In an animal which neither has a fovea nor exhibits vergence the problem is less well constrained (Fig. 7). Theoretically, one is faced with the problem of examining all possible shifts of all portions of the images on the two retinas which contain information from the binocular region of the visual field. Thus it is difficult to limit the range of disparities which will be tested. Further, there is no way to resolve local ambiguities since there is no apriori information present to determine which translation of a local region (i.e. which disparity) will result in the best overall match of the images within that particular region. Binocular depth information can still be extracted under these circumstances. However, some other mechanism must be present by which a "most likely" disparity can be determined for each local region of the image. Since the mechanism of

accommodation is apparently present in frog and toad it is reasonable to expect that it is used to furnish the required bias.

The Computational Mechanism - Competition and Cooperation

Amari and Arbib [1] present a general cooperative/competitive model which has both a plausible neural basis and which solves the problems of memory (hysteresis) and selection outlined above. They envision a homogeneous neural field interacting with an inhibitory neuron pool. Fig. 8 shows how this model might be configured to handle the accommodation problem for the simplified case of the projection of a two-dimensional scene onto a one-dimensional retina.

The cooperative field is two-dimensional with coordinates representing retinal position in one direction and depth in the other. The input to the model is the depth likelihood determined at each local region of the retina by the accommodation system. Regions of the field which are close in both retinal position and depth are mutually excitatory, with the local spread of excitation fairly broad along the retinal position axis and quite narrow along the depth axis. All depths within a narrow annulus about a retinal position excite the portion of the inhibitory pool assigned to that retinal position. That portion of the inhibitory pool in turn sends inhibitory feedback to all elements at that retinal position. If parameters are properly chosen the field will reach an equilibrium state where one depth region at each retinal position will be above threshold and all others will be below threshold. Fig. 9 shows a cut-away view of the net effect on the field due to both the excitatory and inhibitory connections when a strong point source of excitatory input is provided.

The model demonstrates hysteresis in that once an equilibrium state is reached, it will be maintained even under significant changes in the input. This is due to the fact that at equilibrium there is a relatively high level of activity in both the cooperative field and the inhibitory pool. The inhibitory pool tends to override any new excitatory input. Mutual reinforcement of nearby cells in the field tends to maintain excitation at a point even when all input is removed.

METHODS

Structure of the Model

The foregoing introduction summarizes our early research on the depth problem. In order to begin the synthesis necessary to construct a model it was decided to represent the initial depth-estimation problem as one with two methods of solution (accommodation and disparity matching). The results obtained from both methods would be used. Similar estimates from the two methods would be mutually reinforcing and thus could provide the biasing necessary to reduce ambiguity. Also, if one of the methods failed to produce adequate estimates the other would still be available.

Thus, the proposed model of depth perception utilizes a pair of interacting Amari/Arbib models, each acting as a depth map. One map receives depth information which has been monocularly inferred via lens accommodation. The other map receives depth information deduced binocularly by shifting the images on the two retinas with respect to each other, testing for similarities, and applying the appropriate geometrical calculations when a local match is found. Auxiliary

excitatory connections between the maps are utilized to provide the means by which the two maps cooperate to refine each other (Fig. 10) Because of these connections a local build up of excitation in one of the maps will act to sympathetically excite the analogous region in the other map. In this way the model uses the monocular map to bias the disparity cued binocular map and in turn the binocular map acts to refine (bias) the monocular map.

Implementation of the model on a computer led to several advances in understanding which might not otherwise have occurred. The structure of the model did not change drastically from its initial conception. However, discoveries were made concerning the meaning and nature of the inputs and outputs implied by the model's structure. The most important of these was that it is not possible to tune the model so that the depth maps it produces can be interpreted as point-wise reconstructions of the visual scene. Rather, the lateral spread of excitation inherent in the model produces a segmentation of the scene into depth-regions (Fig. 11). To determine the spatial location of an object the current retinal stimulation is necessary to determine visual angle. The depth of an object occuring at this position on the retina may then be read from the depth-map. This small conceptual shift has important behavioral implications (see DISCUSSION -- Directions for Future Research).

Another discovery was that the model is quite sensitive to the relative strength of the binocularly and monocularly derived inputs It was found that no change in model parameters could affect the biasing of the model in favor of either monocular or binocular depth-cues more than changing these inputs. Adjusting internal

parameters has comparatively little effect upon performance. This insensitivity to internal changes suggests a robustness of the model that was not initially expected. It also necessitated the addition of extra parameters used merely to adjust input strengths.

Physiological Justification

In order for the model to be justified from a physiological standpoint there must be cross-tectal connections sufficient to account for the high degree of accuracy in determination of depth which both frogs and toads exhibit during prey-catching behavior. Gruberg [12] reports that such connections via the nucleus isthmus number in the neighborhood of 4000 in each direction. A similar number of fibers project recurrently from each isthmus to the ipsilateral tectum. If we assume that these fibers evenly innervate a retino-tectally projected hemisphere of 180 x 90 degrees then we would expect the corresponding signals to have an error of up to 2-degrees. This error will translate into a corresponding disparity error. Fig. 12 shows the approximate relationship between angular disparity and depth for objects located in the center of the binocular field. This curve was calculated by the author using simple pin-hole optics and an assumed eye separation of about 3 cm. It was intended merely to give an "order of magnitude" estimate of the true curve. It can be determined from this curve that the effect on depth estimation of a cumulative 4 degree error in angular disparity would be less than a millimeter for objects at 5 centimeters from the animal At 10 centimeters the depth error increases to 3 millimeters and at 15 centimeters it is nearly 2 centimeters. These figures appear to be well within the range required for accurate snapping at short

distances, and navigation at longer distances.

Mathematical Expression of the Model

The assumptions of the Amari/Arbib model dictate that the point potential $F(x,y,t)$ of the neural field should vary at a rate $1/\tau_F$ proportional to the difference between the algebraic sum of its inputs and its current potential (where x and y represent the two spatial coordinates and t the time parameter). In a similar fashion the point potential $P(x,t)$ of the inhibitory pool should vary at a rate $1/\tau_P$ proportional to its inputs and current potent. The model can thus be described in terms of these rates by the simultaneous partial differential equations

$$\tau_F \frac{\partial F}{\partial t} = -F(x,y,t) + \iint_{-\infty}^{\infty} w_1(x-\xi)w_2(y-\eta)f_1[F(\xi,\eta,t)]\,d\xi d\eta - \int_{-\infty}^{\infty} w_2(x-\xi)f_2[P(\xi,t)]\,d\xi + I(x,y,t),$$

$$\tau_P \frac{\partial P}{\partial t} = -P(x,t) + \iint_{-\infty}^{\infty} w_3(x-\xi)f_3[F(\xi,\eta,t)]\,d\xi d\eta. \qquad (1)$$

The inputs to a point in the field come from laterally excitatory recurrent connections within the field, inhibitory connections from the inhibitory pool, and external connections from the input source, I. It is assumed that the inhibitory neuron pool is externally undriven so that the only input to the pool will be from the excitatory field. We make the additional assumption that connectivity is symmetric in each spatial variable about any arbitrary point and so can be represented (along either axis) by a weighting function w which is a function only of absolute distance from the point. Finally, we require that the effect of a potential at any point upon any other

point is a function of connectivity and a monotonically non-decreasing function, f, of that potential. (A useful analogy may be drawn between this function and the saturation-threshold curve of the firing rate of a neuron versus its level of excitation).

The equations can be easily extended to include the mutual excitation inherent in the cooperating pair of Amari/Arbib models which are envisioned in the depth perception model. With these extensions the equations of the complete depth-perception model become

$$\tau_M \frac{\partial M}{\partial t} = -M(q,d,t) + \iint_{-\infty}^{\infty} w_{m_1}(q-\xi)w_{m_2}(d-\eta)f_{m_{12}}[M(\xi,\eta,t)]\,d\xi d\eta + \iint_{-\infty}^{\infty} w_{m_3}(q-\xi)w_{m_4}(d-\eta)f_{m_{34}}[S(\xi,\eta,t)]\,d\xi d\eta - \int_{-\infty}^{\infty} w_{m_3}(q-\xi)f_{m_5}[U(\xi,t)]\,d\xi + A(q,d,t),$$

$$\tau_U \frac{\partial U}{\partial t} = -U(q,t) + \iint_{-\infty}^{\infty} w_{u_1}(q-\xi)f_{u_1}[M(\xi,\eta,t)]\,d\xi d\eta,$$

$$\tau_S \frac{\partial S}{\partial t} = -S(q,d,t) + \iint_{-\infty}^{\infty} w_{s_1}(q-\zeta)w_{s_2}(d-\eta)f_{s_{12}}[S(\zeta,\eta,t)]\,d\zeta d\eta + \iint_{-\infty}^{\infty} w_{s_3}(q-\zeta)w_{s_4}(d-\eta)f_{s_{34}}[M(\zeta,\eta,t)]\,d\zeta d\eta - \int_{-\infty}^{\infty} w_{s_3}(q-\xi)f_{s_3}[V(\zeta,t)]\,d\zeta + D(q,d,t),$$

$$\tau_V \frac{\partial V}{\partial t} = -V(q,t) + \iint_{-\infty}^{\infty} w_{v_1}(q-\zeta)f_{v_1}[S(\zeta,\eta,t)]\,d\zeta d\eta. \qquad (2)$$

In these equations the monocularly driven field M and its associated inhibitory pool U are now externally driven not only by the accommodative inference system A but also by excitatory connections

from the stereoptically driven field S. The stereoptic field and its inhibitory pool V are in turn driven by the disparity inference system D and excitatory connections from the monocular field. The cross-field connections obey the same symmetry constraints as the recurrent connections in projecting visuo-topically similar points from one field to the other. To complete this expression of the model we define the spatial coordinates q to represent angular position on a one dimensional circular retina, and d to represent disparity (angular shift between right and left retinas).

Implementation of the Model for Computer Simulation

Certain simplifying assumptions were required in order to ease the computational load of simulating the above equations and to reduce the number of parameters whose adjustment would be required. These assumptions all took the form of eliminating one or more of the spatial dimensions from the integrals of eqs. (2). The spatial weighting functions w which were thus eliminated were replaced, where necessary, by simple multiplicative gains k. In each case the justification for removal of the spatial weighting was that the spread of excitation represented by the weight would be negligible compared with the lateral spread of excitation along the retinal position axis in the neural fields. Further, the eliminated spatial weights were envisioned as having a smaller spread effect than the spread effect inherent in representing the continuous fields as coarse discrete grids in the computer implementation. (A similar step was taken by Amari and Arbib [1] in the development of their original analytical model when they chose to quantize their depth dimension while keeping their positional coordinate continuous in their eqs. 2.5.) With these

simplifications the equations of the implementation model were reduced to

$$\frac{\partial M}{\partial t} = \frac{1}{\tau_M}\left\{-M(q,d,t) + \int_{-\infty}^{\infty} w_{m_1}(q-\zeta) f_{m_{12}}\left[M(\zeta,d,t)\right] d\zeta + k_{m_1} f_{m_{34}}\left[S(q,d,t)\right] - k_{m_2} f_{m_5}\left[U(q,t)\right] + k_a A(q,d,t)\right\},$$

$$\frac{\partial U}{\partial t} = \frac{1}{\tau_U}\left\{-U(q,t) + k_{u_1}\int_{-\infty}^{\infty} f_{u_1}\left[M(q,\eta,t)\right] d\eta\right\}, \qquad (3)$$

$$\frac{\partial S}{\partial t} = \frac{1}{\tau_S}\left\{-S(q,d,t) + \int_{-\infty}^{\infty} w_{s_1}(q-\zeta) f_{s_{12}}\left[S(\zeta,d,t)\right] d\zeta + k_{s_1} f_{s_{12}}\left[M(q,d,t)\right] - k_{s_2} f_{s_5}\left[V(q,t)\right] + k_d D(q,d,t)\right\},$$

$$\frac{\partial V}{\partial t} = \frac{1}{\tau_V}\left\{-V(q,t) + k_{v_1}\int_{-\infty}^{\infty} f_{v_1}\left[S(q,\eta,t)\right] d\eta\right\}.$$

where it is seen that all spreading effects but the self-excitation in the field have been ignored. Eqs. (3) also show the additional multiplicative weights which were found to be necessary in order to adjust the relative strengths of the accommodative and disparity inputs.

The computer implementation of eqs. (3) was viewed as being a qualitative approximation to a hypothethized structure. Thus, no attempt was made to represent the true density of connections or coarseness of the underlying neural mechanisms. Therefore, with computational tractability and simplicity in mind the fields M and S were modeled as 41 x 41 arrays, and the inhibitory pools U and V as vectors of length 41. Again with simplicity in mind the spatial

integrals of eqs. (3) were computed using the trapezoidal rule and the differential equations were solved approximately using Euler's method. The system was taken as being initially inert (zero potential in all fields and inhibitory pools) with zero boundary conditions.

In order to provide input to the model a system of computer programs was developed which uses interactive graphics and simple optics to construct a two dimensional scene, project it onto two semicircular one-dimensional retinas, and infer the accommodative and disparity inputs [15]. The input was broken up into separate "bug" and "barrier" channels emulating the retinal discriminatory mechanisms inherent in the frog's visual system [19]. The work of Ewert [9] points to the possibility that processing of prey stimuli may be localized to the tectum whereas contraindicative stimuli may be processed in the pretectal region. This work inspired the construction of two separate but complete depth models, one to process the "bug" information (tectal processing), and one to process the "barrier" information (pretectal processing).

Since there was no attempt to construct a model of the accommodation system, this input was mechanically created by building Gaussian weighted depth estimates at each retinal position. The disparity coordinate of the retinal angle vs. disparity coordinate system was used to measure depth when creating these estimates since the geometry of this system reflects the decrease with distance from the viewed object of the depth resolving ability of optical focusing systems. The ability to approximate the presence of a lens in front of the eye was provided by a parameter governing systematic error in the centering of the depth estimate curve about the true depth of a

point. The curves resulting from the construction of the depth estimates were scaled and stored in the accommodative input plane A.

The binocular disparity input to D was computed by shifting the projected retinal images over each other and noting the coordinates (retinal position and disparity) of each positive match of information. The shift of one retina over the other was constrained to 25% of the binocular field. The retinas themselves were modeled as vectors of length 161. Again, no attempt was made to emulate actual numbers but merely to obtain a qualitative feel for the model's performance. Provision for modeling the presence of prisms in front of the eyes was also made. Their effect was simulated by modifying the retinal projections so as to introduce a disparity bias consistent with a parametrically indicated prismatic strength.

The depth system model was only fully implemented on the computer for the left tectal and pretectal surfaces. Thus, it avoided the computations and complications associated with concurrent processing in both tectal lobes and the resulting control arbitration problems.

RESULTS

The configuration of the scene which was used to test the model is shown in Fig. 13. The simulated animal is directly facing and about 20 cm. from the center of a paling fence which is oriented perpendicular to its body axis. This arrangement, when processed through the accommodation and disparity matching mechanisms outlined above, resulted in the input planes shown in Figs. 14a-d. These displays are in the retinal-angle vs. disparity coordinate system used by the model. Here can be seen the extent of the spread of the

depth estimates envisioned as being provided by accommodation and the ambiguity due to spurious matching of estimates provided by disparity. Figs. 14e-f show how the same information would appear if transformed back into the coordinate system of Fig. 13 and overlaid upon the original scene. They give a coarse visual feel for the extent of uncertainty in the input. For these figures the lens, and prism parameters were all set to zero so that none of the corresponding effects are seen.

Fig. 15 shows the time course of the model as it proceeded from its initial state with the inputs described above. The displays are temporally spaced at intervals of 1-1/3 time-constants of the excitatory field and thus represent somewhat less than 7 time-constants of simulated activity. The initial lack of excitation in the neural fields is depicted in Fig. 15a. The build-up of excitation and the corresponding response in the inhibitory pools may be noted in Fig. 15b. The growth of inhibition began to shrink the widths of the excited areas of the fields as depicted in Fig. 15c. Figs. 15d through 15f show further steps towards reaching a satisfactory depth segmentation. It may be noted that the monocularly and binocularly driven fields tended towards virtually identical states. Field excitation was maintained only in narrow bands along the disparity axis but showed significant spread in the retinal angle direction as nearby elements reinforced each other. The potential in the inhibitory pool reached a fairly high level to cancel the broad spread of the input in the disparity direction. Fig. 16 is a transformation of the equilibrium state of the monocularly driven field back into translation vs. depth coordinates. This display is

shown overlayed upon the original scene and indicates the extent to which the model was successful in constructing a depth segmentation of its spatial distribution. The decrease of depth acuity with increasing distance may also be noted here.

To more graphically illustrate the depth segmentation effect of the model the simulation was allowed to continue running to nearly 14 field time-constants. The resulting state is shown in Fig. 17a. The additional spread of excitation in the retinal angle direction may be compared with Fig. 15f. The transformation of this state back into spatial coordinates is shown in Fig. 17b. Here the depth segmentation is even more dramatically evident than in Fig. 16. Finally, Fig. 17c demonstrates that this segmentation can be used to spatially localize objects by sampling at only those retinal positions currently receiving stimulation.

Fig. 18 shows the depth segmentations which resulted from simulation runs using the same input scene but with interposed lenses (Fig. 18a) and prisms (Fig. 18b). The emulated lens and prism strengths were chosen to each produce a 20 percent shift in the disparity coordinate of the corresponding monocular and binocular input planes. Inspection of the results for prey (bug) stimuli will show that the shift in the depth segmentation produced by lenses is quite small compared with that produced by prisms. These results are qualitatively consistent with those obtained in the previously described behavioral experiments. On the other hand, the barrier (fence) results appear confusing. Here the lens produces a large shift in the depth segmentation whereas the prisms not only produce a smaller shift but the shift is in the wrong direction. This effect is

mediated by the close disparity spacing of the spurious binocular depth estimates derived from the spatially-periodic fenceposts. Any mismatch between monocular and binocular estimates which exceeds this disparity spacing leads to a reinforcement of one of the spurious estimates rather than the correct one. Thus, the net result is rather arbitrary. For visually sparse data such as occur with prey stimuli this shift to a spurious estimate can only occur with extremely strong optical distortion.

Results from a final test of the model are shown in Fig. 19. Here a monocular animal was emulated by artificially removing the binocularly derived input. The figure shows that the model was again successful in producing a correct depth segmentation. Although accuracy was not noticably impaired, the length of time required to reach a satisfactory segmentation was nearly doubled (to circa 14 field time-constants).

DISCUSSION

Evaluation of the Model

The efferent pathways from the cooperative system envisioned by the model are pictured as emanating from the monocularly driven map. Further, it has been shown that it is possible to tune the model so that it exhibits adequate convergence properties both when binocular information is present and when it is absent. Therefore, the monocularly driven map may be used to direct motor coordination whether or not binocular information is available. If binocular information is available it refines the map and may even be the dominant factor in the resulting depth estimation. However, if it is

not available then monocular information is sufficient for a somewhat degraded but adequate performance. Thus, the model is capable of emulating the depth processing capabilities which both binocular and monocular animals display while engaged in prey-catching behavior.

Further, it is possible to tune the model so that its ability to discriminate spatial location of prey-like stimuli is only slightly affected by the presence of moderate systematic error (lens effect) in the accommodative mechanism. On the other hand, the same tuning results in a high degree of sensitivity to error (prism effect) in the disparity matching mechanism. These results bear a strong qualitative resemblance to the behavioral results mentioned earlier.

The model, however, was not so successful in handling the determination of the depth of spatially periodic data such as are presented by a fence-like barrier. Fence depth was correctly ascertained when both the monocular and the binocular mechanisms were perfectly tuned. However, a small detuning of either mechanism led to a breakdown in consistent discrimination capability. This result, far from being discouraging, points to the likelihood that the (presumably) tectal prey-location process is implemented via a more complex and accurate mechanism than the barrier-location process. The latter process may be purely monocular in nature.

Anatomy and Physiology of the Model

The model depends heavily upon the presence of cross-tectal projections via the nucleus isthmus. Although there are no definitive results concerning the utility of these connections, it is plausible to assume that they play a role in binocular image processing. It has

already been shown that the density of these connections is sufficient to account for the exhibited accuracy of depth discrimination.

The hypothesis concerning the function of the isthmal connections is strengthened by the distribution of fiber terminals in the layers of the tecta (Fig. 20). Fibers from both isthmi terminate in layer 8 where there is a dearth of optic nerve terminals. The isthmal terminals carry information originating only from tectal efferents and thus may be assumed to result from optical events "highly significant" to the animal. In particular, prey activity in the visual field would presumably excite a high degree of activity. Signals from both isthmi will experience similar delays between the original optic input and their arrival in layer 8. Thus they will be properly aligned in both retinotopy and in time, will carry significant information, and will be free from the presence of unprocessed optic nerve input. This is a configuration which seems particularly well suited for efficiently carrying out the process of image matching necessary in a binocularly cued depth perception system.

Fig. 20 also shows that just below layer 8 in layer G is a region innervated by the optic nerve but without isthmal input. This is precisely what would be required for depth estimation via lens accommodation. If the accommodation control system is to be effective it must have input which would provide a fairly pure measure of contrast in the retinal image. Layer G could provide that measure.

Although not of importance to the model in question it appears that the presence of input from the ipsilateral nucleus isthmus together with optic nerve input in layers A through F could play a

role in the phenomenon of facilitation reported by Ingle [16] and modeled by Lara et al. [18]. This same configuration could possibly play a role in motion detection, by exploiting the delay between the optic nerve input and the resulting feedback from the nucleus isthmus.

Directions for Future Research

The depth-perception mechanism presented in this model depends upon accommodation as a secondary depth estimator which is required to remove ambiguity from the binocular estimate. Disambiguation, however, will only be a serious problem when multiple prey-objects are present in the visual field. Therefore, a definitive test of the model would be to observe prey-catching behavior in animals in which the accommodative mechanism has been "frozen". These animals should have little trouble estimating the depth of single targets presented in the frontal binocular field. However, multiple targets should cause a marked tendency toward either reduced feeding behavior or snapping between targets with a significant undershoot.

The model indicates that binocular information might be used only when determining the depth of prey objects. This suggests that the coarse but unambiguous accommodative process may, by itself, be sufficient for the depth resolution necessary for navigation. It would be useful to perform behavioral experiments to test this conjecture. For instance, cine-recordings could be made of test animals orienting to negotiate a fence-like barrier during prey catching. These recordings could then be analyzed to look for differences in orientation angle between control animals, monocular animals, and animals with various configurations of lenses or prisms. To date experiments directed at determining the relative efficacies of

binocular and monocular depth cues in determining the spatial location of barriers have not been successful. This is due in part to the difficulty of motivating test animals to negotiate barriers under the necessary experimental conditions [6].

The observations, above, concerning the anatomy of the tectal afferent connections indicate that tectal layer 8 is concerned with binocular depth estimation. This hypothesis can be tested by selective lesions of the pathways between the tecta and the isthmi. The hypothesis implies that it is by comparing signals from the two isthmi that disparity matching is done. The raw optic input would have no effect on this process. Thus, severing either the ipsilateral or the contralateral isthmal connections would have an equal effect in eliminating the ability of an animal to do binocular processing.

The model depends upon current retinal angle as well as a calculated depth-segmentation of the visual field in order to compute the spatial position of an object. This fact directly predicts responsiveness of frogs and toads to various types of motion in the visual field. Response to small lateral movements of prey stimuli will have only an angular effect. Thus, recomputation of spatial location is merely a matter of changing the retinal angle (essentially instantaneous) and accessing the corresponding position in the segmented depth-map. Therefore, the animal should be very responsive and accurate in compensating for it. However, movement either away from or towards the animal would require a change in the current depth segmentation and would thus have to overcome the hysteresis effect of the depth-mapping process. We would predict that correction for this type of prey motion would be considerably more sluggish.

The sensitivity of the model to relative monocular and binocular input strengths and the slow-down experienced with solely monocular input suggest the likely presence of connections which could provide automatic input scaling. It would be useful to extend the model to include such a scaling mechanism and to explore for the presence of corresponding neural structures.

The model assumes that frogs and toads are able to simultaneously maintain separate depth segmentations of "bug" and "barrier" features within the visual field. It is also a feature of the model that optic nerve input provides angular information concerning spatial orientation of prey objects, while the depth (segementation) map can be interrogated to determine the depth of an object at that point in the visual field. These aspects of the depth model are being exploited in our current efforts to develop a model of orienting behavior.

ACKNOWLEDGEMENTS

The research reported in this paper was supported in part by NIH grant NS14971-03. M. A. Arbib, principal investigator on this grant, was responsible for providing the initial questions, thoughtful criticism, guidance, encouragement, and stimulating research environment which made this work possible.

REFERENCES

1) Amari, S. I., Arbib, M. A., Competition and Cooperation in Neural Nets. In J. Metzler (Ed.), Systems Neuroscience, Academic Press, 1977, pp. 119-165.

2) Arbib, M. A., A View of Brain Theory. In F. Yates (Ed.), Self Organizing Systems, The Emergence of Order, Plenum Press, in press.

3) Burt, P. J., A Procedure for Evaluating Cooperative Models for Stereopsis. Brain Theory Newsletter, University of Massachusetts at Amherst, Center for Systems Neuroscience, 3 (1977), 31-35.

4) Collett, T., Stereopsis in Toads. Nature, 267 (1977), 349-351.

5) Collett, T., Do Toads Plan Routes? A study of the Detour Behavior of Bufo Veridis, to appear.

6) Collett, T., private communication at the Visuo-Motor Coordination Workshop, University of Massachusetts at Amherst, Nov. 1981.

7) Dev, P., Perception of Depth Surfaces in Random-Dot Stereograms: a Neural Model. Int. J. Man-Machine Studies, 7 (1975), 511-528.

8) Epstein, S., Vermin Users Manual. Unpublished project report, University of Massachusetts at Amherst, COINS Department, 1979, 25 pp.

9) Ewert, J.-P., The Visual System of the Toad: Behavioral and Physiological Studies on a Pattern Recognition System. In K. Fite (Ed.), The Amphibian Visual System A Multidisciplinary Approach, Academic Press, 1976, pp. 141-202.

10) Fite, K. V., Scalia, F., Central Visual Pathways in the Frog. In K. Fite (Ed.) The Amphibian Visual System A Multidisciplinary Approach, Academic Press, 1976, pp. 87-118.

11) Frisby, J. P., Mayhew, J. E. W., Spatial Frequency Tuned Channels: Implications for Structure and Function from Psychophysical and Computational Studies of Stereopsis, Phil. Trans. Royal Society Lond. B, 290 (1980), 95-116.

12) Gruberg, E. R., private communication, Jan. 1982.

13) Gruberg, E. R., Udin, S. B., Topographic Projections Between the Nucleus Isthmi and the Tectum of the Frog Rana Pipiens. Comp. Neur., 179 (1978), 487-500.

14) Gruberg, E. R., Lettvin, J. Y., Anatomy and Physiology of a Binocular System in the Frog Rana Pipiens. Brain Research, 192 (1980), 313-325.

15) House, D. H., A Test-Bed for Visuo-Motor Coordination Models. in preparation as a COINS Technical Report, University of Massachusetts at Amherst, COINS Department.

16) Ingle, D., Spatial Vision in Anurans. In K. Fite (Ed.) The Amphibian Visual System A Multidisciplinary Approach, Academic Press, 1976, pp. 119-140.

17) Julesz, B., Foundations of Cyclopean Perception, The University of Chicago Press, Chicago, 1971, 406 pp.

18) Lara, R., Arbib, M. A., Cromarty, A. S., The Role of the Tectal Column in Facilitation of Amphibian Prey-Catching Behavior: A Neural Model. Journal of Neuroscience, 2 (1982), 521-530.

19) Lettvin, J. Y., Maturana, H. R., McCulloch, W. S., Pitts, W. H., What the Frog's Eye Tells the Frog's Brain, Proceedings of the IRE, 47 (1959), 1940-1951.

20) Lock, A., Collett, T., A Toad's Devious Approach to its Prey - A Study of Some Complex Uses of Depth Vision. J. Comp. Physiol., 131 (1979), 179-189.

21) Lock, A., Collett, T. The Three -- Dimensional World of a Toad. Proc. Royal Society Lond. B, 206 (1980), 481-487.

22) Marr, D., Poggio, T., Cooperative Computation of Stereo Disparity. Science, 194 (1976), 283-287.

23) Marr, D., Poggio, T., A Computational Theory of Human Stereo Vision. Proc. Royal Society Ser. B, 204 (1979), 301-328.

24) Selker, T. An Image Based Focusing System: An Alternative for Cameras, a Model of Eye Accommodation. COINS Technical Report 81-19, University of Massachusetts at Amherst, COINS Department, 1981, 34 pp.

FIGURE 1

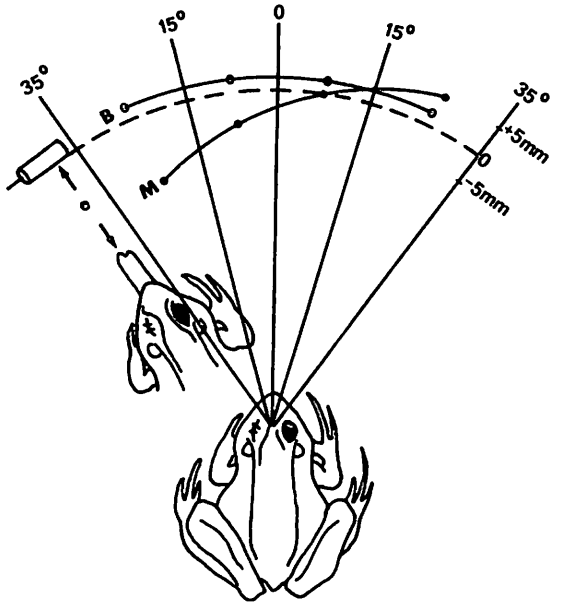

Fig. 1 - Snapping Errors After Monocular Binding of Left Eye

Reprinted by permission. From Ingle in The Amphibian Visual System A Multidisciplinary Approach, K. Fite (ed.), pg. 125, Copyright (c) 1976, Academic Press. Measurements are from cine-recordings. Solid lines mark the deviation of the tip of the wet tongue mark from the near edge of the cylindrical target (dashed line). Line B shows the mean tongue extension for binocular frogs. It slightly overlaps the stimulus across the entire rostral binocular field. Monocular frogs (Line M) fell short of the target for locations 15-35 degrees from the midline, within the contralateral visual field. Errors within the ipsilateral visual field are not significantly greater for monocular animals than for binocular animals. Thus, it may be concluded that monocular information is sufficient for depth perception in frogs. The data allude to the use of accommodation for monocular depth information since the error is consistently worse for more peripheral images where the accommodative power of the lens is the least.

FIGURES

Fig. 2 - Effect of Prisms and Lenses on Depth Perception

Reprinted by permission. From Collett in Nature, Vol. 267, No. 26, pp. 350-351, Copyright (c) 1977 Macmillan Journals Limited. (a) This diagram shows the effect on binocular depth cues caused by base-out prisms mounted in front of the two eyes of a binocular animal. If the animal depends upon these binocular cues for determining depth it will perceive objects as being closer than they really are. (b) Control Results. These scatter-plots from behavioral tests show that both binocular and monocular animals are able to judge snapping distance accurately. The oblique line represents the exact distance of the target from the animal. The overshoot shown by Ingle (Fig. 1) is also seen here. (c) Lens Effect. This plot shows that a lens in front of the good eye of a monocular frog produces the reduction in snapping distance predicted from optical considerations (Line M) assuming lens accommodation is being used to judge depth. In binocular animals lenses cause very little deviation from the correct snapping distance (Line B). This shows that binocular depth cues dominate monocular ones. (d) Prism Effect. Depth-estimation is distorted by prisms placed in front of the eyes of binocular animals. This is a further confirmation of the dominance of binocular cues.

FIGURES

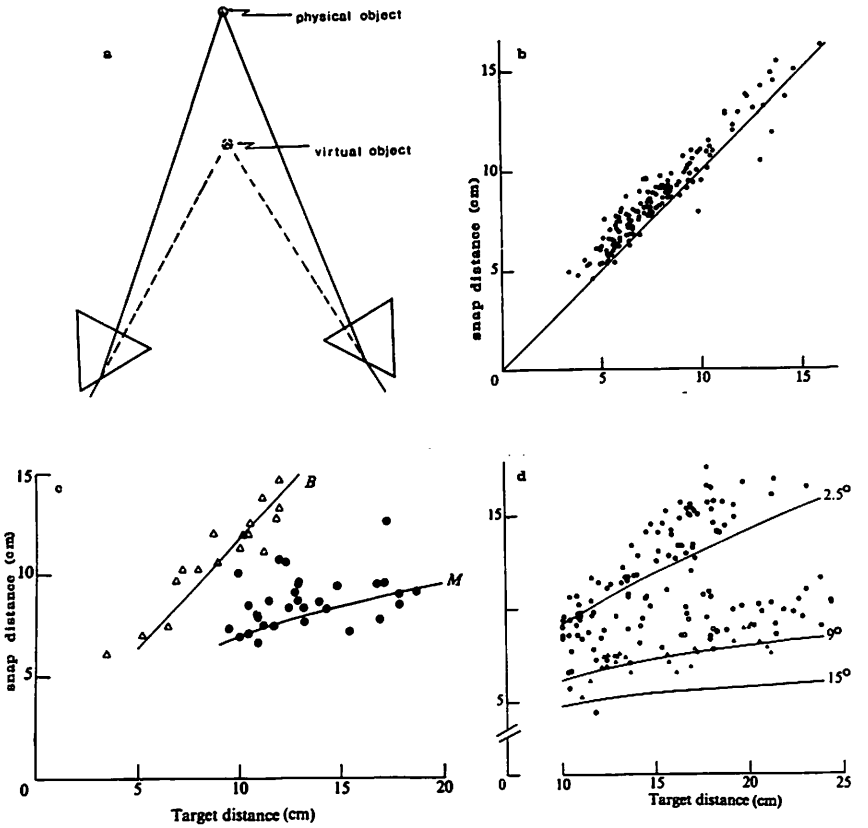

Fig. 2

FIGURES

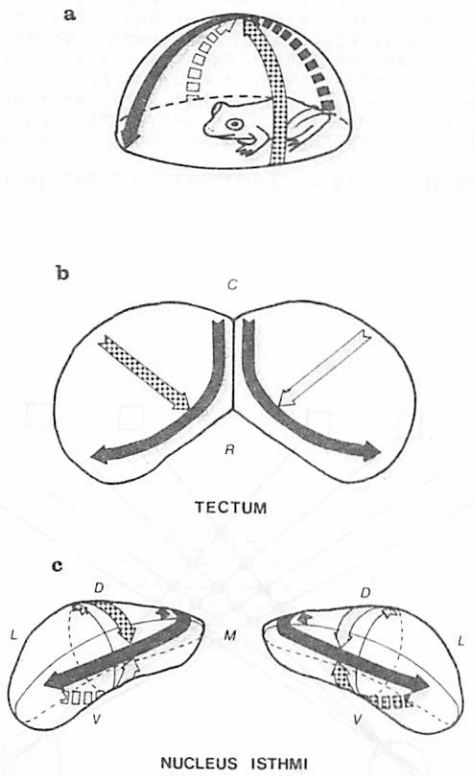

Fig. 3 - Retino-Tectal and Isthmio-Tectal Projections

Reprinted by permission. From Gruberg and Udin Journal of Comparative Neurology, Vol 179, pg. 492, Copyright (c) 1978 Wistar Inst. Press. (a) The upper visual field is represented by arrows. These arrows are used in the other illustrations to schematically represent projections of the visual field in neural structures. (b) This dorsal view of the tectum shows the projection of the visual field formed by terminals of retinal ganglion cells. (c) The nuclei isthmi are represented as shells in a view facing the rostral pole. The locations in the tectum to which the cells on the surface of the nuclei project are shown by the corresponding arrows.

FIGURES

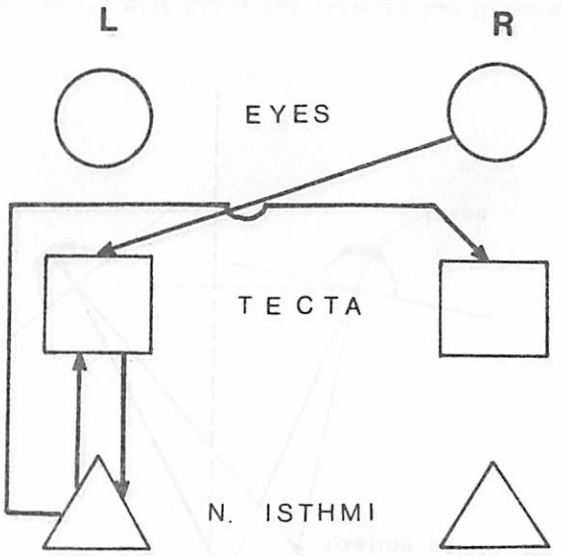

Fig. 4 - Block Diagram of Isthmio-Tectal Projections

Reprinted by permission. From Gruberg and Lettvin in Brain Research, Vol. 192, pg. 321, Copyright (c) 1980 Elsevier/North-Holland Biomedical Press. This diagram schematically shows the pathways from the right eye to the right and left tectal lobes. It illustrates both the ipsilateral and contralateral connections between the tectum and the nucleus isthmus. An identical set of connections exist for the left eye and right tectum.

FIGURES

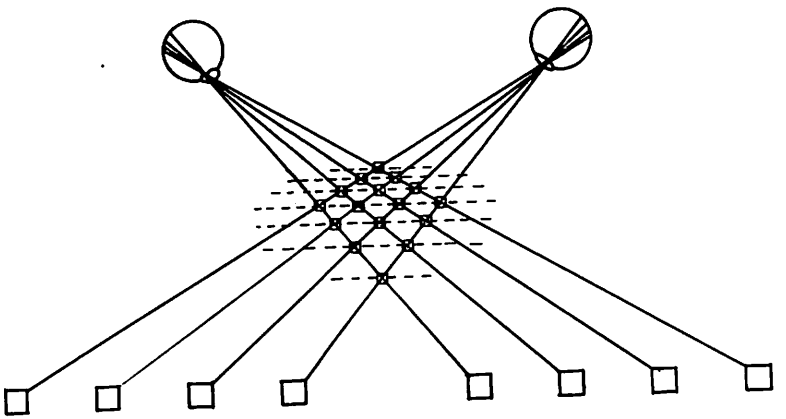

Fig. 5 - Ambiguity of Depth Estimation From Binocular Matching

Redrawn by permission. From Julesz, Foundations of Cyclopean Perception, pg. 119. Copyright (c) 1971 The University of Chicago Press. There are various ways in which it is possible to match binocular visual information from a simple spatially periodic scene. Only the match which superimposes the images of identical objects will result in correct depth estimation. Currently hypothesized low-level neural mechanisms for selecting the correct match all require some means of biasing the selection process via some other source of depth information.

FIGURES

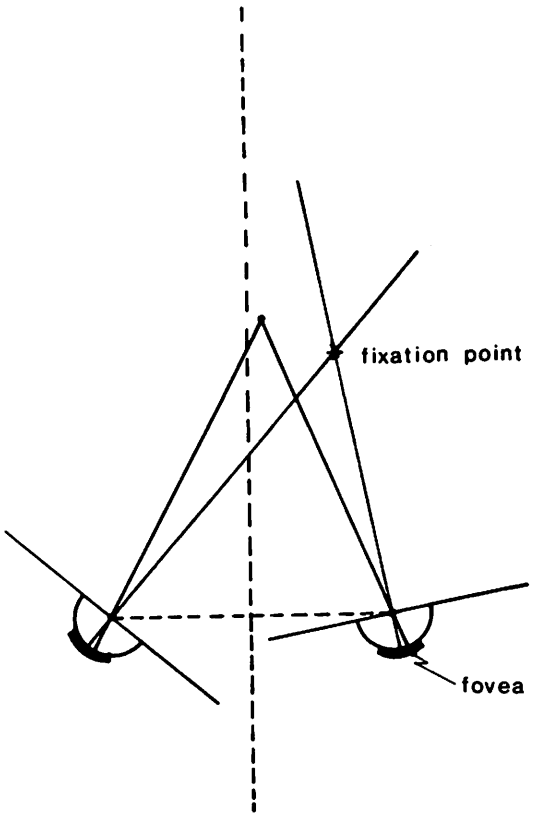

Fig. 6 - Visual System With Fovea and Vergence Eye Movements

In a visual system with vergence the two eyes are directed at the approximate point in space which is currently holding the attention of the system. If only the part of the image on the small high-resolution foveal area of the retina is considered then disparity matching between the two eyes is highly biased in favor of zero shift. Thus, if there are competing depth estimates the competition may be resolved in favor of the one which is supported by the smallest disparity

FIGURE 7

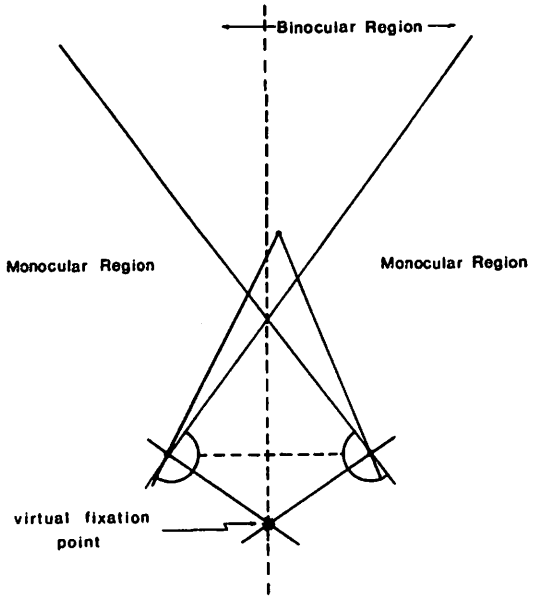

Fig. 7 - Visual System Like That in Frog and Toad

Frogs and Toads do not exhibit vergence eye movements. Likewise there is no distinct foveal area of the retina. Between the extensive binocular regions of the retinas quite large disparities may occur. More troublesome to computational models is the fact that there is apparently no inherent mechanism for biasing the selection among competing depth estimates.

FIGURE 8

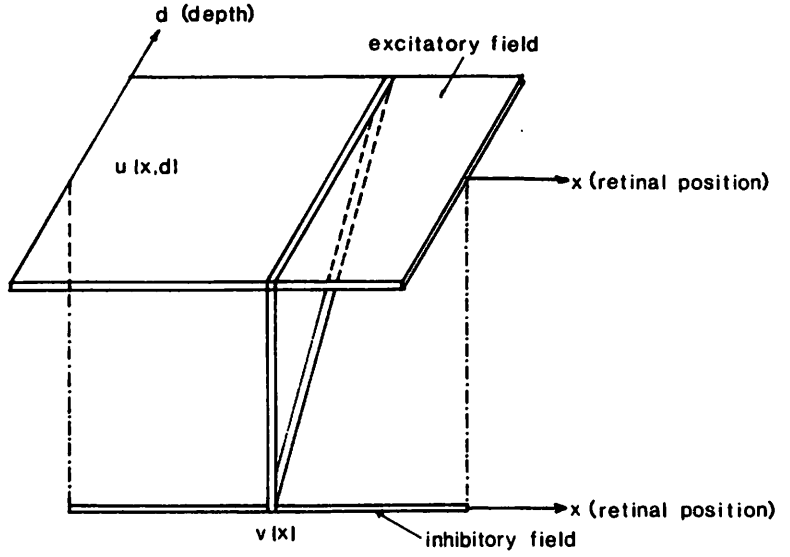

Fig. 8 - The Amari/Arbib Model

Redrawn by permission. From Amari and Arbib in Systems Neuroscience, J. Metzler (Ed.), pg. 126, Copyright (c) 1977 Academic Press. This diagram is meant only to suggest the structure of the model and not the detailed connectivity. The labeling is appropriate for the solution of the depth-mapping problem for a one dimensional retina with one source of depth cues. The excitatory field receives depth cued input. The inhibitory field receives an average level of excitation for all depths at each retinal position and sends an inhibitory feed-back to the excitatory field. There is lateral facilitation in both fields. Thus, nearby elements within a field are mutually reinforcing.

FIGURES

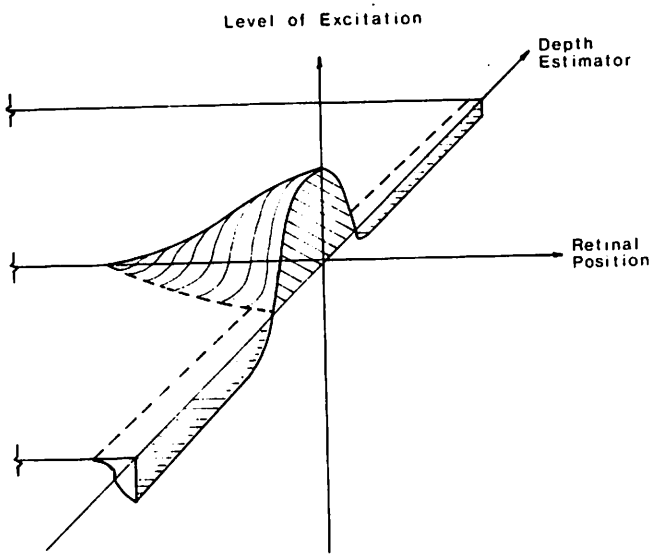

Fig. 9 - Spread of Excitation and Inhibition in Amari/Arbib Model

This is a cut-away view of the net spread of excitation and inhibition around a point-source of external stimulation. It shows the sympathetic excitation of points in the field at nearby retinal positions and similar depths. Within a narrow annulus about the retinal position of the stimulus there is a spread of inhibition along the entire depth axis. Thus other depths at the same retinal position tend to be suppressed.

FIGURES

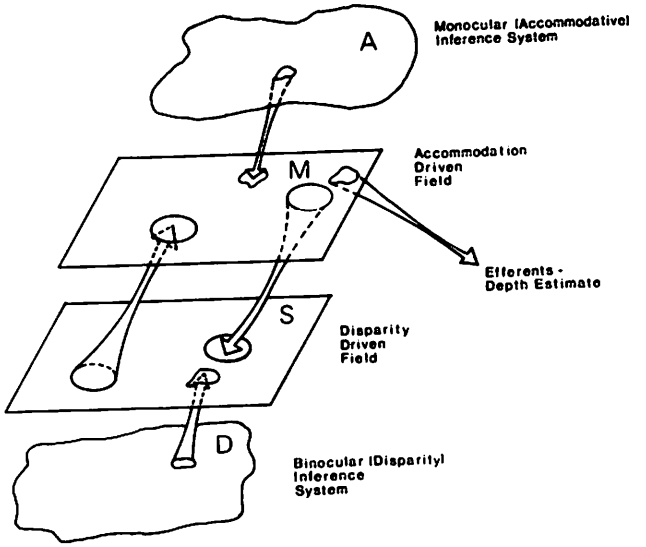

Fig. 10 - Connectivity of the Complete Cooperative Depth System

The sources of excitatory input to the monocularly and binocularly driven Amari/Arbib fields are shown. Besides the external inputs derived from other parts of the visual system, points of high excitation in one field provide additional excitation to corresponding points in the other field. There is a high degree of synergy wherever similar points are externally excited in both fields. Due to the competition among depth estimates points which are excited in only one field will have little chance to sustain excitation unless there are no such mutually excited points at the same retinal position. Depth system efferents are shown coming from the monocularly driven field. This is to allow the system to function if the animal loses binocular vision. Even though output is from the monocular field, the model can be tuned so that binocular depth cues dominate if they are present.

FIGURE 11

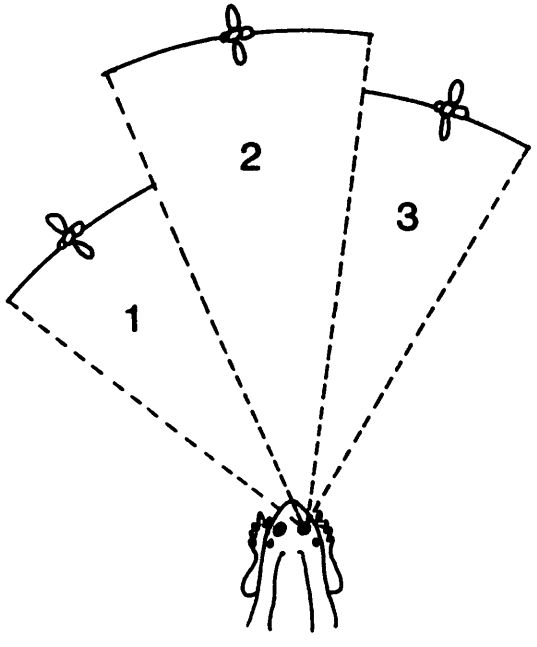

Fig. 11 - Visual Field Depth Segmentation Produced by the Model

Instead of producing a depth-map of each point in the entire visual space, the model produces a map which is really a segmentation of this space into depth-regions. Each attention-fixating point in the visual field (such as a prey object) will result in the addition of a segment. Thus, with three bugs in front of the animal the scene is divided into three depth regions. It is hypothesized that for prey-catching the animal will determine the correct visual angle from the current retinal stimulus, and will then infer depth by reference to the corresponding portion of the depth-map.

FIGURE 12

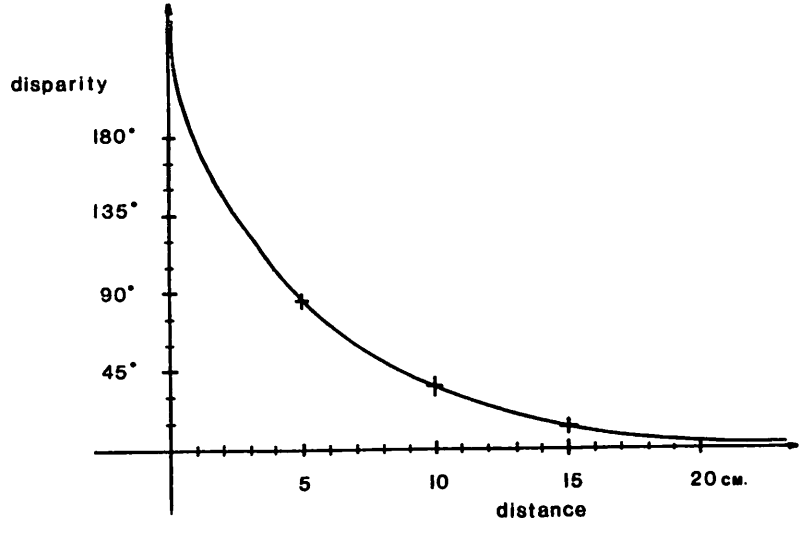

Fig. 12 - Angular Disparity vs. Distance From Viewer

This curve is computed from geometric considerations with the assumptions of pin-hole optics, spherical retinas, and an eye seperation of 3.3 cm. It shows the angular shift between the two retinas of the projection of a centrally-located point light-source. This shift or disparity is displayed as a function of distance of the light-source. Distance is measured along the perpendicular drawn from the mid-point of the line connecting the two pupils.

FIGURE

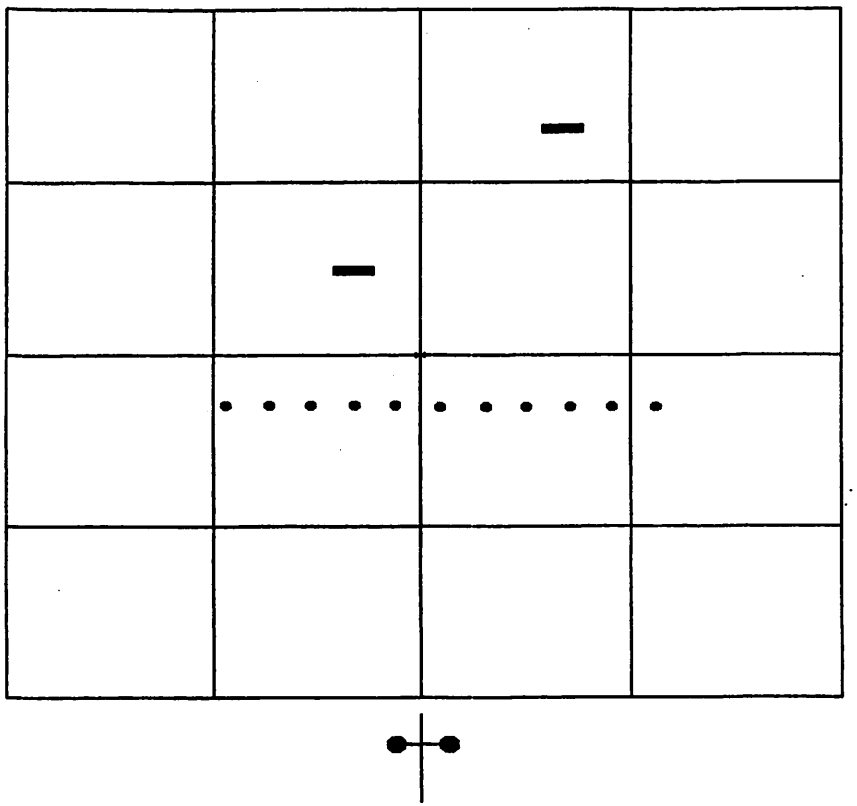

Fig. 13 - Scene Configuration Used for Testing the Model

Experiments with the model were conducted using visual input derived from the scene which is depicted here in top-view. In this scene each grid element represents a 10 cm. by 10 cm. area. The two rectangular objects represent prey (bugs) and the circular objects represent the posts of a paling fence interposed between the animal and its prey. The simulated animal is indicated by the cross-like object below the grid area. The circles on the cross-bar indicate eye position. The current model considers only the simplified case of one-dimensional retinas. Retinal images are formed by taking a horizontal slice through the scene.

FIGURE

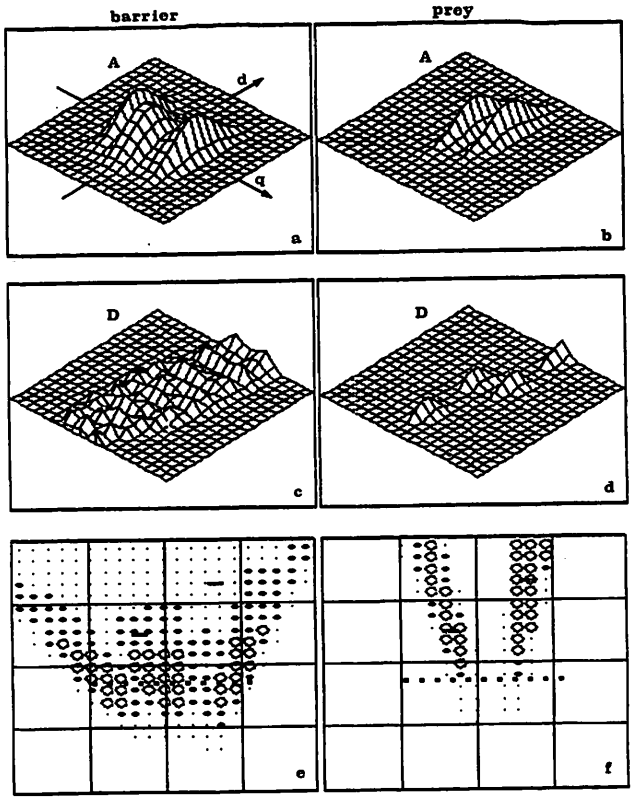

Fig. 14 - Monocular and Binocular Input Planes - Base Case

These graphs show the monocular and binocular raw depth estimates derived from the scene shown in Fig. 13. The left-hand column of figures is for the barrier process and the right-hand column is for the prey process. (a) thru (d) are in the retinal position (q) vs. angular disparity (d) coordinate system. In these figures the height of the curve above the grid-like plane indicates the estimated likelihood of the particular disparity being the correct one for the corresponding retinal position. (e) and (f) show the monocular estimates displayed in the original spatial coordinate system. Here, the estimates are shown superimposed upon the original scene, and are size encoded. The size of each small oval represents the relative strength of the estimate at that portion of the visual field.

FIGURES

Fig. 15 - Time Course of the Model - Base Case

The time course of the depth model from its initially-inert state (a) to a satisfactory depth segmentation (f) is shown here. The full monocular/binocular model was used with the input planes shown in Fig. 14. All figures are in the retinal angle vs. disparity coordinate system. Thus, the elapsed simulation time represented is nearly 7 time-constants. Successive figures are temporally spaced 1-1/3 field time-constants apart. The two-dimensional grids show the level of excitation of the various fields, and the line-graphs under the grids indicate the intensity and localization along the retinal angle axis of excitation in the inhibitory pools.

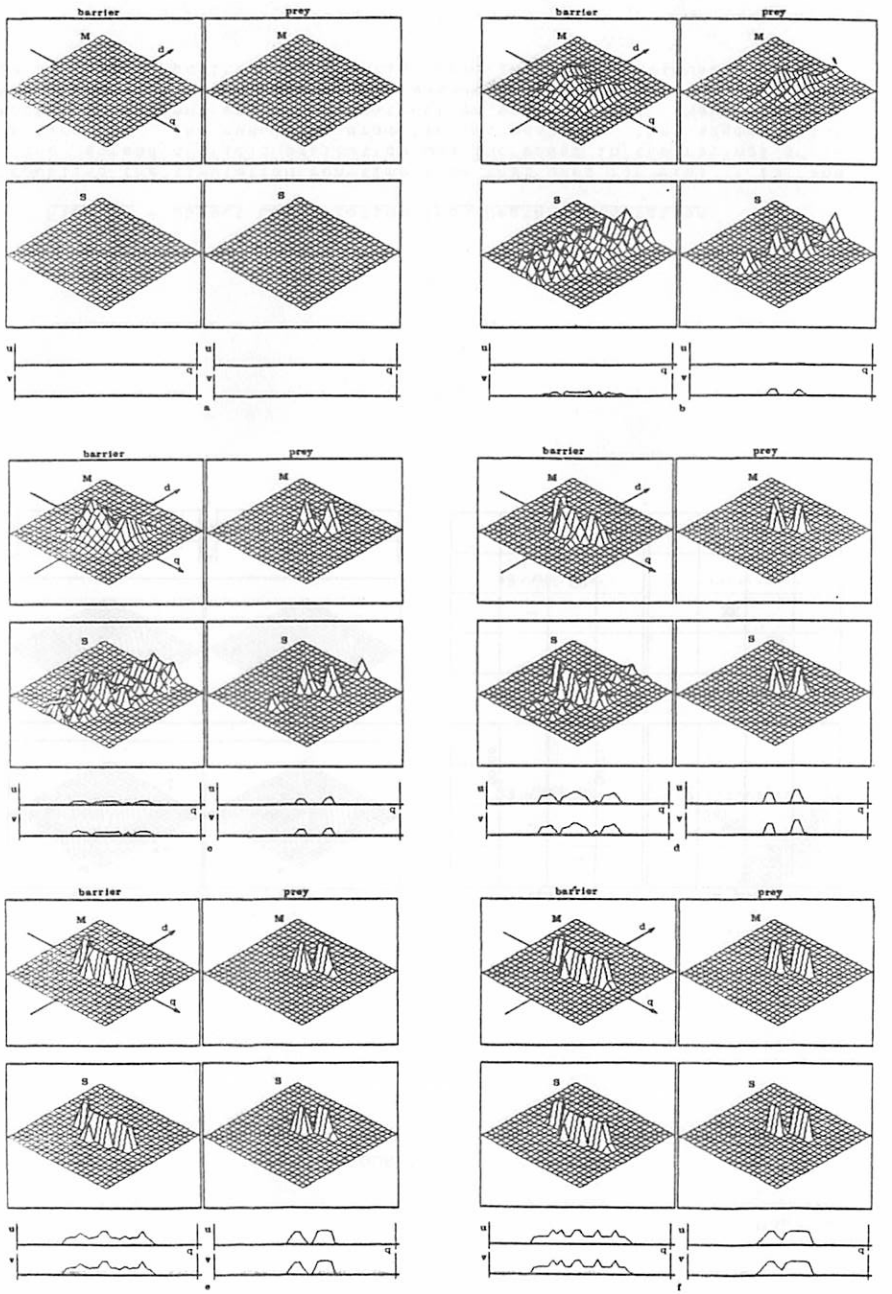

FIGURE 6

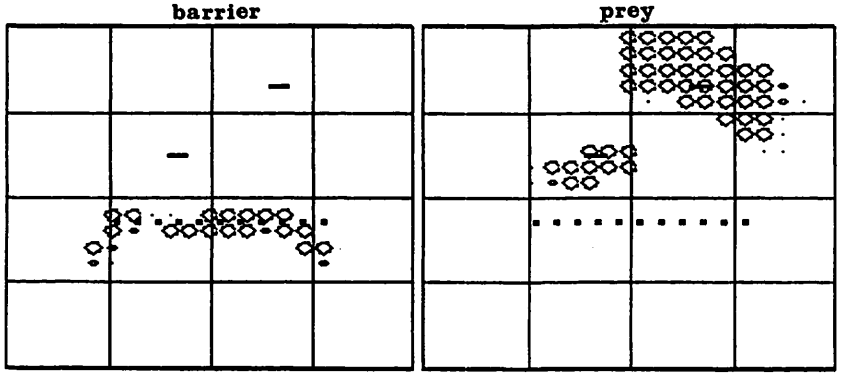

Fig. 16 - Scene Reconstruction from Depth Segmentation

The final depth segmentation shown in Fig. 15f was used to produce the reconstruction shown here. Both the barrier and the two "bugs" were correctly located spatially. The reconstruction is shown over-laid upon the original scene for ease of comparison. The relatively broad spread of the estimate in the depth-direction for the rear "bug" is due to the reduction of fine depth discrimination ability with distance.

FIGURE 6

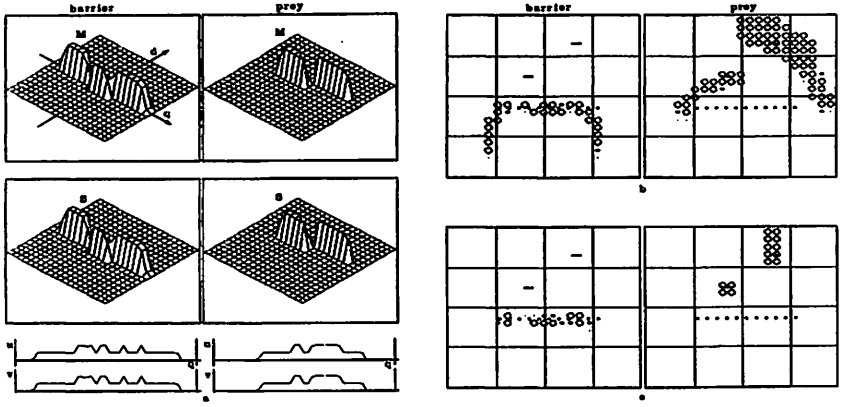

Fig. 17 - Object Localization from Depth Segmentation

By doubling the simulation run-time from that used for Figs. 15 and 16 the spread of field-excitation was increased in the retinal angle direction (a). The resulting dramatic increase in the segmentation effect is apparent in the reconstruction shown in (b). Nevertheless, objects can still be accurately localized by sampling the depth-map only at retinal positions currently receiving direct stimulation (c).

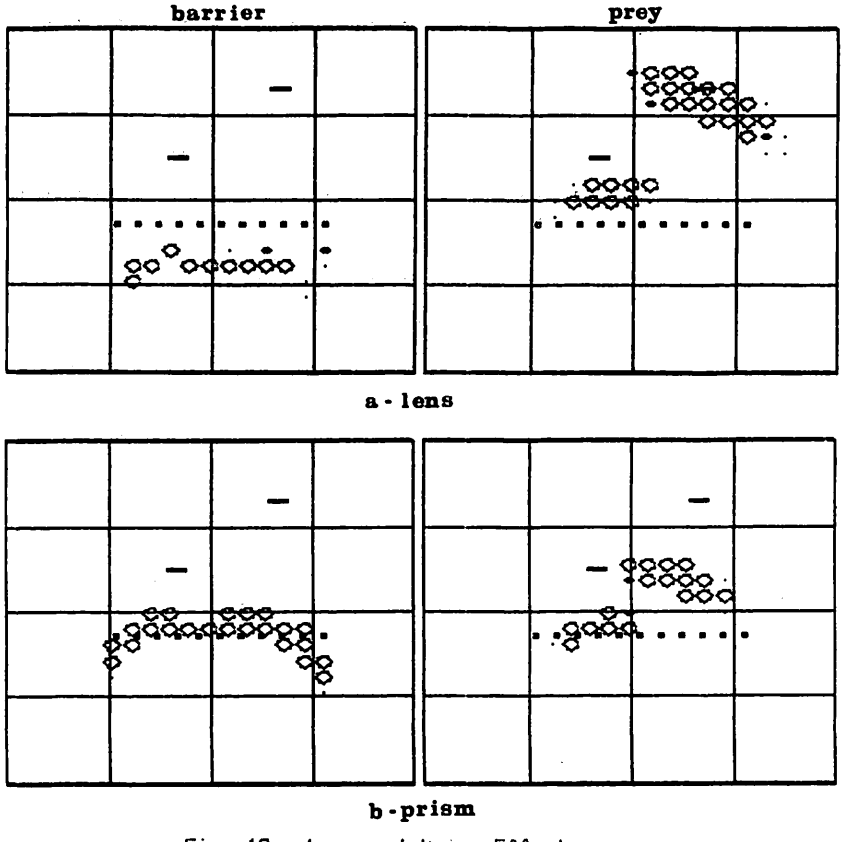

Fig. 18 - Lens and Prism Effects

A simulated lens, set to produce a 20% shift in the disparity coordinate of the monocular input, was used in obtaining the reconstruction shown in (a). Only a small shift in the model's depth estimate for prey stimuli occurred. The barrier estimate was more grossly affected. A simulated prism, producing a 20% binocular shift, was used in producing (b). The large shift apparent in the prey depth-estimate compared with that obtained with the lens is consistent with behavioral results. The inconsistent lens and prism results obtained for barriers are explained by the close spacing and spatial periodicity of the fence-posts. No behavioral results currently exist for this type of stimulus data.

FIGURE

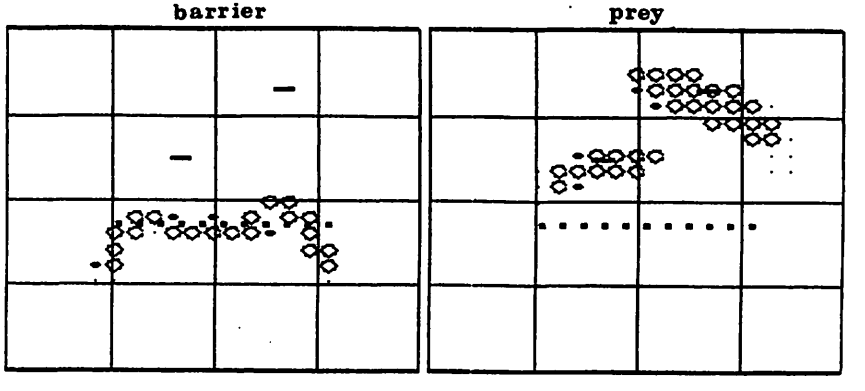

Fig. 19 - Monocular Response

This figure shows the depth segmentation obtained by suppressing binocular input to the model. The resulting monocular segmentation compares well with that obtained from the full monocular/binocular model. However, the amount of time (13 field time-constants) required to achieve a satisfactory segmentation was nearly double that of the full model.

FIGURE 6

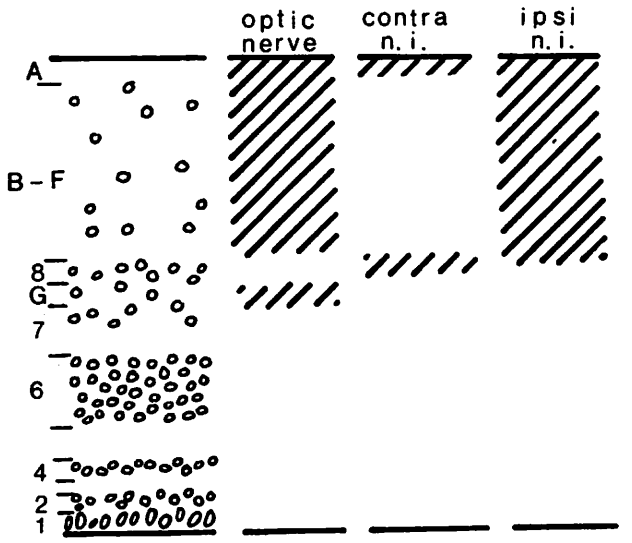

Fig. 20 - Distribution of Fiber Terminals in the Tectal Surface

Reprinted by permission. From Gruberg and Lettvin in Brain Research, Vol. 192, pg. 321, Copyright (c) 1980 Elsevier/North-Holland Biomedical Press. The layers of tectum are shown from the most superficial layer (A) to the ependymal layer (1). The shaded areas show the distribution of terminals of the optic nerve, the contralateral nucleus isthmus, and the ipsilateral nucleus isthmus. Of particular interest to the depth model are the layer labeled 8 where contralateral and ipsilateral isthmal input are present without optic nerve input, and the layer labeled G where only optic nerve input is present. It is proposed that layer 8 provides the right conditions for binocular disparity matching, and layer G is well suited for providing input to the monocular lens accommodation process.

Chapter 5: Development

S.C. Sharma: THE DEVELOPMENT OF SPECIFICITY OF RETINAL CENTRAL CONNECTIONS

Stephen A. George: CELLS AND SYNAPSES IN VISUAL SYSTEMS OF DIFFERENT PLOIDY

Susan B. Udin: THE DEVELOPMENT OF ORDERLY CONNECTIONS BETWEEN THE NUCLEUS ISTHMI AND THE TECTUM IN XENOPUS

Kenneth J. Overton and Michael A. Arbib: THE EXTENDED BRANCH-ARROW MODEL OF THE FORMATION OF RETINO-TECTAL CONNECTIONS

S.C. Sharma: THE DEVELOPMENT OF SPECIFICITY OF RETINAL CENTRAL CONNECTIONS

> From the functional point of view the growth cones of the retinal ganglion cells may be regarded as a sort of club or battering ram, endowed with exquisite chemical sensitivity, with rapid amoeboid movements, and with a certain impulsive force, thanks to which it is able to press forward and overcome obstacles met in its way, forcing cellular interstices until it arrives at its destination.
>
> --Ramon y Cajal, 1899, pp.544-545

The above-cited statement describes perhaps most elegantly the initial concept of how neurons may form synaptic connections. In the decades following Cajal's observation, it was recognized that vertebrate neurons send their axons in the embryonic CNS to form highly specific point-to-point connections with specific types of target neurons at particular loci in the brain (for review, see Gaze, 1970; Jacobson, 1978; and Lund, 1978). For the present review, fundamental work apparently started with Sperry's observation of the early 1940's. Sperry (1943, 1944) found that when the optic nerve of lower vertebrates was cut or crushed, the optic fibers regenerated back to their original position. This conclusion was based upon behavioral testing of the animals following eye rotation and consideration of other surgical procedures. Later Sperry (1950) wrote: "the optic fibers differ from one another in quality according to the particular locus of the retina in which the ganglion cells are located. The retina apparently undergoes a polarized field-like differentiation within the retina and the tectum during development, which brings about specification of the ganglion cells and the tectal cells." The functional relations established by the optic axon in the brain centers are patterned in a systematic manner.

In essence Sperry (1945) postulated that specific regrowth of axons following optic nerve section was mediated by specific chemoaffinities. Implicit in this particular notion was an idea that during development, cells of the retina and tectum acquire cytochemical labels denoting their position within the retina or the tectum. Growing axons then read these labels by a kind of surface chemotaxis and are thus guided to the tectal cells having corresponding labels. Subsequent experiments by Sperry and co-workers on the retinotectal system apparently gave credence to his theory and indicated that the matching process was very precise and rigid. However, most of the support for Sperry's theory came from indirect evidence, primarily behavioral studies of animals whose eye cup had been rotated 180° at various stages of development. Eyes so manipulated developed normal vision if the operations were perfomred at a sufficiently early stage; whereas inverted visuomotor behavior developed if eyes were rotated at later stages.

The studies of Székély (1954) suggested that the nasotemporal axis of the eye was fixed before the dorsoventral axis. These studies were further tested electrophysiologically by Jacobson (1968a) who identified a critical period in the developing eye of the embryo organizing the future visual pathways of the animal. In Xenopus this critical period was between stage 28-31. When the optic cup was rotated through 180° at stage 28/29, the toad developed a normal visual projection. When similar operations were performed at stage 30, the visual projection was abnormal in the sense that the map in the mediolateral direction across the tectum was normal (i.e. dorsoventral

across the retina) but inverted in the rostrocaudal direction across the tectum (anteroposteriorly across the retina). Eyes rotated at stage 31 or later showed inverted maps on both directions across the tectum (Jacobson, 1968a). Jacobson (1968b) also demonstrated that the first ganglion cells in the retina become post-mitotic shortly before the specification of the ganglion cells' central connections. Hence, the cessation of DNA synthesis in the differentiating ganglion cells was followed closely by the specification of the cells' central connections.

In a detailed series of subsequent experiments, Jacobson, in collaboration with Dr. R.K. Hunt, suggested that in the long sequence of "developmental programming" events, the critical period is but one irreversible step. In one experiment these authors showed that when the presumptive optic vesicle reaches the periphery of the stage 22/23 Xenopus embryo, it already possesses a pair of primitive retinal axes, basically aligned with anteroposterior and dorsoventral axes of the eye. These axes are stable (Hunt & Jacobson, 1973a). However, until the eye reaches stage 28, the primitive retinal axes are replaceable. In 2 to 6 hours following 180° eye rotation, the existing axes are replaced by a new pair or orthogonal axes which are themselves "stable but replaceable" and which are once again aligned with the major axes of the embryo's body (Hunt & Jacobson, 1972a, 1974).

In just 2 steps as the optic cup develops from stage 28 to 31, the capacity to undergo axial replacement is lost and the existing "replaceable axes" are locked-in and specified as permanent reference axes for the generation of locus specificity in the retina (Hunt and Jacobson, 1972a, b). These authors further concluded that after

stage 31, the specified axes and subsequently their ganglion cell central connections cannot be modified by either a) rotation of the eye transplanted into a pre-stage 28 host orbit; b) prolonged organ culture of the eye; c) serial reintroduction into younger embryos; d) depriving the retina of its central connections for 4-6 weeks; or e) disrupting the normal pattern of retinal growth (Hunt & Jacobson, 1972a, b; Hunt, 1975).

The relationship between the post-mitotic state of retinal ganglion cells and the time when the ganglion cell central connections become specified has been shown in only one species (Xenopus, Jacobson, 1968). Since these remarkable observations are of central importance in understanding the principles of specification of neuronal connections, Dr. Hollyfield and I were prompted to test whether the earlier observations of Xenopus are valid in a different species, Rana pipiens. We studied the cessation of DNA synthesis in the retinal rudiment in order to determine the time the first ganglion cells become post-mitotic. We also examined the retinotectal projection maps from eyes rotated at various stages of development in order to determine the time of specification of the retinal axes.

In direct contrast to the studies of Hunt & Jacobson, our experiments exploring the timing of axial specification in the developing retina of Rana pipiens showed that ganglion cell central connections were specified before the first ganglion cells became post-mitotic (Sharma & Hollyfield, 1974a). We observed that specification of the retina had occurred prior to early tail-bud stages while all cells in the retinal neuroepithelium continue to divide. Furthermore, the visual maps in these studies with Rana could be predicted prior to actual electrophysiological mapping by the position of the choroidal

fissure on the rotated eye. In the normal animal a small notch or cleft is present along the ventral margin of the iris. Closely associated with the fissure position is a large blood vessel on the inferior aspect of the globe. When these morphological markers were present in any position out of register with their normal alignment, the retinotectal map was always shifted through the same angle as was the eye (Sharma & Hollyfield, 1974a). Although this prominent ventral marker is also present in Xenopus laevis, none of the earlier studies by Jacobson (1968a,b) or Hunt & Jacobson (1972a,b, 1973a,b) has commented on the relative position of the choroidal fissure in relation to orientation of the retinotectal map.

The consistency of our results in Rana pipiens prompted us to reinvestigate in Xenopus the orientation of retinotectal maps relative to choroidal fissure position in eyes rotated at various stages of development or reciprocally exchanged between left and right orbit (Sharma & Hollyfield, 1974b; 1980). The position of choroidal fissures in Xenopus laevis is prominent at tadpole stages as well as in postmetamorphic animals when all of our electrophysiological mapping was performed. The choroidal fissure was prominent in each of the experimental animals used in these studies.

The normal visual field of each eye in Xenopus projects to the contralateral optic tectum; the nasal visual field to the rostral tectum; temporal field to the caudal tectum; dorsal field to the medial tectum; and inferior field to the ventral tectum (See Fig. 1-a). In Xenopus whose eye was rotated 180° between embryonic stage 24-28, the resultant visuotopic projection was also rotated 180° (Fig. 1-b). This result was consistent regardless of the stage of eye rotation. However, in

very few cases, duplicate maps were found. In these maps, the dorsal visual hemifield projected to the extent of the dorsal tectum; whereas, the ventral hemi-visual field projected to the extent of the dorsal tectum but was rotated by 180°. These animals had two choroidal fissures, one directed dorsally and the other ventrally.

In animals where eyes were reciprocally exchanged with 0° rotation, the choroidal fissure appeared at its normal ventral position. In these cases, the nasotemporal axis of the eye was reversed and the dorsoventral axis was normal. The resultant map was rotated 180° in the nasotemporal axis but was normal in the dorsoventral axis (Fig. 1-c). In animals with 180° reciprocal eye exchange, the nasotemporal axis of the maps was normal, but the dorsoventral axis was rotated (Fig. 1-d). In both instances the projections were consistent with the position of the eye, whether the exchanges were done at stage 27 or later. Similar results have been obtained by Gaze and his co-workers (Gaze et al., 1979) in Xenopus.

From these studies, the following conclusions can be made: a) the degree of rotation of the visuotectal map always corresponds to the degree of rotation of the choroidal fissure; b) the reciprocal eye exchange, with or without eye rotation, expresses retinotectal connections according to the original axes of the eye and were never respecified by axial cues from the new orbit; c) eyes reciprocally exchanged to contralateral orbit projected invariably to the contralateral optic tectum indicating the absence of side specificity.

Recently published studies by Gaze et al. (1979) have also found that the results of visuotectal map orientation always corresponded to the orientation of the eye at the time of mapping except for a few cases in which "compound" maps were recorded. In the latter

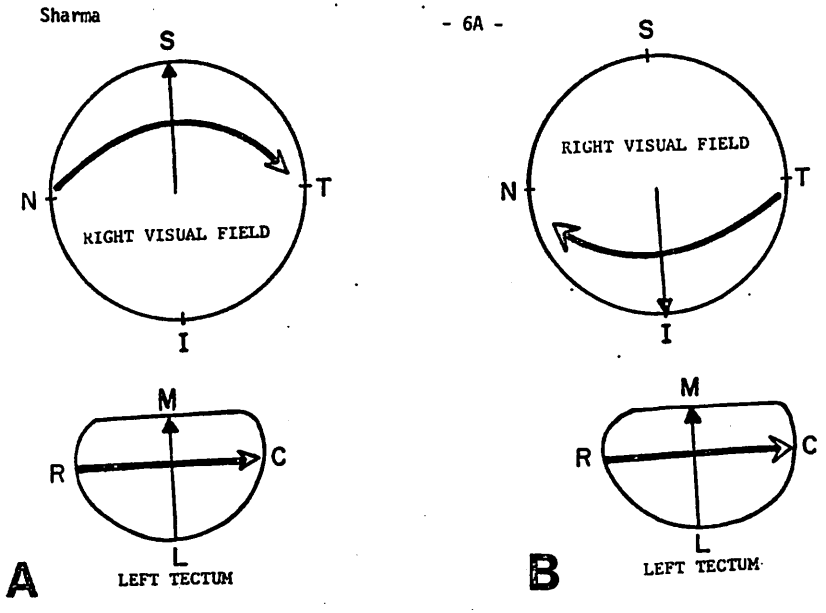

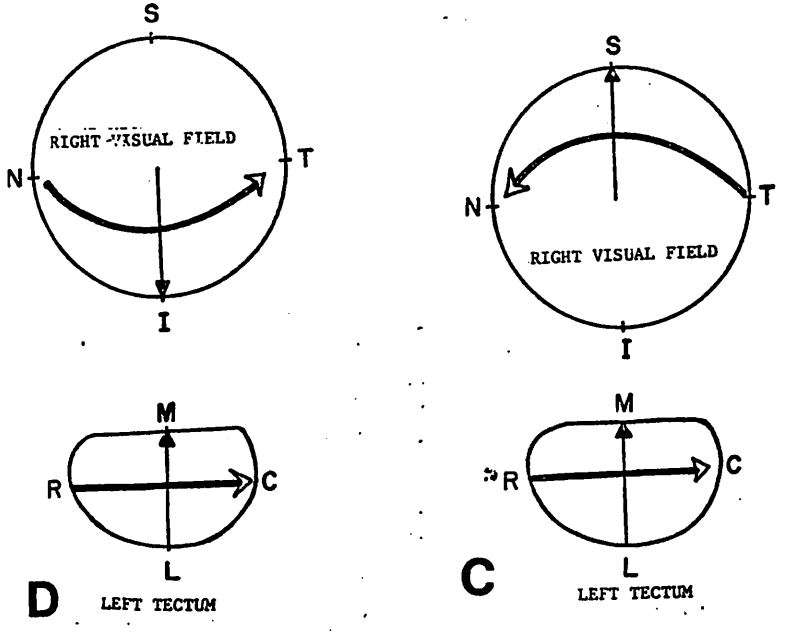

Explanation of the Figures

Fig. 1-a Diagrammatic representation of the visuotopic map from the normal right eye to the left optic tectum. The connections for this and for subsequent figures are the same: N, nasal; T, temporal; S, superior; I, inferior; R, rostral; C, caudal; M, medial; and L, lateral. In the normal map, the nasal visual field projects to the rostral tectum and the temporal field to the caudal tectum (represented by a heavy line with open arrow). The superior visual field is represented onto the medial tectum and the central and inferior visual field onto the lateral and ventral tectum (represented by thin line with closed arrow).

Fig. 1-b Right visual field map onto the left tectum in an animal whose eye was rotated 180° at embryonic stage 24. This map is rotated 180°.

Fig. 1-c The diagrammatic representation of the visuotopic map in which a left eye was transplanted into the right orbit at stage 27 without rotation. In this case, N-T axis of the field was rotated but the dorsoventral axis was normal (compare with Fig. 1-a).

Fig. 1-d In this case the left eye was transplanted into the right orbit at stage 27 with 180° rotation. The dorsoventral axis was rotated but the N-T axis was normal.

cases, the portion of the map which was oriented like the eye came from the originally operative eye tissue, while the other portion of the map came from eye tissue apparently newly grown from the optic stalk.

Using chimeras (albino/wild type) Xenopus, Gaze et al. (1979) showed that resultant eyes were of "compound type" with two fissures. The origin of the dorsal eye was graft derived, whereas the ventral eye with a normal fissure was derived from the host tissue. Gaze et al. suggested that the normal ventral eye of the "compound eye" was probably derived from the optic stalk of the host, giving rise to a normal map.

The evidence of ocular respecification following eye rotation in chick embryo (Goldberg, 1976a) could be the consequence of a new fissure and the development of ventral retina from the optic stalk.

The question of the position of the choroidal fissure is an important aspect of recent studies. From the time of its appearance in the ventral rim of the early optic cup, its location is evident throughout the life of the animal. It is not known when choroidal fissure position is determined in Xenopus laevis. In histological preparation of Xenopus retinas the fissure can be identified as early as stage 27, but it is not readily apparent in the living embryo until the appearance of melanin in the pigment epithelium of stages 31 and 32. The determination of choroidal fissure position has been discussed elsewhere (Sharma & Hollyfield, 1974a).

The recent elegant studies of Holt (1980) showed that during normal development of the eye in Xenopus, the optic stalk cells migrate outward and upward during the optic cup stage of the eye and that these cells form the ventral retina where the future choroidal fissure appears. In those experiments, the eye rudiment at stages

22-37 was excised either partially or completely and was incubated in a medium containing ^{3}H-thymidine. After washing, the eye anlage was replaced in the socket of the same embryo. These embryos were fixed at stages 36-42. When the ventral half eye anlage at stage 24-27 was treated, the labelled cells appeared in the upper half of the ventral retina. Cells surrounding the choroidal fissure were unlabelled. In a second series of experiments, when the whole eye (stage 22-28) was incubated, the resultant autoradiographically labelled cells were present all over the eye except in the ventral most retina containing the choroidal fissure. Unlabelled cells in the ventral retina were not found in studies where the eye was incubated after fissure formation was completed. This study showed, therefore, that there is a progressive movement of cells from the ventral towards the dorsal aspect of the retina during the optic cup formation stage.

From these results, it was inferred that in 180° eye rotation experiments, different fissure positions in the eye could be attributed to the extent of the surgery and the stage at which such operations were performed. The dorsally positioned fissure could be the consequence of deeper surgery at the optic vesicle stage or shallow surgery at the early eye cup stage. If, however, surgery was shallow at the optic vesicle stage, a normal ventral choroidal fissure would develop, assuming, of course, that stalk cells giving rise to ventral retina were still intact and that healing was excellent. When, during surgery, the stalk cell population was divided, a double fissure would result. It was further inferred that

incomplete eye rotation leading to the formation of double fissures (a stage which has been considered by previous workers as the stage where the polarity of the eye is thought to be determined -- Sato, 1933; Beckwith, 1927; Stone, 1966; Goldberg, 1976a, b) may be the explanation for calling the early eye stages "labile" for the determination of axes of the eye.

The question of timing of cessation of DNA synthesis in the ganglion cells of the central retina in relation to the specification of their central connections also deserves comment. Jacobson (1968b) reports that all cells in the retinal neuroepithelium incorporate ^{3}H thymidine until stage 28, at which time a few cells drop out of the mitotic cycle and subsequently differentiate (become specified). Cima & Grant (1978) have recently reported that a bundle of axons, which they interpret as of ganglion cell origin, is present in the optic nerve head of Xenopus as early as stage 28. Since it is usual for axonal development to occur only in post-mitotic cells, it is unlikely that axons would be elaborated prior to withdrawal of these cells from the mitotic cycle. These observations of Cima and Grant suggest that some cells stop dividing much earlier than the stage reported by Jacobson (1968b). Furthermore, the polarization of the developing retina also occurs much earlier than previously reported by Jacobson (1968a). The exact relationship with respect to the relative timing of these two events is not clear at present.

Experimental evidence suggests that the retinotectal projections from eyes either rotated in the orbit or exchanged between left and right orbit were expressed according to the original axis of the eye at the time of the manipulations. In no case was a normally oriented

map obtained from a rotated eye when the choroidal fissure position indicated that the eye was indeed rotated. There is no compelling evidence to indicate that orbital cues can influence or respecify the axial coordinates within the retinal rudiment. There is also no evidence from recent studies that anterior-posterior and dorsal-ventral axes are specified as separate developmental events.

The preceeding discussion leads to an obvious two-fold question: 1) how are retinal axes generated and 2) what role do the axes play in the final projection of the map over the extent of the tectum?

The answer to the second part of the question is that in every study conducted to date in the retinotectal system, the indication is that whatever one does with the tectum (remove, rotate, implant, explant, or partially ablate -- Sharma, 1972, 1981; Schmidt, 1978), the resultant retinal map is always polarized; that is, the nasotemporal and dorsoventral axes of the projection are always maintained. This is perhaps essential for generation of visuotopic order in the projection.

The answer to the first part of the question is, on the other hand, somewhat more intricate, and I shall describe the few models and some experimental work which is pertinent here.

It has been argued that since the eye grows concentrically, i.e. radially, the spatially ordered sequence of cell division may specify the position of new cells. Hence, the specification of retinal cells according to Cartesian coordinates system (orthogonal axes) can also be thought of in terms of a polar coordinate system (MacDonald, 1977). The position of a ganglion cell is defined by

the distance from the center (a radial coordinate) and its angular distance or position along the circumference (the circumferential coordinate). The positional information of ganglion cells, accordingly, arises gradually during retinal development when cells become post-mitotic, thereby determining position by the radial distance from the center and angular coordinate by the angle of the fascicle that guides its axon to the optic nerve head. Each fascicle contains axons from an area in a common wedge-shaped sector of the retina, with oldest axons near the optic nerve head and youngest on the periphery. Therefore, it would be the first fascicle in the developing retina which would assign the angular coordinates for all the axons which will develop later. The spatio-temporal model for the development of optic nerve fiber topography is, therefore, consistent with the polar coordinate positional information hypothesis.

Bodick and Levinthal (1980) showed that a large optic bundle in developing zebra fish arises from cells in a pie-shaped sector of the retina and that cells from the opposite side of the choroidal fissure do not merge into the same bundle. The separation, leading to the formation of a crescent pattern by fibers leaving the eye, is a consequence of the barrier presented by the choroidal fissure. These authors suggested that the opening in the crescent pattern in the developing retina is important since it leads to inversion of the overall topography of the optic axons in the optic nerve, where youngest fibers are on one side of the nerve and the oldest fibers are on the opposite side. (See also Scholes, 1979). Bodick and Levinthal (1980) suggested that the polar coordinates of the cell body position in the retina correspond

to the rectangular coordinates in the optic nerve because of the inversion of overall topography of optic axons in the nerve. They proposed that the ganglion cell axons follow pathways that are determined by the substrate along which they grow and that locus specificity of ganglion cells is determined by the time and place at which they initiate the growth of an axon. These rules, then, may perhaps give rise to (a) locus specificity of the ganglion cells and (b) the ordering of optic axons within the optic nerve. However, whether similar rules apply to the mode of selective synapse formation on the target centers remains to be determined.

Dr. Gunther Rager (see review, 1980) has proposed that the position of a ganglion cell can be specified by spatiotemporal coordinates with respect to the developing optic fiber layer. The ganglion cells formed in incremental rings of growth are transformed into a crescent at the entrance of the optic stalk during eye development. It was asserted that the mode of growth of the optic axons and the tectum were sufficient to the development of a retinotectal map. Rager's hypothesis for the connection formation includes a) temporal and spatial order; b) gradient of cell generation and maturation; c) contact guidance; and d) cell death. This hypothesis does not require Sperry's initial suggestion of a chemoaffinity hypothesis.

In systems where aggregation and sorting of dissociated cells in the retina have been studied (for review, see Moscona, 1976), it has been shown that selective cell adhesion exists. For example, in the retinotectal system, Halfter et al.(1981) showed that a gradient of adhesion between retinal and tectal cells exists. A preferential adhesion of tectal cell membranes in 6-day old chick embryonic retinal explants in cultures was shown to the nasal

retinal ganglion cell axons but not from the temporal retina. Furthermore, the preferential adhesion of the retinal neurite was independent of the dorsoventral quadrant of the retina. These authors argued that the preferential adhesion by the nasal neurite suggested a continuous gradient in the nasotemporal retina. The molecular nature of the adhesion gradient, however, remained elusive.

A recent paper (Trisler et al., 1981) has, for the first time, demonstrated the existance of the concentration gradient of a particular molecule in the chick retina. These authors showed that a monoclone antibody bound more strongly to the dorsal retina as compared to the ventral one. The dorsal retina binds 35-fold more of this antibody than does the ventral retina. These authors referred to the specific antigen which is detected by the monoclonal antibody as "Toponymic," i.e. "marker of the position." This probably cell-surface protein is present in all layers of the 14-day old chick retina. The binding gradient represented differences in the amount of antigen per cell. A similar gradient was observed as early as in a 4-day old embryonic eye. Furthermore, in one animal with an ectopic eye (situated in the middle of the forehead) with abnormal orientation, the toponymic molecule gradient on it had normal orientation with respect to its choroidal fissure. This last example indirectly supports our earlier suggestion that topography of the retina for its subsequent map is always aligned by the position of the eye with respect to its choroidal fissure.

The question of how the molecular gradient of the retina expresses itself in the optic tectum for the generation of a topographic map remains, at present, unclear.

In conclusion, recent experiments on eye rudiments give absolutely no reason to suppose that specification of the eye for subsequent map formation involves polarization of the eye rudiment in Cartesian coordinates. Rather, specification of the eye may be controlled by polar coordinates or some other spatio-temporal order of cell generation. I have here outlined current concepts of eye specification. It is not clear exactly how position-dependent properties for each ganglion cell are acquired both in the polar coordinate system as well as the formation of the topographic molecule gradient which is ordered in relation to the axis of the retina. Certainly, the monoclonal antibodies-antigen approach opens an exciting chapter in the determination of specification of retinotectal connections.

REFERENCES

Beckwith, C. J. 1927. The effect of the extirpation of the lens rudiment on the development of the eye in Amblystoma punctatum with special reference to choroidal fissure. J. Exp. Zool. 49; 217-259.

Bodick, N. and C. Levinthal. 1980. Growing optic nerve fibers follow neighbours during embryogenesis. Proc. Natl. Acad. Sci. U.S.A. 77; 4374-4378.

Cima, C. and P. Grant. 1978. Ultrastructure evidence of early retinal ganglion cell differentiation in Xenopus laevis. Soc. for Neuroscience Abst. 4; 622.

Gaze, R.M. 1970. The Formation of Nerve Connections. Academic Press. New York.

Gaze, R.M., J. D. Feldman, J. Cook and S. H. Chung. 1979. The orientation of the visuotectal map in Xenopus: developmental aspects. J. Embryol. Exp. Morph. 53; 39-66.

Goldberg, S. 1976a. Progressive fixation of morphological polarity in the developing retina. Develop. Biol. 53; 126-127.

Goldberg, S. 1976b. Polarisation of the avian retina. Ocular transplantation studies. J. Comp. Neurol. 168; 379-392.

Halfter, W., M. Claviez and U. Schwarz. 1981. Preferential adhesion of tectal membranes to anterior embryonic chick retina neurites. Nature. 292;67-70.

Holt, C. 1980. Cell movements in Xenopus eye development. Nature. 287; 850-852.

Hunt, R. K. 1975. Developmental programming for retinotectal patterns. pp. 131-150. In Cell Patterning, Ciba Foundation Symposium 29, Elsevier, New York.

Hunt, R. K. and M. Jacobson. 1972a. Development and stability of positional information in Xenopus retinal ganglion cells. Proc. Natl. Acad. Sci. U.S.A. 69; 780-783.

-- 1972b. Specification of positional information in retinal ganglion cells of Xenopus: stability of the unsepcified state. Proc. Natl. Acad. Sci. U.S.A. 69; 2860-2864.

-- 1973a. Specificaiton of positional information in retinal ganglion cells of Xenopus: Assay system for analysis of the unspecified state. Proc. Natl. Acad. Sci. U.S.A. 70; 507-511.

-- 1973b. Neuronal locus spceificity: Altered pattern of spatial deployment in fused fragments of embryonic Xenopus eyes. Science. 180; 509-511.

-- 1974. Specification of positional information in retinal ganglion cells of Xenopus laevis: intra-ocular control of the time of specification. Proc. Natl. Acad. Sci. U.S.A. 71; 3616-3620.

Jacobson, M. 1968a. Development of neuronal specificity in retinal ganglion cells of Xenopus. Develop. Biol. 17; 202-218.

Jacobson, M. 1968b. Cessation of DNA systhesis in retinal ganglion cells correlated with the time of specification of their central connections. Develop. Biol. 17; 219-232.

Jacobson, M. 1978. Developmental Neurobiology. 2nd Ed. Plenum Press. New York.

Lund, R. D. 1978. Development and Plasticity of the Brain. Oxford University Press. New York.

McDonald, N. 1977. A polar coordinate system for positional information of the vertebrate neural retina. J. Theor. Biol. 69; 153-165.

Moscona, A.A. 1976. In Neuronal Recognition (ed. Barondes, J.S.) pp. 205. Plenum Press. New York.

Rager, G. H. 1980. Development of the retinotectal projection in the chicken. Adv. Anat. Embryol. Cell. Biol. 63; 1-92.

Ramon y Cajal, S. 1899-1904. Textura del sistema nervioso del hombre y del los vertebrados estudios sobre el plan estructural y composicion histologica de los centros nerviosos, adicimados de-consideraciones fisiologicas fundadas in los nuevos des cubrimientos. Vol. 1. 566 PP. Madrid. N. Moya.

Sato, T. 1933. Uber die determination der fetal Augenspalts bei Triton taeniatus. Arch. F. Entwmech. d. Org., Bd. 128; 342-377.

Schmidt, J. T. 1978. Retinal fibers alter tectal positional markers during the expansion of the half retinal projecticn in goldfish. J. Comp. Neurol. 177; 279-300.

Scholes, J. H. 1979. Nerve fiber topography in the retinal projection to the tectum. Nature. 278; 620-624.

Sharma, S. C. 1972. Retinotectal connections of a heterotopic eye. Nature. 238; 286-287.

-- 1981. Retinal projection in a non-visual area after bilateral tectal ablation in goldfish. Nature. 291; 66-67.

Sharma, S. C. and J. G. Hollyfield. 1974a. Specification of retinal central connections in Rana pipiens before the appearance of the first post-mitotic ganglion cells. J. Comp. Neurol. 155; 395-408.

-- 1974b. The retinotectal projection in Xenopus laevis following right-left exchange of eye rudiment. Soc. for Neuroscience. Abst. 4; 421.

-- 1980. Specification of retino-tectal connections during development of the toad Xenopus laevis. J. Embryol. Exp. Morph. 55; 77-92.

Sperry, R. W. 1943. Visuomotor coordination in the newt (Triturus viridescens) after regeneration of the optic nerves. J. Comp. Neurol. 79; 33-55.

-- 1944. Optic nerve regeneration with return of vision in anurans. J. Neurophysiol. 7; 57-69.

-- 1945. Restoration of vision after uncrossing of optic nerves and after contralateral transposition of the eye. J. Neurophysiol. 8; 15-28.

-- 1950. Neuronal specificity. pp. 232-239. In Genetic Neurology (P. Weiss, ed.). Univ. of Chicago Press, Chicago.

Stone, L. S. 1966. Development, polarisation and regeneration of the ventral iris cleft (remnant of choroid fissure) and protector lentis muscle in urodele eyes. J. Exp. Zool. 161; 95-108.

Székély, G. 1954. Zür ausbildung der lokalen funktionellen spezifitat der retina. Acta Biol. Hung. 5; 157-167.

Trisler, G. D., M. D. Schneider and M. Nirenberg. 1981. A topographic gradient of molecules in retina can be used to identify neuron position. Proc. Natl. Acad. Sci. U.S.A. 78; 2148-2149.

Stephen A George: CELLS AND SYNAPSES IN VISUAL SYSTEMS OF DIFFERENT PLOIDY

If nervous systems are thought of as ordered assemblies of structurally and functionally distinct classes of neurons connected together in specific ways, then among the important characteristics of nervous systems must be the size, shape, and number of neurons they contain. The importance of neuron size and shape has been recognized in many theoretical studies of electrical activity in model individual neurons, in which space constants, interaction between postsynaptic potentials, and effects of dendritic branching are obviously functions of neuron geometry. The number of neurons in a given neural structure may also be a potentially important consideration in models, not of individual neurons, but of neural circuits. However, neuron number has not appeared as a critical parameter in most models published so far. In part this is because structures that have been modelled, e. g. cerebellum (Marr, 1969) and tectum (Lara, 1981), consist of some basic circuit repeated many times, and the operation of each unit circuit may be to some extent independent of the number of such circuits included in the whole structure. In part, also, the absence of neuron number in models is due to the paucity of experimental work on the role of cell number in neural function that might inspire or constrain neural modellers. One noteworthy model that does indicate how function depends on neuron number is that of Hall (1965) on binaural localization . Cats can discriminate differences of about 10 μsec in the time of arrival of sound at the two ears, although single brainstem auditory neurons cannot reliably distinguish differences less than about 1 msec. Hall was able to account for the cat's ability on the basis of probabilities of response in an ensemble of neurons, in a model in which the minimum discriminable time-of-arrival difference turned out to be proportional to the square root of the number of neurons in the ensemble.

One approach to providing information about the role of cell number

is to study the effects of varying it. Previous work has involved simply removing tissue from an embryo or adult. Cooke (1981) showed that removing any part of an amphibian early embryo led to a smaller later embryo, but with the correct proportions of cells in each type of tissue. This is the latest of studies over many decades that point to plasticity in the "fate" of embryonic cells, and to the existence of mechanisms that can adjust the scale of multicellular structures when cell number is altered. Most of the studies on visuomotor systems that are relevant to cell number, if only indirectly so, have been aimed at understanding how spatially ordered projections are formed, for example by creating "half-eye" or "half-tectum" animals (Sharma, 1972; Berman & Hunt, 1975; Schmidt et al., 1978). Rules of neuronal connectivity in visual systems have emerged from these experiments, such as the idea that optic nerve fibers may interact with each other to form an ordered projection during development, and may then impose some sort of "specificity" on the tectum, which can guide later regeneration. If a post-regeneration disparity exists between retina and tectum because part of one of these structures has been removed, fiber interactions may later come into play to induce a change to an appropriately compressed or expanded projection (Schmidt, 1978). These features have been included in a detailed model of retinotectal connections presented in this volume (Overton, 1982). Useful as disparity preparations have been in establishing rules for the formation of ordered projections, they do not address directly the role of cell number in the operation of neural circuitry, because they always involve gross changes in the amount of neural tissue, as well as in cell number. Such gross changes may lead to unknown adjustments that may effectively restore the tissue that was removed. For example, when half of an eye anlage is removed at an early embryonic stage , the resulting half-eye usually "rounds up" and projects normally to the tectum. However, even if measurements were made to rule out hypertrophy of the remaining half eye (which has not been done in any

published study so far), it is still difficult to rule out "regulative" changes that may reorganize the positional information in the half eye, in much the same way that the fates of cells were reorganized in the experiment by Cooke cited above. In the end, we cannot be sure whether the normal projection from a half eye results from changes in the eye, the ganglion cell/axon terminals, or the postsynaptic tectal cells. This, then, was the point of departure for the recent work in my laboratory: the need for a preparation in which effects of cell number could be studied, in a situation in which regulative changes would not occur. My solution has been to use alterations in the ploidy, i. e. the chromosome number, of Rana and Xenopus frogs. Here I will review those results that are relevant to visuomotor systems, in the hope that their bearing on considerations of cell size and number will prove stimulating to neural modellers who may wish to include such considerations in their models.

Normal individuals of animal species are diploid (2N), i. e. each of their cells contains two complete sets of chromosomes. In several classes of animals, notably fish, amphibians, and insects, triploid (3N) individuals with three sets of chromosomes in each cell, and individuals of even higher ploidy, occasionally occur spontaneously and can be produced in quantity in the laboratory. A remarkable feature of polyploid amphibians that was recognized years ago in a qualitiative way by Fankhauser (1941) is that they have larger but fewer cells than normal diploids. As a result of the reciprocal relation between cell size and cell number, polyploid animals and each of their constituent organs are normal in size, even though made up of larger cells. Although apparently healthy and qualitatively normal in behavior, 3Ns differ from 2Ns in subtle and interesting ways. For example, Fankhauser et al. (1955) showed that 3N salamanders learned a Y-maze task significantly more slowly than 2Ns. Since 2N and 3N brains are the same size, this finding shows that the way the brain is divided into cells is relevant to learning ability, an intriguing, if not finally very astonishing,

result.

The work in my laboratory has involved documenting quantitatively the cell size and cell number differences between 2N and 3N nervous systems, and, as it relates to visuomotor function, in making visual systems of hybrid ploidy through embryonic eye transplantation, in order to study spatial order and synaptic density in interacting 2N and 3N tissue. Triploid frogs have been prepared by delivering a hydrostatic pressure shock to fertilized eggs (Dasgupta, 1962). The ploidy of treated animals was checked by measuring the length of erythrocytes, which are suitable because of their uniform size in animals of each ploidy (George & Lennartz, 1980). The range of brain weights and body lengths, and the relation between brain weight and body length, were essentially identical in 2N and 3N Xenopus, confirming that 2Ns and 3Ns are similar in overall size and organ proportions. Brain cells were counted by homogenizing tissue and counting suspended nuclei using a fluorescence method. Differences between 2Ns and 3Ns in total brain cell number in a batch of sibling frogs are illustrated in Figure 1, from which it can be calculated that on the average 2N brains of a given size contained 30% more cells than 3N brains of the same size (Steer, 1981). Similar differences were found at each larval stage. Two reasons may be given why this difference was less than the 50% that might be expected based simply on the ratio of chromosome numbers. First, the fraction of brain volume occupied by extracellular space is smaller in 3Ns, because only the cells, and not the intercellular clefts, are enlarged in 3Ns. This factor would have little effect on total cell number if extracellular space were as it appears in conventional electron microscopy, amounting to about 3% of the total volume. However, impedance measurements, diffusion studies, and modified electron microscopy all yield a value of about 20% for the extracellular space fraction (reviewed by Gardner-Medwin, 1980), which we estimate may be reduced to 12% - 15% in 3Ns. Thus an extra 5% - 8% of the brain volume would be available to be occupied by cells, in

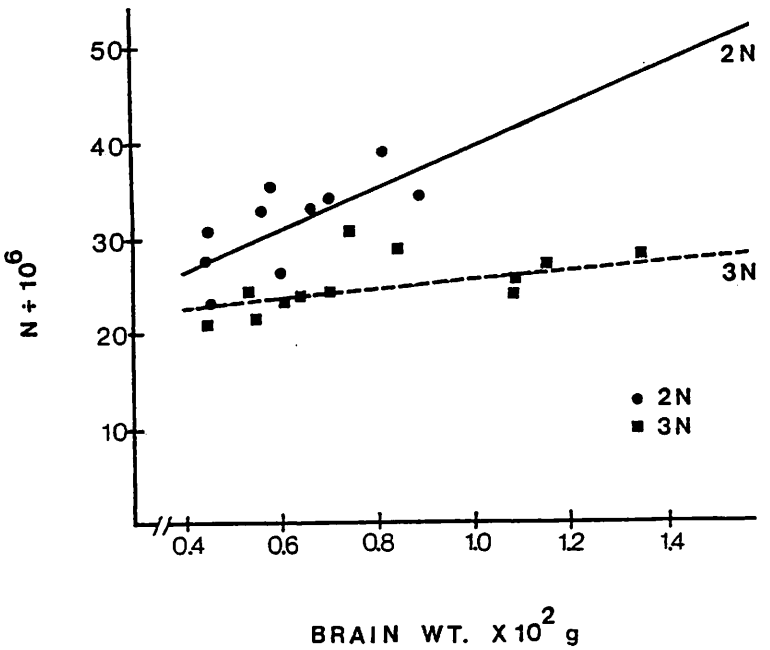

Figure 1. Total cell number in brains of sibling diploid and triploid Xenopus. Brains were homogenized and cells suspended in a solution containing Ethidium bromide, which causes DNA to fluoresce. Small samples of the suspension were placed in a counting chamber, and the number of nuclei in a known volume was counted using a fluorescence microscope. Each point represents the average of 20 determinations on the suspension from a single brain. The straight lines are linear regressions for the 2N and 3N data. This counting method does not distinguish between nuclei of different types of cells, so the counts include glia, blood vessel ependymal cells, and cells of the pia mater, as well as neurons.

3Ns. Second, although the average volume of nuclei of 3N neurons was found to be approximately 50% greater that that of 2N cell nuclei, as expected, there is much more to a neuron than its nucleus, and all parts of the neuron are not uniformly enlarged in 3Ns. In fact, 3N axons and dendrites could not be enlarged in every dimension, or neural pathways would be longer, and plexiform layers thicker, in 3Ns, which they are not. Thus the average total volume of 3N neurons, including cell prooesses far from the nucleus, is less than 50% greater than that of 2Ns. Ploidy does have some effect on dendrites and axons; an example is shown in Figure 2, in which the diameter distribution of 3N sciatic nerve fibers was shifted towards higher values compared with 2Ns (George & Lemanski, 1978); a similar result was found for optic nerve fibers. As an example of changes in dendrites, we found that 2N rod outer segments were thicker, but not longer, than 2N outer segments. These and other measurements we have made confirm that 3N frog nervous systems contain larger but fewer cells than 2N nervous systems.

Exchanges of eye rudiments between 2N and 3N tailbud-stage embryos have been made. Diameters of the transplanted eyes were checked and found to be normal as the eyes grew in hosts of a different ploidy (Figure 3). Thus, as hypothesized, there are no differences in tissue mass here that might trigger regulative changes. Retinotectal projections were mapped at a late larval stage and also found to be normal in order and extent, showing that cell number per se is not a factor in establishing a correct projection. We also transplanted eye rudiments from haploids (animals with one set of chromosomes) into normal diploids. Cell number and size differences might be expected to be even greater here, based on the ratio of chromosome numbers. However, haploid amphibians do not survive past an early larval stage because of many developmental abnormalities. Haploid eyes did survive in diploid hosts in some cases and projected to the tectum, but the eyes were misshapen and the electrophysiologically mapped projections, though qualititatively normal, were diffuse and responses were weak.

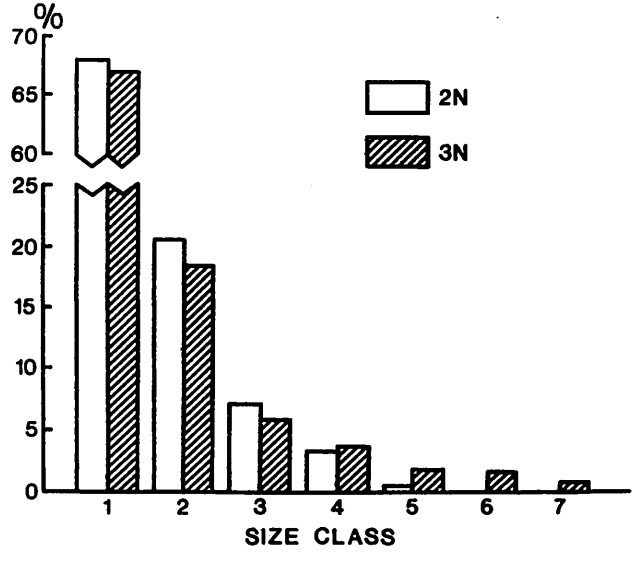

Figure 2. Distribution of cross sectional areas of 2N (open bars) and 3N (hatched bars) Xenopus sciatic nerves. Size class 1 contains fibers with areas from 0 - 100 μm^2, class 2 from 100 - 200 μm^2, etc. To obtain these distributions, sections of sciatic nerves embedded in paraffin were photographed, and the areas of all fibers in each photo were found using a perimeter. At the level of resolution of the light microscope, only myelinated fibers are seen. Note that there are more 2N than 3N fibers in each of the 3 smaller size classes, but more 3N fibers in the 4 larger classes.

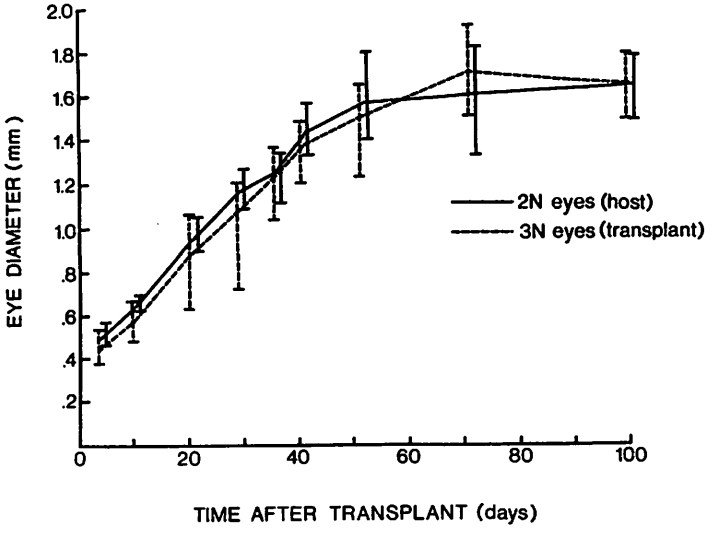

Figure 3. Growth of 3N Xenopus eyes transplanted at the tailbud stage into 2N hosts. The left eye rudiment of the host embryo was removed just before inserting the donor eye rudiment. These data are from 7 animals; points are mean ± range. Similar results were found in 3N hosts receiving 2N eyes. The good correspondence between the size of the host eye and the transplanted eye suggests the absence of conditions that might induce changes in cell number in the transplanted eye.

The possibility of making visual systems of hybrid ploidy has also permitted us to approach a different problem in the area of retinotectal connections, namely the question of what determines the density of synapses made by optic nerve axons on tectal cells. That these synapses constitute a substantial fraction of the synapses in the tectal neuropil was shown by Ostberg & Norden (1979) who observed a large decrease in synaptic density in the neuropil after the contralateral optic nerve was cut. With 2N/3N hybrids, we could test whether a subtle alteration in the optic nerve input--a change in the way that input is divided up into fibers--affects synaptic density. We found that it does (Lynch et al., 1980). Figure 4 shown that three measures of synaptic density were affected by the ploidy of the optic nerve, in that an optic nerve consisting of a larger number of smaller fibers (a 2N nerve) generated a higher density of synapses than a nerve divided more "coarsely" into fibers (a 3N nerve). Postsynaptic factors were less important in the determination of tectal synaptic density, since in our study density did not depend significantly upon the ploidy of the tectum. In another approach to the same question, Marotte (1981) reported that goldfish half tecta receiving a compressed projection contained a higher density of synapses than control tecta, but the measure of density used (the number of synapses per unit area on the screen of the electron microscope) may be inadequate. In the same preparation, Murray et al. (1980) failed to find increased density in tecta receiving a compressed projection using more careful counting procedures. An increased density in compressed projections would seem to correspond to our finding that optic nerve fiber number (as determined by retinal ploidy) affects synaptic density.

In summary, the 2N/3N system provides an opportunity to alter cell number and cell size in an approximately reciprocal fashion. The study of amphibian visual systems of hybrid ploidy, created by embryonic eye

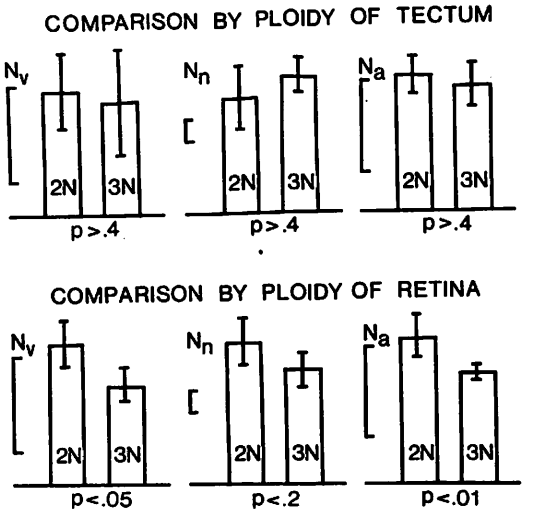

Figure 4. Synaptic density in the tecta of animals with a transplanted eye. Three measures of density were calculated from counts of synapses found in mosaics of electron micrographs covering the entire depth of the tectal superficial neuropil. "N_v" is the number of synapses per unit volume of neuropil. "N_n" is the number of synapses per postsynaptic cell nucleus. (The density of nuclei was determined from light micrographs of adjacent semithin sections.) "N_a" is the number of synapses under a unit area of tectum. It is important to consider all three measures of density under circumstances like these, in which changes in the input to the tectum may affect the thickness of the neuropil and/or the density of postsynaptic cells.

The density measurements summarized in the Figure were made on 10 tecta from 5 animals: 2 diploids with one triploid eye, 2 triploids with one diploid eye, and a control triploid that had received a transplanted triploid eye from another animal. In the top row of the Figure, the density measurements of each type from all tecta of each ploidy have been averaged, and are shown as mean ± 2 S. E. Thus, the first bar shows the number of synapses per unit volume (N_v) in all 2N tecta, both those receiving 2N input and those receiving 3N input. The adjacent bar shows the average of N_v in all 3N tecta, again without regard to the ploidy of the optic nerves innervating them. The Mann-Whitney U-test indicates that N_v in 2N tecta should not be regarded as different from N_v in 3N tecta. However, when values of N_v in all tecta receiving 2N optic nerve input are compared with N_v in tecta receiving 3N input (first pair of bars in lower half of Figure), the difference is now conventionally significant ($P < .05$). Thus synaptic density appears to depend on the nature of the presynaptic fibers, but not on the size and number of postsynaptic cells, at least within the range of variation between diploids and triploids.

transplantation, indicates that cell number per se is not a factor in the establishment of visual pathways with normal spatial order, nbut that cell number does affect the density of synapses formed by optic nerve axons.

Acknowledgment

M. Ballew, L. Douville, D. Fite, M. Kelleher, and P. Rauch assisted in the technical aspects of the research reported here. Some of the eye transplant experiments were performed in the laboratory of R. M. Gaze, whose assistance and support is gratefully acknowledged.

BIBLIOGRAPHY

Berman, N. and Hunt, R. K. Visual projections to the optic tecta in Xenopus after the partial extirpation of the embryonic eye. J. Comp. Neurol. 162: 23-42, 1975.

Cooke, J. Scale of body pattern adjusts to available cell number in amphibian embryos. Nature 290: 775-778, 1981..

Dasgupta, S. Induction of triploidy by hydrostatic pressure in the leopard frog, Rana pipiens. J. Exp. Zool. 151: 105-122, 1962.

Fankhauser, G. Cell size, organ and body size in triploid newts (Triturus viridescens). J. Morphol. 68: 161-177, 1941.

Gardner-Medwin, A. R. Membrane transport and solute migration affecting the brain cell microenvironment. NRP Bull. 18: 208-226, 1980.

George, S. A. and M. J. Lemanski. Peripheral nerve myelin morphology in animals of different ploidy. Neurosci. Abstr. 5: 502, 1979.

George, S. A. and M. R. Lennartz. Methods for determining ploidy in amphibians: nucleolar number and erythrocyte size. Experentia 36: 687-688, 1980.

Hall, J. L. Binaural interaction in the accessory superior-olivary nucleus of the cat. J. Acoust. Soc. Am..37: 814-823, 1965.

Lara,

Lynch, A.E., Brunette, J. J. and S. A. George. Synaptic density in the tectum: effects of number and size of optic afferents. Neurosci. Abstr. 6: 567, 1980.

Marotte, L. R. Density of optic terminals in half tecta of goldfish with compressed retinotectal projections. Neuroscience 6: 697-702, 1981.

Marr, D. A theory of cerebellar cortex. J. Physiol. 202: 437-470, 1969.

Murray, M., Sharma, S. C., and M. A. Edwards. Target regulation of synaptic density in the regenerated optic projection to a halved optic tectum in goldfish. Neurosci. Abstr. 6: 411, 1980

Ostberg, A. and J. Norden. Ultrastructural study of degeneration and regeneration in the amphibian tectum. Brain Res. 168: 441-455, 1979.

Overton, K. This volume.

Schmidt, J. T. Retinal fibers alter tectal positional markers during expansion of the half retinal projection in goldfish. J. Comp. Neurol. 177: 279-300.

Schmidt, J. T., Cicerone, C. M. and S. S. Easter. Expansion of the half retinal projection to the tectum in goldfish: an electrophysiological and anatomical study. J. Comp. Neurol. 177: 257-278, 1978.

Sharma, S. C. Redistribution of visual projections in altered optic tecta of adult goldfish. P. N. A. S. 69: 2637-2639, 1972.

Steer, R. B. Cell number and density in diploid and triploid Xenopus laevis. A. B. Thesis, Amherst College, 1981.

Susan B. Udin: THE DEVELOPMENT OF ORDERLY CONNECTIONS BETWEEN THE NUCLEUS ISTHMI AND THE TECTUM IN XENOPUS

The adult frog has a binocular visual field which is represented on each tectum. The contralateral eye projects directly to the tectum via the optic nerve but the ipsilateral eye projects to the tectum via a roundabout relay involving the nucleus isthmi (NI) (see Figures 1 and 2). The two projections are in register: each position seen by both eyes is represented at one point in each tectum.

The retinal and the crossed and uncrossed isthmic projections all terminate in close proximity in the superficial layers of the tectum (see Fig. 3). Electrophysiological mapping reveals that there is a 30 msec delay between arrival of contralateral input and ipsilateral input; this delay results from the extra stages of tectal and isthmic processing which the ipsilateral activity undergoes. The ipsilateral units are similar in their response properties to retinal units in that most respond best to dark moving objects; some respond best to net dimming. However, ipsilateral units have somewhat larger receptive fields and habituate more readily than retinal receptive fields. In addition, each electrode penetration encounters fewer ipsilateral units than contralateral units because there are far fewer isthmo-tectal fibers than retinotectal fibers (approximately 1000 vs. 50,000 in Xenopus laevis and 4000 vs. 500,000 in Rana pipiens). We currently know nothing about the activity of the uncrossed isthmo-tectal projection.

How do the ipsilateral and contralateral maps come to be in register? What developmental processes bring together isthmic and retinal inputs for the same receptive field locations? Electrophysiological studies by Keating ('74) revealed that early visual experience is a major determining factor.

If the normal relationship of the two eyes is altered during development, for example by rotation of one eye around its optic axis, then the ipsilateral map responds by shifting to become in register with the contralateral map. If one eye is rotated by 180° a few weeks before metamorphosis, each part of the retina still projects to its normal tectal position. A ganglion cell which is normally in the nasal position but has been shifted to a temporal position due to the eye rotation will see the nasal visual fields rather than the temporal. (See ganglion cell "a" in the left retinas shown in Figure 4.) That cell still projects to caudal tectum, which therefore "sees" the nasal visual field rather than temporal. What part of the visual field does the ipsilateral pathway from the normal eye transmit to this part of the tectum? Electrophysiology shows that the ipsilateral activity now also is from the nasal field. Subsequent anatomical studies using localized tectal injections of horseradish peroxidase show that the early rotation of one eye has caused nucleus isthmi cells to shift their terminals on the tectum. (See Fig. 5.)

The most plausible hypothesis to explain this phenomenon is that coincident firing of isthmic and retinal inputs to the same tectal site stabilizes isthmic terminals. We know that the retinotectal map is well-organized prior to the arrival of most isthmo-tectal units (Udin, '81), and isthmic axons appear initially to arborize over a relatively wide area of tectum (Keating and Kennard, '78); perhaps some part of an isthmic arbor with a given receptive field will be close to retinal arbors which have the same receptive field and that part of the isthmic arbor will prosper and grow while the remainder atrophies. In support of the idea that visual input is the source of information is the fact that dark-rearing (beginning at late pre-metamorphic stages) prevents normal acquisition of a fully organized ipsilateral map in normal frogs or of a rotated map in eye-rotated frogs. There does appear to be some innate topographic organization even in these

animals, however, especially along the mediolateral tectal axis (S. Grant, pers. comm.). It is possible that timing of cell genesis plays a role here; the first-born NI cells (ventral) enter the tectum at its oldest portions (lateral) and the last-born NI cells (dorsal) enter the tectum at the youngest part of the tectal margin (medial). This order could give an approximately correct mediolateral orientation to the isthmo-tectal projection even though a simple scheme of this sort would not provide appropriate information for the rostrocaudal tectal axis (see Fig. 6). Furthermore, the eye-rotation experiments demonstrate that such low-level initial orientation can be completely reversed during development.

REFERENCES

Gaze, R.M., M.J. Keating, G. Szekely, and L. Beazley (1970) Binocular interaction in the formation of specific intertectal neuronal connections. Proc. R. Soc. Lond. B. 175: 107-147.

Glasser, S. and D. Ingle (1978) The nucleus isthmus as a relay station in the ipsilateral visual projection to the frog's optic tectum. Brain Res. 159: 214-218.

Grobstein, P., C. Comer, M. Hollyday, and S.M. Archer (1978) A crossed isthmo-tectal projection in Rana pipiens and its involvement in the ipsilateral visuotectal projection. Brain Res. 156: 117-123.

Gruberg, E.R. and J.Y. Lettvin (1980) Anatomy and physiology of a binocular system in the frog Rana pipiens. Brain Res. 192: 313-325.

Gruberg, E.R. and S.B. Udin (1978) Topographic projections between the nucleus isthmi and the tectum of the frog Rana pipiens. J. Comp. Neurol. 179: 487-500.

Keating, M.J. (1974) The role of visual function in the patterning of binocular visual connexions. Brit. Med. Bull. 30: 145-151.

Keating, M.J. and C. Kennard (1978) The effect of visual deprivation on the maturation of neuronal connections in the visual system of Xenopus. Neurosci. Lett. Suppl. 1: 392.

Udin, S.B. (1981) Development of the nucleus isthmi in Xenopus laevis. Soc. Neurosci. Abst. 7: 406.

Udin, S.B. and M.J. Keating (1981) Plasticity in a central nervous pathway in Xenopus: anatomical changes in the isthmotectal projection after larval eye rotation. J. Comp. Neurol. 203: 575-594.

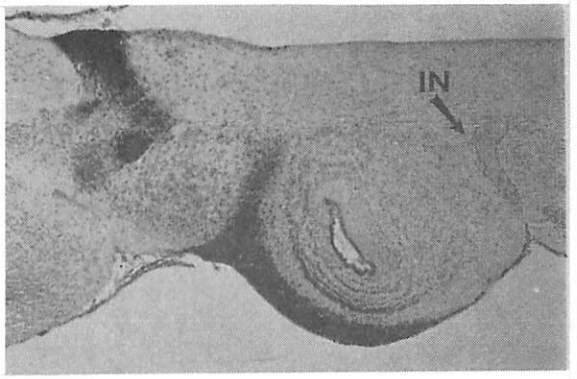

Fig. 1. Parasaggital section through Xenopus brain. Rostral is to right and dorsal above. The heavy black label represents ^{3}H-proline which was transported from the eye, via the optic tract seen at lower right, to the superficial layers of the tectum.

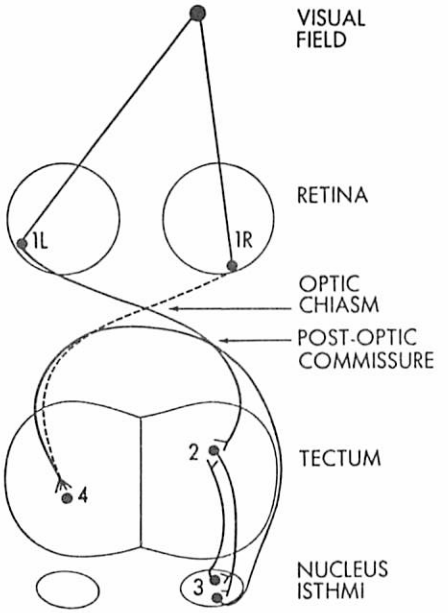

Fig. 2. Schematic diagram of the neural pathways underlying the ipsilateral visuotectal projections in Rana. One locus in the binocular visual field is viewed by retinal position 1 in the left eye. Retinal ganglion cells at position 1 project directly to position 2 on the right optic tectum. This tectal site projects, in turn, to position 3 in the right nucleus isthmi. Cells at position 3 in the right nucleus isthmi project back to position 2 on the right optic tectum via the uncrossed isthmo-tectal projection. Other fibers leave position 3 in the NI, run along the medial aspect of the optic tract, cross the mid-line in the post-optic commissure and reach position 4 in the contralateral tectum. Retinal fibers from position 1r in the right eye also project to position 4.

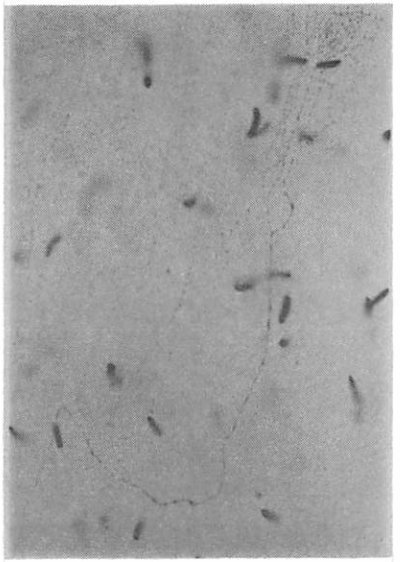

Fig. 3. Crossed isthmo-tectal axon labeled by anterograde transport of horseradish peroxidase which had been injected into the nucleus isthmi. The tectum was flattened, reacted without sectioning, and is viewed from the dorsal surface. Note that this axon has a zig-zag trajectory; however, the majority of axons appear to follow fairly straight pathways when they have entered the tectum.

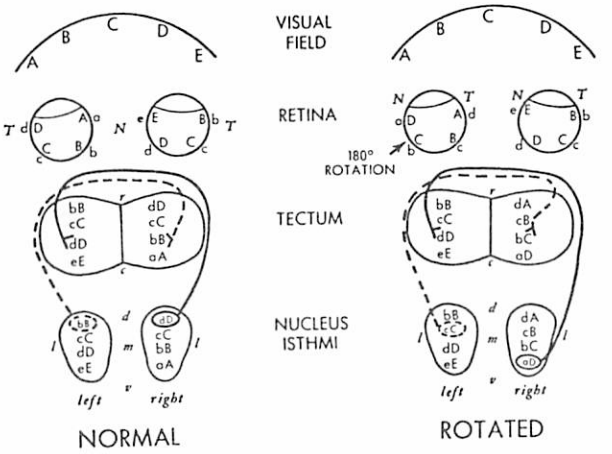

Fig. 4. Schematic diagrams illustrating the morphological changes in the crossed isthmo-tectal projections which are expected following 180° rotation of the left eye. Capital letters represent visual field locations; lower case letters represent sites in the retina, tectum, and NI. Left: Normal frog. Right: Frog in which left eye was rotated 180° during larval life. Matched HRP injections at site b in the right tectum label cells at position b in the left NI of the normal frog and cells at position c in the eye-rotated animal. Matched HRP injections at site d in the left tectum label cells at position d in the right NI of the normal frog and at position a in the eye-rotated frog.

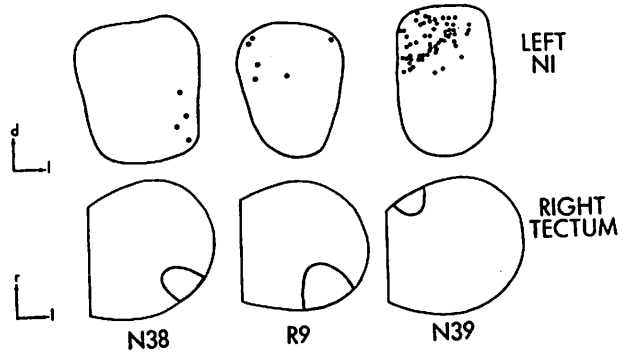

Fig. 5. The crossed isthmo-tectal projection in Xenopus R9 compared with two matched controls. In the lower part of the figure, the left optic tecta of the three animals are shown in dorsal view. The sites of the localized HRP injections are indicated by the filled regions. In the upper part of the figure, the right NI of the three animals is shown in rostral view. The positions within the NI of cells labelled by the tectal injection of HRP are indicated by black dots. Comparison of R9 and N38 shows that comparable sites of HRP injection lead to different locations of cell labeling in the NI after early eye rotation. Comparison with N39 shows that cells in dorsomedial NI usually project to rostromedial tectum rather than to the caudolateral site where they are found in R9.

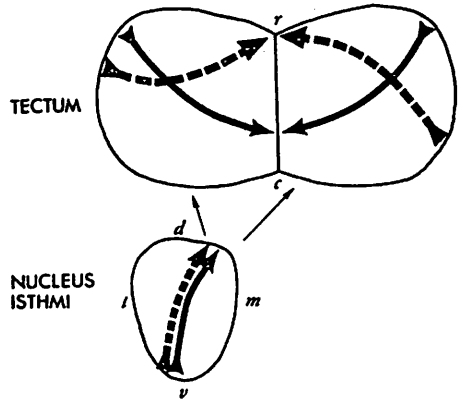

Fig. 6. The solid arrow shows the spatiotemporal gradients of cell birthdays in the tectum and NI based on autoradiography of frogs injected with ^{3}H-thymidine at various stages of development. The first cells born in the NI are at the ventral tip (tail of solid arrow) and the last are born at the dorsomedial tip (head of solid arrow). The first-born tectal cells are rostrolateral (tail of solid arrow) and the last are caudomedial (head of solid arrow). The dashed arrows show the topography of the isthmo-tectal connections. Ventral NI connects to rostrolateral tectum on the same side of the brain and caudolateral tectum on the other side of the brain. Dorsal NI projects to both tecta rostromedially. A simple scheme whereby "old" NI cells project to "old" tectal cells and "young" NI cells to "young tectal cells would produce maps with proper orientation along the mediolateral tectal axis but incorrect order rostrocaudally.

Kenneth J. Overton and Michael A. Arbib: THE EXTENDED BRANCH-ARROW MODEL OF THE FORMATION OF RETINO-TECTAL CONNECTIONS

Abstract

This paper presents XBAM (the Extended Branch-Arrow Model), a new model of the development of the retino-tectal topographic mapping as observed in frog, toad, and goldfish visual systems. The updating process employed by XBAM is distributed in nature and depends upon interactions between branches of retinal fibers, the branches and the boundaries of the tectum and grafts, and the branches and the tectal surface. Results of computer simulation of the model are related to experimental data obtained from tectal and retinal graft and lesion studies, and comparisons are also made with other models.

I. Introduction

Many experiments study the development of the topographic mapping between the retina and tectum of various lower vertebrates. Goldfish, frog, and toad visual systems have generally been the targets of these studies. In these animals the fibers from each retina project to the contralateral tectum. Early behavioral

studies (Sperry 1943, 1944, 1945, Gaze 1959, Maturana et al. 1959) showed that the retinal projections of these animals would regrow to map in an orderly way after surgical interruption. With the development of electrophysiological recording techniques, investigators have been able to better understand the details of the mapping (Gaze et al. 1963, 1965, 1970, 1974, Jacobson 1965). Stimuli in the superior section of the visual field project to the medial section of the contralateral tectum while those in the inferior field project to the lateral side. Similarly, stimuli in the nasal portion of the visual field project to the rostral end and temporal stimuli to the caudal end of the contralateral tectum (see Figure 1). As the body of experimental data has grown, numerous models of the process by which the mapping is formed have been proposed. The models can be divided into two general classes: those subscribing to the idea of a point-to-point chemoaffinity between the retinal and tectal cells and those using the idea of systems-matching.

Figure 1

Sperry (1944, 1945, 1963) first proposed the idea of chemoaffinity between the layers of cells. Under this hypothesis, each retinal cell is uniquely labeled according to its position on the retina. The tectal surface is considered to be labeled in a similar manner and organization of the map is the result of each retinal cell axon seeking the point on the tectum which matches its own retinal label. The Marker Induction model of Willshaw and von der Malsburg (1979) may be viewed as a sophisticated development of this idea in that the tectal "addresses" are not prespecified, but rather develop as a result of the interactions among retinal fibers.

In system matching models, the information available to the retinal fibers is considerably less specific. Retinal fibers do not seek a particular point on the tectum, but rather seek a neighborhood where the interactions with the surrounding

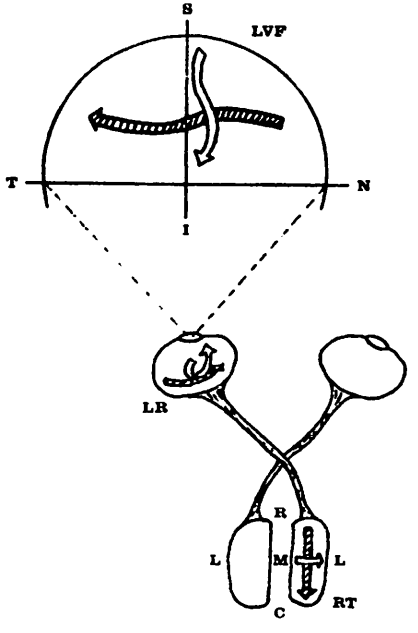

Figure 1. Schematic of the frog visual system. Fibres from the retina project onto the contralateral tectum. Tectum: R - Rostral, C - Caudal, M - Medial, L - Lateral. Visual Field: N - Nasal, T - Temporal, S - Superior, I - Inferior.

fibers match the activity on the retina. The Arrow model proposed by Hope et al. (1976) may be placed in this class.

While the Marker Induction and Arrow models employ different underlying assumptions as to the amount and type of information required by the organization process, they both exhibit many aspects of the experimental data. The model presented in this paper combines new ideas with concepts from both of these approaches to produce a hybrid model which explains a wide body of experiments.

II. An Overview of the Model

We present an overview of four models of increasing complexity: the Arrow Model, our first extension of it (Overton and Arbib, 1982), the Branch Arrow Model (BAM) which is still a systems matching model, the Marker Induction Model, and then the Extended Branch Arrow Model (XBAM) which incorporates both systems matching and certain chemoaffinity features. The mathematical specification of the models is provided in the Appendix.

In the Arrow Model, the tectum is modelled as a discrete grid with retinal fibers allowed to terminate only at the intersections of the grid lines, called tectal sites. Each iteration of the sorting process may assume one of the two forms: switching interaction or random walking.

Switching interaction (see Appendix A) is, essentially, a two-dimensional "bubble-sort" -- retinal fibers with adjacent positions on the retina will switch the position of their terminations if the relative positions on tectum differs from relative positions on the retina. Note, then, that the model uses relative position, not "absolute addressing". Switching interaction is applied to all fibers in such a way that no fiber interacts with more than one other fiber during any iteration. Repeated application of this process produces an ordered mapping from

one in which the initial positions were originally randomly assigned.

Using this mechanism alone, there is no way for fibers to move into previously unoccupied termination sites, an ability required in the case of a hemiretina projecting onto a complete tectum. In order to circumvent this problem, the fibers are periodically allowed to take random steps.

During an iteration of random walking, a site adjacent to each fiber is chosen at random. If the site is empty, the fiber moves to occupy that location. If the site is occupied or one or more other fibers are trying to move into it the fiber retains its original location. One iteration of random walking consists of applying this process to each fiber on the tectum. The updated positions form the initial state for the succeeding iteration.

The overall sorting method in the Arrow Model involves the use of switching interaction and random walking. These are combined by alternating which method is used during successive iterations. The majority of the iterations employ the switching interaction while a few, spaced at predetermined intervals, employ the random walk. This use of the random walk allows the fibers to disperse to all parts of the tectum while the switching interaction provides a degree of ordering in the mapping.

Our Branch-Arrow Model (BAM) redefines the Arrow model in several ways. In the Arrow Model, retinal fibers must terminate at discrete points on a grid; in BAM, retinal fibers form several branches as they reach the tectal surface which is now modelled as a continuum rather than a grid. The termination of each branch is surrounded by a circle which represents its area of interaction with other branches (see Figure 2). The circle is meant to model the area of synaptic efficacy of the branch. Further, each branch explicitly interacts with the tectal and graft boundaries. These changes also dictate that the neighborhood interaction rules be modified. In our model the neighborhood interaction process is applied to each

branch so that the actual position of a fiber as a whole is determined implicitly by the locations of its branches. The resultant model, BAM, seems to more closely resemble the physiology of fiber movement. The reader is referred to Appendix B for a complete development of BAM. However, there is a small number of experiments which cannot be accounted for by either the Arrow Model or BAM. The Extended Branch-Arrow Model, XBAM, adds fiber-surface interaction to the Branch-Arrow model.

Figure 2

In (X)BAM, then, the movement of a retinal fiber is determined by the overall trend of the movements of its individual branches. Rather than the discrete 'pick a neighbor, and switch if appropriate' of the Arrow Model, (X)BAM has the move of a branch determined as a vector sum of the 'nudges' applied by all other branches within its circle of interaction. The direction for each 'nudge' is very similar to that given by the interchange rule used in the Arrow Model. The main difference lies in the stipultation that if the somas are separated by a distance greater than a specified value, the direction of the influence is chosen at random. The authors feel that retinal cells may communicate in a meaningful way only if their somas are within a certain distance, e.g. if their receptive fields overlap. Thus if the cells are separated by a great distance, no communication is possible. When the somas of two interacting branches are within the distance allowing meaningful communication, the direction is chosen as in the Arrow Model. When the branch terminations are oriented on the tectum the same relative to some axis system as are the somas on the retina, relative to the corresponding axis system, the influence tends to force the branches apart. If, however, the branch positions are reversed compared to the relative soma locations on the retina, the influence tends to force the branches to move past one another, i.e. interchange positions. In the case where both of the interacting branches in question belong to the same fiber, the

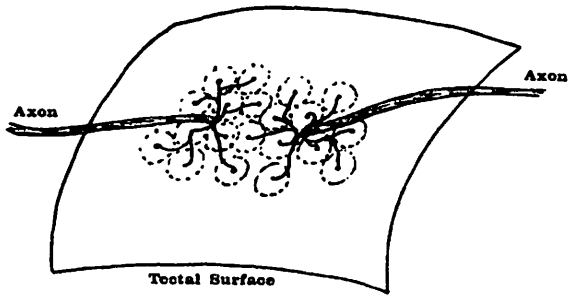

Figure 2. Axonal arborization: retinal fibre termination configuration used in BAM and XBAM.

influence felt by one from the other always tends to force the branches apart thereby attempting the maximize the area of the tectum covered by a fiber. The second component of the physical influence involves the interaction between the branches and the tectal and graft boundaries.

Tectal and graft edges are physical discontinuities in the surface of the tectum. We thus hypothesize that it is more difficult for a branch to migrate across such a boundary than to move across an unobstructed surface. In addition, we propose that communication between fibers separated by such a boundary is more difficult than between fibers on an unobstructed surface. Thus, in (X)BAM, we model the influence of boundaries as restrictions on the movements of the branches.

As we have verified in computer simulations reported elsewhere (Overton and Arbib, 1982), BAM, using the principles of system matching, accounts for a great deal of the experimental data. Relative retinal and tectal orientation information is sufficient to produce behavior similar to most of the experimental results when utilized by neighborhood and boundary interaction mechanisms. If the effect of retinal separation on the ability of two retinal cells to communicate is investigated, degraded behavior results. Restricting the distance allowing a meaningful exchange to a fraction of the retinal expanse results in a locally continuous yet globally discontinuous mapping. However, we found that BAM cannot accurately produce the graft rotation and translocation behavior seen experimentally. The systems matching approach lacks specific information differentiating individual tectal locations and the ability for information to be shared over distances which are large relative to the neighborhood interaction. Unlike the system matching ideas, point-to-point chemoaffinity provides specific information describing every point on the two surfaces.

We now briefly discuss the Marker Induction model of Willshaw and von der Malsburg as a sophisticated representitive of the point-to-point chemoaffinity

approach. The Marker Induction model (Willshaw 1979) involves the specification of the tectal surface by actions of the incoming fibers with the specificity determining, and determined by, the differential growth of synapses between retinal fibers and tectal cells. The retinal surface is posited to possess concentration gradients of a number of transportable substances, with at least one for each spatial dimension. Each retinal cell continually absorbs each of these substances at rates proportional to the concentrations at the cell's location. Thus the cell's retinal location can be uniquely determined by the vector of concentrations. The substances are moved to the synapses by axonal transport where they are injected into the postsynaptic cells at a rate proportional to their concentration and the strength of the synapse.

Each synapse between a retinal fiber and a tectal cell is described by two quantities: strength and fitness. The strength is an indication of the rate of transfer of the substances between pre- and postsynaptic cells. The fitness describes the similarity between the substance concentration vectors of the pre- and postsynaptic cells. The actual interaction between synapses is governed by a set of three rules:

1. The strength of a synapse is proportional to its fitness. The greater the fitness, i.e. the closer the concentration vectors, the greater the strength.
2. The sum of the strengths of all of the synapses of each presynaptic cell is stipulated to be fixed. This accomplishes two things: first, no synapse can grow without bound; and second, this provides competition between synapses of the same cell. If a particular synapse is to be strengthened, the other synapses must be weakend accordingly.
3. Finally, each axon forms new branches in the neighborhood of existing ones and branches with synapses whose strengths are below a minimum value are removed.

The above assumptions and rules provide a method for producing locally continuous maps. However, since the model contains no specific orientation information, there is no preference for one particular final organization over another. In computer simulations of the one dimensional version of this model, an initially random organization resulted in piecewise continuous maps with no particular global organization -- this is similar to the results we report for BAM in the next section (Experiment I). Willshaw and von der Malsburg provide orientation information by giving the initial map some order. This is accomplished by placing the presynaptic fiber terminations in sections of the tectum which approximate the desired final locations. With this, the model is able to produce mapping behavior consistent with experimental data from both regeneration and developmental experiments.

It is our opinion that both the system matching and chemoaffinity approaches have their merits. We now present a hybridization of these two ideas which is posited to have available information which is more specific than that used by the system matching models yet not as specific as that used by the chemoaffinity models. Our Extended Branch-Arrow Model (XBAM) adds a branch-surface interaction mechanism to the neighborhood and boundary interaction mechanisms of BAM. In the Arrow Model, each fiber would interact with at most one of its eight adjacent sites at each iteration. Switching interaction alone was sufficient to account for much of the experimental evidence but random stepping had to be added to account for the expansion results (Schmidt 1978a, 1978b). Even with this addition, the Arrow Model cannot account for the small class of graft translocation experiments (Hope 1976). In addition, when the distance on the retina allowing an effective exchange of information is reduced from the entire retinal expanse to a fraction of that distance, the global behavior degrades markedly. By contrast, the XBAM model is able to account for essentially all of the significant experimental results.

A fiber interacts with the surface of the tectum by way of its branches. Each branch of a fiber is thought to be marked in some manner according to the retinal position of its soma. The marker need not be an indicator of its exact position but rather a marker encoding its general location, e.g. the position should be accurate to within plus or minus the distance allowing effective retinal communication. That is, the marker here is to be considered in the sense of a general position indicator as opposed to a point to point chemoaffinity. The tectal surface is also posited to be marked in a similar manner. Each of the branches sample the marker on the tectal surface. The surface influence contains a weight which is proportional to the difference between the retinal and tectal labels. For a detailed discussion of the model the reader is referred to Appendix C.

III. Experiments

In (Overton and Arbib, 1982), we report a series of experiments on the BAM model. Of these, we simply present one on the effect of retinal 'communication distance'. We then turn to a series of experimens on XBAM.

The results presented below were obtained through computer simulation of a one-dimensional retina/tectum pair containing 40 fibers, each with 4 branches. A one-dimensional simulation was utilized due to the amount of computation required. (A sample set of simulations of two-dimensional arrangements have been performed and the results yield concordant behavior.) In the figures, the one-dimensional tectal surface is represented along the horizontal side of the display. Similarly, the visual field (or retina) appears along the vertical axis. Each horizontal row of symbols represents one fiber with each symbol marking the position of the termination of an individual branch of the fiber. Thus for each branch of each fiber, the position in the visual field of the stimulus exciting the fiber, and thus

the retinal location of the branch's soma is indicated by the height of the row on which the symbol appears. The position of the branch on the tectum is indicated by the horizontal position along the row. Further, the lower end of the visual field display maps to the leftmost end of the tectum and the upper end of the visual field display maps to the rightmost end of the tectal representation. Thus a normal mapping is depicted by a diagonal line of symbols from the lower left corner of the display to the upper right. The physiological data are inherently two dimensional. To compare the simulation results with these data, equate the vertical axis of the simulation display in Figure 3a with the bar, V_t, in Figure 3b and the horizontal axis with bar L_t in 3b. The left end of the tectal representation corresponds to the lower, rostral, end of the bar in the upper half of Figure 3b while the lower end of the retinal representation corresponds to the right, nasal, end of the bar in the lower half of 3b.

Figure 3

Experiment I.

The purpose of this experiment was to study the effects of varying the maximum distance allowing effective communication between cells on the retina. The initial distribution of branch terminations on the tectum was random as illustrated in Figure 3a. Figure 4a shows the organization resulting after 8000 iterations with the radius set to allow effective communication over roughly two thirds of the retina. That is, if two cells are separated by a distance greater than two thirds of the total retinal expanse, then they cannot meaningfully communicate. Thus branches at opposite ends of the retina interact at random. The resulting configuration shows two organized maps on the tectum. The simulation results depicted in Figure 4b show the state after 8000 iterations with the radius set to roughly one half of the total retinal size. In this case, three maps are produced.

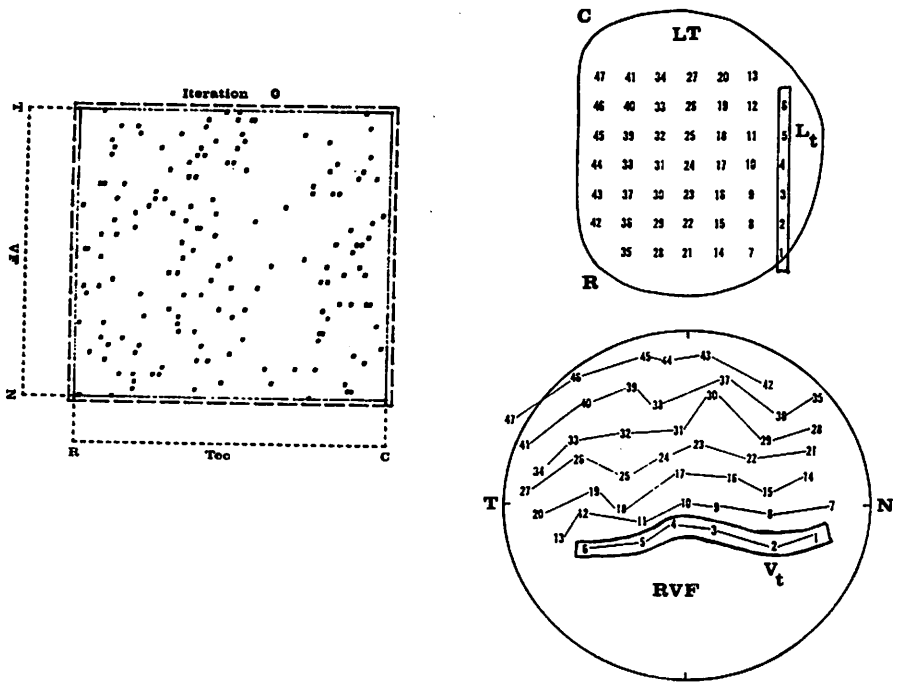

(a) (b)

Figure 3. (a) The initial distribution of branch terminations for the BAM simulation. 40 fibres with 4 branches/fibre.

(b) The projection of right visual field onto the left tectum in a normal animal (Gaze 1974). L_t: a single line of electrode positions which is analogous to the one-dimensional tectum in BAM and XBAM. V_t: the corresponding single row of points in the visual field which excite the tectal positions -- analogous to the vertical axis of the BAM/XBAM display.

Figure 4c shows the map resulting when the distance is reduced to one fifth of the retinal size. Again, several organized pieces are seen. With the radius reduced to one tenth, the configuration in Figure 4d results. The map contains many small pockets of organization yet lacks global organization. The final subfigure, Figure 4e, shows the resulting map when the retinal interaction distance is reduced to approximately one twentieth of the total retinal expanse. Some areas of organization can be seen, although no global organization is apparent.

Figure 4

This experiment demonstrates that as the distance on the retina within which an effective exchange of information can take place is reduced, the amount of global organization is also reduced. The Arrow Model is essentially the discrete analog of the Branch-Arrow Model when the retinal interaction distance in the latter is equal to the width of the retina. It seems to us that the physiology of the visual systems being studied would indicate that an assumption of effective communication between any two retinal cells regardless of their separation is questionable. Alternately, the distance should be reduced to some fraction of the total width. The exact amount is unknown. The lack of global organization which results when the distance is reduced is evidence that a local neighborhood interaction mechanism alone is insufficient to account for the organizational behavior observed in the physiological experiments. This point will be addressed in greater detail with XBAM.

With this, we now turn to the study of XBAM (see Appendix C for the formal specification of XBAM by the addition of some tectal specificity to BAM):

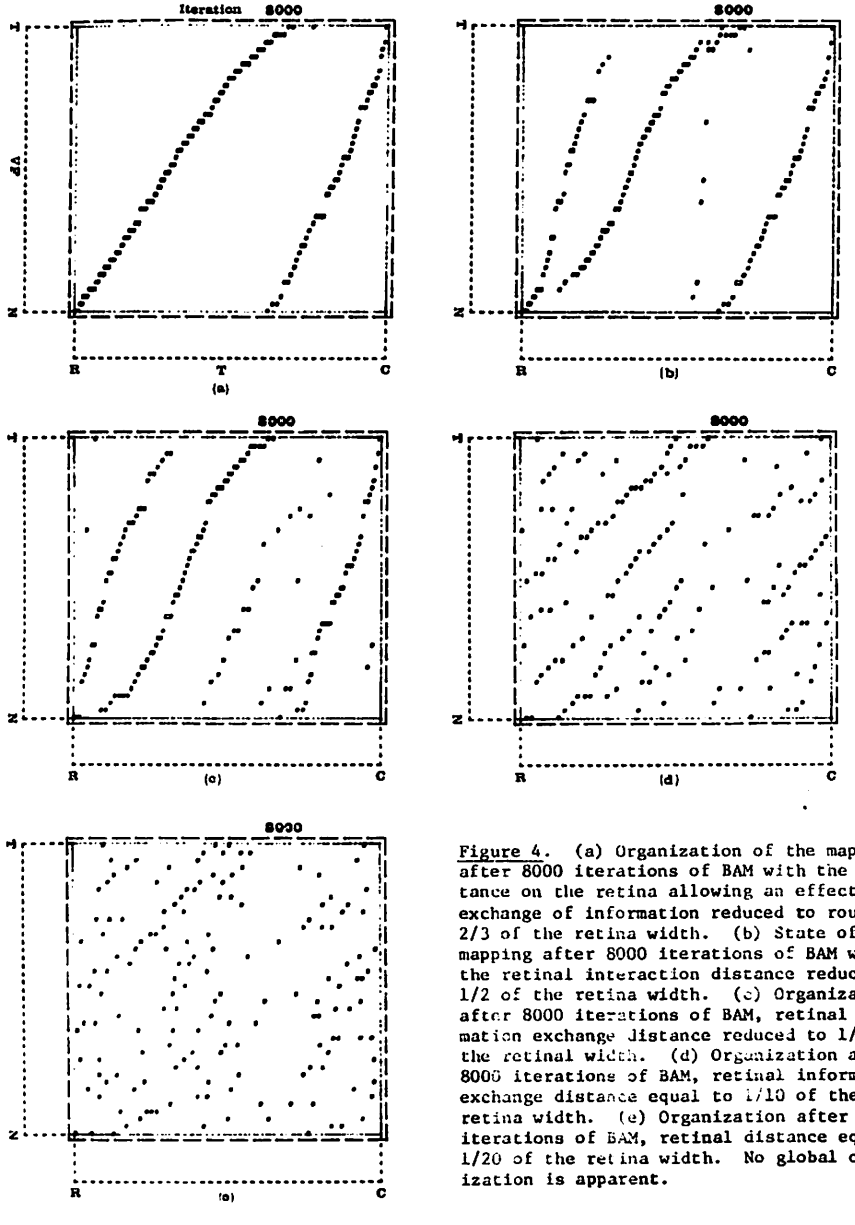

Figure 4. (a) Organization of the mapping after 8000 iterations of BAM with the distance on the retina allowing an effective exchange of information reduced to roughly 2/3 of the retina width. (b) State of the mapping after 8000 iterations of BAM with the retinal interaction distance reduced to 1/2 of the retina width. (c) Organization after 8000 iterations of BAM, retinal information exchange distance reduced to 1/5 of the retinal width. (d) Organization after 8000 iterations of BAM, retinal information exchange distance equal to 1/10 of the total retina width. (e) Organization after 8000 iterations of BAM, retinal distance equal to 1/20 of the retina width. No global organization is apparent.

Experiment II.

In this experiment, the development of the projection from a normal retina onto a normal tectum was studied for XBAM. Figure 5 illustrates the initial random positioning of the branches. Figure 6 contains the state of the mapping after 10,000 iterations of XBAM. Retinal cells were allowed to exchange information regardless of the distance between them. XBAM produced an ordered mapping.

Figures 5 and 6

We next tested the effect of reducing the distance allowing effective communication on the retina, cf. Experiment I. Figure 7 contains the mapping after 28,000 iterations of XBAM with the retinal distance reduced to roughly one half of the retina. XBAM produced a globally ordered map while BAM produced several superpositioned maps, cf. Figures 7 and 4b. The surface interaction term added enough information to allow the neighborhood and boundary mechanisms to produce a completely organized projection.

Figure 7

Experiment III.

Work has been conducted in regard to the compression of the projection onto tectum of which one half has been completely ablated. Udin (1977) and others (Sharma 1977, Yoon 1976) have studied the form of the retino-tectal projection in such a paradigm in the frog visual system. The results obtained from these experiments are generally consistent. An ordered mapping of the entire visual field is found on the intact portion of the tectum. The projection is compressed to fill the available space. The physiological results are displayed in Figure 8, from (Udin 1977).

Figure 8

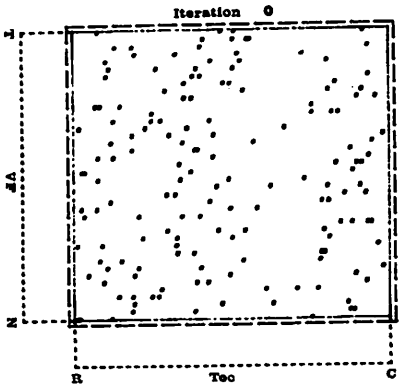

Figure 5. Initial branch distribution for the XBAM simultions. 40 fibres with 4 branches/fibre.

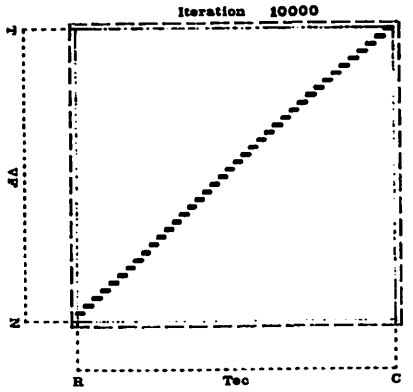

Figure 6. Mapping organization after 10,000 iterations of XBAM with the retinal distance allowing effective communication equal to the entire retina width.

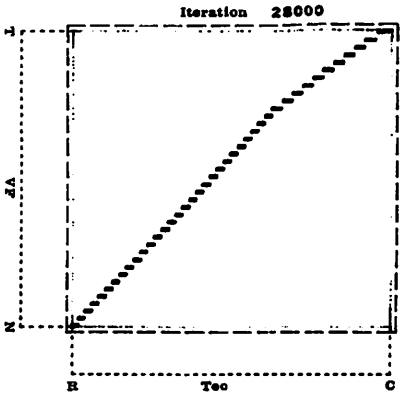

Figure 7. Projection after 28,000 iterations of XBAM with the retinal interaction distance reduced to roughly 1/2 of the retina width.

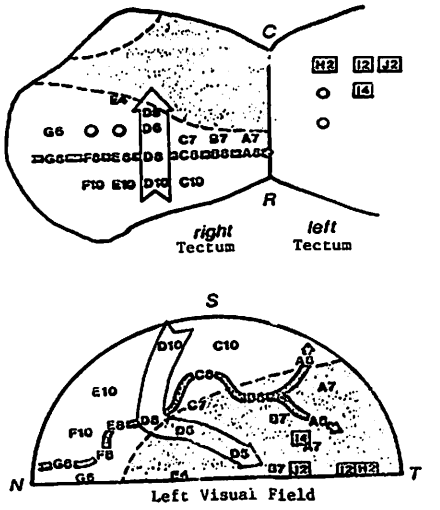

Figure 8. Physiological data from caudal 1/2 tectal ablation experiment (Udin 1977). The mapping from the entire visual field is compressed onto the remaining tectal surface.

The key features to note here are the facts that the entire visual field is represented along the dimension where only half of the original surface remains and that along the other dimension, all of the space is utilized.

This simulation experiment involved the same experimental paradigm in that the caudal half of the tectum was ablated. Figure 9 contains the results from the XBAM computer simulation. The initial termination locations were randomly distributed over the tectal surface. The surface was reduced to one half of its original size. The organization of the projection after 15,000 iterations of XBAM is shown in the figure. This map shows excellent global organization. The branches in the extreme lower left portion of the field have been forced off of the tectal surface. The magnitude of the effect is determined in part by the relative values of the weighting constants in equations (10) and (11) of Appendix B.

Figure 9

Some investigators have noticed that a mapping identical to the original mapping with the normal tectum appears first, followed by a trend toward a complete, compressed projection (Sharma 1977, Cook 1974). Horder (1977) found duplicate maps initially which later appeared compressed. He further found that if one third or less of the surface were ablated, the projection moved immediately to a compressed state. It has been posited that this initial mapping is due, in part, to the debris left on the tectum when the optic nerve is sectioned and then degenerates. The fibers which originally mapped to the rostral half of the tectum may be guided by the debris remaining from the prior mapping. Sharma (Sharma 1977) performed an experiment to test this hypothesis and found that when the fibers are forced to reinnervate a tectum previously devoid of fibers, the compressed mapping appeared with no initially uncompressed projection.

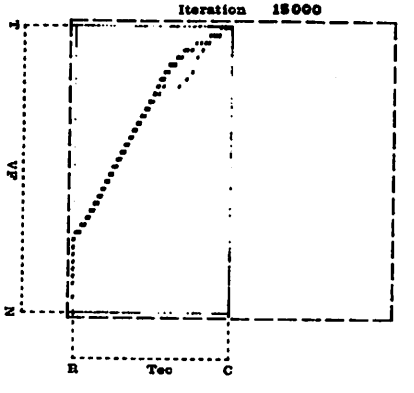

Figure 9. XBAM simulation results of a full retina mapping onto a half tectum. 15,000 iterations.

Another tectal ablation experiment involves removing 1/4 of the tectal surface and mapping the projection after regeneration. Schmidt and Easter (1978c) have performed experiments in which the medial-caudal quarter of the left tectum of the goldfish has been surgically ablated. A similar experiment designed to investigate the effect of removing part of the tectal surface was performed by Sharma (1972) and involved the ablation of a rostroventral strip on the tectal surface. An organized mapping was found compressed onto the remaining surface. The purpose of these experiments was to determin the degree to which the axes of the tectum are independent with respect to the compression of the mapping. They found that, after reinnervation of the tectum, the entire visual field was represented on the tectum. Further, the mapping was completely ordered and was compressed with respect to both axes. The compression appears to have been uniform across the tectum, that is, the fiber arbors appeared to organize in a fashion which resulted not only in an ordered representation of the visual field but also in a uniform distribution across the available tectal surface. While we cannot duplicate this paradigm due to the one dimensional nature of our simulation, we can predict the behavior of the two dimension version of the model in such a case.

Since our model tends to minimize the overlap of adjacent projection fields, as illustrated in the compression results above, and produces a continuous mapping, we would predict that the projection resulting when 1/4 of the tectal surface is removed would be uniformly compressed in all directions.

Experiment IV.

Another class of experiments involves studies of the map resulting between a hemiretina and an intact tectum (Schmidt 1978a, Horder 1971). In this case, the projection of the half of the visual field represented on the remaining hemiretina expands in an orderly manner to completely fill the available space on the tectum.

Typical results are found in Figure 10, from (Schmidt 1978b). Feldman (1975) conducted an experiment in which one eye was removed before it differentiated and the fibers from the other eye were directed to the ipsilateral tectum. He found a normal projection of the entire visual field on the ipsilateral tectum. However, some of the retinal fibers had managed to innervate the contralateral tectum to produce an expanded projection of the represented area of the visual field.

Figure 10

The simulation results for this situation are given in Figure 11. The projection of the half of the visual field represented on the remaining hemiretina expands in an orderly manner to completely fill the available space on the tectum. The XBAM simulation results for this situation are given in Figure 11. The initial locations for the branches were randomly assigned. The state after 10000 iterations shows complete organization with half of the normal number of fibers mapping onto the complete tectal surface. The mapping does not fill the entire rostral section of the tectum. This is due to a slight imbalance in the weighting constant values.

Figure 11

Experiment V.

A direct extension to the hemiretina, full tectum experiments involves studying the projection resulting when hemiretinae from different eyes are fused to form a single eye. Once the nerve connections have regenerated, the mapping is determined electrophysiologically. Gaze et al (1963, 1965) and Hunt (1973) have conducted such experiments. Their results are shown in Figure 12.

Figure 12.

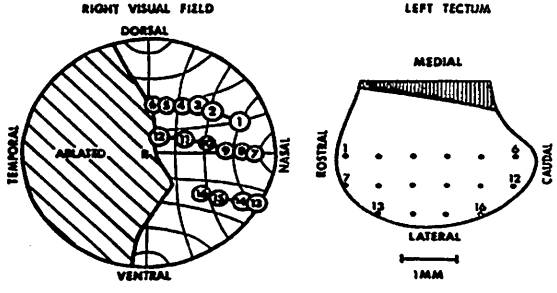

Figure 10. Physiological data from an animal in which the nasal half of the retina has been ablated. The remaining visual field is represented by an ordered projection covering all of the tectal surface (Schmidt 1978b).

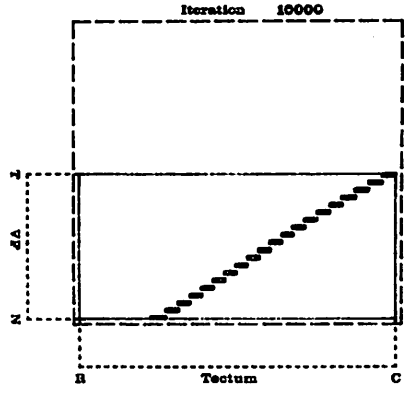

Figure 11. XBAM simulation results of a hemiretina projecting onto a full tectum, 10,000 iterations.

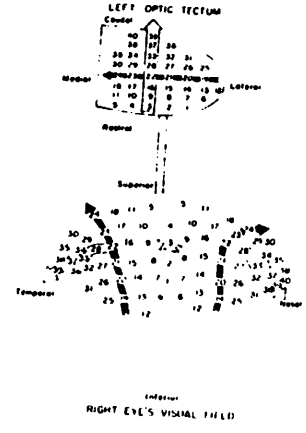

(a)

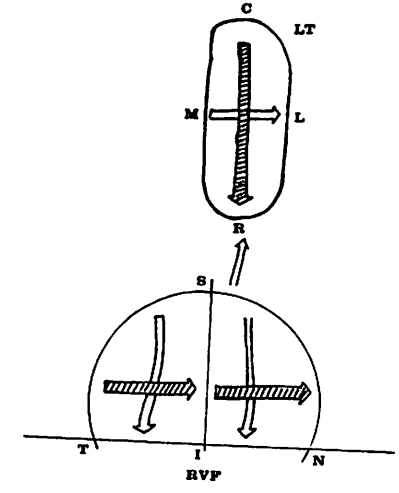

(b)

Figure 12. (a) Projection of the visual field from a double-nasal compound eye onto a normal tectum (Hunt 1973). Notice that there are two overlapping projections, one from each half of the eye.

(b) Schematic of the projection resulting from a compound eye composed of the nasal hemiretina from one eye and the temporal hemiretina from another.

In the case of Figure 12a, (Hunt 1973), the compound eye was composed of the nasal hemiretinae of two eyes with the division along the superior-inferior axis. The interesting point to note is that the projection from the two halves of the compound eye are superimposed. That is, the projection from each hemiretina expanded in an organized way to cover the entire tectal surface. The projection from one of the hemiretina is rotated 180 degrees. This is the case since one of the hemiretinae had to rotated through 180 degrees in order to create the complete eye. Figure 12b contains a schematic of the results from a compound eye composed of two temporal hemiretinae. The projections are ordered the same since neither piece required rotation when the eye was constructed.

Figures 13 and 14 contain the results from computer simulations of the XBAM when a double nasal eye maps onto the tectum. Figure 13 results from hemiretinae with their orientations retained so that the maps are oriented the same. Figure 14 was produced with the orientation of one half of the retina reversed.

Figures 13 and 14

Notice that in both cases the global organization of the field represented on each hemiretinae is maintained. However, the projection has expanded to cover most of the available tectal surface.

To this point, the experiments have focused on the mappings when there is a mismatch in the size or type (e.g. the compound eye experiments) of retinal versus tectal tissue. Another class of experiments involves the excision of a section of the tectum and its subsequent reimplantation after some form of inversion or rotation. Yoon (1975) and Sharma and Gaze (1971) have studied the projection following a 90 degree rotation of the graft tissue about the dorsoventral axis. Completely ordered projections are found both within and surrounding the graft. The projection within the graft, however, is found to be rotated in the same manner

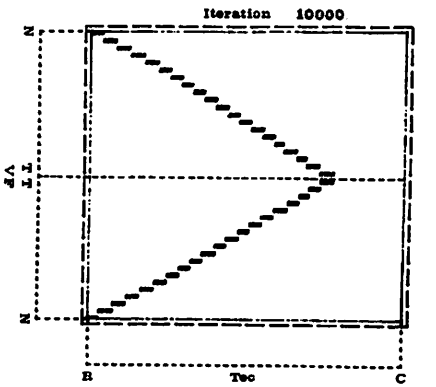

Figure 13. XBAM results of double-nasal compound eye experiment. 10,000 iterations.

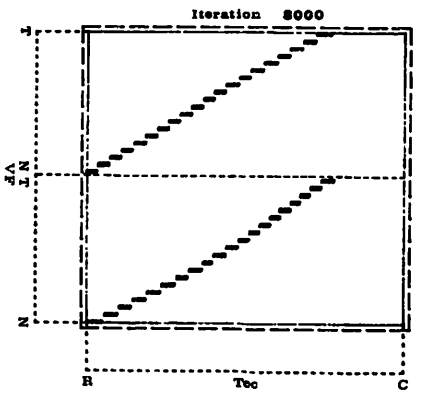

Figure 14. Results of XBAM simulation of nasal-temporal compound eye experiment. 8,000 iterations.

relative the the tectum as the graft. Figure 15, taken from (Yoon 1975) illustrates these results.

Figure 15

Several neurophysiologists (Yoon 1973, 1975, Levine 1974) have experimented with animals in which a single tectal graft has been rotated 180 degrees, again about the dorsoventral axis. Once the tectum has been reinnervated the mapping is found to be completely ordered both within and around the graft. The orientation of the map within the graft is again found to be rotated in a manner identical to the graft, see Figure 16, again from (Yoon 1975).

Figure 16

Yoon (1975) has also performed experiments in which a graft has been excised, rotated 180 degrees about the rostrocaudal axis, and reimplanted. This rotation causes the graft to retain its normal orientation along the rostrocaudal axis while having an inverted orientation along the superior-inferior axis. The resulting projection map is illustrated in Figure 17 (Yoon 1975), and shows that the map retains its normal rostrocaudal organization while the mediolateral organization within the graft is reversed. Again, the local orientation of the map follows that of the underlying tectal surface.

Figure 17

Experiment VI.

The simulation of the XBAM is one dimensional as was BAM so that the 90 degree rotation experiments cannot be performed; the two forms of the 180 degree rotation are equivalent. Figure 18a illustrates the state of organization of the branch termination locations after 8000 iterations. The initial configuration was again

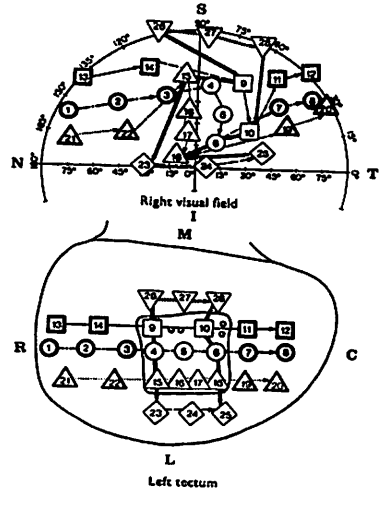

Figure 15. Mapping recorded after section of the optic nerve and 90 degree counterclockwise rotation of a graft (Yoon 1975).

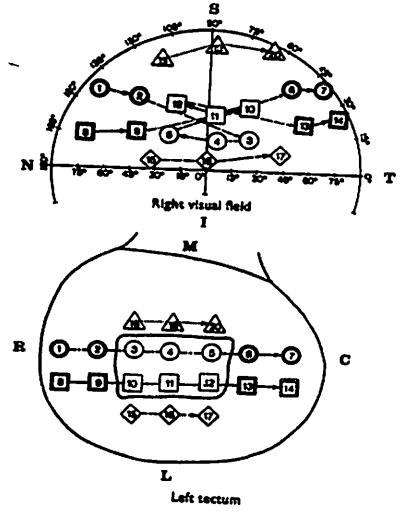

Figure 16. Visual field projection organization after optic nerve section and 180 degree rotation about the dorsoventral axis of a graft (Yoon 1975).

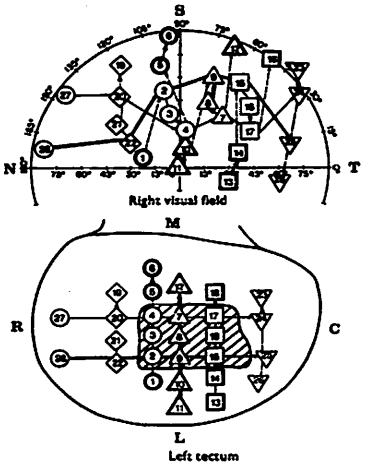

Figure 17. Projection organization after optic nerve section and graft inversion along the rostrocaudal axis (Yoon 1975).

random.

Figure 18

Notice that the most caudal section of the tectum receives information only from the temporal area in the visual field. The projection in that area is reasonably well ordered. The fibers from the nasal section of the visual field are moving toward the rostral section of the tectum. The fibers which should project onto the grafted area are trapped between those in the rostral one third of the tectum and those moving toward that end. The organization in the rostral one third of the tectum is also reasonably well ordered.

An extension to the graft rotation experiments consists of excising two pieces of tissue from the surface of the tectum and reimplanting them without rotation yet with their positions switched (Hope 1976). This is a difficult experiment to perform physiologically and the few available results are not totally consistent. In some cases, a completely normal projection is seen. This result would favor the "systems matching" theory of organization. However, different results have been obtained. In these cases the projection is ordered both within and surrounding the grafts but the grafts retain their original spatial mapping. Thus two sections of the mapping are interchanged. Since no information is available to differentiate between two tectal locations, these data support the "point-to-point chemospecificity" approach. Physiological results from such experiments are given in Figure 19, from (Hope 1976).

Figure 19

Previous experiments, cf. Overton and Arbib (1982), illustrated that the simple BAM cannot produce the behavior found in graft rotation or translation experiments. Simulation results from the translocated graft experiment appear in Figure 18b. Perfect organization in the one dimensional case would appear as line segments

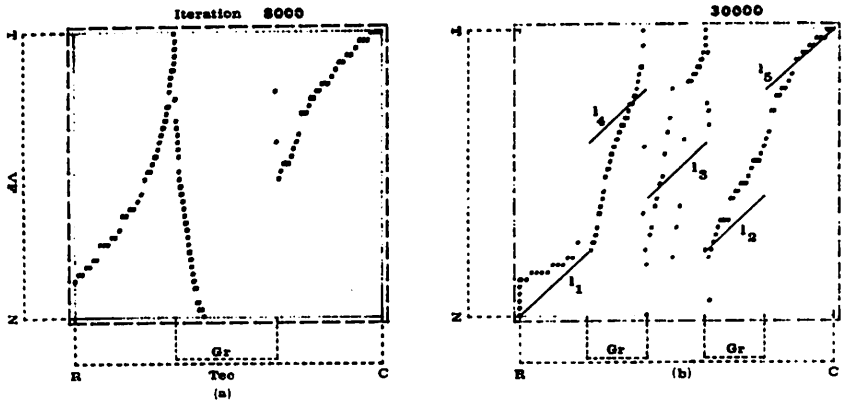

Figure 18. (a) XBAM simulation results of full retina projecting onto a tectum with one graft excised and inverted.

(b) XBAM results of a full retina mapping onto a tectum with two grafts translocated.

l_1 through l_5. BAM produced a completely normal mapping (Overton and Arbib, 1982). XBAM produces behavior closer to that observed experimentally. The disorder in the map is the result of conflicting information from the surface and neighbour interactions. Behavior more closely resembling the ideal case could be produced by appropriately adjusting the weighting constants in equations (10) and (11) of Appendix B.

Experiment VII.

This experiment is designed to compare the behavior of the XBAM simulation with the physiological results obtained during development. The retinal and tectal cell sheets grow at different rates and with different geometries. The retina tends to develop from the center outward in all directions at a uniform rate. The first section of the tectum to develop is the rostrocaudal section. Growth occurs primarily in the caudal and lateral direction. Figure 20 illustrates physiological results produced by Gaze (1974).

Figure 20

The figure contains mappings of the projection of the visual field at various larval stages. There are two interesting features in the data. First, the projection is ordered and initially covers only part of the tectal surface. As the organism continues to develop, the projection expands to fill the entire tectal surface. Second, the projection of the temporal visual field is quite large in comparison to to those of the medial and nasal field. Only after all of the tectal space has been filled does the projection begin to adjust to its normal proportions.

Figure 21a-g contains the XBAM simulation results. In this case, the retina is "grown" from the center outwards. The branches of two fibers are added every 200 iterations. In all cases, the branches of the new fibers are randomly distributed

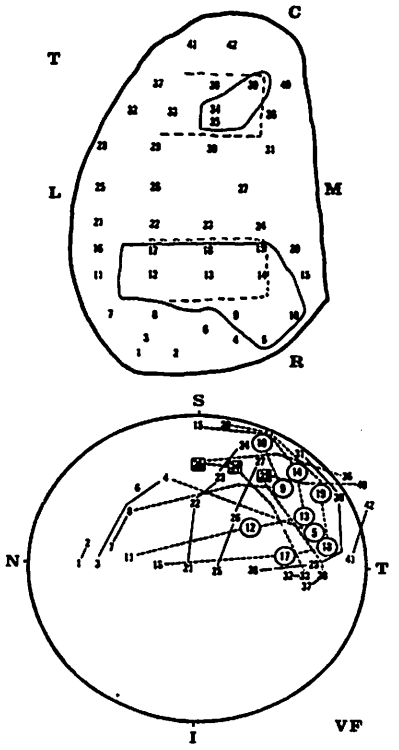

Figure 19. Mapping data from an animal with the positions but not orientations changed for two grafts (Hope 1976).

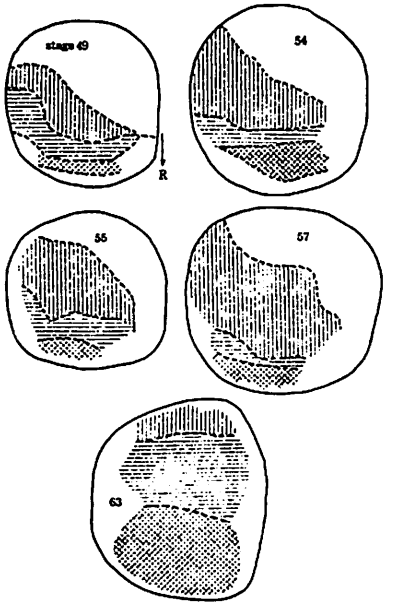

Figure 20. Physiological data of visual field projection mapping during various larval stages (Gaze 1974).

over the tectal surface as delimited in Figure 21a. During the same iteration, the tectal surface is increased in size. The rate of growth in the caudal direction is three times that in the rostral direction. Notice that the middle of the projection onto the tectum is organized as early as iteration 600, cf. Figure 21b, with only 8 fibers represented. As fibers are added from the edges of the retina, the projection remains organized. The tight packing and steep angle seen in the center of the projection indicates that the projection of the medial section of the visual field is compressed as seen in the physiological data. A distinctive "S" shape is evident in the mapping after iteration 2400, Figure 21e. The tails of the projection curve since they cover proportionally more of the tectal surface than does the center. In Figure 21g the branches of the fibers near the center of the projection are tightly packed while the branches of the fibers near the ends are spead out. It should also be noted that the projection is slowly moving in a caudal direction. Continued iteration of the simulation would result in a shift of the mapping in the caudal direction until a mapping projection uniformly covers the entire tectal surface as in Figure 6.

Figure 21

IV. Discussion.

The systems matching theory of the process by which the retino-tectal mapping is produced in lower vertebrates has been discussed. In this light, we presented the Branch-Arrow Model, BAM, as an extension to the Arrow Model of Hope et al. BAM is continuous in nature and includes a generalized neighborhood interaction mechanism as well as explicit boundary interaction. Its behavior was demonstrated through the use of computer simulations. Experiments demonstrate that the systems

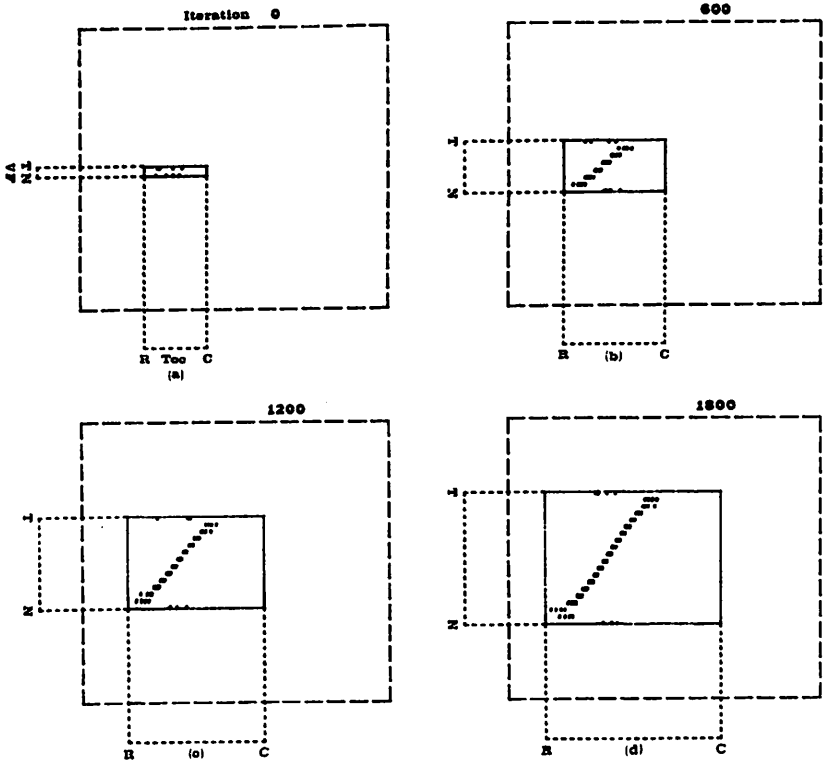

Figure 21, a-d. XBAM simulation of developing visual field and tectum. The visual field grows uniformly out from the center while the tectum grows three times as fast in the caudal direction as in the rostral direction. (a) initial state, (b) 600 iterations, (c) 1200 iterations, (d) 1800 iterations.

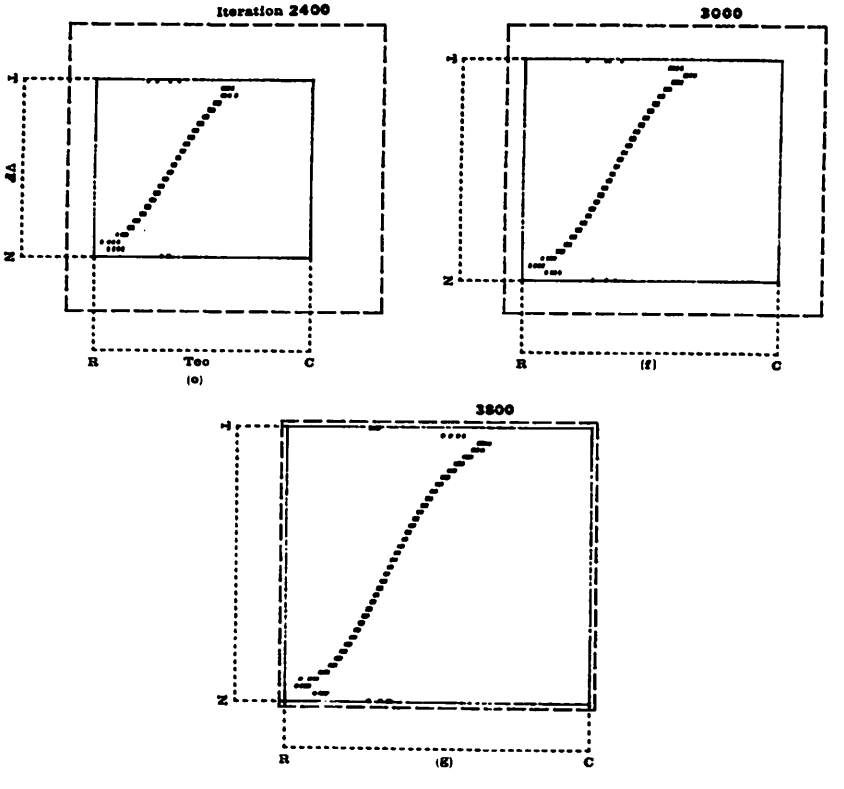

Figure 21, e-g. XBAM simulation of developing visual field and tectum. (e) 2400 iterations, (f) 3000 iterations, (g) 3800 iterations.

matching approach utilizing effective communication between any two retinal cells can account for the majority of the physiological experimental results. However, if the retinal distance allowing communication is reduced to a fraction of the total retinal expanse, the behavior degrades considerably. This suggests that neighborhood interaction mechanisms alone lack sufficient information to produce global organization.

The Marker Induction Model of Willshaw and von der Malsburg can produce behavior similar to the experimental results but requires a degree of initial organization in order to produce a final map which is globally continuous. While this requirement may not be unreasonable, the more general question of the amount of information, or specificity, required by a model to explain the physiological results remains. The Extended Branch-Arrow Model, XBAM, was presented as a compromise between these two approaches.

XBAM combines the local systems matching mechanisms apparent in BAM with a component describing a rough, inaccurate global positioning mechanism derived from the chemoaffinity theory. The behavior of this hybrid model was investigated through computer simulation and was shown to be in good agreement with the physiological data.

The design of (X)BAM reflects the physical structure of the system. Details such as axonal arborization, boundary interaction, and multiple fiber interactions have been included to increase the realism of the model. Expressing our model in a form amenable to computer simulation required the explicit definition of a number of parameters, e.g. the interaction field radius. It has been determined through empirical observation that the model is robust in regard to the settings of these various parameter values. It is not our intent that the actual parameter settings used for our simulations be taken as the quantities on which the validity of our model rests but rather that the model be considered as a possible conceptual

mechanism through which the retino-tectal connections can be organized.

In particular, the values of the parameters were chosen simply to make their relative magnitudes believable. Experimentally determined values for the radius of interaction, average number of branches per retinal fiber, the effect of tectal and graft boundaries, and the ease with which fiber branches can move across surgically induced discontinuities could add a great deal to the model. Our simulations showed that during the course of organization, the density of fiber branch terminations along a graft boundary increased as the boundary became more difficult to cross. A detailed physiological study of the fiber densities seen along graft boundaries in animals could be very useful in evaluating this aspect of model behavior.

The simulation results presented in this paper are one-dimensional in nature. Limited simulations of the two-dimensional analog were conducted. However, they were limited in number and size due to the amount of computation required. The increase in computation was on the order of 100 fold, thus making the use of two-dimensional simulation as a research tool premature. While most of the two-dimensional behavior of a given model can be deduced from the one-dimensional version, certain interesting behavior trends did appear during the time course of organization on our few two-dimensional simulations.

In the one-dimensional experiment involving a rotated graft, some branches were found to remain at the graft boundary due to the conflicting influence felt by the branches on either side: one set inside and the other outside the graft. In the two-dimensional case, branches can again be trapped along a graft boundary. This trapping, however, occurs along one dimension with organizing influence felt along the other dimension. This results in the branches traversing the perimeter of a graft in order to move to the portion of the tectal surface to which they belong instead of crossing the grafted portion. Physiological data indicating the paths across the tectum taken by fibers projecting to different areas would be of great

value in determining the validity of the observed simulation behavior.

A second behavioral anomaly observed in the two-dimensional simulation concerned the shape of the fiber projection fields. Recall that we defined the projection field as the area of the tectum influenced or covered by the branches of a fiber. In the one-dimensional case, we can only conclude that the branches of a particular fiber are grouped together with a uniform overlap in their fields and that the entire surface exhibits reasonably uniform coverage. In the two-dimensional simulation of a normal retina projecting onto a normal tectum, the branches are grouped in such a way as to cover a circular area. The fields are arranged so as to fit the branches in the smallest possible tectal area, given a particular allowable amount of overlap. Again the distribution was such that all of the tectal surface was uniformly covered. When a section of the tectum was excised and rotated, the resulting branch terminations were still grouped, although the shape of the grouping appeared elliptical rather than spherical. The major axis of the set of terminations was in the direction of the rotation of the graft. This suggests the need for physiological experimentation to determine the shape of the area covered by the set of branch terminations for a given fiber. Any differences seen under the conditions of a normal mapping and one with a rotated graft could be compared with the behavior predicted by the simulation.

A final point for discussion concerns the mechanism by which one fiber "knows" how it relates to another. This paper presents a conceptual model which assumes that this information is available to the fibers but does not propose a model of the availability. Several mechanisms have been suggested such as correlation of discharge and chemical gradient (Willshaw and von der Malsburg). The restriction on the distance between two fibers allowing effective communication could be modelled by the latter approach in a rather straightforward manner. If the extent of the indiviual gradients was greatly reduced, then it would be possible for two fibers

which are separated by a distance on the retina large with respect to the extent of the gradients to be marked by different sets of substances. This would result in a lack of information defining the relationship of the somas of the fibers. Physiological work needs to be conducted to determine the types and extents of any position markers on the retina and tectum. In addition, new mechanisms must be sought and further experimental evidence gained if the process by which organizational information is exchanged is to be understood.

Bibliography

Cook, J.E. & Horder, T.J. 1974 Interactions between optic fibers in their regeneration to specitic sites in the goldfish tectum. J. Physiol. 241, 89-90P.

Feldman, J.D., Keating, M.J., & Gaze, R.M. 1975 Retino-tectal mismatch: a serendipitous experimental result. Nature, Lond., 253, 445-446.

Gaze, R.M., Jacobson, M., & Szekely, G. 1963 The retino-tectal projection in Xenopus with compound eyes. J. Physiol., 165, 484-499.

Gaze, R.M., Jacobson, M., & Szeleky, G. 1965 On the formation of connections by compound eyes in Xenopus. J. Physiol., 176, 409-417.

Gaze, R.M. & Sharma, S.C. 1970 Axial differences in the reinnervation of the goldfish optic tectum by regenerating optic fibers. Expl. Brain Res. 10, 171-181.

Gaze, R.M. & Keating, M.J. 1972 The visual system and "neuronal specificity". Nature 237, 375-378.

Gaze, R.M., Keating, M.J., & Chung, S.H. 1974 The evolution of the retinaotectal map during development in Xenopus. Proc. R.Soc. Lond. 185, 301-330.

Hope, R.A., Hammond, B.J., & Gaze, F.R.S. 1976 The arrow model: retinotectal specificity and map formation in the goldfish visual system. Proc. R. Soc. Lond. 194, 447-466.

Horder, T.J. 1971 Retention by fish optic nerve fibers regenerating to new terminal sites on the tectum, "chemospecific" affinity for their original sites. J. Physiol. Lond. 216, 53-55.

Horder, T.J. & Martin, K.A.C. 1977 Translocation of optic fibers in the tectum map be determined by their stability relative to surrounding fiber terminals. J. Physiol., Lond., 271, 23-24P.

Humphery, M.F. and Beazley, L.D. 1981 An electrophysiological study of early patterns of the retinotectal projection during optic nerve regeneration in Hyla Moorei. submitted to Brain Research.

Hunt, R.K. & Jacobson, M. 1973 Development of neuronal locus specificity in Xenopus retinal ganglion cells after surgical transection or after fusion of whole eyes. Dev. Biol., 40, 1-15.

Jacobson, M. & Gaze, R.M. 1965 Selection of appropriate tectal connections by regenerating optic nerve fibers in adult goldfish. Exp. Neurol., 13, 418-430.

Levine, R. & Jacobson, M. 1974 Development of optic nerve fibers is determined by positional markers in the frog tectum. Exp. Neurol. 43, 527-538.

Maturana, H.R., Lettvin, J.Y., McCulloch, W.S., & Pitts, W.H. 1959 Evidence that the cut optic nerve fibers in a frog regenerate to their proper places in the tectum. Science, 130, 1709-1710.

Overton, K.J. & Arbib, M.A. 1982 Systems matching and topographic maps: The branch-arrow model (BAM). In: Competition and Cooperation in Neural Nets (S. Amari and M.A. Arbib, Eds.), Lecture Notes in Biomathematics, Springer-Verlag.

Schmidt, J.T. 1978 Expansion of the half retinal projection to the tectum of in goldfish: an electrophysiological and anatomical study. J. comp. Neurol. 177, 257-278.

Schmidt, J.T. 1978 Retinal fibers alter tectal positional markers during the expansion of the half retinal projection in goldfish. J. comp. Neurol. 177, 279-300.

Schmidt, J.T. & Easter, S.S. 1978 Independant biaxial reorganization of the retinotectal projection: a reassessment. Exp. Brain Res. 31, 155-162.

Sharma, S.C. 1972 Redistribution of visual projections in altered optic tecta of adult goldfish. Proc. Nat. Acad. Sci. U.S.A. 69, 2637-2639.

Sharma, S.C. & Romeskie, M. 1977 Immediate 'compression'of the retinal projection to a tectum devoid of degenerating debris, Brain Res. 134, 367-370.

Sperry, R.W. 1943 Visuomotor coordination in the newt (Triturus viridescens) after regeneration of the optic nerve. J. Comp. Neurol., 79, 33-55.

Sperry, R.W. 1944 Optic nerve regeneration with return of vision in Anurans. J. Neurophysiol. 7, 57-70.

Sperry, R.W. 1945 Restoration of vision after crossing of optic nerves and after contralateral transplantaion of eye. J. Neurophysiol. 8, 15-28.

Sperry, R.M. 1963 Chemoaffinity in the orderly growth of nerve patterns and connections. Proc. Natl. Acad. Sci., U.S.A. 50, 701-709.

Willshaw, D.J. & von der Malsburg, C. 1979 A marker induction mechanism for the establishment of Ordered neural mappings: its application to the retinotectal problem. Phil. Trans. Proc. R. Soc. Lond. B, 287, 203-243.

Udin, S.B. 1977 Rearrangements of the retinotectal projection in Rana Pipiens after unilateral caudal half-tectum ablation. J. comp. Neurol. 173, 561-582.

Yoon, M.G. 1973 Retention of the original toopgraphic polarity by the 180 degree rotated tectal reimplant in young goldfish. J. Physiol. 233, 575-588.

Yoon, M.G. 1975 Readjustment of retinotectal projection following reimplantation of a rotated or inverted tectal tissue in adult goldfish. J. Physiol. 252, 137-158.

Yoon, M.G. 1976 Progress of topographic regulation of the visual projection in the halved optic tectum of adult goldfish. J. Physiol. 257, 621-643.

APPENDIX A

Arrow Model Interchange Rules

One iteration of switching interaction applies the following interchange rule to each retinal fiber, T_k. One of the eight sites immediately adjacent to the present tectal site of T_k (see Figure A.1a) is chosen at random until one containing another fiber, T_n, is found. It should be noted that the boundaries of the tectum are only implicitly considered in that a termination site on a boundary has only five neighbors. The retinal locations, R_k and R_n, of the somas from which fibers T_k and T_n, respectively, emanate are compared and the following process is used to determine the new grid location of the termination of the fibers (Figure A.1b).

* Construct a line, L_t, on the tectum which passes through the site of termination of fiber T_k and is orthogonal to the line connecting the termination sites of both fibers, T_k and T_n.

* Construct a line, L_r, on the retina which passes through the retinal position, R_k, of the soma of fiber T_k and is orthogonal to the line passing through the retinal locations of both fibers, R_k and R_n (Figure A.1b).

* With the superior-inferior retinal axis mapped onto the medial-lateral tectal axis and the nasal-temporal retinal axis mapped onto the rostral-caudal tectal axis, switching is determined as follows: if T_n resides on the same side of line L_t as R_n does with respect to line L_r, then T_k and T_n retain their original locations, otherwise they switch positions.

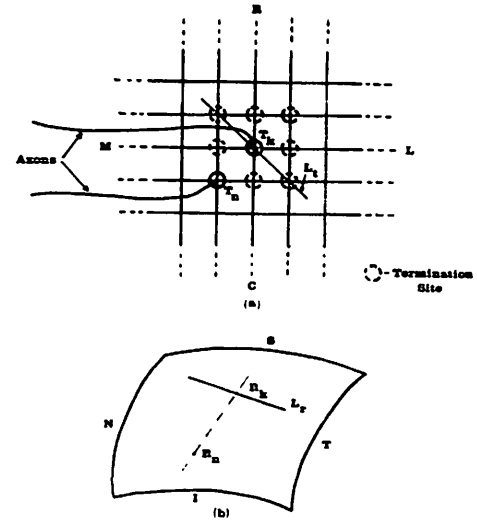

Figure A.1. (a) The grid configuration used in the Arrow Model.
(b) Retinal locations R_k and R_n of the somas of fibres terminating at tectal sites T_k and T_n. R - Rostral, C - Caudal, M - Medial, L - Lateral, N - Nasal, T - Temporal, S - Superior, I - Inferior.

APPENDIX B

Mathematical Specification of BAM

The BAM updating process is obtained by averaging three components: the interaction influence, $\vec{I}_b$, the boundary effect, $\vec{E}_b$, and the average influence, $\vec{A}_b$. The interaction influence component, $\vec{I}_b$, is a continuous analogue of the Arrow-Model interaction process, employed at the level of the branches of a fiber combined with a term describing the local interactions between the branches and the boundaries of the tectum and the various grafts. The average of the physical influence, $\vec{A}_b$, felt by all of the branches of a given fiber is calculated. The ultimate movement of a particular branch is then determined as the weighted sum of these influences.

$$\vec{M}_b = a_1\vec{I}_b + a_2\vec{E}_b + a_3\vec{A}_b \tag{1}$$

where a_1, a_2, and a_3 are weighting constants, $\vec{I}_b$ and $\vec{E}_b$ are described in equations (3) and (4) below, and the average influence is given by

$$\vec{A}_b = \frac{1}{m}\sum_{k\epsilon F_b}(a_4\vec{I}_k + a_5\vec{E}_k) \tag{2}$$

where the sumation ranges over the set F_b of all branches k from the same retinal fiber as b, m is the number of branches in F_b, and a_4, a_5 are weighting constants.

The first term in the physical influence component provides the extension of the Arrow Model. In the Arrow Model, only one of a fiber's eight immediate neighbors is involved during each iteration of its updating. As a result, the fiber in question receives no influence from any of the other neighbouring fibers, nor

from any of the fibers which do not occupy immediately adjacent sites. In BAM, the continuous nature of the tectal surface, the fact that each fiber has a set of branches, and the circle of interaction for each branch eliminate these restrictions. Due to the continuous nature of the tectal surface, the updating process is truly a neighbourhood interaction rather than an interchange. During each iteration, a branch interacts with all other branches whose circles of interaction have a non-empty intersection with the circle of the branch in question to produce the interaction component, $\vec{I}_b$.

To see the shape of this interaction, let B_b be the set of fiber-branches whose interaction circles intersect that of branch b. Let $\vec{U}(b,k)$ be the unit vector in the "interchange direction" for the current position of b and that of k. Then the movement of b induced by its interaction with k is

$$W_d(b,k)\ W_g(b,k)\ \vec{U}(b,k)$$

where the weights W_d (due to the distance of separation) and W_g (due to interaction across a boundary) are described below in equations (4) and (5). Thus the total interaction component is given by

$$\vec{I}_b = \sum_{k\epsilon B_b} W_d(b,k)\ W_g(b,k)\ \vec{U}(b,k) \tag{3}$$

In the Arrow Model, the interchange of two fibers occurs in discrete steps. When it has been determined that two branches are oriented in the reverse of their retinal locations, they simply exchange positions. In BAM, the influence between two branches, W_d, is graduated depending upon separation. The weight is linear in nature with a value of 1 when the two branches terminate at the same point and 0 when the branches are separated by a distance of twice the radius of their circles of interaction:

$$W_d(b,k) = \begin{cases} 1 - \frac{d(b,k)}{2r} & \text{if } d(b,k) < 2r \\ 0 & \text{otherwise} \end{cases} \quad (4)$$

where r is the radius of interaction on the tectum and d(b,k) denotes the distance between the tectal terminations of fibers b and k.

The weight due to intervening graft boundaries, W_g, is intended to model the discontinuous nature of such edges. Since the edges of grafts are actual surgical disruptions of the surface, wee feel that communication across a graft edge should be attenuated. This is expressed mathematically by including a mulplicative constant for each boundary between the two branches, so that two branches separated by a boundary exhibit less influence on one another than do two branches separated by a similar distance but with no intervening boundaries.

$$W_g(b,k) = a_g^n \quad (5)$$

where a_g is the mulplicative constant determining cross-boundary communication effectiveness, $0 \leq a \leq 1$, and n is the number of graft boundaries intersecting the line segment connecting the terminations of branches b and k.

The simple Arrow Model does not include the boundary of the tectum nor the edges of the grafts as influencing factors. The second term of equation (1) includes this factor explicitly as $\vec{E}_b$.

$$\vec{E}_b = \sum_{q \in Q} W_d(b,q)\, W_g(b,q)\, \vec{U}(b,q) \quad (6)$$

where Q is the index set of all tectal and graft boundaries; $\vec{U}(b,q)$ is the unit vector along the line perpendicular to boundary q and passing through the

termination of branch b; W_d is the weight due to the distance of separation; and W_g is the weight due to graft boundaries.

Tectal and graft edges are physical discontinuities in the surface of the tectum. It should, therefore, be more difficult for an axon to migrate across such a boundary than to move across an unobstructed surface. The boundaries thus have influence by restricting the movements of the branches. As in the case of interacting branches, the magnitude of the influence, W_d, is proportional to the distance from the center of the branch circle to the boundary along a line perpendicular to the boundary.

$$W_d(b,q) = \begin{cases} 1 - \frac{d(b,q)}{r} & \text{if } d(b,q) < r \\ 0 & \text{otherwise} \end{cases} \quad (7)$$

where r is the radius of interaction on the tectum and d(b,q) denotes the distance between the termination of branch b on the tectum and boundary q. In addition, due to the physically discontinuous nature of a boundary, the influence of one branch on another across a boundary is decreased, via W_g. Mathematically, the influence due to boundary interaction felt by branch k is given in (5). The direction of the influence, $\vec{U}$, is always away from the boundary along a line perpendicular to the boundary through the point of termination of the branch in question.

The actual influence, $\vec{M}_b$, used to update the position of a branch b during an iteration is determined as the weighted sum of the physical influences $\vec{I}_b$ and $\vec{E}_b$ felt by the branch and the average $\vec{A}_b$ of the physical influences of the branches from the same fiber, as we saw in equation (1). Since, by definition, the branches of a fiber are connected to one another, we feel that this form of information transfer can take place.

APPENDIX C

Mathematical Specificiation of XBAM

The XBAM physical infuence component consists of three factors. The first two are exactly the neighborhood interaction and boundary influences defined in BAM, see Appendix B. The final factor, $\vec{S}_b$, provides the degree of global information required to account for the translocation experiments. This factor describes the interaction between the branches and the tectal surface. As in BAM, these components are combined with the average influence felt by all of the branches of a fiber to form the total influence felt by each branch during a given iteration,

$$\vec{S}_b = W_s(M(P_r(b),P_t(b)))\,\vec{U}_s(P_r(b),P_t(b)) \tag{8}$$

where the weight W_s (due to difference of the markers) is described below in equation (9); $P_r(b)$ is an encoding of the retinal position of the soma of the cell emitting branch b; $P_t(b)$ is an encoding of the tectal position of branch b corresponding to the encoding P_r; $M(p,q)$ is a measure of the difference between the retinal and tectal positions; and $\vec{U}_s$ is the unit vector from the branch's current position to its desired final position.

A fiber interacts with the surface of the tectum by way of its branches. Each branch of a fiber is thought to be marked in some manner according to the retinal position of its soma. The marker need not be an indicator of its exact position but rather a marker encoding its general location, e.g. the position should be accurate to within plus or minus the distance allowing effective retinal communication. That is, the marker here is to be considered in the sense of a general position indicator

as opposed to a point to point chemoaffinity. The tectal surface is also posited to be labelled in a similar manner. Each of the branches sample the marker on the tectal surface. The surface influence contains a weight, W_s, which is proportional to the difference between the retinal and tectal labels.

$$W_s(M(a,b)) = \begin{cases} 1 & \text{if } M(a,b) > t_2 \\ \dfrac{M(a,b)-t_1}{t_2 - t_1} & \text{if } t_1 \le M(a,b) \le t_2 \\ 0 & \text{otherwise} \end{cases} \tag{9}$$

where t_1 and t_2 are thresholds which determine the interval on the retina allowing effective communication.

The average of the influences, $\vec{A}_b$, felt by the branches of a particular fiber is given by

$$\vec{A}_b = \frac{1}{m}\sum_{k\in F_b}(a_7\vec{I}_k + a_8\vec{E}_k + a_9\vec{S}_k) \tag{10}$$

where the sumation ranges over the set F_b of all branches k from the same retinal fiber as b, m is the number of branches in F_b, and a_7, a_8, and a_9 are weighting constants.

The updating processes used in the Extended Branch-Arrow Model consists of four components. For each of the branches, the interaction influence, boundary influence, surface influence, and the average influence components are combined in a weighted average to form the movement of the branch.

$$\vec{M}_b = a_{10}\vec{I}_b + a_{11}\vec{E}_b + a_{12}\vec{S}_b + a_{13}\vec{A}_b \tag{11}$$

where the a's are weighting constants.

Chapter 6: Habituation and Learning

Jorg-Peter Ewert: CONFIGURATIONAL PREY-SELECTION BY INDIVIDUAL EXPERIENCE IN THE TOAD

Rolando Lara: A NEURAL MODEL OF STIMULUS-SPECIFIC HABITUATION IN AMPHIBIA

B.A. Cartwright and T.S. Collett: HOW HONEY BEES USE LANDMARKS TO GUIDE THEIR RETURN TO A FOOD SOURCE

Jorg-Peter Ewert: CONFIGURATIONAL PREY-SELECTION BY INDIVIDUAL EXPERIENCE IN THE TOAD

The variety of the shapes and patterns of natural prey objects should allow toads to link individual experience to particular visual cues and to store this information in order to recall it when faced with the appropriate stimulus (Eibl-Eibesfeldt, 1951; Freisling, 1948). This phenomenon can be studied in habituation experiments.

1. Behavioral Responses

a) Time Course of Habituation in a Stimulus Series. If a common toad is stimulated during a long-term stimulus series with the same prey dummy, the prey-catching orienting activity decreases, which indicates that the toad habituates to the stimulus. The average orienting activity $\bar{R}_s$ decreases approximately according to the formula:

$$\ln \bar{R}_s = - \sigma (s-1) + \ln \bar{R}_1 \quad [\ln(\text{orienting responses} \times \text{min}^{-1})]$$

$$\bar{R}_s = \bar{R}_1 e^{- \sigma (s-1)} \quad [\text{orienting responses} \times \text{min}^{-1}]$$

where s is the time, measured in successive 1 minute intervals (Ewert, 1970a). The value $\bar{R}_1$ refers to the number of orienting responses during the first minute interval (s=1). The exponent describes the linear relationship between s and the natural logarithm of $\bar{R}_s$. The constant $\bar{R}_1$ depended upon the toad's motivational level (e.g., hunger state, time of the day) and stimulus parameters (size, configuration, contrast, velocity, etc.) The reasons for the decrease of prey-catching activity according to Eq. are stimulus-specific "after

effects", which accumulate during successive stimulations and decrease the probability of stimulus responses (Ewert, 1967b). Stimulus specificity means that following habituation to a dummy form A another form B presented immediately thereafter will be effective, a phenomenon which is to be discussed in a later paragraph (Birukow and Meng, 1955; Meng, 1958; Ewert and Kehl, 1978). Toads habituate the orienting response also selectively for the eye and the specific area on the retina being stimulated. This phenomenon is called locus specificity (Eikmanns, 1955; Ewert, 1965, 1967a; Ewert and Ingle, 1971). The biological significance of stimulus and locus specific habituation may be to keep the innate releasing mechanism (IRM) for prey-catching alert toward "new" stimuli. The orienting mechanism per se is not affected.

b) Time Course of Recovery. Toads do recover from habituation in a stimulus series (Ewert, 1970a). The decrease of stimulus and locus-specific after-effects can be measured by the recovery rate R^*_t / R^*_o to the same prey stimulus presented to the same retinal locus at different recovery times, t. R^*_o is the number of responses in the first habituation stimulus series,

..... and R^*_t the number of responses in a second habituation stimulus series, both separated by a recovery pause, t[minutes]. From these data it is evident that two (or more) storage processes are involved - a short-term (first 10 min) and a long-term process. Some 6 to 24 hours after habituation of prey-catching in response to repeated stimulation with the same prey dummy, there is full recovery, i.e., $R^*_t / R^*_o = 1$.

c) Habituation in a sequence of Stimulus Series. Stimulus and locus-specific aftereffects summate during successive stimulus series, each separated by a constant recovery pause, i.e., the number of prey-catching responses per stimulus series decreases. Taking R^*_1 as the number of orienting responses during the first series until no reaction occurs (habituation), the number of responses R^*_i in the ith series is given by:

$$R^*_i / R^*_1 = e^{-\xi (i-1)}$$

Different experimental (stimulus parameters) and motivational conditions (animal's prey-catching activity) produce variations in the overall prey-catching activity, R^*_1, and the length of the habituation series. The habituation rate depends upon the length of the interseries recovery pauses. For 5 min recovery pauses a value of $\xi = -0.23$ was calculated.

Following habituation of the prey-catching orienting response in a sequence of stimulus series, recovery is significantly longer (days) than after habituation with only one stimulus series. This may be due to the involvement of long-term after effects. A hypothesis in this context was presented by Ewert (1965).

Stimulus habituation also occurs after repeated release of escape behavior with a predator dummy. So far as the results of B. viridis and B. bufo are concerned, toads do recover after habituation within a predator-stimlus series much faster than after habituation in a prey-stimulus series - which seems to be biologically meaningful.

d) Stimulus Specificity. The following conclusions were reached (Meng, 1958; Ewert and Kehl, 1978): (i) If the toad, after habituation of the orienting response to the prey dummy with the pattern A, immediately shows orienting activity to another pattern B projected at the same retinal locus, we can conclude that the animal discriminated between the two patterns provided all other stimulus parameters were held at constant values; (ii) If, following (i), in the reverse type of experiment, the pattern A releases no prey-catching responses following habituation of the response first to B, it can be concluded that toads prefer B over A. (iii) If in both habituation series the second pattern "renewed" the toad's prey-catching activity by equal amounts, it can be concluded that both are almost equally attractive as prey. On the basis of paired tests of prey-dummies with different patterns and shapes, a hierarchical ordering of significant features can be constructed (Ewert and Kehl, 1978). For example, if b>c, and c>g, then logically c>g. All these patterns have in common the same maximal expansion in direction of their movement ($x1_1$ = 20 mm) and perpendicular to it ($x1_2$ = 5 mm). The experimental results confidently demonstrate that stimulus specific habituation is based on configurational cues of the stimulus and not only on its newness. The main features governing prey selection are, as far as has been investigated: (1) area components, (2) leading edges of the stimulus, (3) isolated dots, and (4) striped patterns. These cues have a significant effect in the experience governed discrimination of prey in common toads. Indeed those patterns are components of natural prey objects.

a) Other Dishabituation Effects. The aim of this investigation was to determine in toads the influence of visual stimulation on the course of habituation of prey-catching orienting in response to a prey-dummy which was repeatedly presented at a constant angle to one eye. Visual "dishabituatory" stimuli were provided by the same prey-dummy, presented immediately after habituation to the other eye or another part of the retina. In this context it is interesting to note that facilitatory effects on the orienting response could also be produced if stimulus series were successively presented from nasal (N) to temporal (T) retinal positions. Thus, habituation of prey-catching orienting to repeated stimulation of the same retinal locus facilitates the response to subsequent stimulation of an adjacent temporal area α_T, but inhibits the response to a more nasal area α_N. Using a two choice experimental paradigm, comparable excitatory effects following habituation of prey-catching have been described in R. pipiens (Ewert and Ingle, 1971).

2. Neurophysiological Results.

a) Electrical Brain Stimulation. Escape behavior of toads B. bufo was elicited in response to electrical point stimulation of the caudal thalamus at currents of about 25% over threshold (Rehn, 1977). Within a stimulus-series stimuli were given at 10 second intervals - the response decreased. The course of recovery from this habituated state was very similar to that obtained by visual stimulation with a predator dummy. Within a sequence of stimulus series (each series separated by constant 5 or 10 minute recovery intervals) escape activity in response to brain stimulation progressively decreased,

quite similarly to that in visual stimulation experiments. Furthermore, these experiments indicated that habituation caused by visual and electrical brain stimulation summated in successive stimulus series.

b) Brain lesions. After bilateral transection of the telencephalon just in front of the preoptic area, the toad's prey-catching activity in response to a repeatedly moving prey object showed a remarkable decrease, i.e., the value of $\bar{R}^*_1$ in Eq. (1) was relatively low (Ewert, 1965, 1967 a-d). But also the course of habituation - (exponent in Eq. (1) - within a sequence of stimulus series was increased in comparison with controls ($\xi = -0.55$). Following TP-lesions, habituation was almost totally abolished in some of the operated animals ($\xi = -0.05$): in others habituation was even stronger than in control animals ($\xi = -0.23$). Thus, TP-lesioned toads exhibited two response types which were maintained after total ablation of the telencephalon. All of these TP-lesioned toads have in common the "disinhibited" prey-catching behavior (i.e., loss of prey/predator recognition) in response to moving visual stimuli.

c) Neuropeptides and Habituation. In a recent quantitative study by Horn et al. (1979) it was shown that administration of ACTH to common toads significantly prolongs the course of recovery after stimulus specific habituation of prey-catching. As a result, habituation within a sequence of stimulus series is increased in ACTH-treated animals against controls.

d) Neuronal Responses. Retinal ganglion cells. Neuronal adaptation

of retinal ganglion cells following stimulus traverse of the ERF was studied in detail in R. esculenta by Grusser and Grusser-Cornehls (1969, 1973). Adaptation after repeated stimulus traverses is strongest in class R2 and weakest in class R3 and R4 neurons. Adaptation in retinal ganglion cells is obviously due to different time constants τ_n of synaptic transfer processes and thus linked with the movement specificity (or sensitivity) of R2 (or R3 and R4) neurons (Grusser and Grusser-Cornehls, 1968a). The greater the values of τ_n, the smaller the exponents γ_n in the neurophysiological power functions describing the relationships between neuronal discharge rate and stimulus angular velocity according to the power function. In common toads the calculated values for the neuronal classes R2, R3, and R4 are $\gamma_2 < \gamma_3 < \gamma_4$ and thus, $\tau_2 > \tau_3 > \tau_4$ (Ewert and Hock, 1972). Local adaptation in the ERF is strongest in class R2 neurons. Here, a stimulus has to be displaced (e.g., moved) in the ERF in order to elicit a response. Neuronal adaption is a precondition of movement specificity. The behavioral findings in TP-lesioned toads of response type 1 clearly show that neuronal adaptation in the retina cannot be the mechanism producing stimulus-specific habituation of prey-catching or avoidance (Ewert and Kehl, 1978).

Tectal neurons. Some of the class T5 neurons investigated in R. pipiens exhibit response properties of "newness detectors" (Lettvin et. al., 1961). They quickly adapt to the same stimulus moving through their receptive fields, but can be reactivated within the same locus of the ERF by "new" visual stimuli, such as change of its movement direction or configuration. Ingle (1973c) discovered in R. pipiens a remarkable deficit of adaptation properties in tectal T5

"newness cells" following ipsilateral thalamic-pretectal lesions. These results have been confirmed for T5 neurons in B. bufo and R. temporaria (Ewert, von Wietersheim and Schurg-Pfeiffer, unpublished data). Both locus-specific and stimulus-specific adaptation properties, including the phenomenon of dishabituation, were also obtained in tectal class T2(1), T2(2), and T4 neurons of B. bufo (Manns and Ewert, unpublished data). There are neurons whose responses upon repeated stimulation of the same locus in the ERF are not adapted but facilitated (Ingle, 1975b). The "attention" property may be distinct from "dishabituation". Both excitatory or inhibitory after effects could be obtained in class T5(2), T2(1)(2), T2(2)(2) and T4(2) neurons following just one stimulus traverse of the ERF. For example, in class T5(2) neurons the antiworm configuration of a moving $2^0 \times 8^0$ stripe was less effective than the worm configuration. However, the absolute discharge rate in response to the antiworm stimulus may depend to some extent on the configuration of the preceding stimulus (Ewert et al., unpublished data).

Thalamic-pretectal neurons. "Memory units" of class TH9 may be involved in particular storage processes. These neurons exhibit relatively long lasting discharges after the stimulus has traversed the ERF. The afterdischarges seemed to be linked to certain cues of the stimulus (Ewert, 1971). With regard to dishabituation of prey-catching in response to cutaneous stimulation, electrophysiological studies (Ewert and Borchers, 1971) have as yet failed to demonstrate tactile influences upon toad's class T5 neurons so that an intratectal route for this kind of bimodal facilitation is without support at present. However, there are striking examples of

"visual tactile" interactions among subtectal class T'2(1) and T'2(2) neurons. Similar neurons (class T4) were also obtained by Fite (1969), Grusser-Cornehls (1970b) and Liege and Galand (1972) in the frog's optic tectum. Bimodal facilitation was also seen among thalamic class TH5 and TH10 neurons in B. americanus (Ewert, 1971; cf. also Vesselkin et al., 1971; Liege and Galand, 1972).

Telencephalic neurons. Independent of the mode of stimulation (one or several field traverses) neither neuronal adaptation nor facilitation effects lasted longer than 90 to 120 seconds, so far as has been investigated in tectal and thalamic-pretectal neurons. Comparable behavioral habituation effects may last up to 24 hours or even longer. However, recent preliminary studies in visual telencephalic neurons indicate neuronal adaptation phenomena which are much longer lasting than that obtained in tectal and thalamic-pretectal neurons (Fite, pers. comm.).

Conditioning

1. Behavioral Responses

According to the results of various investigators, frogs and toads are capable of learning to prefer or to avoid particular stimuli due to "positive" or "negative" experience (Pache, 1932; Cott, 1936; Honigman, 1944; Eibl-Eibesfeldt, 1951; Buytendijk, 1918, 1941; Freisling, 1948; Parriss, 1963a, b; Schmajuk et al. 1980). Studies on escape and avoidance learning from an electric shock revealed contradictory results (Bajandurov and Pegel, 1933; McGill, 1960; Crawford and Langdon, 1966; Boice, 1970; Yaremko et al., 1974).

Appetitive learning has been successfully demonstrated by van Bergeijk (1967) and Schmajuk et al. (1980).

a) Combined Visual Cues. In qualitative experiments by Brzoska and Schneider (1978) and quantitative investigations by Burghagen (1979) adult common toads were allowed to eat mealworms (unconditioned stimulus) out of the experimenter's hand (conditioned stimulus). In the course of time (4 months, one trial per day) animals came to associate the presence of the hand (or the entire moving investigator) with food, and they finally responded to the moving hand alone. However, this phenomenon was not specific to configurational features of the investigator's hand! Association of the hand during feeding was generalized to include other large objects as prey. Quantitative experiments showed that prey-catching activity of trained toads was significantly increased even in response to antiworm-like stripes and large square objects. However, among long black stripes of equal sizes, antiworm configurations were never preferred against worm configurations! In summary, the configurational selectivity for prey was decreased in trained toads, and the entire response spectrum became wider. The accuracy of the releasing mechanism had been modified in relation to individual experience based on learning. After subsequent "normal feeding" with mealworms - without other moving visual stimuli being present - the configurational sensitivity again increased. But even after 1 month of "normal feeding" the selectivity in some animals was not as sharp as before the training.

In a second experimental group, adult animals were fed with mealworms from a particular moving holder (Burghagen, unpublished data). The holder had the configuration of a 5 x 60 mm^2 antiworm-like black stripe and was moved to and from in the horizontal plane against a white background. Thus, during feeding toads were presented two kinds of stimuli: the natural prey (unconditioned stimulus) and the antiworm configuration of the holder (conditioned stimulus). After this kind of training toads responded more frequently to the antiworm configuration of a 2 x 30 mm^2 black (C=0.95) test stimulus, but they never preferred it over the worm configuration. Therefore, this kind of training mainly increases in general the probability that stimuli of inappropriate shape are classified as prey.

b) Combined Visual and Olfactory Cues. Common toads were exposed to the familiar odor of mealworm excrement (Ewert, 1965, 1968b). During a process of self- training, toads associated olfactory stimuli with visual cues of the prey. If "known odor" was then offered in the experimental situation along with a visual dummy, the stimulus efficacy could be increased, even in response to those stimulus configurations which previously had poorly or never resembled prey, such as long black worms. Odor-naive control animals showed no comparable phenomenon. However, olfactory training would never invert worm over antiworm preference (as far as black stripes are concerned). It seems as if association of large moving objects during handfeeding is mediated by olfactory cues in an initial phase of training. Facilitation of prey-catching behavior in the presence of known olfactory cues has also been obtained in B. calamita by Heusser (1958), in B. cognatus by D. Ingle (pers. comm.), and in R. pipiens (Shinn and Dole, 1978, 1979a,b). B. cognatus appears to be able to search for food, guided exclusively by olfactory stimuli. For the role of olfaction among salientian amphibia see Martof (1962b).

Sometimes common toads, when exposed to known mealworm odor, exhibited an unexpected behavior in response to large moving objects of the size of conspecifics. The excited toad oriented toward the conspecific and snapped at its moving head or eyes. When the conspecific was walking, the excited toad followed and clasped it - quite similar behavior to that seen during mating. The observation was independent of the season (Ewert, unpublished data).

c) Combined Visual and Gustatory Cues. In a study by Brzoska (1976), bugs or flies were soaked in a solution of quinine. Initially, guided by visual cues toads B. bufo caught these prey objects. But some animals spat them out. Toads behaving in this manner also linked this kind of negative gustatory experience with visual cues of the "prepared" prey objects, and they stored this information and called it into play when faced with the visual stimulus.

Similar results were obtained in R. pipiens by Schaffer (1911) and Sternthal (1974). These toads also avoided "unprepared" flies. Comparable observations have been reported for B. americanus and B. marinus following prey experience with bombardier beetles (Dean, 1980a,b). Another study by Mikula et al. (1980) explored the ability of B. terrestris to discriminate between palatable and unpalatable prey objects (dipped in 2%HCl solution) based on prey color and background color.

d) Other Cue Combinations. Cott (1936) investigated the modification of prey-catching in B. bufo in relation to acquired individual experience of pain and/or taste after feeding with hive-bees. Toads may associate the appearance of the bee with the painful sting which they received after the bee had been snapped. (Hive-bees are very distasteful, so that gustatory stimuli may also set cues of negative experience). Whereas bee-naive toads readily caught bees, animals with "bee experience" when placed in the same situation exhibited avoidance or even escape behavior. However, these toads immediately returned to their normal prey-catching habits when faced with prey of other visual appearance, such as a mealworm. The number of bees required to be eaten before the association of threat was established varied from 1 to 17 bees during a period of 1 to 7 days. In 30% of the cases only one experience was necessary to establish bee-avoidance. Once learned, this experience could be recalled for up to 14 days. Other studies by Brower and Brower (1962) and Brower et al. (1960) have shown that toads can learn to avoid bees (honeybees and bumblebees) and their mimics (dronflies and robberflies, respectively). Clarke (1974) and Smith and Bragg (1949) found that toads in the field often digest quantities of potentially painful food objects.

Most dramatic is the wide range of interindividual variability shown by common toads in training experiments. A proportion of only 20 to 30% "good learners" (Cott, 1936) was observed throughout all of the described training groups (a) to (d). Whether such variability is due to different (motivational) states of the animal or whether toads exhibit constant interindividual variability are important questions

that need quantitative treatment in future investigations.

2. Neurophysiological Data

Common toads which have learned to avoid bees will further snap toward bees, if they received a thalamic-pretectal lesion (Ewert, unpublished data). However, the conclusion cannot necessarily be drawn at present that TP-lesioned animals have lost their memory capacities. The phenomenon may be explained by the loss of visual pattern recognition. At present there are no single cell studies in frogs or toads indicating neuronal properties of coding "known" and "unknown" stimuli.

With respect to intraindividual variability of pattern recognition, it may be important to note that at least some of class T5(1) neurons can change the directional dependency of their configurational sensitivity over time (Ewert et al., 1979a). In two single neurons in which responses have been recorded over 4 to 5 h., the same stimulation program was repeated 4 or 5 times. Interestingly, the response to the worm-configuration was relatively constant over time, whereas the response to the antiworm could show remarkable changes. Grusser and Crusser-Cornehls (1976) noted in some T5 neurons another kind of changeability which was concerned with the exponents γ_n of the velocity power functions. Furthermore, some T5 neurons sometimes exhibit in their discharge particular burst patterns, where activation is interrupted by regular pauses (Lettvin et al., 1961); fast moving stimuli cause this pattern to disappear (Grusser and Grusser-Cornehls, 1968a). Following TP-lesions T5 neurons lose not only their configurational selectivity, but also the

interrupted burst characteristic (Ewert et al., unpublished data). It seems likely that under normal conditons (certain) neurons may alter their response characteristics in relation to variable system components in neural networks - according to conditions which are unknown at present.

References:

Ewert, J.-P. (1982) Tectal Mechanisms Underlying Prey-Catching and Avoidance Responses in the Toad, in: "Neurology of the Optic Tectum, (H. Vanegas, ed.), Plenum Press, New York.

References

Birukow, G., and Meng, M., 1955, Eine neue Methode zur Prufung des Gesichtssines bei Amphibien, Naturwissenschaften 42:652-653.

Boice, R., 1970, Avoidance learning in active and passive frogs and toads, J. comp. Physiol. Psycho). 70:154-156.

Brower, J.V.Z., and Brower, L.P., 1962, Experimental studies of mimicry.6. The reaction of toads (Bufo terrestris) to honeybees (Apis mellifera) and their dronfly mimics (Eristalis vinetorum), Amer. Naturalist 96:297-307.

Brower, L.P., Brower, J.V.Z., and Westcott, P.W., 1960, Experimental studies of mimicry.5. The reaction of toads (Bufo terrestris) to bumblebees (Bombus americanorum) and their robberfly mimics (Mallophora bomboides), with discussion of aggressive mimicry, Amer. Naturalist 94:343-356.

Brzoska, J., 1976, "Verhaltensphysiologische Untersuchungen uber das Horvermogen einheimischer Anuren, Dipl. Thesis, University of Bonn.

Brzoska, J., and Schneider, H., 1978, Modification of prey- catching behavior by learning in the common toad (Bufo b. bufo L., Anura, Amphibia): Changes in response to visual objects and effects of auditory stimuli. Behav. Processes 3:125-136.

Burghagen, H., 1979, Der Einfluss von Figuralen, visuellen Mustern auf das Beutefangverhalten verschiedener Anuren, Ph.D. Thesis, University of Kassel.

Buytendijk, F.J.J., 1918, Instinct de la recherche du nid et experience chez les crapauds (Bufo vulgaris et Bufo bufo), Arch. neerl. Physiol. 2:1-50.

Buytendijk, F.J.J., 1941, "Wege zum Verstandnis der Tiere", Zurich.

Clarke, R.D., 1974, Food habits of toads, genus Bufo (Amphibia: Bufonidae), Amer. Midland Naturalist 91:140-147.

Cott, H.B., 1936, The effectiveness of protective adaptations in the hive-bee, illustrated by experiments on the feeding reactions, habit formation and memory of the common toad (Bufo bufo bufo), Proc. Zool. Soc. Lond. 1:113-133.

Crawford, F.T., and Langdon, J.W., 1966, Escape avoidance responding in the toad, Psychonomic Sci. 6:115-116.

Dean, J., 1980a, Encounters between bombardier beetles and two species of toads (Bufo americanus, B. marinus): Speed of prey- capture does not determine success, J.comp.Physiol. 135:41-50.

Dean, J., 1980b, Effect of thermal and chemical components of bombardier beetle's chemical defense: Glossopharyngeal response in two species of toads (Bufo americanus, B. marinus), J. comp. Physiol. 135: 51-59

Eibl-Eibesfeldt, I., 1951, Nahrungserwerb und Beuteschema der Erdkrote (Bufo bufo L.), Behavior 4: 1-35.

Eikmanns, K.-H., 1955, Verhaltensphysiologische Untersuchungen uber den Beutefang und das Bewegungssehen der Erdkrote (Bufo bufo L.), Z. Tierpsychol. 12: 229-253.

Ewert, J.-P., 1965, "Der Einfluss peripherer Sinnesorgane und des Zentralnervennsystems auf die Antwortbereitschaft bei der Richtbewegung der Erdkrote (Bufo bufo L.), Ph.D. Thesis, University of Gottingen.

Ewert, J.-P., 1967a, Der Einfluss von Storreizen auf die Antwortbereitschaft bei der Richtbewegung der Erdkrote (Bufo bufo L.), Z. Tierpsychol. 24: 208-312.

Ewert, J.-P., 1967b, Untersuchungen uber die Anteile zentralnervoser Aktionen an der taxisspezifischen Ermudung beim Beutefang der Erdkrote (Bufo bufo L.), Z. vergl. Physiol. 57: 263-298. .

Ewert, J.-P., 1967c, Elektrische Reizung des retinalen Projektionsfeldes im Mittelhirn der Erdkrote (Bufo bufo L.), Pflugers Arch. 295: 90-98.

Ewert, J.-P., 1967d, Aktivierung der Verhaltensfolge beim Beutefang der Erdkrote (Bufo bufo L.) durch elektrische Mittelhirnreizung, Z. vergl. Physiol. 54: 455-481.

Ewert, J.-P., 1968b, Der Einfluss von Zwischenhirndefekten auf die Visuomotorik im Beute- und Fluchtverhalten der Erdkrote (Bufo bufo L.), Z. vergl. Physiol. 61: 41-70.

Ewert, J. P.: Neural mechanisms of prey-catching behavior and avoidance in the toad (Bufo bufo I). Brain Behav. Evol. 3, 35-56 (1970).

Ewert J. P., 1971, Single unit response of the toad's caudal thalamus to visual objects. Verg. Physiologie 74. 81-102.

Ewert, J.-P., and Borchers, H.-W., 1971, Reaktionscharakteristik von Neuronen aus dem Tectum opticum und Subtectum der Erdkrote Bufo bufo (L.), Z. vergl. Physiol. 71: 165-189.

Ewert, J.-P., and Hock, F.J., 1972, Movement sensitive neurones in the toad's retina, Exp. Brain Res. 16: 41-59.

Ewert, J.-P., and Ingle, D., 1971, Excitatory effects following habituation of prey-catching activity in frogs and toads, J. comp. Physiol., Psychol. 77: 369-374.

Ewert, J.-P., and Kehl, W., 1978, Configurational prey-selection by individual experience in the toad Bufo bufo, J. Comp. Physiol. 126: 105-114.

Ewert, J.-P., Borchers, H.-W., and Wietersheim, A.v., 1979a, Directional sensitivity, invariance and variability of tectal T5 neurons in response to moving configurational stimuli in the toad Bufo bufo (L.), J. Comp. Physiol. 132: 191-201.

Fite, K.V., 1969, Single unit analysis of binocular neurons in the frog optic tectum, Exp. Neurol. 24: 475-486.

Freisling, J., 1948, Studien zur Biologie und Physiologie der Wechselkrote (Bufo viridis Laur.), Osterr. Zool. Zeitschr. (Wien) 1: 383-440.

Grusser, O.-J., and Grusser-Cornehls, U., 1968a, Neurophysiologische Grundlagen visueller angeborener Auslosemechanismen beim Frosch, Z. vergl. Physiol. 59: 1-24.

Grusser, O.-J., and Grusser-Cornehls, U., 1969, Neurophysiologie des Bewegungssehens. Bewegungsempfindliche und richtungspezifische Neurone im visuellen System, Ergebn. Physiol., 61: 178-265.

Grusser, O.-J., and Grusser-Cornehls, U., 1970b, Die Neurophysiologie visuell gesteuerter Verhaltensweisen be Anuren, Verh. Dtsch. Zool. Ges. Koln 1970, pp. 201-218.

Grusser, O.-J., and Grusser-Cornehls, U., 1973, Neuronal mechanisms of visual movement perception and some psychophysical and behavioral correlations. In: Handbook of Sensory Physiology (H. Autrum, R. Jung, W.R. Loewenstein, D.M. McKay, and H.L. Teuber, eds.), Vol. VII/ 3A: Central Processing of Visual Information: Integrative Functions and Comparative Data (R. Jung ed.), Springer Verlag, Berlin, Heidelberg, New York, pp. 333-429.

Grusser, O. J., and Grusser-Cornehls, V.: Neurophysiology of the anurans visual system. In: Frog Neurobiology (Llinas, R., and Precht, W. eds.), Springer Verlag, New York, 1976, pp. 297-385.

Heusser, H., 1958, Zum geruchlichen Beutefinden und Gahnen der Kreuzkrote (Bufo calamita Laur.), Z. Tierpsychol. 15: 94-98.

Honigman, H., 1944, The visual perception of movement by toads, Proc. Roy. Soc. London 132: 291-307.

Horn, E., Greiner, B., and Horn, I., 1979, The effect of ACTH on habituation of the turning reaction in the toad Bufo bufo L., J. Comp. Physiol. 131: 129-135.

Ingle, D., 1973c, Disinhibition of tectal neurons by pretectal lesions in the frog, Science 180: 422-424.

Ingle, D., 1975b, Selective visual attention in frogs, Science 188:1033-1035.

Lettvin, J.Y., Maturana, H.R., Pitts, W.H., and McCulloch, W.S., 1961, Two remarks on the visual system of the frog. In: Sensory Communication (W.A. Rosenblith, ed.), M.I.T. Press, Cambridge, Mass.

Liege, B. and Galand, G., 1972, Single unit visual responses in the frog's brain, Vision Res. 12:609-622.

Martof, B.S., 1962b, Some reservations on the role of olfaction among salient amphibia, Physiol. Zool. 35:270-272.

McGill, T.E., 1960, Response of the leopard frog to electric shock in an escape learning situation, J. comp. Physiol. Psychol. 53: 443-445.

Meng, M., 1958, Untersuchungen zum Farben- und Formsehen der Erdkrote (Bufo bufo L.), Zool. Beitr. 3:313-363.

Mikulka, P., Hughes, J., and Aggerup, G., 1980, The effect of pre-training procedures and discriminative stimuli on the development of food selection behaviors in the toad (Bufo terrestris), Behav. and Neur. Biol. 29:52-62.

Pache, J., 1932, Formensehen bei Froschen, Z. vergl. Physiol. 17:423-463.

Parriss, 1963b, Retention of shape discrimination after regeneration of the optic nerves in the toad, Quart. J. exp. Psychol. 15: 22-26.

Parriss, J.R., 1963a, Visual discrimination in the toad, Quart. J. exp. Psychol. 15:13-23.

Rehn, B., 1977, Cerebrale Repräsentation des Fluchtverhaltens der Erdkrote (Bufo bufo L.), Ph.D. Thesis, University of Darmstadt.

Schaeffer, A.A., 1911, Habit formation in frogs, J. Anim. Behav. 1:309-335.

Schmajuk, N.A., Segura, E.T., and Reboreda, J.C., 1980, Appetitive conditioning and discriminatory learning in toads, Behav. and Neur. Biol. 28:392-397.

Shinn, E.A., and Dole, J.W., 1978, Evidence for a role for olfactory cues in the feeding response of leopard frogs, Rana pipiens, Herpetologia 34:167-172.

Shinn, E.A., and Dole, J.W., 1979b, Lipid components of prey odors elicit feeding responses of Western Toads (Bufo boreas, Copeia 1979(1):163-165.

Shinn, E.A., and Dole, J.W., 1979, Evidence for a role for olfactory cues in the feeding response of Western Toads, Bufo boreas, Copeia 1979(1):163-165.

Sternthal, D.E., 1974, Olfactory and visual cues in the feeding behavior of the leopard frog (Rana pipiens), Z. Tierpsychol. 34:240-246.

Van Bergeijk, W.A., 1967, Anticipatory feeding behaviour in the bullfrog (Rana catesbeiana), Anim. Behav. 15: 231-238.

Vesselkin, N.P., Agayan, A.L., Nomokonova, L.M., 1971, A study of thalamo-telencephalic afferent systems in frogs, Brain, Behav. Evol. 4:295-306.

Yaremko, R.M., Jette, J., and Utter, W., 1974, Further study of avoidance conditioning in toads, Bull. Psychonomic Soc. 3:340-342.

Rolando Lara: A NEURAL MODEL OF STIMULUS-SPECIFIC HABITUATION IN AMPHIBIA

The most important properties of habituation of prey orienting behavior in amphibia are the following[1-6] : 1) habituation is produced by the repeated presentation of the same stimulus; 2) if the stimulus is witheld, spontaneous recovery of the response occurs; 3) habituation is dependent on the frequency of stimulation, the higher the frequency, the higher the level and rate of habituation; 4) indirect evidence indicates that habituation is dependent on the amplitude of the stimulus: the weaker the stimulus, the strongest the rate and level of habituation; 5) habituation of the orienting response shows short and long term effects dependent on the number of habituation trials; 6) habituation is stimulus specific: when the habituated stimulus is changed the orienting response reappears; this fact suggests that habituation implies pattern recognition; in amphibia dishabituation has a hierarchy order where only certain types of stimulus will dishabituate a previously habituated object; 7) habituation in amphibia is a local spatial located process; and 8) habituation of prey orienting behavior is modulated by the motivational state of the animal.

We have proposed a neural model of the processing of information required for the phenomenon of habituation of prey orienting behavior to occur. The model is constituted by the bidimensional model of the interactions between retina-tectum and pretectum used to simulate recognition between prey-non prey stimuli[7], and the model of the possible neural mechanisms responsible

for habituation of the orienting reflex in mammals[8] (Fig. 1). Both models are based, as much as possible, on the anatomical, physiological and behavioral studies of this phenomenon.

The main postulates of the model are the following: 1) the retina extracts useful information about contrast, configuration and speed of the stimulus; 2) this information is sent both to the thalamus and tectum where further feature extraction occurs: the thalamus processes the information of the ganglion fibres 3 and 4 to define the properties of predator like stimulus; while the tectum integrates the information from retinal ganglion cells 2,3 and 4 and thalamic afferents to discriminate different stimuli (fig. 2); 3) the tectum through the integration of the processing of information of the retina and thalamus generates a spatio-temporal pattern which represents the general properties of the stimulus; 4) this spatio-temporal pattern is sent to the thalamus-telencephalon where a model of the spatio temporal pattern is generated; 5) After repeated presentations of the stimulus, the model of the spatio-temporal pattern and the actual spatio-temporal pattern produced in the tectum are compared in the thalamus-telencephalon; 6) if model and stimulus match, habituation as build up of inhibition over the tectum develops; while if model and stimulus does not match, then, if the new pattern is stronger, measured as the number and frequency of the pattern, dishabituation occurs (Figure 3).

With this model we have been able to reproduce most of the general properties of stimulus specific habituation of prey orienting response, showing how this animal could recognize different stimuli (see fig.4). The hypothesis of the model are clearly established so it could be tested experimentally.

REFERENCES

1. Ewert, P., The visual system of the toad: behavioral and physiological studies on a pattern recognition system, In: The amphibian visual system. A multidisciplinary approach, (Fite, K. ed.), Academic Press, New York, 1976.

2. Ingle, D., Disinhibition of tectal neurons by pretectal lesions in the frog, Science, 180, 442-444 (1973).

3. Ingle, D., Selective choice between double prey objects by frogs, Brain Behav. Evol. 7, 127-144 (1973).

4. Ewert, P., and Ingle, D., Excitatory effects following habituation of prey catching activity in frogs and toads, J. Comp. Physiol. Psychol. 3, 369-374 (1971).

5. Ewert, P. and Kehl, N., Configurational prey selection by individual experience in the toad Bufo bufo, J. Comp. Physiol. 126, 105-114 (1978).

6. Ingle, D., Reduction of habituation of prey catching activity by alcohol intoxication in the frog, Behav. Biol. 8, 123-129 (1973).

7. R. Lara, F. Cervantes and M.A. Arbib.
Bidimensional model of the interaction among retina-tectum pretectum for the control of prey-predator recognition and size preference in amphibia. Submitted for publication.

8. R. Lara and M.A. Arbib
A model of the neural mechanisms responsible for stimulus specific habituation of the orienting reflex invertebrates. Accompanying paper.

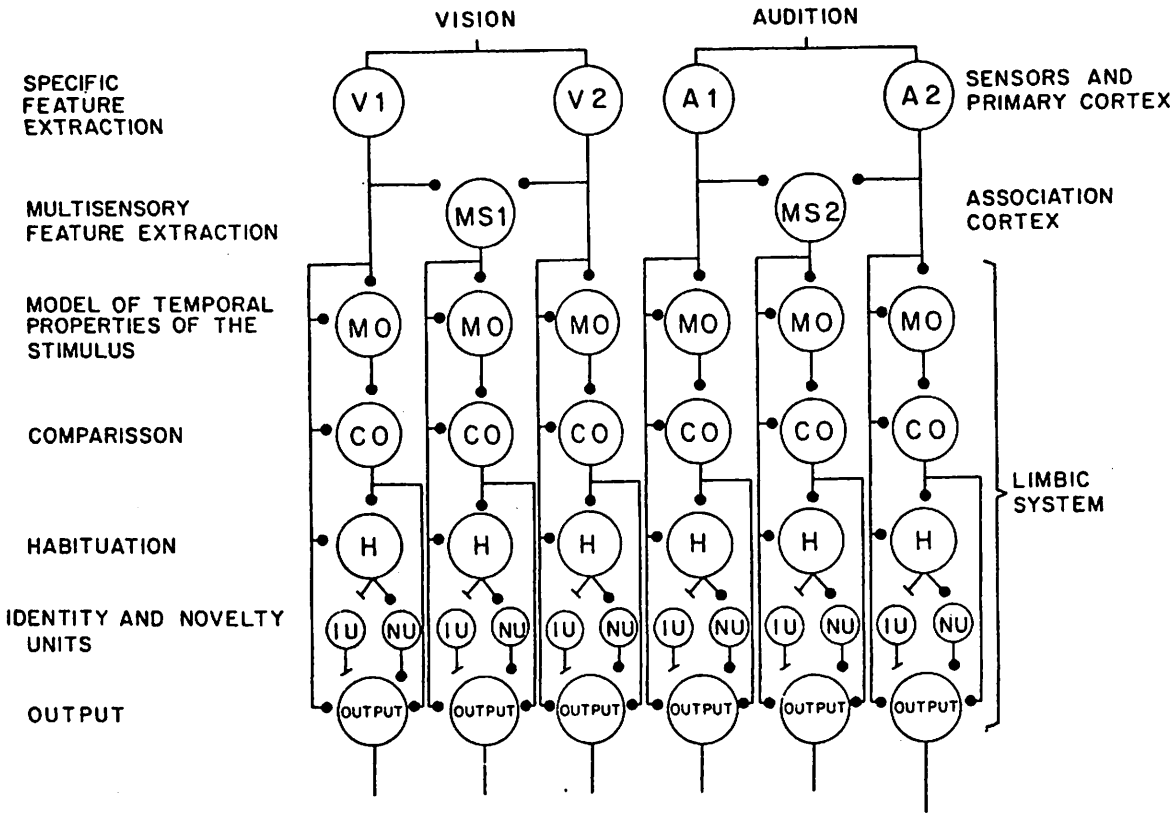

Fig. 1.- Diagram of the different steps in the processing of information required for stimulus specific habituation of the orienting reflex. The first step is feature extraction represented in the diagram by visual and auditory information. The regions that may be performing this process may be located in the senses and primary cortex. The second step is multisensory coding, possibly performed in the association cortex, and is represented in the diagram by two multisensory cells, each receiving visual and auditory information. The third step is the creation of the temporal properties of each feature of the stimulus. The fourth step is the comparisson between model and stimulus. The fifth step is habituation when stimulus and model match, through IU, or dishabituation when a mismatch occurs, through NU. The final step is the output neuron which receives the excitation from the feature extractor, IU, NU and CO, defining the novelty of a given situation. The last four steps may be performed in the limbic systems.

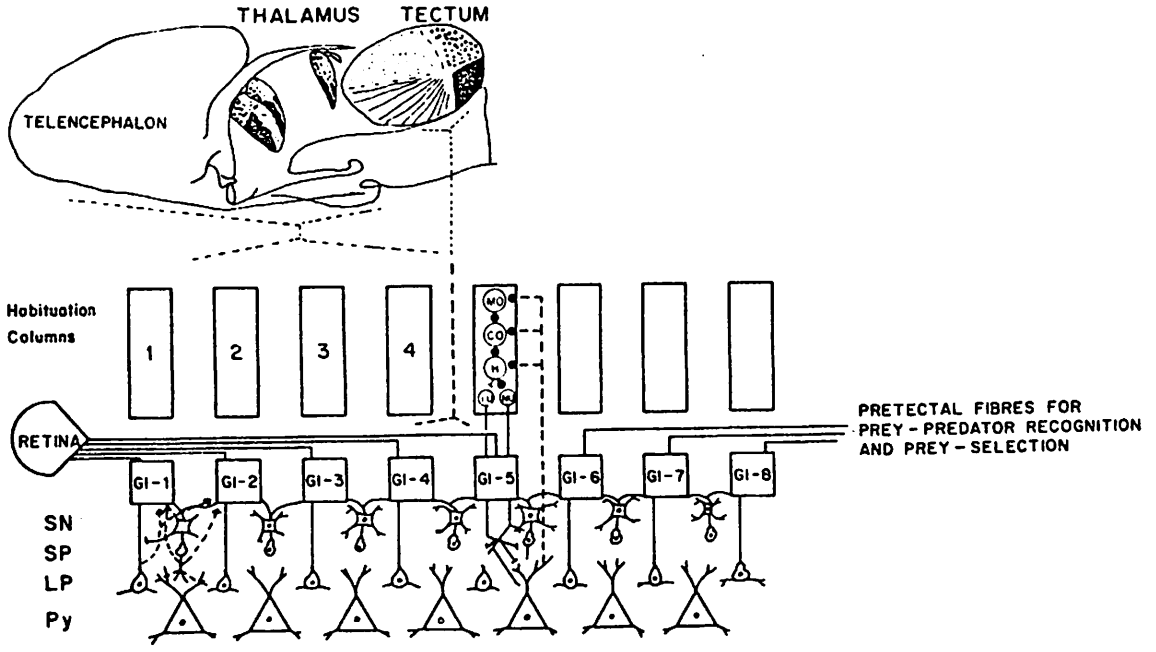

Fig. 2.- Model of interactions among retina-tectum and pretectum. The retina sends ganglion cells type 2, 3 and 4 to the tectum and ganglion cells type 3 and 4 to the pretectum. The pretectal cell inhibits the large pear shaped, small pear shaped and pyramidal neurons of each tectal column.

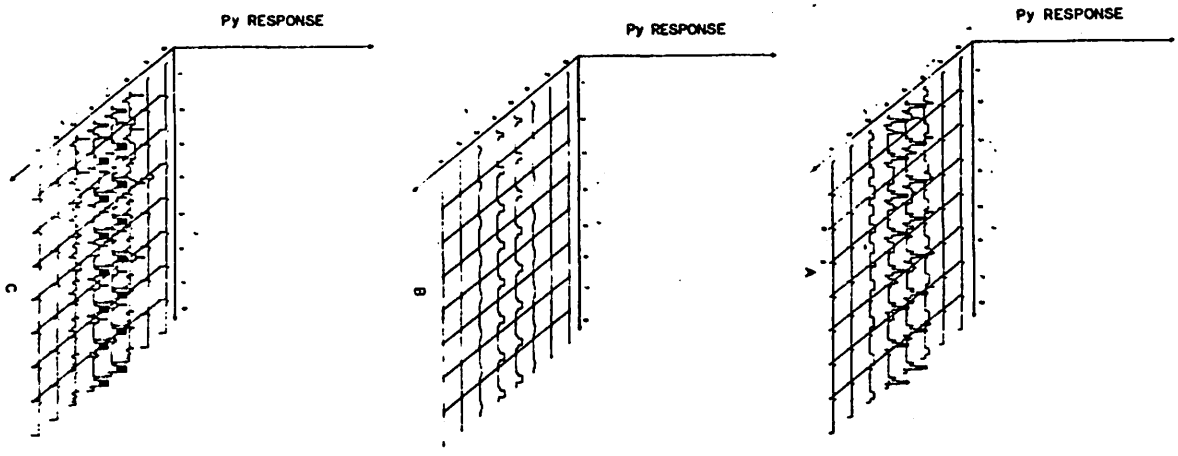

Fig. 3.- Computer simulation of the response of the 64 PY neurons of the bidimensional model of the tectum to the presentation of a given stimulus (Fig. 3 A), its habituation (Fig. 3 B), and dishabituation when a new stimulus is presented (Fig. 3C). The response of each PY neuron is measured for 5 units of time and the action potential is represented as a vertical line. The object moves from left to right.

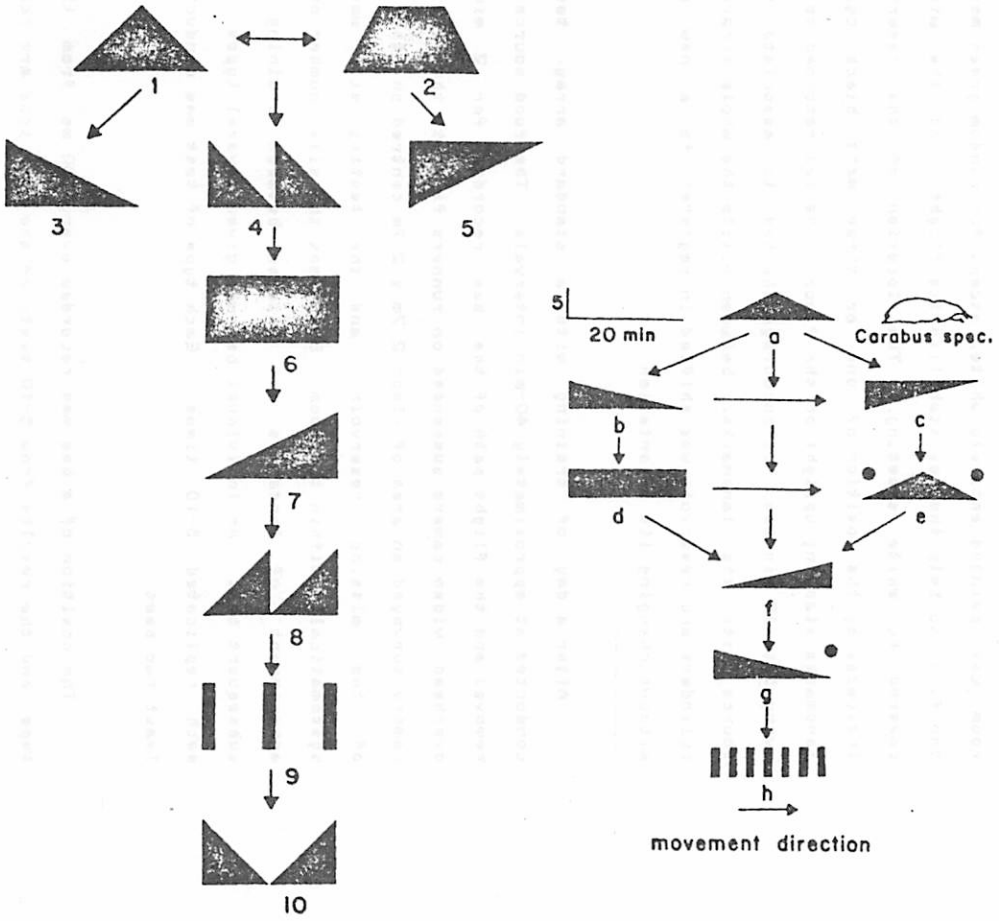

Fig. 4.- Hierarchy of dishabituation for the stimuli used in the computer simulation of the bidimensional model of retina-thalamus-telencephalon-tectum for stimulus specific habituation. The upper stimuli can dishabituate any of the other stimuli on the lower parts. For comparison with experimental results the right section of the figure shows the hierarchy found by Ewert and Kehl (1980).

B.A. Cartwright and T.S. Collett: HOW HONEY BEES USE LANDMARKS TO GUIDE THEIR RETURN TO A FOOD SOURCE

Bees trained to forage at a place specified by landmarks do not construct a cartesian map of the arrangement of landmarks and food source. Instead they store something like a two-dimensional snapshot of their surroundings taken from the food source. To return there, bees move so as to reduce discrepancies between the snapshot and their current retinal image. A computational model embodying these principles mimics the bees' behaviour.

Honey bees can learn the position of a source of sugar by reference to nearby landmarks (reviewed in ref. 1). We describe here what bees seem to learn about the spatial layout of landmarks and how this information might guide their approach to the source. Our experimental results strongly support earlier proposals [1-4] that to identify a place to which it will return an insect learns no more than the appearance of the landmarks viewed from that spot - just as though it takes and stores a panoramic snapshot of the landmarks from that position. Then, to find its way back, it compares the image on its retina with the stored snapshot and moves until the two match. It is not immediately obvious that this hypothesis can work, and we have therefore developed a computational model to show that it does.

Bee Tests

Single marked bees were trained to fly through an open window into an experimental room (floor area 4m x 4m) to collect sugar solution from a small reservoir (diameter 1.5 cm) on the floor. The

room was painted entirely white, except for random green markings on the floor to help the bee stabilize its flight, and the window was covered by white sheeting. The location of the reservoir was indicated by the position of one or three matt black cylindrical landmarks standing upright on the floor. The bee returned to the room every 5 to 10 minutes. To encourage the bee to associate the food source with the landmarks, between visits the whole arrangement of cylinders and reservoir was shifted in register to a new position, without changing its orientation.

After a day of training with a standard array, tests were conducted at approximately 40-min intervals. The food source was then removed and the flight path of the bee recorded for 2 min by an overhead video camera suspended on runners fixed to the ceiling. The camera surveyed an area of floor 2.7m x 2.7m centred on the position of the missing reservoir, and the testing site was varied systematically within the room. Sometimes the size, number or spatial arrangement of landmarks was altered between training and the subsequent test. An individual bee was given several types of test, each replicated 5-10 times. Each type of test was conducted on at least two bees.

The position of a bee was recorded every 100 ms from the video tape and the results from 5-10 tests of the same type are combined to show in Figs 1 and 2 how an individual bee distributed its time in the vicinity of the landmark array. Our aim was to infer from the bee's

searching pattern where it thought the reservoir was to be found, and from this to deduce what it knew about the arrangement of landmarks.

When a bee was trained to a food source at a constant distance from a single cylindrical landmark, and then tested with the food source removed, it searched roughly where it had previously foraged with respect to the landmark (Fig. 1a). Although a radially symmetrical landmark does not define direction, the bee does not fly in a circle around the landmark, implying that some other cue (possibly the window) must specify in which direction from the landmark the food lay. Tests with single landmarks smaller (or larger) than the training size result in a search area shifted closer to (or further from) the landmark (ref. 5 and B.A.C. and T.S.C. in preparation). This suggests that the bee has not learnt the distance between landmark and food source but rather how large the landmark appears when viewed from the food source, and also that to find the reservoir the bee flies to where the image of the landmark on the retina is of the right size.

Experiments using three landmarks, when the search area is rather more sharply defined (Fig. 1b), reinforce these conclusions. If a bee is trained to a particular configuration of landmarks and then tested with a different spatial arrangement of those same landmarks, it always searches in an area where the inter-landmark angles (as shown in Fig. 2) are the same as when seen from the food source. The actual distances of the landmarks from each other or from the search

area are of minor importance.

Figure 2a, b shows a bee's search area when it was confronted with an array in which the distances between landmarks differed from those with which it was trained. The bee spent most of its time where the inter-landmark angles matched those experienced during training. Furthermore, if the test configuration was such that a bee could search where either the distances from the landmarks or the inter-landmark angles were correct, it chose to do the latter (Fig. 2c).

A bee tested with cylinders that were larger or smaller than the ones used in training also searched where the inter-landmark angle was approximately correct. Figure 2d illustrates that this behaviour persists for very dramatic changes of landmark shape and size, when cubes with 30-cm edges were substituted for the training cylinders (4 cm diameter, 40 cm height). We conclude that to a bee the most important feature of the landmark array is the retinal position of the landmarks as seen from the food source.

At first sight, the bee's neglect of landmark size would seem to conflict with their behavior when they are trained to a single landmark and its size is changed. However, whatever the size of a single test landmark, a bee can always find a position where there is a perfect match between its 'snapshot' and the retinal image of the test landmark. But with three landmarks both their sizes and the

distances between them must be changed in a coordinated way for a position to exist where retinal image and snapshot are congruent. If just one of these parameters is varied, then wherever the bee searches there will be some degree of mismatch. Simple geometry suggests that in this case the retinal sizes of landmarks is correct, the positions of the other landmarks on its retina would be very wrong.

It seems, then, that a bee will search within a circumscribed area without requiring a perfect match between its postulated snapshot and its current retinal image. This can be shown in another way by testing bees with landmarks added to or taken away from the training array. Figure 2e shows that with two extra landmarks the bee's search area, although slightly larger than normal, is roughly in its usual position. When a bee was tested with any of the three landmarks removed, it still spent most of its time looking where the inter-landmark angle formed by the remaining two landmarks was the same as it was during training (not illustrated). This test also demonstrates that the bee must learn the sizes of the landmarks, for it is only their size that tells the bee whether or not the two remaining landmarks are neighbors and whether the inter-landmark angle should be 60 degrees or 120 degrees.

The Snapshot Model

All the above findings argue that the representation of landmarks in the bee's memory can be described in terms of a snapshot taken from the food source (see also ref. 1 for somewhat similar experiments on

desert ants). The bee does not seem to be equipped with anything akin to a floor plan or cartesian map. We have therefore explored how well a model bee can guide itself using a representation of this kind. The basic idea is that the direction in which the bee moves at any moment is governed by the discrepancy between the snapshot annd its current image (Fig. 3).

To construct such a model we must make assumptions about the way images are coded in the visual system and the snapshot. In part these are arbitrary. However, we have some evidence that the most important features of the retinal image are the edges between the dark landmarks and the light ground (B.A.C. and T.S.C., in preparation). Accordingly, in the model the retinal image consists of edges lying on a circular retina and the snapshot is represented in a compatible way (Fig. 3). The positions of the edges on both retina and snapshot are defined as compass bearings with respect to Earth-based coordinates. This assumption is supported by several experimental results. First, the tests with single landmarks (Fig. 1a) imply that cues external to the landmark specify the direction of the food source from the landmark. Second, when bees were tested with a three-landmark array rotated by 90 degrees from the training orientation, the search area shifted away from the position predicted by the inter-landmark angles experienced during training. Third, bees find it difficult to use landmarks if, during training, the array is rotated between each of the bee's foraging visits. The simplest way to picture how edges in the snapshot can be given Earth-based coordinates is to suppose that

the snpshot is fixed in the bee's head and that the bee always maintains the same orientation. This is not in fact so, and one needs to assume that as the bee turns, the snapshot counter-rotates.

Algorithms for Calculating Flight Direction

We have examined two algorithms for generating the bee's direction of flight. These were programmed in Basic and run on a PDP8/a computer. The first, the simplest we could devise, fails to mimic all the bee's behaviour, but the second and more elaborate version performs very much as real bees do.

In the first algorithm (Fig. 4a) a unit vector is associated with each edge in the snapshot. The direction of the vector depends on the bearing of the closest edge of the same sign (that is, dark-light or light-dark) on its retina. Imagine each edge in the snapshot putting out an extensible arm to reach the nearest retinal edge. Once the edge is located, a unit vector is generated lying perpendicularly to the bearing of the retinal edge and pointing away from the paired edge in the snapshot, tending thus to align the two edges. These unit vectors are then summed, in the conventional way for adding vectors, to give the bee's flight direction. As the bee moves through the field of landmarks, it will continually update its direction as the edges shift over its retina. Note that it is not necessary for all edges in the retina to be matched to partners in the snapshot. Some may have more than one partner and others none at all. Furthermore, the bee is not required to assess the goodness of fit

between its snapshot and the retinal image.

Figure 4b shows the computed vector directions for different points within the field of landmarks for a bee which is trained and tested with the same array of three landmarks. If the algorithm is to be successful, then from any starting point the vectors must lead the bee to the food source. The extent to which this is the case is shown in Fig. 4c. For most starting points the bee does indeed end up at the food source. However, there are mishaps which arise because partial matches exist. There is one position within the field, for instance, where the two outer landmarks form an inter-landmark angle of 60 degrees. The bee is trapped there because within a region on either side the vectors have opposite directions, pointing towards the partial match. Real bees do not make this mistake. The algorithms performance can be improved if it takes into account the amplitude of the summed vectors. However, it still does not work in all the situations we have tested. In particular it fails if the array of landmarks rotated by 30 degrees from the orientation to which the bee was trained - a situation with which the bee can cope (Fig. 2f). Because the algorithm depends on the positions of edges defined with respect to external coordinates, a changed orientation of the landmark array will generate several points in the field where the edges of two landmarks can be roughly matched with edges in the snapshot, but none where all edges can be correctly matched.

To overcome these problems the second algorithm requires the bee

to assess not only the position of each edge, but also the angular distance between them (Fig. 4d). Its first step is to decide on the basis of the signs of neighbouring edges whether the angles between them are dark or light. It then measures the size of each dark and light angle in the snapshot and on the retina, and locates the positons of their bisectors. Next, each bisector in the snapshot searches out the closest bisector on the retina with the same sign (dark or light), so pairing angles in the snapshot with angles on the retina. As in the first algorithm, a unit vector (the positional component) is associated with each pair, tending to move the bee perpendicularly to the bearing of the bisector on the retina, pointing away from the bisector in the snapshot (or toward it if the retinal angle is greater than 180 degrees). The additional feature of this algorithm is a second unit vector (an angular component) which depends on the differences between the sizes of the paired angles. This vector faces centripetally along the bisector on the retina if the angle in the snapshot is the smaller, and centrifugally if it is the larger. It thus takes the bee away from retinal angles that are too big and towards those that are too small. All the component vectors are then summed to determine the bee's flight direction, which is shown by the arrow in the centre of Fig. 4d.

Figure 4e illustrates the directions of the summed vectors within the standard three-landmark array. The improvement over the first algorithm is obvious: there are paths from all points to the food source, and when the bee is flown from different starting points it

now always finishes there (Fig. 4f). It is easy to see that neither the positional nor the angular component of the summed vector would by itself be sufficient to locate a food source specified by a single landmark, although either can do so when there are three landmarks. With one landmark the positional component defines direction but not distance, so that the bee would search along a line originating at the landmark and passing through the food source. The angular component, on the other hand, only specifies distances and would leave the bee flying in an annulus centred on the landmark. The two acting together are needed to identify the intersecting point.

This algorithm copes with all the one- and three-landmark tests we have tried, including those with landmarks added or deleted. The 30 degree rotation of the three-landmark configuration on which the first algorithm founders is taken care of by the angular component. However, to prevent aberrant solutions, the angular component must be given a greater weighting than the positional one (3:1), a weighting which works in all situations. When the landmark array was rotated through 90 degrees from the training orientation, the search area was displaced for the model, as it was for real bees.

The algorithm will not only move bees to the right position within an array of landmarks, but it will also bring a bee successfully to a foraging position in the centre of a ring of eight landmarks from points well outside the circle, as in tests with real bees. [6]

The model does not specify how directional information is abstracted. The information is assumed to be provided by an independent system. We have attempted, but failed, to generate a simple alternative model in which direction can be automatically obtained from an array of close and distant landmarks.

Despite the success of the model in our artificial environment, it is rash to conclude that this is how bees operate in the real world. For a start, sensory processing is undoubtedly more complicated than we have allowed it to be here. However, what does seem to be certain is that bees do not need a three-dimensional representation of their immediate surroundings in order to use nearby landmarks to locate a food source. A much simpler model will work: one in which the bee is not required to identify landmarks as such, or even to separate figures from the background. There is, of course, a price to be paid for simplifying one's visual world in the way the experiments suggest that the bee has done. It is that the bee can only use the information provided by its snapshot of the landmarks to return to the food source. The snapshot provides it with no means of navigating to anywhere else within the array of landmarks.

We thank David Blest, Mike Land, Christopher Longuett-Higgins, Peter Slater and Geoff Sullivan for their comments and Jo Harper for typing. Financial support came from SRC.

References

1. Wehner, R., in Handbook of Sensory Physiology Vol. VII/6C (ed. Autrum, H.J.) (Springer, Berlin, 1981).
2. Collett, T.S. Land, M.F., J. Comp. Physiol. 100, 59-84 (1975).
3. Wehner, R., Raber, F., Experientia 35, 1569-1571 (1979).
4. Holldobler, B., Science 210, 86-88 (1980).
5. Cartwright, B.A. , Collett, T.S., J. Exp. Biol. 82, 367-372 (1979).
6. Anderson, A.M., J. Comp. Physiol. 114, 335-355 (1977).

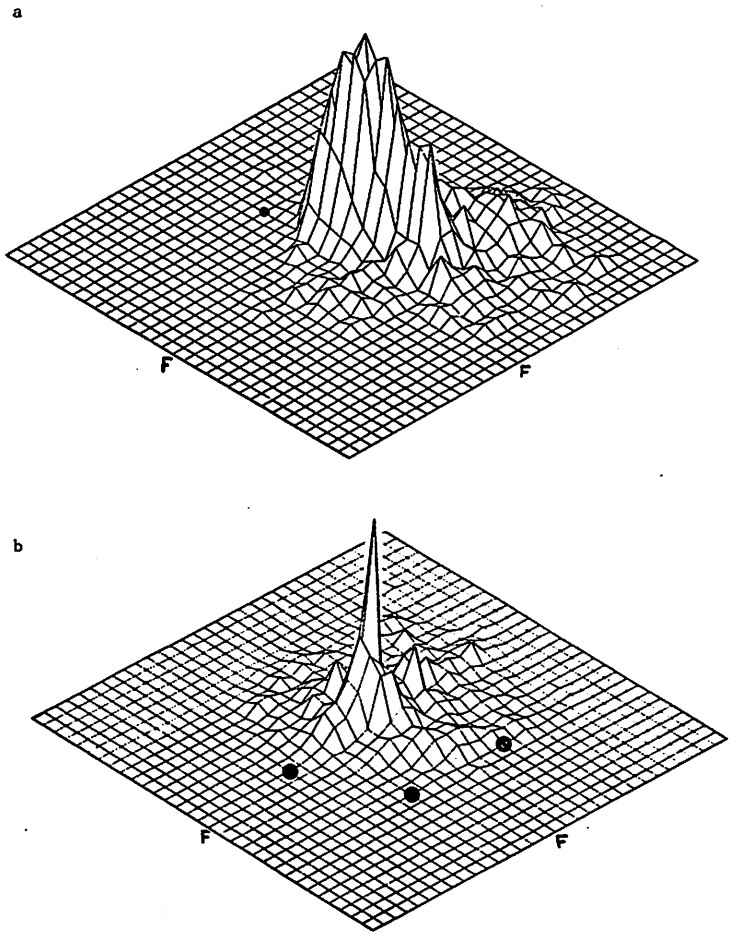

Fig. 1 a) Distribution of a single bee's flight time within the area surveyed by the camera when trained to a food source 50 cm from a single cylindrical landmark and tested with the same-sized landmark (4 cm diameter and 40 cm high). The position of the food source during training is marked by 'F' on the x and y axes. The position of the base of the landmark is indicted by filled circles. Height shows relative times spent in different regions of the testing area. Lines on grid are 8.7 cm apart. b) Distribution of bee's flight time when trained and tested with three landmarks in the standard array described in Fig. 2.

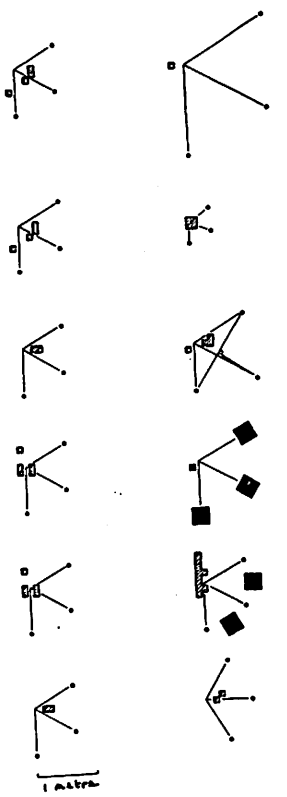

Fig. 2 Tests with three landmarks. The training configuration is shown in plan view in the left-hand column. The food source was placed 76 cm from each landmark at the intersection of the three lines drawn from the landmarks. Inter-landmark angles refer to the angles between these lines. In a and b, the cylinders were 5 cm in diameter and 50 cm high. In c to f they were 4 cm x 40 cm. Each row of the figure presents a pair of test arrays. The left half shows where a single bee searched when presented with the training array. On the right is the same bee's search area when presented with a variant of the training array. The hatching represents the search area defined as those squares within the test area (as in Fig. 1) that are at least 80% as high as the peak value. a) Distance between landmarks doubled; b) distance halved; c) landmarks arranged so that bee could search either where the inter-landmark angles or where the distances from the landmarks were the same as during training; d) cubes substituted for cylinders; e) cubes added to landmark array; f) landmark array rotated through 30 degrees from training orientation. The point of intersection of the lines in the right-hand column show where the bee would need to search to see the same inter-landmark angles that it experienced when foraging at the food source. This is generally where the bee spends most of its time.

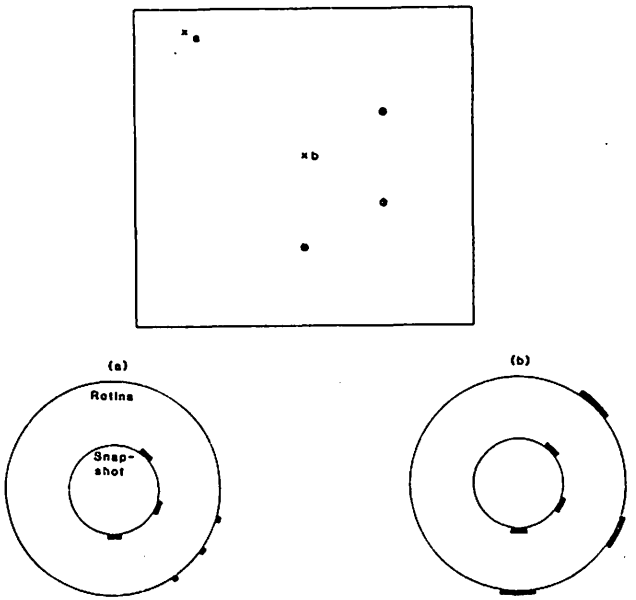

Fig. 3 The snapshot model. Positions of images of landmarks on circular retina (outer circle) and in snapshot (inner circle) viewed from two points within the landmark array as shown by crosses. a) Distance from the food source; b) at food source, where snapshot and retinal image match. The aim of the model is to move the insect from a to b using the discrepancy between retinal image and snapshot as a guiding cue. Note that positions of edges on the circular snapshot and retina are compass bearings with respect to external coordinates. Frame round landmark array shows area viewed by video camera.

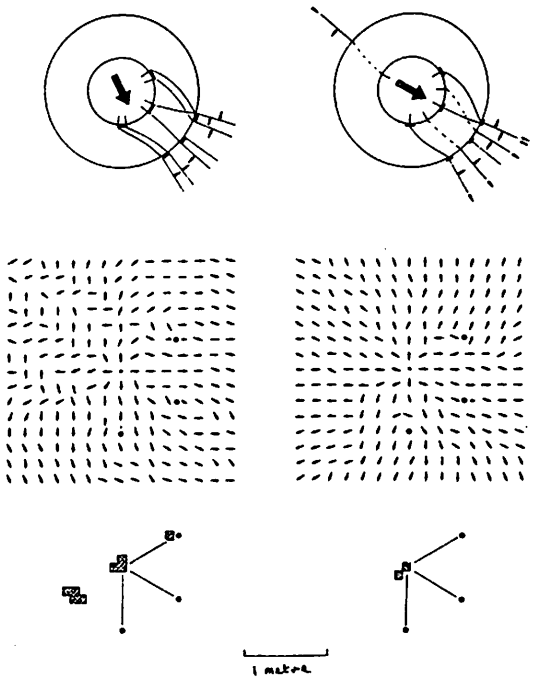

Fig. 4 Two algorithms for transforming retinal image to snapshot. a) Edge algorithm. Each edge in snapshot paired with closest edge on retina. Unit vector, shown by arrows around outer circle, is associated with each pair and lies perpendicularly to edge on retina, pointing away from edge in snapshot. Larger arrow in centre of circle shows flight direction of bee obtained by summing the unit vectors. b) The flight direction for different positions of the bee within landmark field, computed as outlined in a. Model bee trained and tested with landmark configuration of Fig. 3. c) Positions of end points are shown by cross-hatching. The bee is started at different positions within the landmark field and it follows the vectors as shown in b until it stops. d) Bisector algorithm. Unit vectors of positional component shown by arrows lying tangentially to outer circle, those of angular component by radially aligned arrows (details in text). e) Vector field for bisector algorithm. f) Position of end points for bisector algorithm.